UNIVERSITY OF CALIFORNIA, SAN DIEGO

Microbe-Metazoan Interactions at Pacific Ocean Methane Seeps

A dissertation submitted in partial satisfaction of the
requirements for the degree Doctor of Philosophy

in

Oceanography

by

Andrew Reichmann Thurber

Committee in Charge:

Professor Lisa A. Levin, Chair
Professor Lihini Aluwihare
Professor Douglas H. Bartlett
Professor William H. Gerwick
Professor Greg W. Rouse
Professor Christopher J. Wills

2010

The Dissertation of Andrew Reichmann Thurber is approved, and it is acceptable in quality and in form for publication on microfilm and electronically:

_____

_____

_____

_____

_____

_____

Chair

University of California, San Diego

2010

DEDICATION

This Dissertation is dedicated to my grandparents, Gunnar and Annelies Dahlquist, who exposed me to the joy and biology of the oceans throughout my earliest memories. Through fishing, collecting invertebrates, and spending countless hours staring in tide pools every year, they provided the foundation for my interest in the oceans. Although tides were explained as King Neptune using a giant sack to collect or release water each day, fish biology and what I later learned was population biology was a part of our everyday lives. We treated the ocean with respect and harvested with conservation in mind and the general rule "if you killed it, you eat it." These experiences gave me direction. Although I quickly steered away from fish, the ocean remained my calling and I dedicate this dissertation to them.

EPIGRAPH

Therefore the sight that is granted to your world penetrates
within the Eternal Justice as the eye into the sea;
for though from the shore it sees the bottom,
in the open sea it does not, and yet the
bottom is there but the depth conceals it.
-Dante

TABLE OF CONTENTS

Signature Page iii

Dedication iv

Epigraph v

Table of Contents vi

List of Figures ix

List of Tables xii

Acknowledgments xiv

Vita xvii

Abstract xviii

Chapter 1. Introduction 1

- Background 1
- Problem 4
- Overview and Approach 4
- Figure 7
- Table 8
- References 9

Chapter 2. Stable isotope signatures and methane use by cold seep benthos 13

- Abstract 13
- Introduction 13
- Regional Settings 15
- Materials and methods 15
- Results 16
- Discussion 19
- Conclusions 21
- Acknowledgments 21
- References 21

Chapter 3. Microbes, Macrofauna, and Methane: The importance of aerobic methanotrophy in fueling a high-biomass, methane seep infaunal community 25

- Abstract 25
- Introduction 26

Methods 29
Results 32
Discussion 37
Conclusions 42
Figures 43
Tables 50
References 56
Acknowledgments 60

Chapter 4. Diet-dependent incorporation of biomarkers: Implications for food-web studies using stable isotopic and fatty acid analyses 62

Abstract 62
Introduction 63
Materials and Methods 65
Results 69
Discussion 74
Conclusion 81
Figures 83
Tables 87
References 89
Acknowledgments 94

Chapter 5. Archaea in metazoan diets 95

Abstract 95
Introduction 96
Materials and Methods 99
Results 105
Discussion 109
Figures 116
Tables 121
References 123
Acknowledgments 129

Chapter 6. Dancing for food in the deep sea: Bacterial farming by a new species of Yeti crab 130

Abstract 130
Introduction 131
Materials and Methods 133
Results and Discussion 136
Species Description 143
Figures 152
Table 159

References..... 161
Acknowledgements..... 165

Chapter 7. Discussion..... 166
References..... 171

LIST OF FIGURES

Figure 1.1 Examples of lipids diagnostic for Crenarchaea or anaerobic methane oxidizing Euryarchaea and ester lipids diagnostic for Eukaryotes and Bacteria. Crenarchaeal lipids modified from Wutcher et al. (2003)..... 7

Figure 2.1 Methane-seep regions sampled for symbiont-bearing megafauna and heterotrophic macrofauna. Omakere Ridge includes LM-9, Kaka, and Bear's Paw. Opouawe Bank includes North Tower, South Tower, and Takahe. For site maps see Greinert et al. (2010) 15

Figure 2.2 Stable isotopic composition of symbiont-bearing invertebrate fauna from New Zealand methane seeps. Range of methane isotopic concentration is from Sommer et al. (2010) 16

Figure 2.3 Stable isotopic composition of heterotrophic invertebrate fauna, filamentous, sulfide-oxidizing bacteria, and plankton samples from New Zealand methane seeps. The range of estimated percent methane-derived carbon in animal tissues is given as a top x-axis (see text for model estimation methods). Range and mean of methane isotopic concentration are from Sommer et al. (2010) 16

Figure 2.4 Mean stable isotopic composition of heterotrophic invertebrate fauna at each site sampled on the New Zealand continental margin. Error bars are ±1SE. Legend gives sampling equipment used at each location using the abbreviations: Sled = epibenthic sled; MUC = blind multicorer; Grab = vanVeen grab; TV-G = video-guided hydraulic grab; TV-MUC=video-guided multicorer; Lander=Bigo and Flufo benthic landers. For more details see Materials and methods and Table 2.1 18

Figure 3.1 Sampling locations of methane seeps off the North Island, New Zealand.. 43

Figure 3.2 A 2D representation of the similarity of New Zealand methane-seep infaunal communities. Significant different groupings as tested by an analysis of similarity (ANOSIM) are indicated by dotted lines..... 44

Figure 3.3 Vertical distribution of dominant taxa within ampharetid bed communities 45

Figure 3.4 A 2D representation of the similarity among fatty acid samples. Significantly different groupings, as tested by an analysis of similarity (ANOSIM), are indicated by dotted lines. Mean isotopic composition for each group are given. 46

Figure 3.5 Ampharetid bed macrofaunal abundance compared to other methane seep communities. For Hydrate Ridge all abundances are from Levin et al. (2010) except for "Acharax" which is from Sahling et al. (2002) since Levin et al. (2010) used the same size sieve as the present study and is thus more comparable 47

Figure 3.6 Wet-weight biomass of ampharetid bed communities from New Zealand in comparison to other seep infaunal communities. Grey bars indicate a combination of heterotrophic and symbiont bearing (chemosynthetic) fauna. Bioturb. Sed. = Bioturbated Sediment; Red. Sed. = Reduced sediment. 48

Figure 3.7 Macrofaunal methane demand from two ampharetid beds in comparison to the total oxygen utilization, standing stock of anaerobic methane oxidation ANMEs (Note: ANME growth rate of was 0.1 mmol C m-2 day-1) and maximum methane emission from ampharetid bed sediment. White bar indicates minimum estimate and grey bar indicates maximum conservative estimate. 49

Figure 4.1 Carbon and nitrogen stable isotopic composition of six food sources and *Ophryotrocha labronica* fed those food sources. Significant differences in food sources are indicated by bars with horizontal bars showing significant differences in carbon and vertical differences in nitrogen. Points which fall under the same bar are not significantly different from each other. An asterisk indicates the isotopic composition of that food source is significantly different from all other food sources. See text for statistical treatment. Error bars are standard error. 83

Figure 4.2 Relationship between A) $\delta^{13}C_{diet}$ and $\delta^{13}C_{tissue}$ and B) $\delta^{15}N_{diet}$ and $\delta^{15}N_{tissue}$ for *Ophryotrocha labronica* fed the indicated diets. Solid lines are linear regressions based on all data. Dotted grey lines indicate a slope of one or the slope of the line predicted by a constant tissue-diet shift independent of food source. Dashed black line in A) indicates the regression fit when *Oryza* sp. is not included in the analysis. See text for regression equations and fit. Error bars are standard error 84

Figure 4.3 Multidimensional Scaling of log(x+1) fatty acid profiles of *Ophryotrocha labronica* fed six food sources. Worms fed eukaryotic food sources are in grey, bacterial in black, and archaeal in white 85

Figure 4.4 Deviation from the mean fatty acid profile for *Ophryotrocha labronica* fed six different diets. Food-source fatty acid distribution is presented in the lower panel in hashed bars.. 86

Figure 5.1 Mean daily growth rate of *Ophryotrocha lobronica* over a 44 to 47 day period as a function of food source. Error bars = 1 SE..... 116

Figure 5.2 Micrograph of ANME aggregate from inside rock "E3" stained with DAPI. Scale bar = 15μm (Credit: Jeffrey Marlow)..... 117

Figure 5.3 Carbon isotopic composition of fatty acids and fatty acid distribution within (upper panel) carbonate rocks and (lower panel) *Dorvillea* sp. Left y-axis and bars are percent fatty acid and right y-axis and points are isotopic composition. Asterisks indicate that isotopic composition was potentially largely impacted by contaminants (see text for more details). Value estimates for this omitted FA ranged between -143 to -45 ‰. 18:2 and 20:1(n-11) were left off this figure as they were <2% in only one individual of *Dorvillea* sp. 118

Figure 5.4 Relationship between carbon isotopic composition and sum of 16:1(n-5) and 18:1(n-5) FAs present within 5 species of polychaete from Eel River and Hydrate Ridge. Solid line is a regression including all dorvilleid polychaetes in which both isotopic and FA data are available within a single sample. Dotted line indicates regression if point to the far right is removed. Symbols indicate species..... 119

Figure 5.5 Most abundant neutral lipids present within the two species of Euryarchaea used in the laboratory feeding study (squalene, A, and B) and those present within methane seep Euryarchaea (PMI, crocetane from Blumenberg et al. 2004). Location of double bonds for A and B are approximate and in Table 5.1 A and B include all isomers of these molecules 120

Figure 6.1 *Kiwa puravida* n. sp. holotype, *in situ* images, and morphologic and behavioral adaptations to harvest its bacteria. *Kiwa puravida* n. sp. male holotype: (A) Dorsal view. (B) Ventral view (A and B scale bar = 10mm; credit: Shane Ahyong, NIWA Wellington). (C) *in situ* next to bathymodiolin mussels (D) scanning electron micrograph of *K. puravida* n. sp.'s 3rd maxilliped and the comb-row setae that it uses to harvest its bacteria (scale bar = 150μm credit; Shana Goffredi, Occidental College]. (E) Setae covered by bacteria from 3rd pereopod (see Figure 6.7E for scale). (F) Dense aggregation *in situ*. (G) Shipboard photo of *K. puravida* n. sp. using its 3rd maxilliped to harvest its epibiotic bacteria. (H) Comb-row setae with bacteria filaments stuck among combs (indicated by arrow) 152

Figure 6.2 Fatty acid composition of muscle tissue and bacteria-laden setae in relation to plankton. Mean fatty acid composition of abundant (>1‰ of the total fatty acids present in any of the samples) fatty acids of muscle and bacteria-laden setae from 3rd or 4th pereopod of *Kiwa puravida* n. sp. subtracted from the fatty acid composition of plankton collected from the overlying water column. Error bars = range. N=2 153

Figure 6.3 Bayesian phylogenetic tree based of 18S rRNA gene sequence, rooted using *Upogebia affinis* 154

Figure 6.4 16S rRNA gene phylogeny of ε-proteobacteria decapod symbionts created using the MUSCLE algorithm (Edgar 2004) 155

Figure 6.5 *Kiwa puravida* n. sp. male holotype. (A) Pereopod 1 (cheliped). (B) Pereopod 2 (1st walking leg). (C) Pereopod 3. (D) Pereopod 4. (E) Carapace. Scale bars = 5mm 156

Figure 6.6 *Kiwa puravida* n. sp. male holotype. (A) Lateral view carapace and abdomen. (B) Antennule and antenna left and anterior part of ptergostomial flap. (C) Basis-ischium of third maxilliped, mesial view. (D) Third maxilliped. (E) Sixth segment of abdomen. (F) Sternal plastron. (G) Male paratype gill arrangement. Scale bars = 5mm 157

Figure 6.7 *Kiwa puravida* n. sp. male holotype. (A) Dorsal carapace. (B) Lateral view. (C) Sternal plastron. (D) Finger and thumb on cheliped (E) Whip-like barbed setae (left), comb-row setae (middle), and stout barbed setae (right). (G) *K. puravida* n. sp. female gonopore on third pereopod. Scale bars: A-D = 10mm; E =500μm. (A-D credit: Shane Ahyong, NIWA Wellington) 158

LIST OF TABLES

Table 1.1 Characteristic lipid biomarkers for microbes with chemoautotrophic pathways. * indicates diagnostic. 8

Table 2.1 Sampling sites, dates, depths, and gear used for faunal collection. 14

Table 2.2 Stable isotopic composition of known symbiont-bearing taxa at New Zealand methane seeps. 16

Table 2.3 Mean, standard error, and range of stable isotope values of heterotrophic fauna collected from each methane-seep station on the New Zealand continental margin 17

Table 2.4 Mean station carbon isotopic signatures for macrofauna obtained by each type of sampling gear used. 18

Table 2.5 Estimates of percent methane-derived carbon (MDC) in tissues of heterotrophic invertebrates in methane-seep sediments. 19

Table 3.1 Study locations, sites, macrofaunal density, number of fatty acid (FA) analysis run from each site, mean carbon stable isotopic signature with standard error and sample size given, and the wet-weight biomass of two samples. Sites in bold are ampharetid bed sites and those in italics had a subset of the samples collected belonging to the "non-seep" habitat. 50

Table 3.2 SIMPER results indicating which macrofaunal taxa differentiated the groupings identified in Figure 3.2. Polychaete* indicates that the family was not identifiable 51

Table 3.3 Composition of infaunal communities along the New Zealand margin. Group A is the ampharetid bed community. Number of cores are given in parentheses and standard error among cores (not stations) is given. 52

Table 3.4 SIMPER results indicating which fatty acids differentiated the groupings identified in Figure 3.4 54

Table 3.5 Fatty acid (FA) and stable isotopic composition of each of the different fatty acid clusters. Percent of FA is given for those FAs which made up more than 1% in any sample. Grey shading indicates aerobic methanotroph biomarkers, red indicates sulfate reducing bacterial biomarkers, and green indicates phytoplanktonic biomarkers .. 55

Table 4.1 Mean tissue-diet shift for carbon, $\Delta^{13}C$, and nitrogen, $\Delta^{15}N$, stable isotopic composition between *Ophryotrocha labronica* and six different diets. Statistical results indicate differences between the diet and tissue with a significant value indicating that they were different, df= degrees freedom and significant p-values are in bold. C:N ratio is given of each food source. SE = standard error 87

Table 4.2 Fatty acid (FA) composition of *Ophryotrocha labronica* reared on six food sources and the fatty acid composition of those food sources. Archaeal food sources had no FAs present. Bold numbers indicate percent of the total FA within

the species (± Standard Error). FAs are named after the number of carbons in their carbon back bone followed by the number of double bonds present. The (n-x) notation indicates the position of the first double bond (x) relative to the terminal end of the FA and those preceded by an a or i are branched. Number of replicates is given in parentheses after the food source. 88

Table 5.1 Percent neutral lipid composition of dorvilleid polychaetes and *Ophryotrocha labronica* fed Euryarchaea in the laboratory. Dorvilleids include those collected from cold-seep habitats. Archaea are identified in bold. tr = trace; nd = not detected potentially due to methodology or concentration analyzed. M.W. = molecular weight of TMS derivative. Other indicates that its mass spectra was not able to be conclusively identified. Asterisks indicates probable identity. A and B are more saturated molecules of squalene (and shown in Figure 5.5). 121

Table 5.2 Fatty acid (FA) fraction of total FA profile of each species included in analysis. Isotopic data are provided for either a fraction of the individual extracted for lipids or from individuals within the same core or scoop sample. Standard error is given. Only data are presented with samples that corresponded to an isotopic measure and only FAs are presented that made up at least 1% of any one sample. * means that double-bond position was estimated from retention time rather than DMDS adduct formation..... 122

Table 6.1 $\delta^{13}C$ and $\delta^{15}N$ and fatty acid composition of abundant (>1‰ in any sample) fatty acids within the 3rd or 4th pereopod from *Kiwa puravida* n. sp. or plankton from the overlying water column. nd – not detected 159

Table 6.2 Relationship between *Kiwa puravida* epibiont fauna and sequence available in GenBank as of 9/15/2009 using 16S rRNA gene sequence data..... 160

ACKNOWLEDGMENT

This work was possible due to the insight and opportunities provided to me by my advisor and mentor, Dr. Lisa Levin. Through guiding me on every aspect of science from proposal writing, carrying out research at sea, leading expeditions, and manuscript preparation, she has always provided encouragement and advice to improve the quality of my science. She has shown me how to put together a scientific paper when I did not see one and how to tell a story in a non-perfect data world. She provided a gold standard of mentorship, giving me a goal to strive for throughout my career during my interactions with future students.

I am also indebted to my committee who facilitated this dissertation. Dr. William Gerwick made his lab and instrumentation available to me and provided key pieces of advice into approaches to take when doing this analysis. Dr. Lihini Aluwihare provided great insight into lipid approaches and also taught me to think about carbon and nitrogen in the ocean in a different manner. Dr. Greg Rouse provided excellent suggestions, taxonomic and photographic advice and wonderful company at sea. Drs. Douglas Bartlett and Christopher Wills also supported this research throughout. To all of them I am grateful.

The community at SIO made this research possible. Emiley Eloe was instrumental on growing bacterial and archaeal cultures for my laboratory-based feeding experiments. Cameron Coates, Jo Nunnery, and Tak Suyama provided many great pieces of advice on lipid analysis and always helped with the gas chromatograph and troubleshooting lipid analysis surprises. Within the Levin Lab, Carlos Neira, Jen Gonzalez, Guillermo Mendoza and Pat McMillan all helped at many points along this research path.

In addition to my official committee, I had my (not so) silent committee of students who constantly provided lively discussion points, thoughts on scientific method and writing,

and a lot of entertainment. Leading this committee was Geoff Cook who was always available to discuss the finer points of a figure or battle over statistical analysis, not to mention reading countless grant proposals, abstracts, manuscripts, and pretty much anything else I asked him to do. In addition Christine Whitcraft, Serena Moseman, Christina Tanner, Ben Grupe, and Mike Navarro all joined in this banter to keep the scientific discourse alive within the lab.

As there were my partners in science there were also my partners in crime. Marco, Renee, and Marin Hatch always kept me entertained and provided a family when I was far from mine. Ben Maurer was a constant source of support, although rarely to do work. He kept me sane during days of hardship and turned a project I was struggling with into a key success. The North Pier Surf group, Marco, Spencer, Talina, Nate, Ben M., Jessica Carrilli, Jen and Rich Walsh, Mike N., Ben Neal, Glen Pezzoli and those random strangers whom I spent many hours with, provided an avenue to clear the mind during my tenure at SIO. The founding members of the "Ride to Lard" also added to the joy which is SIO: Erdem, Kate, Rich, Ian, C.A.Tanner.

The SIO Grad Department, Ship Scheduling and Development offices, UC Ship Funds, and IOD business office all made my time at SIO as joyful and exciting, with as minimal paperwork as possible. They always found ways to support my research in one way or another. This research, as all oceanographic studies, is the work of many including ship's captains, and crews, Alvin pilots, and enough different science party members that I would fill this dissertation merely by listing the names of those whom I have had the privilege to sail with.

My wife, Rebecca Vega Thurber, joined me in many adventures and supported me throughout my dissertation. With my family and her behind me I knew that no matter how

high my p-value or heterogeneous my data were, I was supported by loved ones and that made all the difference.

Chapter 2, in full, is a reprint of the material as it appears in Marine Geology 2010, Thurber, Andrew R., Kroger, K., Neira, Carlos, Wiklund, Helena, Levin, Lisa A. The dissertation author was the primary investigator and author of this material.

Chapter 3, in part, currently being prepared for submission for publication of the material. Thurber, Andrew R.; Levin, Lisa A.; Rowden, Ashley A. The dissertation author was the primary investigator and author of this paper.

Chapter 4, in full, has been submitted for publication of the material as it may appear in Oecologia, 2010, Thurber, Andrew R. The dissertation author was the primary investigator and author of this paper.

Chapter 5, in part, is currently being prepared for submission for publication of the material. Thurber, Andrew R.; Levin, Lisa A.; Orphan, Victoria J. The dissertation author was the primary investigator and author of this paper.

Chapter 6, in part, has been submitted for publication of the material as it may appear in PLoS ONE, 2010, Thurber, Andrew R.; Jones, William J.; Schnabel, Kareen. The dissertation author was the primary investigator and author of this paper.

VITA

2001 Bachelor of Science, Hawaii Pacific University
2005 Master of Science, Moss Landing Marine Laboratories - California State University, Stanislaus
2010 Doctor of Philosophy, University of California, San Diego

PUBLICATIONS

Kim S, Hammerstom KK, Conlan KE, Thurber AR, 2010. Polar ecosystem dynamics: Recovery of communities from organic enrichment in McMurdo Sound, Antarctica. Integrative and Comparative Biology. doi:10.1093/icb/icq058

Conlan KE, Kim SL, Thurber AR, Hendrycks E, 2010. Benthic changes at McMurdo Station, Antarctica following local sewage treatment and regional iceberg-mediated productivity decline. Marine Pollution Bulletin 60: 419- 432.

Levin LA, Mendoza G, Gonzalez J, McMillan P, Thurber AR, 2010. Diversity of bathyal macrobenthos on the northeastern Pacific margin: the influence of methane seeps and oxygen minimum zones. Marine Ecology 34: 94-110.

Thurber AR, Kröger K, Neira C, Wiklund H, Levin LA, 2010. Stable isotope signatures and methane use by New Zealand cold seep benthos. Marine Geology. 272:260-269.

Glover AG, Smith CR, Minks SL, Sumida PY, Thurber A, 2008. Temporal and spatial variability in macrofaunal abundance and community structure on the West Antarctic Peninsula continental shelf. Deep-Sea Research II 55:2491-2501.

Thurber AR, 2007. Diets of Antarctic sponges: links between the pelagic microbial loop and benthic metazoan food web. Marine Ecology Progress Series 351:77-89.

Kim SL, Thurber A, Hammerstrom K, Conlan K, 2007. Seastar response to organic enrichment in an oligotrophic polar habitat. Journal of Experimental Marine Biology and Ecology 346:66-75.

Kim SL and Thurber A, 2007, Comparison of seastar (Asteroidea) fauna across island groups of the Scotia Arc. Polar Biology 30:415-425.

Detrich HW, Jones CD, Kim S, North AW, Thurber A, Vacchi M, 2005. Nesting behavior of the icefish *Chaenocephalus aceratus* at Bouvetoya Island, Southern Ocean. Polar Biology 28:828-832.

ABSTRACT OF THE DISSERTATION

Mircrobe-Metazoan Interactions at Pacific Ocean Methane Seeps

by

Andrew Reichmann Thurber

Doctor of Philosophy in Oceanography

University of California, San Diego, 2010

Professor Lisa A. Levin, Chair

Methane seeps host a diversity of metazoans that co-occur with chemoautotrophic Bacteria and Archaea, providing a model system to study trophic microbe-metazoan interactions. The goal of this dissertation is to characterize and quantify the types of microbial production consumed by methane-seep fauna. Through combined laboratory and field studies from four methane seep locations (11 New Zealand sites; Eel River; Hydrate Ridge; and Costa

Rica's Mound 12), I found that aerobic methane-oxidizing bacteria and the syntrophic partnership which mediates the anaerobic oxidation of methane are consumed within metazoan food webs. In New Zealand, two communities were largely fueled by methane: (1) a sponge which provided a habitat and trophic conduit of methane-derived production to a diversity of fauna and (2) ampharetid polychaete beds. These ampharetid beds formed a distinct community which was fueled by aerobic methane-oxidizing bacteria, as shown through stable isotopic and fatty-acid analysis coupled to a mass-specific mixing model. The Dorvilleidae, a polychaete family which excels at inhabiting areas with high microbial production, provided a ideal taxa to study metazoan trophic linkages to Archaea. In the laboratory, I raised *Ophryotrocha labronica,* a dorvilleid, from egg to reproduction on monocultures of archaeal, bacterial and eukaryotic food sources. This demonstrated that all domains of life can support viable metazoan populations. In contrast to current biomarker paradigms, this species exhibited isotopic enrichment (not composition) which was food-source specific whereas fatty-acid signature was largely not; a finding that explained many of the patterns observed in the field studies. Although archaeal biomarkers were not transferred from diet to consumer, sulfate-reducing bacteria, a member of the assemblage responsible for the anaerobic oxidation of methane, provided a mechanism that identified archaeal aggregates as a food source for dorvilleids in both authigenic-carbonate and soft-sediment habitats. As a final example of microbial-metazoan interactions, during the formal description of a novel species of Yeti crab, I identified how this crab farms chemosynthetic-epibiotic bacteria by waving its bacteria-covered setae in methane-seep fluid. This research demonstrates the ubiquity of strong trophic links between chemoautotrophic microbes and heterotrophic metazoans while highlighting how these interactions vary among site and habitat at seeps.

CHAPTER 1.

INTRODUCTION

Background

Chemoautotrophic bacteria have been studied since 1897 (Pfeffer 1897), but it was not until hydrothermal vents (Lonsdale 1977) and later methane seeps (Paul et al. 1984) were discovered that the importance of this chemical fueled production for metazoan fauna was identified. Studies of symbiont-bearing taxa in chemosynthesis-based ecosystems have been paramount in identifying a key pathway by which microbial production supports metazoan fauna (Felbeck 1981; Cavanaugh et al. 1981; Childress et al. 1986). What has received less attention is the role of free-living Bacteria and Archaea in the nutrition of heterotrophic fauna. This understanding is necessary considering the ubiquity of non-symbiotic chemosynthetic production throughout the oceans (Wuchter et al. 2003). The diversity of microbial metabolisms represented in seep sediments populated by metazoans makes methane-seep ecosystems an ideal place to elucidate microbial heterotrophy. The goal of this dissertation is to characterize and quantify the types of microbial production consumed by methane-seep fauna.

Sedimented cold seeps, fueled by methane, are inhabited by bacteria and archaea that fix carbon through a diversity of chemoautotrophic processes. In anoxic sediment, the anaerobic oxidation of methane (AOM) is performed by a syntrophic partnership between methanotrophic archaea and sulfate-reducing bacteria that produces energy and hydrogen sulfide (Boetius et al. 2000; Orphan et al. 2001; 2002). Methane that is not consumed through anaerobic processes is respired aerobically by both free-living and symbiotic bacteria including α-, δ-, γ- proteobacteria, or it is released into the hydrosphere (Murase and Frenzel

2007; Ding and Valentine 2008). The sulfide produced by AOM is oxidized by bacteria. Each one of these processes, AOM, aerobic methanotrophy, sulfide oxidation and sulfate reduction, result in autotrophic carbon fixation and provide a potential food source for the metazoans that co-occur with these chemosynthetic Archaea and Bacteria at methane seeps (Levin and Michener 2002; MacAvoy et al. 2005).

Polychaetes in the family Dorvilleidae are one metazoan taxon that may consume these diverse forms of microbial production. In certain seep habitats (e.g. microbial mats) this family of polychaete makes up more than 80% of the infaunal community (Levin et al. 2003). A potential cause of dorvilleids dominance is their ability to handle high sulfide concentrations (Dahlgren et al. 2001); hydrogen sulfide can reach milli-molar concentrations within seep sediments where dorvilleids occur (Levin et al. 2003; 2006; Ziebis and Haese 2005). This sulfide tolerance would potentially allow them access to a diversity of chemosynthetic bacteria. Early observation of light $\delta^{13}C$ signatures indicated that this family might consume the microbial aggregates that perform AOM (Levin and Michener 2002). Yet neither methods nor conclusive evidence currently exist to identify AOM in the diet of any metazoan taxon, even dorvilleids.

The main technique that has been used to identify the consumption of chemosynthetic energy sources is stable isotopic analysis (Conway et al. 1994). Due to enzymatic preferential incorporation of carbon 12 over 13, both metabolic substrate and fixation pathways impart a unique although sometimes overlapping signature. When organic matter is consumed its signature is retained in consumer tissue with a small trophic enrichment of carbon 13, resulting in a biomarker that can resolve dietary sources. This technique has been successfully used to identify metazoan use of chemosynthetic production (e.g. Levin and Michener 2002; Eller et al. 2005; MacAvoy et al. 2005; Deines et al. 2007). Yet the relative importance of

specific metabolic substrates are difficult to resolve since in many cases an intermediate value can either be indicative of a mixed diet of two sources or a third source entirely. The other chemical species that may identify consumption of microbial biomass is nitrogen. Although the isotopic composition of nitrogen (the relative abundance of ^{15}N to ^{14}N) has traditionally been used to look at trophic position due to its approximate +3‰ enrichment with each trophic step (^{14}N is preferentially excreted by consumers), it also varies as a function of N_2 fixation and form of nitrogen assimilated. Species-specific, highly negative values are reported from both vents and seeps (Colaco et al. 2002; Van Dover 2002; Levin and Mendoza 2007). The source of these light $\delta^{15}N$ values is unknown.

Lipid signatures offer an alternative technique for elucidating food web linkages. Fatty acids (FAs) have characteristic branching and bonding patterns that loosely follow taxonomic lineages within producers (Figure 1.1; Table 1.1), and are either incorporated directly from a heterotroph's diet or synthesized along a known pathway. Importance of bacterial production or recycling has been demonstrated through the lipid signature within organisms (Kharlamenko et al. 2001; Howell et al. 2003; Hudson et al. 2004; Kiyashko et al. 2004; Thurber 2007). This technique has begun to be applied to cold seep ecosystems (MacAvoy et al. 2003; Van Gaever et al. 2009), and has demonstrated species- and location-specific use of differential sources of microbial production at hydrothermal vents (Pond et al. 1997; Rieley et al. 1999; Colaco et al. 2007). One use for lipid analysis that has not currently been evaluated is its ability to identify archaeal consumption. Archaea, rather than having membranes made up of carbon chains connected through ester linkages to glycerol molecules, are composed of repeating isoprene units connected to glycerol with ether bonds. These lipids are not only unique structurally, but in methanotrophic species also have very light $\delta^{13}C$ values, in many cases <-100‰ (Elvert and Suess 1999; Boetius et al. 2000; Hinrichs et al. 2000). It has yet to be demonstrated that (1) eukaryotes consume or assimilate Archaea or (2)

what lipid biomarkers can be used to identify archaeal biomass incorporation into eukaryotic tissues.

Problem

Although our understanding of microbial processes has increased exponentially in the last thirty years, the input of bacterial and archaeal biomass into metazoan food webs has not been quantified. This information represents a critical component of carbon sources, flow, and recycling within the marine ecosystem. Two challenges that currently limit this understanding are a lack of methods to (1) identify archaeal consumption by metazoans and (2) quantify microbial sources in food webs. Methane seeps provide an ideal system in which to study microbial roles in food webs due to an abundance of microbes with diverse metabolisms juxtaposed with heterotrophic metazoans. The goal of this dissertation is to answer the overarching question:

How is microbial production from different metabolic pathways incorporated and used in methane-seep metazoan food webs?

Overview and Approach

The overall goal of my dissertation is to identify and, when possible, quantify different types of microbial production in methane seep food webs using both laboratory experiments and field observations. In **Chapter 2**, I use a classical carbon-isotopic approach to identify the extent of methane-derived carbon that fuels both symbiont-bearing and heterotrophic fauna at methane-seep sites from New Zealand. As the first description of the trophic pathways in this novel location, this chapter highlights both the power and limitations of isotopic mixing models in identifying the role of chemoautotrophic production in food webs. I build upon these findings in **Chapter 3** by identifying ampharetid beds as a unique

community within New Zealand methane seeps, characterized by high density and biomass. I provide a conservative estimate of the amount of methanotrophic biomass that this community consumes. This chapter combines fatty acid data, biomass, and species-specific isotopic mixing models to identify aerobic methanotrophy as the chemosynthetic energy source for the most dense seep community currently known.

The next two chapters of my dissertation address the role of Archaea in metazoan food webs. **Chapters 4** identifies the influence of diet (bacteria, archaea, spinach, rice) on stable isotope trophic shifts and fatty acid representation in dorvilleid polychaetes via a laboratory experiment, information needed to interpret stable isotopic and FA data from the field. The results show that $\delta^{15}N$ is not uniformly enriched compared to a species food source, in contrast to the literature, and that $\delta^{13}C$ results in food-specific enrichment instead of food specific composition. In addition, species fed a diet of archaea did not have a unique FA signature. This highlights the challenges associated with applying both stable isotopic and fatty acid analysis to infaunal food webs. The results of the laboratory-based study are further discussed in **Chapter 5,** which examines dorvilleid species from three methane seep locations in addition to those fed a diet of archaea in the lab. After discovering that neutral lipids do not provide insight into the diet of dorvilleids, I track sulfate-reducing bacterial carbon, which belongs to the syntrophic partners of archaea that perform AOM, into the diet of dorvilleids. This provides the first direct evidence of archaea being consumed by metazoa.

No discussion of the interaction between microbes and metazoans at seeps would be complete without discussion of symbiont-bearing metazoans. In **Chapter 6**, I provide a formal description of the second species of "Yeti Crab," discovered on the Costa Rica margin during my exploration of Pacific seeps, and I identify a novel form of symbiosis involving epibiotic bacteria on the crabs pereopods. This species harvests a group of chemosynthetic bacteria

belonging to the γ– and ε- proteobacteria by waving these epibiotic bacteria in fluid being released from methane seeps. These bacteria are closely related to hydrothermal-vent decapod epibionts. Divergent host and bacterial phylogenies suggest that this group of bacteria has either separately colonized the two yeti crab taxa from across the ocean or its identity is selected for by local environmental conditions from a pan-oceanic pool of reducing-habitat, decapod-specific symbionts.

Together in these chapters I use a variety of techniques, habitats, fauna, and locations from around the Pacific to add to our understanding of energy flow and trophic interactions at deep-sea methane seeps.

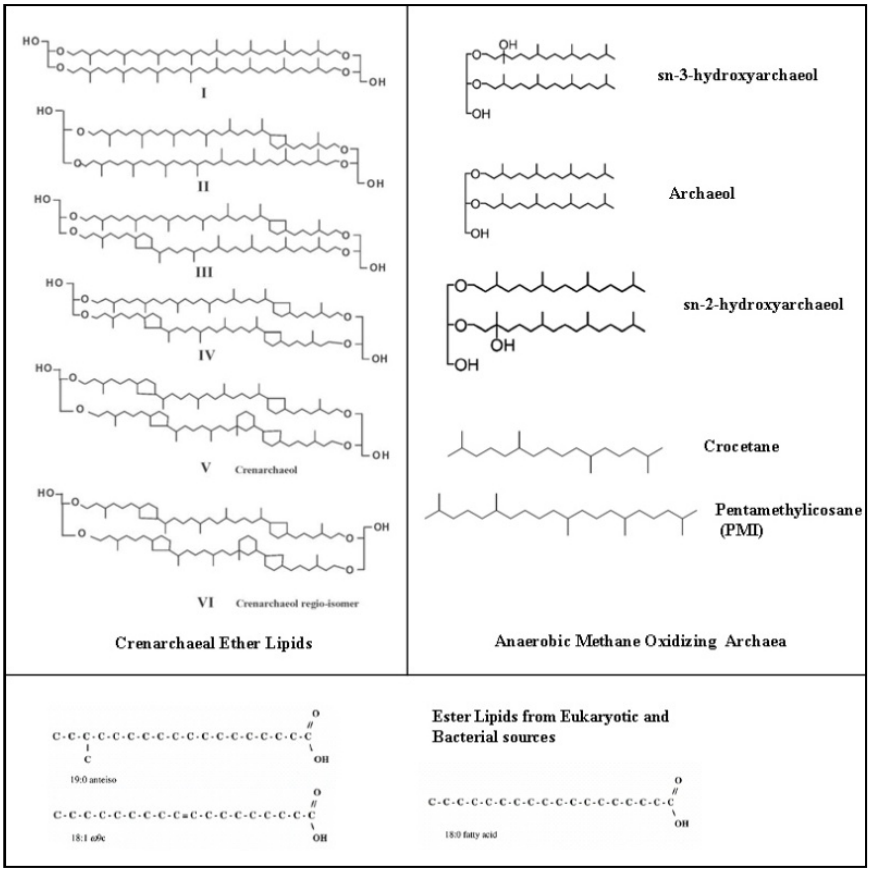

Figure 1.1 Examples of lipids diagnostic for Crenarchaea or anaerobic methane oxidizing Euryarchaea and ester lipids diagnostic for eukaryotic and bacterial sources. Crenarchaeal lipids modified from Wutcher et al. (2003).

Table 1.1 Characteristic lipid biomarkers for microbes with chemoautotrophic pathways. * indicates diagnostic.

Metabolic source	Taxon	Biomarker	Reference
Aerobic Methane Oxidation	Methanotrophic bacteria (Type I)	16:1(n-8)*; 16:1(n-6)*	Bowman et al.(1991)
Ammonia Oxidation	Crenarchaea	Crenarchaeol* GDGTs	Wutcher et al. (2003)
Anaerobic Methane Oxidation	Euryarchaea	Archaeol; Pentamethylicosane (PMI); *sn*-2-hydroxyarchaeol*; *sn*-3-hydroxyyarchaeol*;	Sprott et al. (1990); Hinrichs et al. (2000); Werne et al. (2002); Pancoast et al. (2000)
	ANME-2	Crocetane; Crocetenes; High ratio of *sn*-2- hydroxyarchaeol:archaeol	Blumberg et al. (2004)
	ANME-1	Glygerol dialkyl glycerol tetraethers (GDGTs)	Blumberg et al. (2004)
Photosynthesis	Eukaryotic phytoplankton	Poly Unsaturated Fatty Acids; 20:5(n-3); 22:6(n-3)	Dalsgaard et al. (2003)
Sulfate Reduction	*Desulfosarcina/ Desulfococcus* group	16:1(n-5); cy17:0 (5,6)*	Elvert et al. (2003)
	ANME–1 Mat	16:1(n-7); 16:1(n-5); cyc17:0(5,6)	Blumberg et al. (2004)
	ANME-2 Mat	ai-C15:0; 18:1(n-7)	Blumberg et al. (2004)
	Desulfovibrio	i17:1(n-7); i15:1(n-7); i19:1(n-7)	Nichols et al. (1986)
	Desulfobacter	10Me16:0; cy18:0	Boon et al. (1977)
Sulfide Oxidation	*Thioploca*	Very abundant 16:1(n-7) and 18:1(n-7)	McCaffrey et al. (1989)

References

Blumenberg M, Seifert R, Reitner J, Pape T, Michaelis W (2004) Membrane lipid patterns typify distinct anaerobic methanotrophic consortia. Proc Nat Acad Sci 30:11111-11116

Boetius A, Rabenschlag K, Schubert CJ , Richert D, Widdle F, Gieske A, Amann R, Jorgensen BB, Witte U, Pfannkuche O (2000) A marine microbial consortium apparently mediating anaerobic oxidation of methane. Nature 407:623-626

Boon JJ, de Leeuw JW, van der Hoek GJ, Vosjan JH (1977) Fatty acids and branched b-hydroxy acids in *Desulfovibrio desulfuricans*. J Bacteriol 129:1183–1191

Bowman JP, Skerratt JH, Nichols PD, Sly LI (1991) Phospholipid fatty acid and lipopolysaccharide fatty acid signature lipids in methane-utilizing bacteria. FEMS Microbiol Ecol 85:15– 22

Cavanaugh CM, Gardiner SL, Jones ML, Jannasch HW, Waterbury JB (1981) Prokaryotic cells in the hydrothermal vent tube worm *Riftia pachyptila* Jones: Possible chemoautotrophic symbionts. Science 213:340-342

Childress JJ, Fisher CR, Brooks JM, Kennicutt MC, Bidigare R, Anderson AE (1986) A methanotrophic marine molluscan (Bivalvia, Mytilidae) Symbiosis: Mussels fueled by Gas. Science 233:1306-1308

Colaco A, Dehairs F, Desbruyeres D (2002) Nutritional relations of deep-sea hydrothermal fields at the Mid-Atlantic Ridge: a stable isotope approach. Deep-Sea Res. 49:395-412

Colaco A, Desbruyeres D, Guezennec J (2007) Polar lipid fatty acids as indicators of trophic associations in a deep-sea vent system community. Mar Ecol 28:15-24

Conway NM, Kennnicult II MC, Van Dover CL (1994) Stable isotopes in the study of marine chemosynthetic-based ecosystems. In: Lajtha K, Michener HR (eds) Stable Isotopes in Ecology and Environmental Science, Blackwell, Oxford, pp. 158–186

Dahlgren TG, Akesson B, Schander C, Halanych KM, Sundsberg P (2001) Molecular phylogeny of the model annelid *Ophryotrocha*. Biol. Bull. 201:193-203

Dalsgaard J, St John M, Kattner G, Müller-Navarra D, Hagen W (2003) Fatty acid trophic markers in the pelagic marine environment. Adv Mar Biol 46:225–340

Deines P, Grey J, Richnow HH, Eller G (2007) Linking larval chironomids to methane: seasonal variation of the microbial methane cycle and chironomid delta C-13. Aquat Microbial Ecol 46:273-282

Ding H and Valentine DL (2008) Methanotrophic bacteria occupy benthic microbial mats in shallow marine hydrocarbon seeps, Coal Oil Point, California. J Geo Res 113:1-11 doi: 10.1029/2007JG000537

Eller G, Deines P, Grey J, Richnow HH, Kruger M (2005) Methane cycling in lake sediments and its influence on chironomid larval $\delta^{13}C$. FEMS Microbiol Ecol 54:339-350

Elvert M, Suess E (1999) Anaerobic methane oxidation associated with marine gas hydrates: superlight c-isotopes from saturated and unsaturated C20 and C25 irregular isoprenoids. Naturwissenchaften 86:295-300

Elvert M, Boetius A, Knittel K, Jorgensen BB (2003) Characterization of specific membrane fatty acids as chemotaxonomic markers for sulfate-reducing bacteria involved in anaerobic oxidation of methane. Geomocrbiol J 20:403-419

Felbeck H. (1981) Chemoautotrophic potential of the hydrothermal vent tube worm, *Riftia pachyptila* Jones (Vestimentifera). Science 213:336-338

Hinrichs KU, Summons RE, Orphan V, Sylva SP, Hayes JM (2000) Molecular and isotopic analysis of anaerobic methane-oxidizing communities in marine sediments. Org Geochem 31: 1685–1701

Howell KL, Pond DW, Billett DSM, Tyler PA (2003) Feeding ecology of deep-sea seastars (Echinodermata: Asteroidea): a fatty-acid biomarker approach. Mar Ecol Prog Ser 225:193-206

Hudson IR, Pond DW, Billett DSM, Tyler PA, Lampitt RS, Wolff GA (2004) Temporal variations in fatty acid composition of deep-sea holothuruans: evidence of bentho-pelagic coupling. Mar Ecol Prog Ser 281:109-120

Kharlamenko VI, Kiyashko SI, Imbs AB, Vyshkvartzev DI (2001) Identification of food sources of invertebrates from the seagrass *Zostera marina* community using carbon and sulfur stable isotope ratio and fatty acid analyses. Mar Ecol Prog Ser 220:103-117Kiyashko et al. 2004

Kiyashko SI, Imbs AB, Narita T, Scetashev Vi, Wada E (2004) Fatty acid composition of aquatic insect larvae *Stictochironomus pictulus* (Diptera: Chironomidae): evidence of feeding upon methanotrophic bacteria. Comp Biochem Physiol B 139:705-711

Levin LA, Mendoza GF (2007) Community structure and nutrition of deep methane-seep macrobenthos from the North Pacific (Aleutian) Margin and the Gulf of Mexico (Florida Escarpment). Mar Ecol 28:131-151

Levin LA, Michener R (2002) Isotopic evidence of chemosynthesis-based nutrition of macrobenthos: the lightness of being at Pacific methane seeps. Limnol Oceanog 47:1336–1345

Levin LA, Ziebis W, Mendoza G, Growney V, Tryon M, Brown K, Mahn C, Gieskes J, Rathburn A (2003) Spatial heterogeneity of macrofauna at northern California methane seeps: the influence of sulfide concentration and fluid flow. Mar Ecol Prog Ser 265:123–139

Levin LA, Ziebis W, Mendoza GF, Growney-Cannon V, Walther S (2006) Recruitment response of methane-seep macrofauna to sulfide-rich sediments: an in situ experiment. J Exp Mar Biol Ecol 330:132-150

Lonsdale P (1977) Clustering of suspension-feeding macrobenthos near abyssal hydrothermal vents at oceanic spreading centers. Deep-Sea Res 24:857-863

MacAvoy SE, Macko SA, Carney RS (2003) Links between chemosynthetic production and mobile predators on the Louisiana continental slope: stable carbon isotopes of specific fatty acids. Chem Geol 201:229-237

MacAvoy SE, Fisher CR, Carney RS, Macko SA (2005) Nutritional associations among fauna at hydrocarbon seep communities in the Gulf of Mexico. Mar Ecol Prog Ser 292:51-60

McCaffrey MA, Farrington JW, Repeta DJ (1989) Geochemical implications of the lipid composition of *Thioploca spp*. from the Peru upwelling region – 15^{o}S. Org Geochem 14:61–68

Murase J, Frenzel P (2007) A methane-driven microbial food web in a wetland rice soil. Environ Microbiol 9:3025-3034

Nichols PD, Guckert JB, White DC (1986) Determination of monounsaturated fatty acid double-bond position and geometry for microbial monocultures and complex consortia by capillary GC-MS of their dimethyl disulphide adducts. J Microbiol Meth 5:49–55

Orphan VJ, House CH, Hinrichs KU, Mckeegan KD, Delong EF (2001) Methane-consuming archaea revealed by directly coupled isotopic and phylogenetic analysis. Science 293:484–487

Orphan VJ, House CH, Hinrichs KU, McKeegan KD, DeLong EF (2002) Multiple archaeal groups mediate methane oxidation in anoxic cold seep sediments. Proc Nat Acad Sci USA 99**:**7663–7668

Pancost, RD, Sinninghe Damste JS, De Lint S, Van Der Maarel MJEC, Gottschal JC, Medinaut Shipboard Scientific Party (2000) Biomarker evidence for widespread anaerobic methane oxidation in Mediterranean sediments by a consortium of methanogenic archaea and bacteria. Appl Environ Microbiol 66:1126–1132

Paul CK, Hecker B, Commeau R, Freeman-Lynde RP, Neumann C, Corso WP, Golubic S, Hook JE, Sikes E, Curray J (1984) Biological communities at the Florida escarpment resemble hydrothermal vent taxa. Science 226:965-967

Pfeffer, W (1897) Planzenphysiology. Engelmann, Leipzig. Vol. 1.

Pond DW, Segonzac M, Bell MV, Dixon DR, Fallick AE, Sargent JR (1997) Lipid and lipid carbon stable isotope composition of the hydrothermal vent shrimp *Mirocaris fortunata*: evidence for nutritional dependence on photosynthetically fixed carbon. Mar Ecol Prog Ser 157:221–231van

Rieley G, Van Dover CL, Hedrick DB, Eglinton G (1999) Trophic ecology of *Rimicaris exoculata*: combined lipid abundance/stable isotope approach. Mar Biol 133:495–499

Sprott GD, Ekiel I, Dicaire C (1990) Novel, Acid-labile, Hydroydiether lipid cores in methanogenic bacteria. J Biological Chem 23:13735-13740

Thurber AR (2007) Diets of Antarctic sponges: links between the pelagic microbial loop and benthic metazoan food web. Mar Ecol Prog Ser 351:77-89

Van Dover CL (2002) Trophic relationships among invertebrates of the Kairei hydrothermal vent field (Central Indian Ridge). Mar Biol 141:761-772

Van Gaever S, Moodley L, Pasotti F, Houtekamer M, Middelburg JJ, Danovaro R, Vanrousel A (2009) Trophic specialization of metazoan meiofauna at the Håkon Mosby Mud Volcano: fatty acid biomarker isotope evidence. Mar Biol 156: 1289-1296

Werne JP, Baas M, Sinninghe Damste JS (2002) Molecular isotopic tracing of carbon flow and trophic relationships in a methane-supported benthic microbial community. Limnol Oceanogr 47:1694-1701

Wuchter C, Schouten S, Boshker HTS, Sinninghe Damste JS (2003) Bicarbonate uptake by marine Crenarchaeota. FEMS Microbiol Lett 219:203-20

Ziebis W, Haese RR (2005) Interactions between fluid flow, geochemistry, and biogeochemical processes at methane seeps. In: Kristensen E, Haese RR, Jostka JE (eds) Interactions between macro- and microorganisms in marine sediments. Coastal and Estuarine studies 60. American Geophysical Union, Washington. p267-298

CHAPTER 2.

Contents lists available at ScienceDirect

Marine Geology

journal homepage: www.elsevier.com/locate/margeo

Stable isotope signatures and methane use by New Zealand cold seep benthos

Andrew R. Thurber [a,*], Kerstin Kröger [b,1], Carlos Neira [a], Helena Wiklund [c], Lisa A. Levin [a]

[a] Integrative Oceanography Division, Scripps Institution of Oceanography, La Jolla, CA, 92093-0218 USA
[b] National Institute of Water and Atmospheric Research, Private Bag 14-901, Wellington, New Zealand
[c] Department of Zoology, University of Gothenburg, PO Box 463, SE-405 30 Göteborg, Sweden

ARTICLE INFO

Article history:
Received 22 July 2008
Received in revised form 19 May 2009
Accepted 1 June 2009
Available online 11 June 2009

Keywords:
macrobenthos
methane-derived carbon
methane seep
methanotrophy
Pogonophora
ecosystem engineer

ABSTRACT

The carbon isotopic composition of seep faunal tissue represents a time-integrated view of the interaction between biology and the biogeochemical gradients within the environment. Here we provide an initial description of carbon and nitrogen stable isotope signatures of dominant symbiont-bearing megafauna and heterotrophic mega- and macrofauna from 10 methane-seep sites on the continental margin of the North Island of New Zealand (662–1201 m water depth). Isotopic signatures suggest that sulfide oxidation supports symbiont-bearing taxa including solemyid and vesicomyid bivalves, and methanotrophic symbionts are present in the seep mussel *Bathymodiolus* sp. Multiple species of Frenulata (Siboglinidae) are present and have a range of isotopic values that are indicative of both thiotroph- and methanotroph-based nutrition. Isotopic composition of the tubeworm *Lamellibrachia* sp. varied by 23.3‰ among individuals although there was no consistent difference among sites. Variation in methane use by heterotrophic fauna appears to reflect the availability of hard vs. soft substrate; macrofauna on hard substrates had high $\delta^{13}C$ signatures, reflecting consumption of photosynthetic-derived organic matter. Two unique, biotic assemblages were discovered to be fueled largely by methane: a hard-substrate, multi-phyla sponge-associated community (inhabiting the sponge *Pseudosuberites* sp.) and a soft-sediment assemblage dominated by ampharetid polychaetes. Isotope signatures yield estimates of 38–100% and 6–100% methane-derived carbon in sponge associates and ampharetid-bed macrofauna, respectively. These estimates are comparable to those made for deeper methane seeps at the Florida Escarpment (3290 m) and Kodiak, Alaska seeps (4445 m). The overall high use of methane as a carbon source by both symbiont-bearing and heterotrophic fauna suggests that New Zealand methane seeps are an ideal model system to study the interaction among metazoans, bacteria, archaea, and their resulting effect on methane cycles.

1. Introduction

Methane seeps are increasingly recognized as a patchy (Luff et al., 2004; Robinson et al., 2004) but widespread feature of the world's continental margins in both the past (Campbell, 2006) and present (Sibuet and Olu, 1998). The use of methane as a carbon source is one of the many unusual features that distinguishes methane-seep fauna from those in other systems. Methane use was first documented for bathymodiolin mussels harboring methanotrophic symbionts in the Gulf of Mexico (Childress et al., 1986). More recently, widespread incorporation of methane-derived carbon (MDC) has been documented for heterotrophic seep invertebrates (e.g., Levin and Michener, 2002; Gebruk et al., 2003; Levin and Mendoza, 2007) and for the surrounding non-seep fauna (MacAvoy et al., 2002, 2003, 2008). Methane-derived carbon may be obtained by seep metazoans in several ways. They can consume chemoautotrophic archaea (anaerobic methane oxidizers; Valentine, 2002), and aerobic methane-oxidizing bacteria (Ding and Valentine, 2008), as well as from sulfide-oxidizing or sulfate-reducing bacteria which can take up methane-derived carbon after it passes into the dissolved inorganic carbon (DIC) pool (Wegener et al., 2008).

Stable isotope signatures provide valuable insight into nutritional sources of seep fauna (Van Dover, 2007). Biogenic methane is isotopically depleted in ^{13}C (usually $\delta^{13}C$ of −50 to −110‰) thus it serves as its own biomarker (Whiticar, 1999). Carbon fixation by other metabolic processes, such as phytoplankton photosynthesis or autotrophy coupled to sulfide oxidation, also results in distinctive $\delta^{13}C$ signatures. $\delta^{15}N$ signatures provide information about local N fixation (often associated with symbiosis) or trophic level in heterotrophs. When novel seep communities are discovered, an initial characterization of trophic structure and key nutritional sources can be obtained from a survey of stable isotope signatures.

During late 2006 and early 2007, the eastern continental margin of New Zealand was intensively surveyed for the presence of methane seeps using a towed camera and acoustic tools to record methane bubble plumes and map the extent of seep-related seabed structures (Baco

* Corresponding author. Tel.: +1 858 534 3579; fax: +1 858 822 0562.
E-mail addresses: athurber@ucsd.edu (A.R. Thurber), kerstin.kroeger@imr.no (K. Kröger), cneira@coast.ucsd.edu (C. Neira), helena.wiklund@zool.gu.se (H. Wiklund), llevin@ucsd.edu (L.A. Levin).
[1] Present Address: Institute of Marine Research, Sykehusveien 23, P-O-Box 6404, N-9294 Tromsø, Norway.

et al., 2010-this issue; Greinert et al., this issue; Jones et al., 2010-this issue; Klaucke et al., 2010-this issue). Here we discuss the isotopic signatures of invertebrate assemblages found at 10 seep sites located at bathyal depths of 662 to 1200 m. The sites are described in more detail in Greinert et al. (2009-this issue) and the general geology in Barnes et al. (2010-this issue). The symbiont-bearing seep megafauna present included siboglinid polychaetes, specifically the vestimentiferan, *Lamellibrachia* sp., and members of the Frenulata (previously known as pogonophorans; Southward et al., 2005), bathymodiolin mussels (*Bathymodiolus* sp.), vesicomyid (*Calyptogena* spp.) and solemyid clams (Baco et al., 2010-this issue). Ampharetid polychaetes formed dense beds in sulfidic sediments (Sommer et al., 2008, 2009-this issue) and small frenulates (*Siboglinum* spp.) formed beds in sediments at the periphery of seep sites. Many of the sites had widespread, blocky carbonates, some covered with sponges (*Pseudosuberites* sp. undescribed, Class Demospongiae: Order Hadromerida: Family Suberitidae) or multiple species of deep-water coral (Baco et al., 2010-this issue). Sled, grab and multicore samples yielded many other invertebrate taxa which are being described elsewhere (e.g. Baco et al., 2010-this issue; Campbell et al., 2010-this issue).

Here we describe carbon and nitrogen stable isotope signatures of dominant mega- and macrofauna at methane seeps on the New Zealand continental margin. We focus on site-specific variability and address the following questions for the New Zealand seep fauna:

(1) What nutritional pathways are likely among the symbiont-bearing megafauna?
(2) What are the nutritional sources of heterotrophic macrobenthos and megabenthos and how variable are they within a seep patch and among seep sites?
(3) Which assemblages and taxa exhibit high concentrations of methane-derived C in their tissues?

Table 1
Sampling sites, dates, depths, and gear used for faunal collection.

Region	Site	Station	Date (mm/dd/yr)	Gear	Depth (m)	Latitude (S)	Longitude (E)
Builder's Pencil		21	11/5/06	Epibenthic sled	812	39°32.62′	178°19.72′
		34	11/6/06	Grab	802	39°32.62′	178°20.01′
		36	11/6/06	Multicorer	794	39°32.62′	178°20.01′
		38	11/6/06	Epibenthic sled	815	39°32.65′	178°19.62′
		32	11/6/06	Epibenthic sled	817	39°32.68′	178°19.70′
		18	11/5/06	Epibenthic sled	780	39°32.83′	178°19.95′
		23	11/5/06	Grab	787	39°32.84	178°19.94′
		30	11/6/06	Epibenthic sled	790	39°33.01′	178°19.91′
		22	11/5/06	Grab	787	39°32.79′	178°19.97′
LM-3		238	3/6/07	TV-Grab	908	39°58.62′	178°14.16′
		216	3/4/07	TV-MUC	662	40°01.52′	178°09.65′
Rock Garden	Knoll	10	11/4/06	Epibenthic sled	760	40°02.22′	178°38.86′
		6	11/4/06	Epibenthic sled	730	40°02.31′	178°08.58′
		11	11/4/06	Grab	752	40°02.38′	178°08.59′
		7	11/4/06	Epibenthic sled	766	40°02.42′	178°09.00′
		12	11/4/06	Epibenthic sled	749	40°02.65′	178°08.91′
Omakere Ridge	LM-9	45	11/7/06	Epibenthic sled	1150	40°00.52′	177°51.38′
		50	11/8/06	Epibenthic sled	1140	40°00.93′	177°51.56′
		57	11/8/06	Multicorer	1143	40°01.04′	177°51.72′
		46	11/7/06	Multicorer	1145	40°01.08′	177°51.59′
		49	11/7/06	Multicorer	1140	40°01.09′	177°51.58′
		58	11/8/06	Grab	1144	40°01.09′	177°51.63′
		59	11/8/06	Grab	1144	40°01.10′	177°51.63′
		60	11/8/06	Grab	1145	40°01.13′	177°51.73′
		61	11/8/06	Grab	1144	40°01.15′	177°51.62′
		164	2/22/07	TV-Grab	1110	40°03.20′	177°49.11′
		174	2/23/07	TV-Grab	1104	40°03.19′	177°49.30′
	Kaka	261	3/9/07	TV-MUC	1165	40°02.12′	177°48.93′
		232	3/6/07	TV-MUC	1169	40°02.15′	177°48.96′
		242	3/7/07	TV-MUC	1172	40°02.15′	177°47.95′
	Bear's Paw	197	3/3/07	TV-MUC	1100	40°03.17′	177°49.17′
		198	3/3/07	TV-MUC	803	40°03.17′	177°49.16′
		186	2/28/07	TV-MUC	1201	40°03.14′	177°49.24′
Uruti Ridge	East	70	11/10/06	Epibenthic sled	720	41°17.18′	176°35.49′
	LM-10	68	11/10/06	Epibenthic sled	716	41°17.49′	176°33.12′
	Hihi	67	11/10/06	Epibenthic sled	740	41°17.65′	176°33.66′
Opouawe Bank	North Tower	122	11/18/06	Epibenthic sled	1040	41°46.77′	175°24.05′
		79	11/13/06	Epibenthic sled	1045	41°46.83′	175°24.25′
		290	3/12/07	TV-MUC	1061	41°46.98′	175°24.27′
		298	3/14/07	Bigo	1059	41°46.95′	175°24.18′
		112/113	11/17/06	Multicorer	1036	41°46.90′	175°24.08′
		277	3/11/07	ELUFO 6	1048	41°46.90′	175°24.11′
		86	11/13/06	Multicorer	1050	41°46.92′	175°24.12′
		84	11/13/06	Multicorer	1053	41°46.99′	175°24.04′
		83	11/13/06	Epibenthic sled	1040	41°46.88′	175°24.14′
	South Tower	81	11/13/06	Epibenthic sled	1050	41°47.27′	175°24.53′
		116	11/18/06	Multicorer	1049	41°47.31′	175°24.45′
		118	11/18/06	Multicorer	1051	41°47.36′	175°24.43′
		82	11/13/06	Multicorer	1059	41°47.37′	175°24.26′
		123	11/18/06	Multicorer	1051	41°47.40′	175°24.45′
	Takahe	309	3/16/07	TV-MUC	1056	41°46.34′	175°24.68′

Latitude and longitude are given for the end of epibenthic sled deployments.

2. Regional settings

The Hikurangi margin is the southern extent of the Tonga–Kermadec–Hikurangi subduction zone where the thick, sediment-rich Hikurangi Plateau region of the Pacific plate is being subducted under the Indo-Australian plate (Lewis and Pettinga, 1993). The region is dominated by a wide (maximum of 80 km) and thick (maximum of 7 km) accretionary prism of sediment (Lewis and Pettinga, 1993), with the sites discussed here occurring on the ridge crests of thrust faults (Barnes et al., 2010-this issue). The geologic underpinnings of our sample locations are discussed in detail in Barnes et al. (2010-this issue).

3. Materials and methods

Sampling took place aboard the *RV TANGAROA* (Cruise – TAN0616) from 5 November to 18 November 2006 and aboard the *RV SONNE* (Cruise – SO191) from 22 February to 14 March 2007. Collection gear included an epibenthic sled (25 mm stretched mesh diameter), vanVeen grab (surface area 0.2 m^2 and 90l volume) and multicore (9.6 cm internal diameter tubes) on TAN0616 and a video-guided multicorer (10.0 cm internal diameter tubes), TV-guided hydraulic grab (1.8 m^2 opening), and benthic landers (sediment opportunistically collected from the chambers) on SO191. A total of 51 stations at 10 seep sites spread over 5 regions were sampled on the 2 cruises within a depth range of 662 to 1201 m (Table 1, Fig. 1). During the SO191 we focused on several faunal associations in particular: ampharetid beds and commensals from sponges as they occurred at locations of seepage. Plankton was collected on either a 63 μm or 150 μm sieve from the ship's unfiltered flow-through seawater supply to constrain the planktonic isotopic signature for the region.

3.1. Stable isotope analyses

Symbiont-bearing megafauna, heterotrophic invertebrates, and filamentous bacteria were collected by hand picking them from dredged material, or by sieving sediment samples through 0.3 mm mesh and sorting the retained material live under a dissecting microscope. Specimens were identified to family level (lower if possible) and allowed to clear gut contents overnight in filtered seawater, washed in milli-Q water and placed in pre-weighed tin boats or combusted vials (500 °C for 4 hours) and frozen at either −20 or −70 °C. In the laboratory, specimens were oven dried (60 °C), weighed and acidified with 1% $PtCl_2$ to remove inorganic C. Stable isotope measurements ($\delta^{13}C$, $\delta^{15}N$) were made on 0.2–1.0 mg of dry weight, usually from single individuals. Samples were analyzed either on a Eurovector elemental analyzer interfaced with a continuous flow Micromass Isoprime isotope ratio mass spectrometer at Washington State University or with a Thermo Finnigan Delta XP Plus with a Costech 4010 Elemental Analyzer at the Scripps Institution of Oceanography analytical facility.

Isotope ratios are expressed as $\delta^{13}C$ or $\delta^{15}N$ in units of per mil (‰). Standards were Pee Dee Belemnite for $\delta^{13}C$ and nitrogen gas for $\delta^{15}N$ (atmospheric). Estimates of the percentage of methane-derived carbon in the macrofaunal carbon pool of each region and habitat were generated using a 2-source, single isotope mixing model as in Fry and Sherr (1984). The formula used is

$$F_m = \left(\delta_t - \delta_{POC/SOB}\right) / \left(\delta_m / \delta_{POC}\right) \quad (1)$$

where F_m is the fraction of methane-derived carbon, δ_t, $\delta_{POC/SOB}$, and δ_m refer to the $\delta^{13}C$ signatures of sample tissue, particulate organic

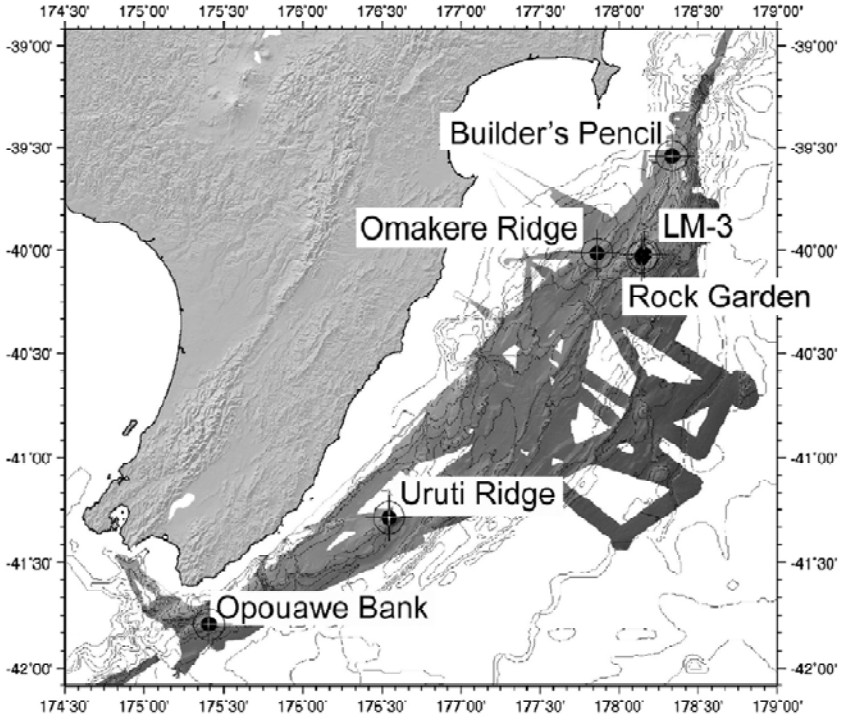

Fig. 1. Methane-seep regions sampled for symbiont-bearing megafauna and heterotrophic macrofauna. Omakere Ridge includes LM-9, Kaka, and Bear's Paw. Opouawe Bank includes North Tower, South Tower, and Takahe. For site maps see Greinert et al. (2009-this issue).

Table 2
Stable isotopic composition of known symbiont-bearing taxa at New Zealand methane seeps.

Taxa	Site	*n*	$\delta^{13}C$		$\delta^{15}N$		$\delta^{13}C$		$\delta^{15}N$	
			Mean	SE	Mean	SE	Min	Max	Min	Max
Mollusc										
Bathymodiolus	LM-3	5	−63.0	1.2	1.1	0.3	−65.8	−60.0	−0.1	2.5
Calyptogena	Builder's Pencil	1	−36.3		2.8					
	LM-9	2	−35.6		0.3		−36.5	−34.7	−0.8	1.3
Solemyidae	Takahe	1	−32.3		4.4					
	LM-9	3	−31.5	0.8	−0.1	0.6	−33.0	−30.2	−1.4	0.6
	North Tower	1	−30.7		−0.7					
Siboglinid polychaetes										
Lamellibrachia sp.	Builder's Pencil	11	−35.9	1.6	4.0	0.4	−43.1	−26.2	0.6	6.7
	LM-3	3	−28.5	2.9	2.2	0.8	−34.4	−22.5	0.8	4.7
	North Tower	4	−28.0	2.9	4.9	0.6	−33.4	−19.8	3.8	6.4
Frenulata	Bear's Paw	4	−43.7	2.0	2.6	1.5	−48.9	−40.1	−0.2	6.6
	Builder's Pencil	2	−66.6		5.6		−72.9	−60.3	5.4	5.8
	LM-9	13	−40.2	2.9	2.4	1.3	−51.8	−18.5	−4.4	14.8
	Takahe	3	−36.4	4.1	7.3	0.5	−44.6	−31.7	6.3	8.2
	Uruti Ridge	2	−43.1		6.0		−50.0	−36.3	1.1	10.9
	North Tower	4	−36.1	1.1	−4.4	1.5	−38.6	−33.5	−7.0	0.1

carbon or sulfide-oxidizing bacteria (POC/SOB) and methane, respectively. The $\delta^{13}C$ of either plankton or sulfide-oxidizing bacteria and the extremes in methane isotopic concentrations were used for $\delta_{POC/SOB}$ and δ_m, respectively, to make a robust, albeit wide ranging, estimate of MDC (see Levin and Michener, 2002 and the results for further explanation.) The $\delta^{13}C$ of methane varies both spatially and temporally (Ziebis and Haese, 2005), therefore extreme values of methane were used. This fine scale variability means measured end points, whether site-specific or not, may or may not reflect the $\delta^{13}C$ value of source methane in contact with the bacteria or archaea fixing carbon. In this instance, use of extremes reflects a realized range rather than a finite estimate based on estimated means. No trophic shift was included as this is negligible (<1‰ per trophic level) for $\delta^{13}C$ and end points for the model were chosen as the maximum values for filamentous free-living microbial sulfide oxidizers, as the isotopic concentration of non-filamentous, sulfide-oxidizing bacteria was not possible to constrain for this system.

3.2. Statistical analyses

Means were calculated for raw isotope data within each site, not pre-averaged within species. Values are given as mean ± 1 standard error unless indicated otherwise. When sampling with an epibenthic sled, species cannot be treated as spatial replicates, as pre-averaging within species would imply. Global comparisons were completed with data averaged by species within a site, to be consistent with the literature. The $\delta^{13}C$ values of *Lamellibrachia* sp. vestimentum and trophosome were compared with a paired *t*-test to determine if the two tissues yield the same isotopic composition. Isotopic values of *Lamellibrachia* sp. were compared among sites using a one-way analysis of variance (ANOVA) using the means of all tissues sampled from within an individual. To elucidate sampling biases inherent to the gear used, the mean isotopic composition of sampling gear was compared with a one-way ANOVA with Tukey post-hoc test. All data met the underlying assumptions of the statistics employed without transformation.

4. Results

Possible invertebrate food sources exhibited a broad range of $\delta^{13}C$ and $\delta^{15}N$ values. The mean $\delta^{13}C$ value of surface water plankton was −22.2 ± 0.5‰ and the $\delta^{15}N$ value was 4.5 ± 0.5‰. The $\delta^{13}C$ of

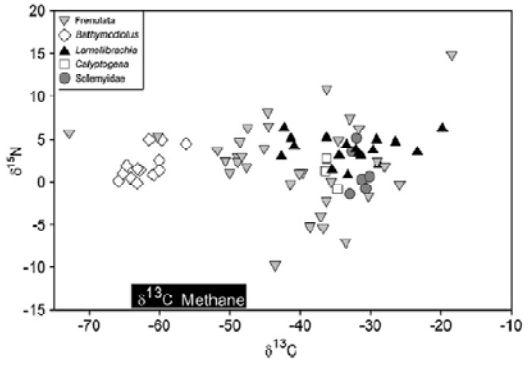

Fig. 2. Stable isotopic composition of symbiont-bearing invertebrate fauna from New Zealand methane seeps. Range of methane isotopic concentration is from Sommer et al. (2009-this issue).

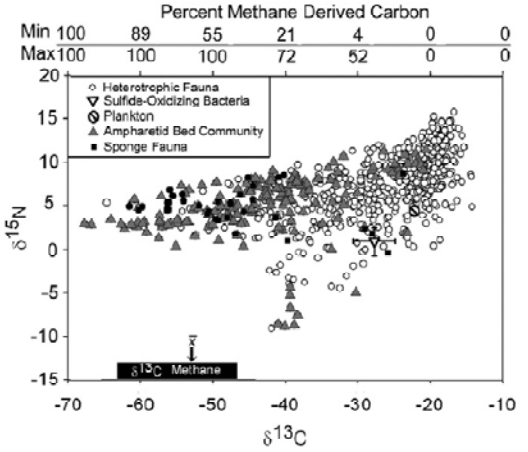

Fig. 3. Stable isotopic composition of heterotrophic invertebrate fauna, filamentous, sulfide-oxidizing bacteria, and plankton samples from New Zealand methane seeps. The range of estimated percent methane-derived carbon in animal tissues is given as a top *x*-axis (see text for model estimation methods). Range and mean of methane isotopic concentration are from Sommer et al. (2009-this issue).

Table 3
Mean, standard error, and range of stable isotope values of heterotrophic fauna collected from each methane-seep station on the New Zealand continental margin.

Region	Sites	Station	N	# of sp.	$\delta^{13}C$ Mean	SE	Min	Max	$\delta^{15}N$ Mean	SE	Min	Max	Seep fauna $\delta^{13}C$ values of most ^{13}C-depleted organisms present
Builder's Pencil		21	3	3	−20.1	0.8	−21.3	−18.6	9.2	1.7	6.2	12.0	Ophiuroidea (−21)
		34	19	16	−21.1	0.7	−26.6	−14.4	8.2	0.5	3.4	11.8	Glyceridae (−27), Amphipoda (−25.4), Ophiuroidea (−23)
		36	3	3	−23.4	0.7	−24.8	−22.5	9.5	1.0	8.3	11.5	Isopoda (−25), Cirratulidae (−23), Cumacea (−23)
		38	18	13	−23.3	1.2	−34.0	−18.4	9.0	1.0	0.4	14.8	L Gastropoda (−34), Nematoda (−27), Isopoda (−25)
		32	5	5	−21.3	2.0	−29.0	−18.0	10.1	1.3	6.7	13.9	P, L Gastropoda (−29), Isopoda (−22)
		18	20	15	−21.4	1.2	−44.0	−16.8	9.8	0.6	5.1	14.9	Sipuncula (−44), Cirratulidae (−23), Syllidae (−23)
		23	13	11	−29.3	2.2	−46.5	−14.4	7.0	0.7	3.1	11.4	*B, F, SH* Oligochaeta (−47), Isopoda (−35), Amphipoda (−35)
		30	15	12	−19.6	0.4	−22.4	−17.3	9.7	0.5	6.8	12.7	Amphipoda (−22), scale worm (−22), Glyceridae (−21)
		22	9	8	−18.5	0.6	−21.4	−16.6	10.4	0.9	7.4	14.2	Amphipoda (−21), Phyllodocidae (−20), Onuphidae (−20)
		Mean			−22.2	0.5	−30.0	−17.5	9.0	0.3	5.3	13.0	
LM-3		238	28	15	−49.5	1.5	−61.5	−23.8	5.5	0.3	1.9	8.9	S, B Scale worm (−62), Terebellidae (−60), Tanaidacea (−56)
		216	20	10	**−52.7**	**1.8**	**−62.1**	**−31.4**	**3.4**	**0.4**	**0.5**	**7.6**	Cumacea (−62), Ampharetidae (−60), Dorvilleidae (−57),
		Mean			−50.8	1.1	−61.8	−27.6	4.7	0.3	1.2	8.2	
Rock Garden	Knoll	10	2	1	−20.5	3.3	−23.8	−17.2	9.8	3.2	6.6	13.1	Pholoidae (−24)
		6	26	15	−19.7	0.4	−27.1	−16.8	10.0	0.6	4.0	15.8	Syllidae (−27), Glyceridae (−22), Amphipoda (−21)
		11	2	2	−19.6	0.0	−19.6	−19.6	10.3	0.9	9.4	11.2	Syllidae (−20), Lumbrineridae (−20)
		7	3	3	−20.8	0.8	−22.2	−19.3	9.7	0.7	8.4	10.8	Glyceridae (−22), scale worm (−21)
		12	7	6	−19.3	0.4	−20.8	−18.0	11.8	0.8	9.1	14.9	Scale worm (−21), Glyceridae (−20), Onuphidae (−20)
		Mean			−19.8	0.3	−22.7	−18.2	10.3	0.4	7.5	13.1	
Omakere Ridge	LM-9	45	5	5	−19.7	0.8	−21.7	−17.6	8.4	0.6	6.8	10.4	B, S, SP Polychaeta (−22), Amphipoda (−22), Maxillopoda (−19)
		50	1	1	−19.7		−19.7	−19.7	10.3		10.3	10.3	F, SP Ophiuroidea (−20)
		57	17	16	−31.0	2.1	−52.3	−14.3	5.7	0.8	−0.2	12.1	Cumacea (−52), Maldanidae (−43), Nematoda (−38)
		46	12	12	−25.7	1.2	−32.4	−20.3	4.4	0.8	0.7	10.0	F Aplacophora (−32), Bivalvia (−31), Spionidae (−30)
		49	3	3	−23.8	1.6	−25.7	−20.6	4.7	1.9	2.4	8.5	F Bivalvia (−26), Amphipoda (−25), Gastropoda (−21)
		58	22	15	−21.4	0.9	−37.4	−17.0	8.1	0.8	−3.7	12.8	B, F Aplacophora (−37), Tanaidacea (−29), Paraonidae (−23)
		59	15	14	−20.0	0.4	−22.4	−16.6	8.3	1.0	0.4	12.7	Oligochaeta (−22), scale worm (−22), Terrebellidae (−22)
		60	19	19	−23.6	0.9	−35.5	−19.5	8.1	0.8	−0.9	15.3	Cumacea (−36), Cirratulidae (−29), Isopoda (−27)
		61	7	6	−19.5	1.3	−27.4	−17.3	10.5	1.6	1.3	13.9	Ophiuroidea (−27), Lumbrineridae (−19), Polychaeta (−19)
		Mean			−23.6	0.6	−30.5	−18.1	7.4	0.4	1.9	11.8	
	Kaka	261	25	19	**−36.7**	**2.0**	**−52.5**	**−21.3**	**7.4**	**0.5**	**2.9**	**10.9**	Ampharetidae (−52), Cumacea (−50), Orbiniidae (−49)
		232	14	10	**−33.0**	**1.8**	**−46.7**	**−23.3**	**7.3**	**0.5**	**3.7**	**9.9**	B Cumacea (−47), Amphipoda (−42), Ampharetidae (−37)
		242	31	22	**−29.5**	**0.9**	**−41.9**	**−18.0**	**7.0**	**0.8**	**−9.0**	**13.9**	Spionidae (−42), Paraonidae (−37), Bivalvia (−37)
		Mean			−32.7	1.0	−47.0	−20.9	7.2	0.4	−0.8	11.6	
	Bear's Paw	197	7	3	**−44.9**	**3.5**	**−54.2**	**−26.1**	**6.6**	**0.7**	**4.5**	**9.7**	Ampharetidae (−54), Orbiniidae (−51), Dorvilleidae (−26)
		198	42	15	**−46.7**	**1.7**	**−64.0**	**−24.3**	**5.4**	**0.4**	**1.7**	**9.6**	Cumacea (−64), Orbiniidae (−61), Amphipoda (−61)
		186	10	9	**−35.4**	**1.7**	**−43.8**	**−27.9**	**6.0**	**0.8**	**2.5**	**9.8**	F Isopoda (−44), Amphipoda (−42), Amphinomidae (−40)
		Mean			−44.6	1.4	−54.0	−26.1	5.7	0.3	2.9	9.7	
Uruti Ridge	East	70	17	12	−22.3	0.9	−28.7	−16.7	10.0	0.6	4.1	13.8	Lumbrineridae (−29), Chrysopetelidae (−29), scale worm (−27)
	LM-10	68	6	6	−20.4	0.5	−22.5	−19.3	11.2	1.4	5.3	14.6	F Lumbrineridae (−23), Nematoda (−21), Maldanidae (−20)
	Hihi	67	6	14	−18.7	0.5	−22.0	−15.4	10.4	0.8	3.8	14.0	Ophiuroidea (−22), Paraonidae (−21), Glyceridae (−21)
		Mean			−20.6	0.5	−24.4	−17.1	10.4	0.4	4.4	14.1	
Opouawe Bank	North Tower	122	14	10	−20.1	0.7	−25.4	−15.8	10.1	0.5	4.4	11.4	Maldanidae (−25), Lumbrineridae (−25), Trichobranchidae (−22)
		83	14	11	−30.4	2.2	−40.8	−19.9	7.5	1.1	−3.4	12.7	Nereididae (−41), Amphipoda (−41), Syllidae (−39)
		86	10	8	−24.9	1.4	−34.0	−19.3	7.3	1.3	0.1	12.4	Amphipoda (−34), Dorvilleidae (−29), Oligochaeta (−28)
		84	9	9	−19.4	0.6	−22.4	−16.3	7.7	0.9	1.2	10.8	Amphipoda (−22), Tanaidacea (−21), Spionidae (−20)
		79	18	15	−32.1	2.8	−50.1	−17.2	7.1	1.2	−1.8	23.2	F, S, L Hesionidae (−50), Maldanidae (−44), Cirratulidae (−44)
		290	12	6	**−48.7**	**3.1**	**−67.7**	**−35.4**	**4.7**	**0.5**	**2.9**	**8.2**	Ampharetidae (−68), Spionidae (−45), Amphipoda (−40)
		298	32	23	**−32.7**	**1.2**	**−47.8**	**−21.2**	**6.2**	**0.5**	**−3.9**	**10.6**	Amphinomidae (−48), Polychaeta (−43), Capitellidae (−41)
		112/113	20	15	−19.8	0.5	−25.8	−15.6	8.8	0.7	3.8	14.0	F, SM *Bathysiphon* (−26), Ophiurnidea (−23), Thyasiridae (−22)
		277	3	3	**−41.9**	**11.8**	**−64.6**	**−25.0**	**5.9**	**0.5**	**5.3**	**6.9**	Capitellidae (−65), Spionidae (−36), Dorvilleidae (−25)
		Mean			−29.3	0.9	−42.1	−20.6	7.0	0.3	0.9	12.2	
	South Tower	81	54	23	−34.7	1.2	−59.4	−19.6	4.4	0.5	−3.2	12.0	Ampharetidae (−59), Lumbrineridae (−49), Spionidae (−47)
		116	11	11	−27.2	1.1	−36.2	−23.3	8.0	0.7	4.8	11.8	B Amphipoda (−36), Bivalvia (−29), Maldaniae (−27)
		118	16	16	−23.8	0.7	−30.4	−20.9	6.9	0.6	1.8	10.6	B Glyceridae (−30), Amphinomidae (−28), Isopoda (−27)
		82	5	5	−17.9	0.5	−19.7	−16.5	8.5	1.1	5.0	11.7	Amphipoda (−20), Cumacea (−18), Opheliidae (−18)
		123	15	14	−21.9	0.9	−33.6	−18.4	8.4	1.2	−4.2	12.6	Tanaidacea (−34), Protista (−23), Isopoda (−23)
		Mean			−25.1	0.4	−35.9	−19.8	7.6	0.2	0.8	11.7	
	Takahe	309	57	23	**−38.4**	**1.1**	**−53.7**	**−20.6**	**5.4**	**0.7**	**−8.8**	**11.5**	Ampharetidae (−54), Spionidae (−47), Capitellidae (−46)

N is the number of samples analyzed. # of species indicates the number of putative species analyzed from each station. Seep fauna include the chemoautotrophic taxa collected (L = *Lamellibrachia* sp., B = sheath-forming bacteria, F = frenulata, S = sponge, SH = *Calyptogena* spp. shell hash, SP = solemyid periostracum, SM = solemyid). Most ^{13}C-depleted values and ID indicate those taxa with the lowest $\delta^{13}C$ values (given in parentheses). Bold values are those from ampharetid beds. Underlined values are fauna collected from a *Pseudosuberites* sp. community.

methane ranged from −46.7 to −63.2‰ with a mean of −52.9‰ (Sommer et al., 2009-this issue). Filamentous, sulfide-oxidizing bacteria had a $\delta^{13}C$ of −33.6 to −22.0‰ (mean = −27.7 ± 2.9, $n = 4$) and a $\delta^{15}N$ of −4.7 to 2.5‰ (mean = 1.0 ± 1.6). Two sets of mixing model end points were used to account for variable inputs. Maximum estimates of methane-derived carbon (MDC) were based on a $\delta_{POC/SOB}$ of −22.2‰ (from the phytoplankton sample) and the least negative value of methane $\delta_m = -46.7$‰. Minimum MDC estimates used a $\delta_{POC/SOB}$ value of −33.6‰ (sulfide-oxidizing bacteria minimum) and the most depleted value of methane ($\delta_m = -63.2$‰) from Sommer et al. (2009-this issue). Use of all other possible mixing model end points yields intermediate estimates of MDC.

Table 4
Mean station carbon isotopic signatures for macrofauna obtained by each type of sampling gear used.

Region	Site	TV-MUC		MUC		TV-Grab		Grab		Sled		Chambers
		Mean	SE	Mean	SE	Mean	SE	Mean	SE	Mean	SE	Mean
All		−40.7	2.8	−23.5	1.1	−49.5		−21.6	1.2	−22.5	1.1	−37.3
Builder's Pencil				−23.4				−23.0	3.3	−21.1	0.6	
LM-3		−52.7				−49.5						
Rock Garden	Knoll							−19.6		−20.1	0.3	
Omakere Ridge	LM-9			−26.8	2.1			−21.1	0.9	−19.7	0.0	
	Kaka	−33.1	2.1									
	Bear's Paw	−42.3	3.5									
Uruti Ridge										−20.5	1.0	
Opouawe Bank	North Tower	−48.7		−21.4	0.7					−28.2	1.5	−37.3
	South Tower			−24.6	0.5					−34.7	1.2	
	Takahe	−38.4										

TV-MUC = video-guided multicore; MUC = blind multicore; TV-Grab = video-guided hydraulic grab; Grab = blind vanVeen grab; Sled = epibenthic sled; Chambers = respiration chambers from benthic lander deployments. SE is not given if <3 samples were present.

4.1. Symbiont-bearing taxa

A total of 5 taxonomic groups of symbiont-bearing fauna, represented by 60 individuals from 7 sites were analyzed (Table 2, Fig. 2). Isotopic signatures indicated the use of two distinct metabolic pathways. The bathymodiolin mussel had a $\delta^{13}C$ isotopic signature ($\delta^{13}C$ of −60‰ to −65.8‰) clearly indicating methanotrophic endosymbiosis, whereas Vesicomyidae and Solemyidae ($\delta^{13}C$ of −36.5 to −30.2‰) almost certainly use the products of symbiont sulfide oxidation to fuel their biomass. A minimum of three frenulate species (Polychaeta, Siboglinidae) were present. These species exhibited a wide range of carbon isotopic signatures among individuals, suggesting the presence of methanotrophic symbionts ($\delta^{13}C = -72.9‰$), sulfide-oxidizing symbionts ($\delta^{13}C = -33.5‰$) and possibly uptake of dissolved inorganic carbon (DIC) from plankton sources ($\delta^{13}C = -18.5‰$). *Lamellibrachia* sp. had $\delta^{13}C$ values ranging from −19.8 to −43.1‰, with no significant difference between the $\delta^{13}C$ of their trophosome and vestimentum (paired *t*-test; $t = 0.71$, df = 13, $p = 0.49$) nor among the sites where they were collected (1-way ANOVA: $F_{2,15} = 1.77$, $p = 0.20$).

4.2. Heterotrophic fauna

A total of 751 heterotrophic individuals were examined from 10 different seep locations. A complete list of the species collected and their respective isotopic values are available upon request from the first author. This assemblage exhibited a 53.4‰ range in $\delta^{13}C$ (from −67.7 to −14.3‰) and a 24.8‰ range in $\delta^{15}N$ (from −9.0 to +15.8‰; Fig. 3, Table 3), reflecting varying nutritional sources across taxa within a site and across sites within a taxon. Incorporation of MDC was estimated in sipunculids, arthropods (cumaceans, tanaids, and amphipods), molluscs (gastropods) and annelids (≥6 families), all had $\delta^{13}C$ values of <−40‰ indicating that 21% to 73% of their carbon was derived from methane.

A comparison of average isotopic values for entire samples, revealed that gear types were not equally effective at collecting seep fauna (Table 4). Assemblages collected with the video-guided multicore, which targeted ampharetid-bed communities, had a more negative carbon isotopic signature than epibenthic sleds, blind multicores, or blind grabs, which were not different from each other ($F_{3,42} = 30.62$, $p \ll 0.01$, Tukey post-hoc test). Insufficient replication did not allow inclusion of video-guided grabs and benthic landers in the analysis.

The Uruti Ridge, Rock Garden, and Builder's Pencil sites, sampled largely by epibenthic sled and blind grabs (Table 1), were covered by extensive carbonate precipitates (rocks, boulders and stones; Campbell et al., 2010-this issue; Greinert et al., 2009-this issue; Liebetrau et al., 2009-this issue; Naudts et al., 2010-this issue). Despite the presence of chemosynthetic, symbiont-bearing megafauna (*Lamellibrachia* sp., *Calyptogena* spp. and frenulates), the majority of heterotrophic taxa from these sites had isotopic signatures similar to photosynthesis-based organic matter. Only 5% of the individuals from Rock Garden, 21% at Uruti Ridge and 24% at Builder's Pencil had $\delta^{13}C$ signatures less than our plankton value of −22.2‰ (Fig. 4, Table 3), suggesting primarily photosynthetic food source utilization by these assemblages. At Builder's Pencil, half of the taxa that consumed chemosynthesis-based organic matter ($\delta^{13}C_{sample} < \delta^{13}C_{plankton}$) were from two samples collected by the blind grab. With the exception of one sipunculan, all of the fauna at Uruti Ridge and Builder's Pencil with evidence of MDC ($\delta^{13}C < -33.6‰$) were collected by cores and grabs. These included two species of amphipod, one gastropod, an isopod, and an oligochaete (Table 3). No specimens collected at Rock Garden appeared to use MDC (i.e. had a minimal estimate of MDC>0%).

Macrobenthos collected from LM-3 (Rock Garden), Bear's Paw (Omakere Ridge) and Takahe (Opouawe Bank) sites exhibited the most negative carbon isotopic signatures (Fig. 4) with 96%, 83% and 80%, respectively, of all individuals analyzed using MDC. A diverse group of annelids including ampharetid and orbiniid polychaetes, as well as amphipods and cumaceans, had $\delta^{13}C$ values <−50‰. The ^{13}C-depleted average and $\delta^{15}N$ values (<6‰) suggest the use of chemosynthetic food sources. However, three or fewer gear deployments were made at these sites (Table 2), and they were selective in targeting ampharetid beds (with the TV-guided multicore) or the *Pseudosuberites* sp. sponge fauna (with the TV-guided grab).

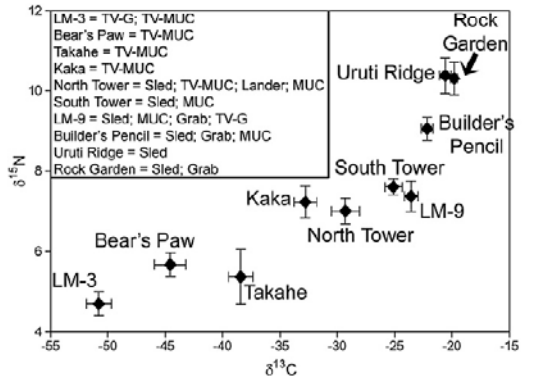

Fig. 4. Mean stable isotopic composition of heterotrophic invertebrate fauna at each site sampled on the New Zealand continental margin. Error bars are ±1SE. Legend gives sampling equipment used at each location using the abbreviations: Sled = epibenthic sled; MUC = blind multicorer; Grab = vanVeen grab; TV-G = video-guided hydraulic grab; TV-MUC = video-guided multicorer; Lander = Bigo and Flufo benthic landers. For more details see Materials and methods and Table 1.

The remaining 4 study sites (LM-9 and Kaka both at Omakere Ridge, North and South Tower both at Opouawe) all had comparable mean $\delta^{15}N$ values (7.2 to 7.6‰) but a 9‰ range in mean $\delta^{13}C$ (−23.6 to −32.7‰). Site-averaged MDC estimates for heterotrophic macrobenthos ranged from limited (LM-9, 0–4% MDC) to higher (Rock Garden, 7–60%) values (Table 5). The most negative heterotroph $\delta^{13}C$ values in the study were from a cumacean at LM-3 (−62.1‰) and an ampharetid at North Tower (−67.7‰). Yet coexisting with these taxa were species with individual $\delta^{13}C$ values as high as −14.3 to −18‰. The most negative $\delta^{15}N$ value for macrobenthos at each of these 5 (LM-3, LM-9, North and South Tower, and Kaka) sites ranged from −9 to 0.5‰, indicating considerable chemosynthesis-derived nutrition. These taxa included a new genus of spionid polychaete ($\delta^{15}N = -5.4 \pm 0.8$‰, $n = 9$), a tanaid ($\delta^{15}N = -4.2$‰, $n = 1$), an aplacophoran ($\delta^{15}N = -3.4$‰, $n = 1$), a second species of spionid ($\delta^{15}N = -3.4$‰, $n = 1$), two species of dorvilleid polychaetes ($\delta^{15}N = -1.0 \pm 1$‰, $n = 3$), a nematode ($\delta^{15}N = -1.8$‰, $n = 1$), and an arborescent foraminiferan ($\delta^{15}N = 0.5$‰, $n = 1$).

There were two multi-species invertebrate assemblages with high levels of MDC: taxa living within the sponge *Pseudosuberites* sp. and the invertebrate assemblage inhabiting ampharetid beds. ^{13}C-depleted *Pseudosuberites* sp. were collected from LM-3 (Station 238; $\delta^{13}C = -56.6$‰, $n = 1$), LM-9 (Station 45; $\delta^{13}C = -57.1$‰, $n = 1$), and North Tower (Station 79; $\delta^{13}C = -50$‰, $n = 1$). At LM-3 the associated fauna, mostly living within the sponge, consisted of 15 species including capitellid, cirratulid, terebellid, amphinomid, syllid, glycerid, and scale worm polychaetes, and tanaid, isopod, and pycnogonid arthropods. The commensal invertebrates had a mean $\delta^{13}C$ of -49.5 ± 1.5‰ indicating 38 to 100% MDC. However, a sponge-associated amphinomid polychaete had a $\delta^{13}C$ signature of −23.8‰; this was the only species with a $\delta^{13}C$ higher than −40‰. At North Tower the sponge-commensal fauna had $\delta^{13}C$ values from −23.7 to −47.0‰. Here the assemblage included ^{13}C-depleted ($\delta^{13}C < -40$‰) maldanid polychaetes and limpets, intermediate ($-40 < \delta^{13}C < -30$‰) sipunculans and a holothurian in the family Psolidae and less ^{13}C-depleted ($\delta^{13}C > -25$‰) lumbrinerid and paraonid polychaetes.

Ampharetid beds contained dense assemblages of two species of Ampharetidae and a host of other invertebrate taxa. These assemblages had $\delta^{13}C$ values indicating high use of chemosynthesis-derived nutrition. At Bear's Paw, Kaka, Takahe, and LM-3, the ampharetid-bed macrofauna had a mean $\delta^{13}C$ value of -39.4 ± 0.7‰. The ampharetid species themselves had a $\delta^{13}C$ of -50.3 ± 1.1‰ or 56–100% MDC and $\delta^{15}N = 4.2 \pm 0.2$‰ ($n = 37$). Associated fauna included cumaceans (mean $\delta^{13}C$ of -52.1 ± 3.8‰, $\delta^{15}N = 3.7 \pm 0.3$‰, $n = 10$), eight species of amphipod (mean $\delta^{13}C$ of -38.7 ± 1.2‰, $\delta^{15}N = 6.8 \pm 0.3$‰, $n = 34$), an orbiniid polychaete ($\delta^{13}C = -49.1 \pm 2.5$‰, $\delta^{15}N = 7.2 \pm 0.3$‰, $n = 10$), at least seven species of dorvilleid polychaete ($\delta^{13}C = -29.7 \pm 1.3$‰, $\delta^{15}N = 6.9 \pm 0.5$‰, $n = 37$). The aforementioned species of spionid ($\delta^{13}C = -39.7 \pm 0.4$‰, $\delta^{15}N = -7.3 \pm 0.6$‰, $n = 8$) and another spionid species ($\delta^{13}C = -38.4 \pm 2.7$‰, $\delta^{15}N = 7.2 \pm 0.7$‰, $n = 10$) were also collected from this habitat.

5. Discussion

5.1. Symbiont-bearing taxa

The fauna of New Zealand methane seeps exhibit a broad range of isotope signatures indicative of multiple trophic pathways, but with a significant role for methane. Bathymodiolin mussels are known to have symbionts with multiple metabolic pathways and their use of methane has been reported frequently (Childress et al., 1986; Brooks et al., 1987; Cary et al., 1988; Van Dover et al., 2003). Sulfide oxidation is a well established source of energy for solemyid and vesicomyid bivalves (Fisher, 1990). *Lamellibrachia* spp. are reported to only have thiotrophic (sulfide-oxidizing) symbionts (Brooks et al., 1987; Fisher, 1990). The $\delta^{13}C$ values (−19.8 to −43.1‰) of the New Zealand *Lamellibrachia* sp. population, however, suggest incorporation of methane-derived carbon into their tissues. The carbon isotopic compositions of *Lamellibrachia* sp. from Builder's Pencil are equivalent to the most negative $\delta^{13}C$ values of *Lamellibrachia* spp. reported in the literature ($\delta^{13}C = -43.7$‰; Brooks et al., 1987). *Lamellibrachia* spp. commonly has a very heavy $\delta^{13}C$ composition compared to other

Table 5
Estimates of percent methane-derived carbon (MDC) in tissues of heterotrophic invertebrates in methane-seep sediments.

Geographic location	Water depth (m)	Habitat	Percent MDC			References
			Minimum	Maximum	Average	
Kodiak Seep, Gulf of Alaska	4413–4444	Frenulate field	32 ± 8	51 ± 6	44 ± 9	1, 2
	4413–35	*Calyptogena* beds	12 ± 8	40 ± 5	39 ± 6	1, 2
Unimak, Aleutian Islands	3283	Frenulate field			11 ± 6	2
	3267	*Calyptogena* beds			21 ± 4	2
Hydrate Ridge, OR	590	Microbial mats	20 ± 5	44 ± 4		1
	590	*Calyptogena* beds	0	27 ± 3		1
Eel River Seeps, CA	520	Microbial mats	0	5		1
	520	*Calyptogena* beds	0	22 ± 5		1
Florida Escarpment, FL	3290	Microbial mats			55 ± 8	2
	3234	Frenulate field			223 ± 7	2
	3290	*Calyptogena* beds			31 + 6	2
Builder's Pencil	780–817	Carbonates, shell hash	0	4 ± 3		3
LM-3	908	Sponge assemblage	53	100		3
	662	Ampharetid bed	51	100		3
Rock Garden	730–766	Mixed	0	0		3
Omakere Ridge — LM-9	1140–1150	Mixed	0	4 ± 3		3
Omakere Ridge — Kaka	1165–1172	Ampharetid beds	6 ± 6	49 ± 11		3
Omakere Ridge — Bear's Paw	803–1201	Ampharetid beds	18 ± 7	77 ± 12		3
Uruti Ridge	716–740	Carbonates, frenulate fields	0	1 ± 1		3
Opouawe Bank — North Tower	1036–1061	Ampharetid beds	22 ± 11	73 ± 15		3
		Mixed	0	15 ± 7		3
Opouawe Bank — South Tower	1040–1059	Mixed	0	14 ± 8		3
Opouawe Bank — Takahe	1056	Ampharetid beds	8	57		3

Data are averages across species for upper and lower estimates of MDC within a geographic location and habitat. Non-New Zealand sites indicate sediment-dwelling macrobenthos. MDC estimates are obtained from a 2-source mixing model (Fry and Sherr, 1984) using the $\delta^{13}C$ of methane and either surface plankton (to obtain a maximum or average estimate) or sulfide-oxidizing bacteria (to obtain a minimum estimate). "Mixed" are samples from more than one type of habitat and all samples collected via epibenthic sled.
1 = Levin and Michener (2002).
2 = Levin and Mendoza (2007).
3 = This study.

thiotrophic seep organisms. For example, $\delta^{13}C$ values are −20.1‰, −22.8‰ and −23.6 to −26.6‰ respectively for *Lamellibrachia luymesi* in the Gulf of Mexico (MacAvoy et al., 2005), for *Lamellibrachia* sp. at a Chilean seep (Sellanes et al., 2008), and for *Lamellibrachia* sp. at a Mediterranean mud volcano (Olu-Le Roy et al., 2004).

Many factors influence the $\delta^{13}C$ of vestimentiferans, including DIC source and size, growth rate and growth form of the individual (Fisher et al., 1990; MacAvoy et al., 2005). The DIC pool used may either be from the overlying water column, as it is in hydrothermal vent vestimentiferans (Fisher, 1990), or potentially sediment pore water DIC taken up through their tube from below the sediment surface (MacDonald et al., 1989; Fisher, 1990; Kennicutt et al., 1992; Dattagupta et al., 2006). A DIC pool that contains relatively high proportions of C recycled from methane would also impart a ^{13}C-depleted signature to faunal symbionts that are fixing carbon from this pool; $\Delta^{14}C$ analyses support uptake of methane-derived DIC by thiotrophic species (Brooks et al., 1987; Paull et al., 1989, 1992). Due to mass balance arguments, DIC limitation to the trophosome of a vestimentiferan results in reduced carbon fractionation (i.e. the realized enzymatic discrimination against ^{13}C) between the source DIC pool and its tissues. This limitation can result from a low respiratory surface to body size ratio, which decreases with increasing size/age (Fisher et al., 1990; Kennicutt et al., 1992). In addition, rapid growth or a high density of vestimentiferans can also impact availability of DIC and resultant carbon isotopic signatures (Kennicutt et al., 1992). These latter factors can help to explain increased $\delta^{13}C$ values in *Lamellibrachia* sp. The uncharacteristically ^{13}C-depleted $\delta^{13}C$ values of some of the *Lamellibrachia* sp. individuals found in New Zealand potentially mirror a DIC pool impacted by methane. The $\delta^{13}C$ signatures from foraminiferan tests and vesicomyid shells from New Zealand, also reflect DIC pools heavily influenced by methane oxidation (Martin et al., 2010-this issue).

The presence of discreet groups of frenulates with widely differing isotope signatures (Table 2) suggests that multiple methanotrophic and thiotrophic species are present off New Zealand. Frenulates with $\delta^{13}C$ values indicative of methanotrophy could result from symbionts which are methanotrophic or symbionts which fix carbon from a methane influenced or derived DIC source. Although vestimentiferans have never been reported to have methanotrophic symbionts, such symbionts have been unequivocally identified in one frenulate species, *Siboglinum poseidoni* (Schmaljohann and Flügel, 1987; Schmaljohann et al., 1990). Methanotrophic symbionts have been suggested in a variety of other frenulate species, yet evidence has either been inconclusive or has rejected this form of symbiosis (see discussion in Dando et al., 2008). *Oligobrachia haakonmobiensis*, a species present at the Håkon Mosby methane seep, is an example of a species with carbon isotopic values indicative of methane oxidization ($\delta^{13}C$ value of −66‰), but its symbionts did not possess characteristic genes indicative of methanotrophy (Lösekann et al., 2007).

The $\delta^{13}C$ values of siboglinid taxa identified Builder's Pencil as a location with a geochemical environment not present or not sampled at the other seep sites. Although the $\delta^{13}C$ values of the sub-population of *Lamellibrachia* sp. present at Builder's Pencil were not statistically different from the other sites, four individuals had $\delta^{13}C$ values 7.3‰ less than those at LM-3 and North Tower. In addition, a highly ^{13}C-depleted frenulate ($\delta^{13}C = -72.9$‰) was sampled at Builder's Pencil from a separate location. Both of these values are indicative of a DIC pool at Builder's Pencil which is impacted by methane oxidation and/or high methane release.

5.2. Heterotrophic fauna

The macrofauna collected from the Bear's Paw ampharetid beds (−44.6 ± 1.4‰) was the most ^{13}C-depleted assemblage among the New Zealand seeps, and also among the most depleted globally. The New Zealand mean $\delta^{13}C$ values are comparable to those of macrobenthos in microbial mats at the Florida Escarpment (−42.8‰; Levin and Mendoza, 2007) and Hydrate Ridge, Oregon (−43.8‰), in frenulate fields and clam beds of Kodiak, Alaska (−46.4‰ and −40.9‰, respectively; Levin and Michener, 2002), in mussel beds on the Blake Ridge (−40 to −50‰; Van Dover et al., 2003), and a frenulate field/bacterial mat in the North Sea (a range of −17 to −44.9‰; Gebruk et al., 2003; Table 5). The ampharetid-bed fauna is more depleted in ^{13}C than macrofauna in vesicomyid clam beds off California (−25.1‰), Oregon (−33.4‰; Levin and Michener, 2002) and Unimak Island, Alaska (−26.5‰; Levin and Mendoza, 2007). These negative $\delta^{13}C$ values are likely the result of periodically high methane release (Linke et al., 2010-this issue; Naudts et al., 2010-this issue), high bottom-water methane concentration (Faure et al., 2010-this issue; Law et al., 2009-this issue) potentially impacting the DIC pool, and from consumption of methanotrophic-microbial biomass, which can have a −30‰ fractionation factor from methane (Summons et al., 1994).

The average $\delta^{15}N$ signatures for macrofauna at 7 of the 10 New Zealand sites studied fell between 4.7‰ and 7.6‰ (Fig. 4). These $\delta^{15}N$ values are consistent with those observed for macrofauna with comparable $\delta^{13}C$ signatures from other Pacific seep sites (Levin et al., 2003), but are 5–10‰ heavier than those observed at the Florida Escarpment (Levin and Mendoza, 2007) and exhibit a smaller range than those present in the Sea of Okhotsk (1.9–8.4‰; Sahling et al., 2003).

Although the mixing model presented here is used to identify methane input into the food web, the role of nitrogen stable isotopic values can also elucidate the contribution of chemosynthetic production to heterotrophic food webs (Van Dover et al., 2003). Twenty-two individuals collected in this study had $\delta^{15}N$ between 0 and −9.0‰. All of their $\delta^{13}C$ signatures were between −29 and −41.8‰, thus these taxa did not reflect the highest MDC. Fourteen of these individuals (~2/3) belong to an undescribed spionid polychaete species that lives deep in seep sediments and was collected from Kaka, Takahe, and North and South Tower. The remainder included 2 dorvilleid polychaetes, 2 nematodes, 1 amphipod, 1 tanaid and 1 cumacean, and an aplacophoran. All of these must be consuming chemosynthetic microbial producers or have microbial symbionts themselves. Negative $\delta^{15}N$ values in symbiont-bearing taxa have been hypothesized to be a function of N_2 fixation (Brooks et al., 1987; Fisher, 1990) and nitrate and ammonium assimilation, with experimental evidence supporting the latter two in both sulfide-oxidizing and methane-oxidizing fauna (Lee and Childress, 1994).

We hypothesize that the sponge *Pseudosuberites* sp. facilitates transfer of methane released from fissures in carbonate rocks into a metazoan food web while mitigating its release into the overlying water column. Studies of estimated MDC assimilation by metazoans have largely been limited to soft-sediment habitats (e.g. Levin and Michener, 2002; Levin et al., 2003; Levin and Mendoza, 2007). In the present study, areas with abundant hard substrate lacked heterotrophic taxa with a high estimated proportion of MDC. The commensal sponge fauna was an important exception. At present the only known methanotrophic sponges are members of the family Cladorhyzidae (Vacelet et al., 1995). These can form large bushes, 1.5–2 m in diameter and 0.4 m high, as observed at the Barbados accretionary prism (Olu et al., 1997). No commensal communities were reported from that site. As cladorhizids lack cavities and many have spicules adapted to catch zooplankton, their other food source (Vacelet et al., 1995), there may be a limited number of taxa that can live within its interstices. *Pseudosuberites* sp. possesses defined structures such as dendritic crevices suitable for commensal living, and is not known to be a carnivore. This sponge may play a novel role as an ecosystem engineer providing habitat and energy via its tissues or symbionts. This sponge community was present at three of the sites (LM-3, LM-9, and North Tower) and is further discussed in Baco et al. (2010-this issue). The function of encrusting sponges as a hard-substrate methane sink,

equivalent to the sediment filter in soft-sediment habitats (Treude et al., 2003; Sommer et al., 2006), is a fertile area for research. Sponges identified to use chemoautrophic food sources have also been observed in the Sea of Okhotsk (Sahling et al., 2003). In addition the interplay between commensal microbial communities within these sponges may add to the burgeoning field of microbial-sponge interactions (Taylor et al., 2007).

Mean $\delta^{13}C$ values of heterotrophic taxa may have been biased by the sampling method employed. Seep fauna (i.e. siboglinid polychaetes, symbiont-bearing clams, and sponges with $\delta^{13}C$ values of $<-50‰$) were found at all sampling sites (Baco et al., 2010-this issue), confirming areas of active seeping at each site. However, the absence of megafauna with chemosynthetic symbionts did not preclude the use of chemosynthetic nutritional sources by consumers. The sampling techniques ranged from epibenthic sleds that integrate large swaths of epifauna and minimal infaunal species to video-guided multicores that selectively sampled infaunal ampharetid-bed habitats. Large carbonate areas and shell hash, which were present at Builder's Pencil, could only be sampled by epibenthic sleds. This sampling method recovered few heterotrophic species which consume methane, with the exception of one sipunculid, a taxon whose high volume of sediment ingested makes it especially sensitive to seep input (Van Dover et al., 2003). At Builder's Pencil, the sampling that was done with the blind grab yielded the greatest abundance of heterotrophs with chemosynthesis-based diets.

Directed sampling with either the video-guided multicore or grab resulted in an average MDC that was much higher than for other sampling methods, largely because these samplers targeted ampharetid beds and a sponge assemblage. It is uncertain whether the fauna in areas that were covered with carbonate (Uruti Ridge and Builder's Pencil) and had to be sampled with sleds, actually had reduced MDC or whether the estimates of MDC reflect gear selectivity (i.e. sleds collected more filter feeders). In other regions, seep carbonates have high abundances of photosynthesis-based fauna that are not reliant on seepage-fueled microbes for nutrition and are taking advantage of the hard substrate (Sellanes et al., 2008). This may be the case at Builder's Pencil and Uruti Ridge, or we may have missed the heterotrophic fauna that used the chemosynthesis-based nutrition.

The New Zealand seeps represent a potential model system for quantifying the role that metazoans play in the oxidation of methane. Seep taxa can enhance conditions for associated organisms by modifying the in-situ chemical and microbial environment (Cordes et al., 2005a). Examples include bio-irrigation and sulfate transport of symbiont-bearing clams to fuel sulfide oxidation (Wallmann et al., 1997; Levin et al., 2003; Luff et al., 2004), or increasing sediment-sulfate concentrations by tubeworms (Cordes et al., 2005a; Dattagupta et al., 2006, 2008). This facilitation can drive community composition (Cordes et al., 2005b). We hypothesize that the sponge and ampharetids in New Zealand enhance the food supply for their associated fauna by funneling methane to oxidizing microbes, potentially increasing the proportion of aerobic methanotrophy within this system (as suggested in Sommer et al., 2009-this issue). Further studies of the interactions between organisms in these communities and the chemistry that fuels them are necessary to quantify the fate of methane and its release into the water column.

6. Conclusions

Methane emissions at seeps are complex and not constant over time (Tryon and Brown, 2001, 2004; Greinert, 2008). The presence and isotopic composition of seep fauna provide a time-integrated proxy for the chemistry and magnitude of the fluid released. This approach can be especially enlightening for hard substrates, where techniques to quantify methane emissions (e.g. benthic chambers) are not currently available. In this study, we compared isotopic composition of symbiont-bearing among sites and identified Builder's Pencil, dominated by carbonate and shell hash, as an area where methane release is potentially high enough to impact the DIC pool, with implications for faunal trophodynamics. Through a comparison of heterotrophic faunal isotopic signatures among different seep habitats, we identified two novel biotic associations which are largely fueled by methane; the presence of sponge cover and ampharetid beds may be useful indicators of high methane-emission areas. This approach identifies the important role for methane in the nutrition of New Zealand seep fauna.

Acknowledgments

We are indebted to (in alphabetical order) Amy Baco, Peter Linke, Olaf Pfannkuche, Ashley A. Rowden, Craig R. Smith, and Stefan Sommer for making this research possible. We thank Jens Greinert, David Bowden, Angelo Bernardino, and the captains, crews, and science parties of *RV SONNE*-SO191 and *RV TANGAROA*-TAN0616 for additional assistance at sea. The map on which Fig. 1 is based was provided courtesy of Jens Greinert. Jennifer Gonzalez assisted tremendously with the processing of isotope samples in the laboratory. We thank Bruce Deck (Scripps Institution of Oceanography — SIO) and Ray Lee (Washington State University) for conducting isotopic analyses and the SIO Graduate Office for supplying funding to analyze many of the samples through the SIO analytical facility. We are grateful to Jens Greinert and two anonymous reviewers for their excellent critical review of this manuscript. Michelle Kelly kindly provided the sponge identification. A. Thurber was supported in part by a University of California Marine Council — Coastal Environmental Quality Initiative (CEQI) grant during the preparation of this manuscript. Funding was provided by the United States NOAA Office of Exploration Grant Nos.: NA17RJ1231 and NA050AR417076, United States National Science Foundation grant OCE 0425317 and NIWA Capability Fund project CRFH073.

References

Baco, A.R., Rowden, A.A., Levin, L.A., Smith, C.R., Bowden, D., 2010. Initial characterization of cold seep faunal communities on the New Zealand margin. Marine Geology 272, 251–259 (this issue).

Barnes, P.M., Lamarche, G., Bialas, J., Henrys, S., Pecher, I., Netzeband, G.L., Greinert, J., Mountjoy, J.J., Pedley, K., Crutchley, G., 2010. Tectonic and geological framework for gas hydrates and cold seeps on the Hikurangi subduction margin, New Zealand. Mar. Geol. 272, 26–48 (this issue).

Brooks, J.M., Kennicutt, M.C., Fisher, C.R., Macko, S.A., Cole, K., Childress, J.J., Bidigare, R.R., Vetter, R.D., 1987. Deep-sea hydrocarbon seep communities — evidence for energy and nutritional carbon-sources. Science 238, 1138–1142.

Campbell, K.A., 2006. Hydrocarbon seep and hydrothermal vent paleoenvironments and paleontology: past developments and future research directions. Palaeogeogr. Palaeoclimatol. Palaeoecol. 232, 362–407.

Campbell, K.A., Nelson, C.S., Alfaro, A.C., Boyd, S., Greinert, J., Nymann, S.L., Grosjean, E., Logan, G.A., Gregory, M.R., Cooke, S., Linke, P., Milloy, S., Wallis, L., 2010e. Geological imprint of methane seepage on the seabed and biota of the convergent Hikurangi Margin, New Zealand: Box core and grab carbonate results. Marine Geology 272, 285–306 (this issue).

Cary, S.C., Fisher, C.R., Felbeck, H., 1988. Mussel growth supported by methane as sole carbon and energy source. Science 240, 78–80.

Childress, J.J., Fisher, C.R., Brooks, J.M., Kennicutt, M.C., Bidigare, R., Anderson, A.E., 1986. A methanotrophic marine molluscan (Bivalvia, Mytilidae) symbiosis: mussels fueled by gas. Science 233, 1306–1308.

Cordes, E.E., Arthur, M.A., Shea, K., Arvidson, R.S., Fisher, C.R., 2005a. Modeling the mutualistic interactions between tubeworms and microbial consortia. Proc. Libr. Sci. Biol. 3, e77.

Cordes, E.E., Hourdez, S., Predmore, B.L., Redding, M.L., Fisher, C.R., 2005b. Succession of hydrocarbon seep communities associated with the long-lived foundation species *Lamellibrachia luymesi*. Mar. Ecol. Prog. Ser. 305, 17–29.

Dando, P.R., Southward, A.J., Southward, E.C., Lamont, P., Harvey, R., 2008. Interactions between sediment chemistry and frenulate pogonophores (Annelida) in the northeast Atlantic. Deep-Sea Res., Part 1 55, 966–996.

Dattagupta, S., Miles, L.L., Barnabei, M.S., Fisher, C.R., 2006. The hydrocarbon seep tubeworm *Lamellibrachia luymesi* primarily eliminates sulfate and hydrogen ions across its roots to conserve energy and ensure sulfide supply. J. Exp. Biol. 209, 3795–3805.

Dattagupta, S., Arthur, M.A., Fisher, C.R., 2008. Modification of sediment geochemistry by the hydrocarbon seep tubeworm *Lamellibrachia luymesi*: a combined empirical and modeling approach. Geochim. Cosmochim. Acta 72, 2298–2315.

Ding, H., Valentine, D.L., 2008. Methanotrophic bacteria occupy benthic microbial mats in shallow marine hydrocarbon seeps, Coal Oil Point, California. J. Geophys. Res. 113, 1–11.

Faure, K., Greinert, J., Schneider von Deimling, J., McGinnis, D.F., Kipfer, R., Linke, P., 2010. Methane seepage along the Hikurangi Margin of New Zealand: Geochemical and physical data from the water column, sea surface and atmosphere. Marine Geology 272, 170–188 (this issue).

Fisher, C.R., 1990. Chemoautotrophic and methanotrophic symbioses in marine invertebrates. Rev. Aquat. Sci. 2, 399–436.

Fisher, C.R., Kennicutt II, M.C., Brooks, J.M., 1990. Stable carbon isotopic evidence for carbon limitations in hydrothermal vent vestimentiferans. Science 247, 1094–1096.

Fry, B., Sherr, E.B., 1984. $\delta^{13}C$ measurements as indicators of carbon flow in marine and freshwater systems. Contrib. Mar. Sci. 27, 13–46.

Gebruk, A.V., Krylova, E.M., Lein, A.Y., Vinogradov, G.M., Anderson, A., Pimenov, N.V., Cherkashev, G.A., Crane, K., 2003. Methane seep community of the Håkon Mosby mud volcano (the Norwegian Sea): composition and trophic aspects. Sarsia 88, 394–403.

Greinert, J., 2008. Monitoring temporal variability of bubble release at seeps: the hydroacoustic swath system GasQuant. J. Geophys. Res. 113. doi:10.1029/2007JC004704.

Greinert, J., Lewis, K., Bialas, J., Pecher, I., Rowden, A., Linke, P., De Batist, M., Bowden, D., Suess, E., 2009-this issue. Methane seepage along the Hikurangi Margin, New Zealand: review of studies in 2006 and 2007. Marine Geology.

Jones, A.T., Greinert, J., Bowden, D.A., Klaucke, I., Petersen, C.J., Netzeband, G.L., Weinrebe, W., 2010. Acoustic and visual characterisation of methane-rich seabed seeps at Omakere Ridge on the Hikurangi Margin, New Zealand. Mar. Geol. 272, 154–169 (this issue).

Kennicutt II, M.C., Burke Jr., R.A., MacDonald, I.R., Brooks, J.M., Denoux, G.J., Macko, S.A., 1992. Stable isotope partitioning in seep and vent organisms: chemical and ecological significance. Chem. Geol. 101, 293–310.

Klaucke, I., Weinrebe, W., Petersen, C.J., Bowden, D., 2010. Temporal variability of gas seeps offshore New Zealand: multi-frequency geoacoustic imaging of the Wairarapa area, Hikurangi margin. Mar. Geol. 272, 49–58 (this issue).

Law, C.S., Nodder, S.D., Mountjoy, J., Jarriner, A., Orpin, A., Pilditch, C., Franz, P., Thompson, K., 2009-this issue. Geological, hydrodynamic and biogeochemical characterization of a New Zealand deep-water methane cold seep during a three-year time-series study. Marine Geology.

Lee, R.W., Childress, J.J., 1994. Assimilation of inorganic nitrogen by marine invertebrates and their chemoautotrophic and methanotrophic symbionts. Appl. Environ. Microbiol. 60, 1852–1858.

Levin, L.A., Michener, R., 2002. Isotopic evidence of chemosynthesis-based nutrition of macrobenthos: the lightness of being at Pacific methane seeps. Limnol. Oceanogr. 47, 1336–1345.

Levin, L.A., Mendoza, G.F., 2007. Community structure and nutrition of deep methane-seep macrobenthos from the North Pacific (Aleutian) margin and the Gulf of Mexico (Florida Escarpment). Mar. Ecol. 28, 131–151.

Levin, L.A., Ziebis, W., Mendoza, G., Growney, V., Tryon, M., Brown, K., Mahn, C., Gieskes, J., Rathburn, A., 2003. Spatial heterogeneity of macrofauna at northern California methane seeps: the influence of sulfide concentration and fluid flow. Mar. Ecol. Prog. Ser. 265, 123–139.

Lewis, K.B., Pettinga, J.R., 1993. The emerging, imbricate frontal wedge of the Hikurangi margin. In: Balance, P.F. (Ed.), South Pacific Sedimentary Basins. Sedimentary Basins of the World 2, Basins of the Southwest Pacific. Elsevier, Amsterdam, pp. 225–250.

Liebetrau, V., Eisenhauer, A., Linke, P., 2009-this issue. Deciphering the geochemical record of cold seep carbonates and cold water corals from the Hikurangi Margin, offshore New Zealand. Marine Geology.

Linke, P., Sommer, S., Rovelli, L., McGinnis, D.F., 2010. Physical limitations of dissolved methane fluxes: The role of bottom-boundary layer processes. Marine Geology 272, 209–222 (this issue).

Lösekann, T., Niemann, H., Pradillon, F., Knittel, K., Boetius, A., Dubilier, N., 2007. Endosymbioses between bacteria and deep-sea siboglinid tubeworms from an arctic cold seep (Haakon Mosby mud volcano, Barents Sea). Appl. Environ. Microbiol. 75, 3348–3362.

Luff, R., Wallmann, K., Aloisi, G., 2004. Numerically modeling of carbonate crust formation at cold vent sites, significance for fluid and methane budgets and chemosynthetic biological communities. Earth Planet. Sci. Lett. 221, 337–353.

MacAvoy, S.E., Carney, R.S., Fisher, C.R., Macko, S.A., 2002. Use of chemosynthetic biomass by large, mobile benthic predators in the Gulf of Mexico. Mar. Ecol. Prog. Ser. 225, 65–78.

MacAvoy, S.E., Macko, S.A., Carney, R.S., 2003. Links between chemosynthetic production and mobile predators on the Louisiana continental slope: stable carbon isotopes of specific fatty acids. Chem. Geol. 201, 229–237.

MacAvoy, S.E., Fisher, C.R., Carney, R.S., Macko, S.A., 2005. Nutritional associations among fauna at hydrocarbon seep communities in the Gulf of Mexico. Mar. Ecol. Prog. Ser. 292, 51–60.

MacAvoy, S.E., Morgan, E., Carney, R.S., Macko, S.A., 2008. Chemoautotrophic production incorporated by heterotrophs in Gulf of Mexico hydrocarbon seeps: an examination of mobile benthic predators and seep residents. J. Shellfish Res. 27, 153–161.

MacDonald, I.R., Boland, G.S., Baker, G.S., Brooks, J.M., Kennicutt II, M.C., Bidigare, R.R., 1989. Gulf of Mexico hydrocarbon seep communities, II. Spatial distribution of seep organisms and hydrocarbons at Bush Hill. Mar. Biol. 101, 235–247.

Martin, R.A., Nesbitt, E.A., Campbell, K.A., 2010. The effects of anaerobic methane oxidation on benthic foraminiferal assemblages and stable isotopes on the Hikurangi Margin of eastern New Zealand. Marine Geology 272, 270–284 (this issue).

Naudts, L., Greinert, J., Poort, J., Belza, J., Vangampelaere, E., Boone, D., Linke, P., Henriet, J.-P., De Batist, M., 2010. Active venting sites on the gas-hydrate-bearing Hikurangi Margin, off New Zealand: Diffusive- versus bubble-released methane. Mar. Geol. 272, 233–250 (this issue).

Olu, K., Lance, S., Sibuet, M., Henry, P., Fiala-Médioni, A., 1997. Cold seep communities as indicators of fluid expulsion patterns through mud volcanoes seaward of the Barbados accretionary prism. Deep-Sea Res., Part I 44, 811–841.

Olu-Le Roy, K., Sibuet, M., Fiala-Medioni, A., Gofas, S., Salas, C., Mariotti, A., Foucher, J.-P., Woodside, J., 2004. Cold seep communities in the deep eastern Mediterranean Sea: composition, symbiosis and spatial distribution on mud volcanoes. Deep-Sea Res., Part I 51, 1915–1936.

Paull, C.K., Martens, C.S., Chanton, J., Neumann, A.C., Coston, J., Jull, A.T., Toolin, L.T., 1989. Old carbon in living organisms and young $CaCO_3$ cements from abyssal brine seeps. Nature 342, 166–168.

Paull, C.K., Chanton, J., Neumann, A.C., Coston, J.A., Martens, C.S., Showers, W., 1992. Indicators of methane-derived carbonates and chemosynthetic organic carbon deposits: examples from the Florida Escarpment. Palaios 7, 361–375.

Robinson, C.A., Bernhard, J.M., Levin, L.A., Mendoza, G.F., Blanks, J.K., 2004. Surficial hydrocarbon seep infauna from the Blake Ridge (Atlantic Ocean, 2150 m) and the Gulf of Mexico (690–2240 m). Mar. Ecol. 25, 313–336.

Sahling, H., Galkin, S.V., Salyuk, A., Greinert, J., Foerstel, H., Piepenburg, D., Suess, E., 2003. Depth-related structure and ecological significance of cold-seep communities — a case study from the Sea of Okhotsk. Deep-Sea Res., Part I 50, 1391–1409.

Schmaljohann, R., Flügel, H.J., 1987. Methane-oxidizing bacteria in Pogonophora. Sarsia 72, 91–98.

Schmaljohann, R., Faber, E., Whiticar, M.J., Dando, P.R., 1990. Co-existence of methane- and sulphur-based endosymbioses between bacteria and invertebrates at a site in the Skegerrak. Mar. Ecol., Prog. Ser. 61, 119–124.

Sellanes, J., Quiroga, E., Neira, C., 2008. Megafauna community structure and trophic relationships at the recently discovered Concepción methane seep area, Chile, ~36°S. ICES J. Mar. Sci. 65, 1102–1111.

Sibuet, M., Olu, K., 1998. Biogeography, biodiversity and fluid dependence of deep-sea cold-seep communities at active and passive margins. Deep-Sea Res., Part II 45, 517–567.

Sommer, S., Linke, P., Pfannkuche, O., Bowden, D.A., Haeckel, M., Greinert, J., Thurber, A.R., 2008. Novel cold seep habitat along the Hikurangi Margin (New Zealand). Geophys. Res. Abstr. 10 (EGU2008-A-02387).

Sommer, S., Pfannkucke, O., Linke, P., Luff, R., Greinert, J., Drews, M., Gubsch, S., Pieper, M., Poser, M., Viergutz, T., 2006. Efficiency of the benthic filter: biological control of the emission of dissolved methane from sediments containing shallow gas hydrates at Hydrate Ridge. Glob. Biogeochem. Cycles 20, GB2019. doi:10.1029/2004GB002389.

Sommer, S., Linke, P., Pfannkuche, O., Treude, T., Niemann, H., 2009-this issue. Carbon flow through a novel seep habitat dominated by dense beds of ampharetid polychaetes. Marine Geology.

Southward, E.C., Schulze, A., Gardiner, S.L., 2005. Pogonophora (Annelida): form and function. Hydrobiologia 235/236, 227–251.

Summons, R.E., Jahnke, L.L., Roksandic, Z., 1994. Carbon isotopic fractionation in lipids from methanotrophic bacteria: relevance for interpretation of the geochemical record of biomarkers. Geochim. Cosmochim. Acta 58, 2853–2863.

Taylor, M.W., Radax, R., Steger, D., Wagner, M., 2007. Sponge-associated microorganisms: evolution, ecology, and biotechnological potential. Microbiol. Mol. Biol. Rev. 71, 295–347.

Treude, T., Boetius, A., Knittel, K., Wallmann, K., Jørgensen, B.B., 2003. Anaerobic oxidation of methane above gas hydrates at Hydrate Ridge, NE Pacific Ocean. Mar. Ecol. Prog. Ser. 264, 1–14.

Tryon, M.D., Brown, K.M., 2001. Complex flow patterns through Hydrate Ridge and their impact on seep biota. Geophys. Res. Lett. 28, 2863–2866.

Tryon, M.D., Brown, K.M., 2004. Fluid and chemical cycling at Bush Hill: implications for gas- and hydrate-rich environments. Geochem. Geophys. Geosyst. 5, 1–7.

Vacelet, J., Boury-Esnault, N., Fiala-Medioni, A., Fisher, C.R., 1995. A methanotrophic carnivorous sponge. Nature 377, 296.

Valentine, D.L., 2002. Biogeochemistry and microbial ecology of methane oxidation in anoxic environments: a review. Antoine van Leeuwenhoek 81, 271–282.

Van Dover, C.L., 2007. Stable isotopes in the study of marine chemosynthetic based ecosystems: an update. In: Michener, R., Lajtha, K. (Eds.), Stable Isotopes in Ecology and Environmental Sciences (Ecological Methods and Concepts). Wiley-Blackwell Scientific Publications, London, pp. 202–237.

Van Dover, C.L., Aharon, P., Bernhard, J.M., Caylor, E., Doerries, M., Flickinger, W., Gilhooly, W., Goffredi, S.K., Knick, K.E., Macko, S.A., Rapoport, S., Raulfs, E.C., Ruppel, C., Salerno, J.L., Seitz, R.D., Sen Gupta, B.K., Shank, T., Turnipseed, M., Vrijenhoek, R., 2003. Blake Ridge methane seeps: characterization of a soft-sediment chemosynthetically based ecosystem. Deep-Sea Res., Part I 50, 281–300.

Wallmann, K., Linke, P., Suess, E., Bohrmann, G., Sahling, H., Schlüter, M., Dählmann, A., Lammers, S., Greinert, J., von Mirbach, N., 1997. Quantifying fluid flow, solute mixing and the biogeochemical turnover at cold vents on the eastern Aleutian subduction zone. Geochim. Cosmochim. Acta 61, 5209–5219.

Wegener, G., Niemann, H., Elvert, M., Hinrichs, K.U., Boetius, A., 2008. Assimilation of methane and inorganic carbon by microbial communities mediating the anaerobic oxidation of methane. Environ. Microbiol. 10, 2287–2298.

Whiticar, M.J., 1999. Carbon and hydrogen isotope systematics of bacterial formation and oxidation of methane. Chem. Geol. 161, 291–314.

Ziebis, W., Haese, R.R., 2005. Interactions between fluid flow, geochemistry, and biogeochemical processes at methane seeps. In: Kristensen, E., Haese, R.R., Kostka, J.E. (Eds.), Interactions Between Macro- and Microorganisms in Marine Sediments. Coastal and Estuarine Studies, vol. 60. American Geophysical Union, Washington, DC, pp. 267–298.

Dattagupta, S., Arthur, M.A., Fisher, C.R., 2008. Modification of sediment geochemistry by the hydrocarbon seep tubeworm *Lamellibrachia luymesi*: a combined empirical and modeling approach. Geochim. Cosmochim. Acta 72, 2298–2315.

Ding, H., Valentine, D.L., 2008. Methanotrophic bacteria occupy benthic microbial mats in shallow marine hydrocarbon seeps, Coal Oil Point, California. J. Geophys. Res. 113, 1–11.

Faure, K., Greinert, J., Schneider von Deimling, J., McGinnis, D.F., Kipfer, R., Linke, P., 2010. Methane seepage along the Hikurangi Margin of New Zealand: Geochemical and physical data from the water column, sea surface and atmosphere. Marine Geology 272, 170–188 (this issue).

Fisher, C.R., 1990. Chemoautotrophic and methanotrophic symbioses in marine invertebrates. Rev. Aquat. Sci. 2, 399–436.

Fisher, C.R., Kennicutt II, M.C., Brooks, J.M., 1990. Stable carbon isotopic evidence for carbon limitations in hydrothermal vent vestimentiferans. Science 247, 1094–1096.

Fry, B., Sherr, E.B., 1984. $\delta^{13}C$ measurements as indicators of carbon flow in marine and freshwater systems. Contrib. Mar. Sci. 27, 13–46.

Gebruk, A.V., Krylova, E.M., Lein, A.Y., Vinogradov, G.M., Anderson, A., Pimenov, N.V., Cherkashev, G.A., Crane, K., 2003. Methane seep community of the Håkon Mosby mud volcano (the Norwegian Sea): composition and trophic aspects. Sarsia 88, 394–403.

Greinert, J., 2008. Monitoring temporal variability of bubble release at seeps: the hydroacoustic swath system GasQuant. J. Geophys. Res. 113. doi:10.1029/2007JC004704.

Greinert, J., Lewis, K., Bialas, J., Pecher, I., Rowden, A., Linke, P., De Batist, M., Bowden, D., Suess, E., 2009-this issue. Methane seepage along the Hikurangi Margin, New Zealand: review of studies in 2006 and 2007. Marine Geology.

Jones, A.T., Greinert, J., Bowden, D.A., Klaucke, I., Petersen, C.J., Netzeband, G.L., Weinrebe, W., 2010. Acoustic and visual characterisation of methane-rich seabed seeps at Omakere Ridge on the Hikurangi Margin, New Zealand. Mar. Geol. 272, 154–169 (this issue).

Kennicutt II, M.C., Burke Jr., R.A., MacDonald, I.R., Brooks, J.M., Denoux, G.J., Macko, S.A., 1992. Stable isotope partitioning in seep and vent organisms: chemical and ecological significance. Chem. Geol. 101, 293–310.

Klaucke, I., Weinrebe, W., Petersen, C.J., Bowden, D., 2010. Temporal variability of gas seeps offshore New Zealand: multi-frequency geoacoustic imaging of the Wairarapa area, Hikurangi margin. Mar. Geol. 272, 49–58 (this issue).

Law, C.S., Nodder, S.D., Mountjoy, J., Jarriner, A., Orpin, A., Pilditch, C., Franz, P., Thompson, K., 2009-this issue. Geological, hydrodynamic and biogeochemical characterization of a New Zealand deep-water methane cold seep during a three-year time-series study. Marine Geology.

Lee, R.W., Childress, J.J., 1994. Assimilation of inorganic nitrogen by marine invertebrates and their chemoautotrophic and methanotrophic symbionts. Appl. Environ. Microbiol. 60, 1852–1858.

Levin, L.A., Michener, R., 2002. Isotopic evidence of chemosynthesis-based nutrition of macrobenthos: the lightness of being at Pacific methane seeps. Limnol. Oceanogr. 47, 1336–1345.

Levin, L.A., Mendoza, G.F., 2007. Community structure and nutrition of deep methane-seep macrobenthos from the North Pacific (Aleutian) margin and the Gulf of Mexico (Florida Escarpment). Mar. Ecol. 28, 131–151.

Levin, L.A., Ziebis, W., Mendoza, G., Growney, V., Tryon, M., Brown, K., Mahn, C., Gieskes, J., Rathburn, A., 2003. Spatial heterogeneity of macrofauna at northern California methane seeps: the influence of sulfide concentration and fluid flow. Mar. Ecol. Prog. Ser. 265, 123–139.

Lewis, K.B., Pettinga, J.R., 1993. The emerging, imbricate frontal wedge of the Hikurangi margin. In: Balance, P.F. (Ed.), South Pacific Sedimentary Basins. Sedimentary Basins of the World 2, Basins of the Southwest Pacific. Elsevier, Amsterdam, pp. 225–250.

Liebetrau, V., Eisenhauer, A., Linke, P., 2009-this issue. Deciphering the geochemical record of cold seep carbonates and cold water corals from the Hikurangi Margin, offshore New Zealand. Marine Geology.

Linke, P., Sommer, S., Rovelli, L., McGinnis, D.F., 2010. Physical limitations of dissolved methane fluxes: The role of bottom-boundary layer processes. Marine Geology 272, 209–222 (this issue).

Lösekann, T., Niemann, H., Pradillon, F., Knittel, K., Boetius, A., Dubilier, N., 2007. Endosymbioses between bacteria and deep-sea siboglinid tubeworms from an arctic cold seep (Haakon Mosby mud volcano, Barents Sea). Appl. Environ. Microbiol. 75, 3348–3362.

Luff, R., Wallmann, K., Aloisi, G., 2004. Numerically modeling of carbonate crust formation at cold vent sites, significance for fluid and methane budgets and chemosynthetic biological communities. Earth Planet. Sci. Lett. 221, 337–353.

MacAvoy, S.E., Carney, R.S., Fisher, C.R., Macko, S.A., 2002. Use of chemosynthetic biomass by large, mobile benthic predators in the Gulf of Mexico. Mar. Ecol. Prog. Ser. 225, 65–78.

MacAvoy, S.E., Macko, S.A., Carney, R.S., 2003. Links between chemosynthetic production and mobile predators on the Louisiana continental slope: stable carbon isotopes of specific fatty acids. Chem. Geol. 201, 229–237.

MacAvoy, S.E., Fisher, C.R., Carney, R.S., Macko, S.A., 2005. Nutritional associations among fauna at hydrocarbon seep communities in the Gulf of Mexico. Mar. Ecol. Prog. Ser. 292, 51–60.

MacAvoy, S.E., Morgan, E., Carney, R.S., Macko, S.A., 2008. Chemoautotrophic production incorporated by heterotrophs in Gulf of Mexico hydrocarbon seeps: an examination of mobile benthic predators and seep residents. J. Shellfish Res. 27, 153–161.

MacDonald, I.R., Boland, G.S., Baker, G.S., Brooks, J.M., Kennicutt II, M.C., Bidigare, R.R., 1989. Gulf of Mexico hydrocarbon seep communities, II. Spatial distribution of seep organisms and hydrocarbons at Bush Hill. Mar. Biol. 101, 235–247.

Martin, R.A., Nesbitt, E.A., Campbell, K.A., 2010. The effects of anaerobic methane oxidation on benthic foraminiferal assemblages and stable isotopes on the Hikurangi Margin of eastern New Zealand. Marine Geology 272, 270–284 (this issue).

Naudts, L., Greinert, J., Poort, J., Belza, J., Vangampelaere, E., Boone, D., Linke, P., Henriet, J.-P., De Batist, M., 2010. Active venting sites on the gas-hydrate-bearing Hikurangi Margin, off New Zealand: Diffusive- versus bubble-released methane. Mar. Geol. 272, 233–250 (this issue).

Olu, K., Lance, S., Sibuet, M., Henry, P., Fiala-Médioni, A., 1997. Cold seep communities as indicators of fluid expulsion patterns through mud volcanoes seaward of the Barbados accretionary prism. Deep-Sea Res., Part I 44, 811–841.

Olu-Le Roy, K., Sibuet, M., Fiala-Medioni, A., Gofas, S., Salas, C., Mariotti, A., Foucher, J.-P., Woodside, J., 2004. Cold seep communities in the deep eastern Mediterranean Sea: composition, symbiosis and spatial distribution on mud volcanoes. Deep-Sea Res., Part I 51, 1915–1936.

Paull, C.K., Martens, C.S., Chanton, J., Neumann, A.C., Coston, J., Jull, A.T., Toolin, L.T., 1989. Old carbon in living organisms and young $CaCO_3$ cements from abyssal brine seeps. Nature 342, 166–168.

Paull, C.K., Chanton, J., Neumann, A.C., Coston, J.A., Martens, C.S., Showers, W., 1992. Indicators of methane-derived carbonates and chemosynthetic organic carbon deposits: examples from the Florida Escarpment. Palaios 7, 361–375.

Robinson, C.A., Bernhard, J.M., Levin, L.A., Mendoza, G.F., Blanks, J.K., 2004. Surficial hydrocarbon seep infauna from the Blake Ridge (Atlantic Ocean, 2150 m) and the Gulf of Mexico (690–2240 m). Mar. Ecol. 25, 313–336.

Sahling, H., Galkin, S.V., Salyuk, A., Greinert, J., Foerstel, H., Piepenburg, D., Suess, E., 2003. Depth-related structure and ecological significance of cold-seep communities — a case study from the Sea of Okhotsk. Deep-Sea Res., Part I 50, 1391–1409.

Schmaljohann, R., Flügel, H.J., 1987. Methane-oxidizing bacteria in Pogonophora. Sarsia 72, 91–98.

Schmaljohann, R., Faber, E., Whiticar, M.J., Dando, P.R., 1990. Co-existence of methane- and sulphur-based endosymbioses between bacteria and invertebrates at a site in the Skegerrak. Mar. Ecol., Prog. Ser. 61, 119–124.

Sellanes, J., Quiroga, E., Neira, C., 2008. Megafauna community structure and trophic relationships at the recently discovered Concepción methane seep area, Chile, ~36°S. ICES J. Mar. Sci. 65, 1102–1111.

Sibuet, M., Olu, K., 1998. Biogeography, biodiversity and fluid dependence of deep-sea cold-seep communities at active and passive margins. Deep-Sea Res., Part II 45, 517–567.

Sommer, S., Linke, P., Pfannkuche, O., Bowden, D.A., Haeckel, M., Greinert, J., Thurber, A.R., 2008. Novel cold seep habitat along the Hikurangi Margin (New Zealand). Geophys. Res. Abstr. 10 (EGU2008-A-02387).

Sommer, S., Pfannkucke, O., Linke, P., Luff, R., Greinert, J., Drews, M., Gubsch, S., Pieper, M., Poser, M., Viergutz, T., 2006. Efficiency of the benthic filter: biological control of the emission of dissolved methane from sediments containing shallow gas hydrates at Hydrate Ridge. Glob. Biogeochem. Cycles 20, GB2019. doi:10.1029/2004GB002389.

Sommer, S., Linke, P., Pfannkuche, O., Treude, T., Niemann, H., 2009-this issue. Carbon flow through a novel seep habitat dominated by dense beds of ampharetid polychaetes. Marine Geology.

Southward, E.C., Schulze, A., Gardiner, S.L., 2005. Pogonophora (Annelida): form and function. Hydrobiologia 235/236, 227–251.

Summons, R.E., Jahnke, L.L., Roksandic, Z., 1994. Carbon isotopic fractionation in lipids from methanotrophic bacteria: relevance for interpretation of the geochemical record of biomarkers. Geochim. Cosmochim. Acta 58, 2853–2863.

Taylor, M.W., Radax, R., Steger, D., Wagner, M., 2007. Sponge-associated microorganisms: evolution, ecology, and biotechnological potential. Microbiol. Mol. Biol. Rev. 71, 295–347.

Treude, T., Boetius, A., Knittel, K., Wallmann, K., Jørgensen, B.B., 2003. Anaerobic oxidation of methane above gas hydrates at Hydrate Ridge, NE Pacific Ocean. Mar. Ecol. Prog. Ser. 264, 1–14.

Tryon, M.D., Brown, K.M., 2001. Complex flow patterns through Hydrate Ridge and their impact on seep biota. Geophys. Res. Lett. 28, 2863–2866.

Tryon, M.D., Brown, K.M., 2004. Fluid and chemical cycling at Bush Hill: implications for gas- and hydrate-rich environments. Geochem. Geophys. Geosyst. 5, 1–7.

Vacelet, J., Boury-Esnault, N., Fiala-Medioni, A., Fisher, C.R., 1995. A methanotrophic carnivorous sponge. Nature 377, 296.

Valentine, D.L., 2002. Biogeochemistry and microbial ecology of methane oxidation in anoxic environments: a review. Antoine van Leeuwenhoek 81, 271–282.

Van Dover, C.L., 2007. Stable isotopes in the study of marine chemosynthetic based ecosystems: an update. In: Michener, R., Lajtha, K. (Eds.), Stable Isotopes in Ecology and Environmental Sciences (Ecological Methods and Concepts). Wiley-Blackwell Scientific Publications, London, pp. 202–237.

Van Dover, C.L., Aharon, P., Bernhard, J.M., Caylor, E., Doerries, M., Flickinger, W., Gilhooly, W., Goffredi, S.K., Knick, K.E., Macko, S.A., Rapoport, S., Raulfs, E.C., Ruppel, C., Salerno, J.L., Seitz, R.D., Sen Gupta, B.K., Shank, T., Turnipseed, M., Vrijenhoek, R., 2003. Blake Ridge methane seeps: characterization of a soft-sediment chemosynthetically based ecosystem. Deep-Sea Res., Part I 50, 281–300.

Wallmann, K., Linke, P., Suess, E., Bohrmann, G., Sahling, H., Schlüter, M., Dählmann, A., Lammers, S., Greinert, J., von Mirbach, N., 1997. Quantifying fluid flow, solute mixing and the biogeochemical turnover at cold vents on the eastern Aleutian subduction zone. Geochim. Cosmochim. Acta 61, 5209–5219.

Wegener, G., Niemann, H., Elvert, M., Hinrichs, K.U., Boetius, A., 2008. Assimilation of methane and inorganic carbon by microbial communities mediating the anaerobic oxidation of methane. Environ. Microbiol. 10, 2287–2298.

Whiticar, M.J., 1999. Carbon and hydrogen isotope systematics of bacterial formation and oxidation of methane. Chem. Geol. 161, 291–314.

Ziebis, W., Haese, R.R., 2005. Interactions between fluid flow, geochemistry, and biogeochemical processes at methane seeps. In: Kristensen, E., Haese, R.R., Kostka, J.E. (Eds.), Interactions Between Macro- and Microorganisms in Marine Sediments. Coastal and Estuarine Studies, vol. 60. American Geophysical Union, Washington, DC, pp. 267–298.

This chapter, in full, is a reprint from a 2010 issue of Marine Geology (Thurber AR, Kröger K, Neira C, Wiklund H, Levin LA, 2010. Stable isotope signatures and methane use by New Zealand cold seep benthos. Marine Geology. 272:260-269.) The dissertation author was the primary investigator and author of this material.

CHAPTER 3.

MICROBES, MACROFAUNA, AND METHANE: THE IMPORTANCE OF AEROBIC METHANOTROPHY IN FUELING A HIGH-BIOMASS, METHANE SEEP INFAUNAL COMMUNITY

Abstract

During the discovery and description of seven New Zealand methane seeps an infaunal assemblage dominated by ampharetid polychaetes was found. Here we ask: (1) if this habitat has a unique community composition compared to other New Zealand seep communities; (2) how does its density and biomass compare to other seep habitats from around the globe; (3) what type of chemoautotrophic microbes fuel this heterotrophic community. Multivariate analysis of total assemblage data revealed that unlike the other macro-infaunal assemblages sampled, the 'ampharetid-bed community' composition exhibited between sample homogeneity, independent of location, highlighting the distinctness of this community. The ampharetid-bed macrofaunal community reached a maximum density of 84,000 individuals m^{-2} and 274 grams m^{-2} wet biomass, both this density and mass are among the greatest known from deep-sea methane seeps. Through application of a mixing model based on species-specific isotopic composition and mass, combined with published respiration measurements, we estimate that this community consumes 34-106 mmol C m^{-2} day^{-1} of methane-fueled biomass; 340 times the carbon produced by anaerobic methane oxidizers in these ampharetid beds. A fatty-acid biomarker approach indicated that microbial biomass derived from the aerobic oxidation of methane fuels much of this metazoan community. As methane flux from the sediment which harbors this community reached twice that of other seep habitats we suggest this community is a model system to study the influence of metazoan grazing on microbially-mediated biogeochemical cycles.

Introduction

Bacteria and Archaea provide key ecosystem services in the ocean from fixing carbon to mitigating the release of the green-house gas methane from our continental margins (Treude et al. 2003; Boetius and Suess 2004; Sommer et al. 2006). These services are especially important at deep-sea cold seeps where methane-fueled chemosynthetic production supports unique metazoan communities, adding to the biodiversity of our margins (Sibuet and Olu 1998; Cordes et al. 2010). Yet our understanding of the interplay among metazoan fauna, microbial population structure and the biogeochemical processes which the microbes facilitate is still in its infancy. Although recent advances have identified how symbiont-bearing fauna impact the sediment-microbial community (Cordes et al. 2005; Dattagupta et al. 2008), the effects of heterotrophic fauna, or "top-down forcing" on seep microbial communities remains largely unknown. Recently a unique seep assemblage with abundant ampharetid polychaetes was discovered off of New Zealand (NZ). Initial studies found methane-derived carbon to fuel this infaunal assemblage, providing a pertinent system to study how metazoan food webs interact with microbial communities and production (Thurber et al. 2010). We build upon the initial reports of this assemblage though evaluating if this seep habitat forms a unique community and identifying what microbial processes fuel this infaunal assemblage.

Sedimented cold seeps consist of a mosaic of distinct habitats commonly identified by faunal groups, including microbial mats, vesicomyid clam beds, frenulate fields, mussel beds, and tubeworm bushes that differ in geochemistry and microbial and metazoan community composition (Sahling et al. 2002; Treude et al. 2003; Boetius and Suess 2004; Orphan 2004; Levin 2005; Cordes et al. 2010). Bacterial mats are fueled by the greatest flux of methane (up to 100 mmol m^{-2} d^{-1}; Tryon and Brown 2001; Torres et al. 2002; Levin et al. 2003; Sommer et al. 2010) whereas clam beds have comparatively reduced and/or oscillating fluid flow (0.2-1.1

mmol m^{-2} d^{-1}; Tryon and Brown 2001; Levin et al. 2003; Sommer et al. 2006) and frenulate fields have even lower methane flux rates (<0.7 mmol m^{-2} d^{-1}; Sommer et al. 2009). Comparable data do not exist for tubeworm bushes or mussel beds. This methane-based energy is respired initially through a syntrophic partnership between anaerobic methane-oxidizing archaea and sulfate-reducing bacteria, resulting in hydrogen-sulfide production (Boetius et al. 2000; Orphan et al. 2001; 2002). This sulfide is aerobically oxidized by large sheath-forming bacteria of the genera *Beggiatoa* or *Thioploca* in addition to a variety of other bacteria. Methane that is not consumed through an anaerobic processes is respired aerobically by both free-living and symbiotic bacteria. Together with the anaerobic methane oxidizers, these aerobic methane oxidizing bacteria mitigate the release of methane by forming the "sediment filter" (Murase and Frenzel 2007; Sommer et al. 2006; Ding and Valentine 2008). Although both aerobic and anaerobic processes remove methane, the dominant sink for methane is thought to be anaerobic (Truede et al. 2003; Linke et al. 2005).

In addition to distinct chemical environments, each of the seep habitats supports a unique metazoan community composed of species that can tolerate these productive but physiologically stressful habitats. Microbial mats are fueled by mmol levels of sulfide formed by the anaerobic oxidation of methane occurring deeper within the sediment (Boetius et al. 2000; Orphan et al. 2002; Sahling et al. 2002; Truede et al. 2003; Levin et al. 2003). Sulfide is a compound that is toxic to many eukaryotic taxa (Bagarinao 1992; Somero et al. 1989). This leads to communities dominated by those fauna that can tolerate this chemical stress, including dorvilleid, capitellid, and ampharetid polychaetes, and vesicomyid bivalves (Sahling et al. 2002; Levin et al. 2003; Levin et al. 2010). The reduced chemical stress in clam beds, partially ameliorated by the bioirrigation of vesicomyid bivalves, allows species that are not as tolerant of sulfide to inhabit these communities; here species from the background community overlap with seep specialists (Levin et al. 2003; 2010). Together this creates macrofaunal

community patterns within the sediment that reflect the biogeochemical, fluid flow, and microbial environment (Sahling et al. 2002; Levin 2005; Olu Le Roy 2007; Menot et al. 2010). As these communities consume the diversity of chemoautotrophic bacteria, and potentially archaea, within the sediment, identifying which prokaryotes are consumed by the heterotrophic metazoan community provides insight into the dominant form of chemical cycling that occurs within the sediment.

The main technique that has been used to identify the type of chemosynthesis-based energy consumed by these communities is stable isotopic analysis (Conway et al. 1994) although fatty acid (FA) analysis can provide additional information as to the diet of different species (Dalsgaard et al. 2003). Due to enzymatic preferential incorporation of Carbon 12 over 13, both metabolic substrate and fixation pathways impart a unique although sometimes overlapping carbon isotopic signature (Conway et al. 1994). When organic matter is consumed its signature is retained in its consumer's tissue with a small trophic enrichment of carbon 13, resulting in a biomarker that can resolve dietary sources. This technique has been successfully used to identify metazoan use of chemosynthetic production (e.g. Levin and Michener 2002; Eller et al. 2005; Deines et al. 2007). Yet the relative importance of specific metabolic substrates are difficult to resolve since in many cases an intermediate value can either be indicative of a mixed diet of two sources or a third source entirely. Fatty acid signatures offer an alternative technique for studying food web linkages (Daslgaard et al. 2003). Constituents of bacterial and eukaryotic lipids, FAs have characteristic branching and bonding patterns that loosely follow taxonomic lineages within producers, and are either incorporated directly from heterotroph diets or are synthesized by the heterotrophs along known pathways. Importance of bacterial production or recycling has been demonstrated through the lipid signature within organisms (Kharlamenko et al. 2001; Howell et al. 2003; Hudson et al. 2004; Kiyashko et al. 2004; Thurber 2007). This technique has received less use in cold-seep ecosystems (but see

MacAvoy et al. 2003; 2005; Van Gaever et al. 2009), but has demonstrated species- and location- specific use of differential sources of microbial production at hydrothermal vents (Pond et al. 1997; Rieley et al. 1999; Colaco et al. 2007).

A variety of methane seeps were recently discovered along the New Zealand margin (Baco et al. 2010; Greinart et al. 2010) but microbial mats were conspicuously absent; instead ampharetid polychaete beds were found in areas of the most intense seepage (Naudits et al. 2010; Sommer et al. 2006). In the ampharetid beds, local methane flux was more than double that previously observed in any seep community (Sommer et al. 2006). Metazoans present gained between 6 and 100 percent of their energy from methane-derived carbon (Thurber et al. 2010), which, with the high rate of methane flux, suggest that these ampharetid beds may be a unique community both in its microbial fueling and its metazoan composition. In this study we describe the faunal composition of the macroinvertebrate community within this habitat and couple FA analysis to an isotopic, mass-based model to answer the questions:

a) Does the species assemblage present within these ampharetid beds form a unique seep habitat on the New Zealand Margin?
b) What microbial processes fuel these ampharetid bed communities?

Methods

Sample collection and processing

Methane seep habitats were sampled during RV Tangaroa (Cruise TAN-0616; 5-18 November 2006) and RV Sonne (Cruise SO191-3; 22 February- 14 March, 2007) at 7 sites along NZ's North Island (Figure 3.1; Table 3.1). Together 7 sites at three different locations were sampled by a total of 22 "blind" and video-guided multicore deployments between 662 m and 1172 m water depth. These samples were used to quantify community abundance and similarity, faunal stable-isotopic and FA composition. Blind cores sampled a continuum

between seep and non-seep samples and video-guided multiple corers targeted ampharetid-bed communities exclusively. Between one and three cores from each successful multicore deployment were preserved in 8% formalin. The top 5cm was vertically fractioned into 0-1, 1-2, 2-3, 3-5 cm layers and preserved unsieved. Three remaining sediment fractions, 5-7, 7-10, and 10-20 cm, were sieved on a 300−μm mesh prior to preservation. After return to the laboratory, all sediment sections were sieved on a 300-μm sieve and sorted to the lowest possible taxon.

Additional cores from those collections, as well as samples from multicore deployments that did not yield quantitative samples, were sieved on a 300-μm sieve and sorted live at sea. Individuals from these cores were placed in 25-μm filtered seawater overnight to allow gut evacuation. They were then placed in pre-weighed tin boats for isotopic analysis or cryovials for FA analysis before being frozen at -20^{o}C or -80^{o}C. Treatment of isotopic samples is described in Thurber et al. (2010) and samples were analyzed on either on a Eurovector elemental analyzer interfaced with a continuous flow Micromass Isoprime isotope ratio mass spectrometer at Washington State University or with a Thermo Finnigan Delta XP Plus with a Costech 4010 Elemental Analyzer at the Scripps Institution of Oceanography analytical facility. Isotope ratios are expressed as $\delta^{13}C$ or $\delta^{15}N$ in units of per mil (‰). Standards were Pee Dee Belemnite for $\delta^{13}C$ and nitrogen gas for $\delta^{15}N$ (atmospheric). Samples for lipid extraction were placed in pre-cleaned glass vials, frozen and then extracted following the method of Lewis et al. (2000) as specified in Thurber (submitted). Blanks were run concurrently with all samples and solvents were ACS grade or better. Due to the small biomass of all samples, Gas Chromatography- Mass Spectrometry was used to measure FA composition due to its increased sensitivity. This means that whereas comparisons of relative FA composition within this study are valid, they cannot be directly compared to FA composition in other studies. Peaks were identified using a combination of dimethyl-disulfide

adduct formation (Nichols 1986), comparison to known standards (as in Chapter 4), and using mass spectra. Analysis of peak area was performed using Xcaliber © software (Thermo scientific) based on total spectra and manually checked to confirm accurate peak extent.

Data analysis

Community composition and fatty acid composition of individuals of different assemblages were used to identify assemblage differences among sites or diet differences among fauna. In both instances multidimensional analysis, based on Bray-Curtis similarity, was used to identify groups within both community (abundance) and FA data sets. Abundance data (square root transformed) and FA data (log(x+1) transformed) were separately put through the SIMPROF routine in Primer (ver. 6) to identify distinct groupings. The maximum similarity cutoff was identified that resulted in significantly different "groups", as identified by analysis of similarity (ANOSIM). This resulted in groupings defined by the community or FA composition that can then be used to identify driving factors for community or FA pattern, independent of *a priori* ideas of what factors may be driving the species distribution. SIMPER analysis was used to identify which taxa or FA drove the groupings identified by the combined SIMPROF and ANOSIM approach. Where replication was sufficient, an Analysis of Variance (ANOVA) test was run on factors that the BVSTEP routine identified as correlated with the community or FA patterns. A Tukey post-hoc test identified pair-wise differences and homogeneity of variance was tested graphically.

For two cores species-specific biomass was measured to allow estimates of the rate of microbial methane oxidation required to fuel these communities. Formalin-fixed samples were sorted to putative species placed on pre-weighted nitex screen and blotted to remove excess water before being weighed. In small samples, triplicate measurements were made with re-wetting in between, which lead to reproducible results. Putative species were identified at sea

for samples destined for isotope analyses. Resulting data allowed application of a two-source mixing model to estimate the amount of methane-derived carbon used by this community. For those species lacking isotope data, the mean core average was used. The mixing model employed uses wide-ranging end points that constrain likely maximum and minimum estimates of methane derived carbon, as discussed in Thurber et al. (2010). We used the respiration rate of ampharetids as a proxy for whole community respiration rate, as measured by Sommer et al. 2010. This was combined with species-specific estimates of methane-derived carbon, to model the amount of methane-derived microbial carbon consumed by this community on a per meter and daily bases, assuming 100% trophic efficiency.

Results

The Ampharetid Bed Community

A total of 10,406 individuals were collected from 18 quantitative multicore deployments from 7 sites (Table 3.1). We used these samples to test if the ampharetid bed fauna formed a unique habitat (i.e. a seep community that was homogeneous in composition independent of location). This is the same approach used to identify clam beds and microbial mats as unique communities at other seep locations (Sahling et al. 2002). To do this we used the most stringent similarity cutoff within the SIMPROF routine that resulted in groupings of community data based on Bray-Curtis similarity which were all significantly different from each other as tested by ANOSIM. In this case a 40% similarity cut off resulted in four distinct assemblages that were different (Figure 3.2 ANOSIM $p<0.05$). Within these groupings, Group A was the most unique and was always more than 61% dissimilar from the remaining assemblages (SIMPER, Table 3.2). The main component that separated Group A from the remaining groups was the abundance of ampharetids (SIMPER, Table 3.2). Based on the distribution of these samples we found that with a “definition” of ampharetid beds as having

greater than 2400 ampharetids m^{-2} caused almost all of the "ampharetid bed" cores to fall within this Group A. Two nuances of this classification were that from Station 259, two of the three cores had less than 400 ampharetids m^{-2}, yet were included within Group A. The third core had 15000 ampharetids per m^{-2} and so this multicorer likely spanned the edge of the bed, and collected samples that were similar in fauna but not dominated by ampharetids. The other station that seemed to span the edge of a bed was station 242 where the ampharetid densities from each core within a single drop were 127, 2419 , and 7000 ampharetids m^{-2}. Only one of these three cores fell in Group A. We treated all multicore deployments that collected more than this 2400 ampharetids m^{-2} cut off as ampharetid beds, as each core within a drop is a psuedoreplicate of the other, and thus should not be treated as a separate community. As shown in the MDS plot, location did not explain the distribution of data points even though 9 of the 21 pair-wise site comparisons did result in significant differences (ANOSIM $p<0.01$). These within-site differences did not result in a difference ($p = 0.092$) between the southern sites (North Tower, South Tower, Takahe) and the northern sites (those remaining). From this we conclude that the ampharetid beds were a unique community amongst those habitats we sampled on the New Zealand margin.

The ampharetid beds were dominated by two novel species, each belonging to a different and novel genus, of the polychaete family Ampharetidae. Mean macrofaunal density was 58000 individuals m^{-2} with the ampharetids making up an average of 21000 individuals m^{-2}. In the densest macrofaunal sample, the infaunal community reached 84000 individuals m^{-2}, where 33000 of those individuals were ampharetids. The second two most abundant polychaete families within this community were Dorvilleidae and Spionidae, which had mean abundances of 7400 individuals m^{-2} and 1700 individuals m^{-2}, respectively. More abundant than either of these two polychaete taxa in the ampharetid beds were cumaceans and a variety of species of gammarid amphipod, with mean densities of 8300 and 8400 individuals m^{-2}.

Together these five taxa made up 84 % of the individuals within the ampharetid bed community.

The ampharetids formed tubes that extended greater than 10cm into the sediment but 92% of the community was found in the top 5 cm of sediment (Figure 3.3). The majority of the community is composed of surface-deposit feeders, including the ampharetids themselves, and 60% of the community was collected in the 0-1cm fraction. Yet ampharetids, as well as cumaceans and gammerid amphipods were also found deeper in the sediment; in the case of the amparetids certain individuals were found deeper than 10cm. At the surface, the dorvilleids were not as abundant as either the gammarids or cumaceans but quickly surpassed all but the ampharetids in density, becoming the second most abundant taxa between 1 and 5cm depth (Figure 3.3); 92% of the community was present within these top 5cm of the sediment column. Spionids were relatively evenly distributed throughout and were not limited to the surface, even though the family commonly feeds on surface-deposits and/or suspended material.

Groups B, C, and D were characterized by less dense assemblages and composed of taxa that are more characteristic of deep-sea fauna. Group C had the second highest density of fauna, with a mean of 25,000 individuals m^{-2} and was mostly made up of spionid polychaetes and isopods, with far reduced ampharetid and dorvilleid polychaete density compared to Group A (Table 3.2; 3.3). Group C was also impacted by seepage as this was the only group where filamentous bacteria were identified within the collected samples. Both Group B and Group D had 6000 individuals m^{-2} and differed from each other due to the abundance of oweniid and “unidentified” polychaetes (Table 3.2). In addition Group B had more arthropods than polychaetes whereas Group D was the opposite; Group D had 63% polychaetes.

Fatty acid distribution

Classification by fatty acid analysis also yielded four groups (again labeled A-D) that were significantly different from each other while at the same time indicated differential use of chemosynthetic food sources and methane (Figure 3.4). A total of 69 samples were analyzed from 7 sites, including 5 ampharetid bed stations, from 11 multicore deployments (Table 3.1). Among the 47 Fatty acids that were identified, photosynthetic biomarkers (22:6(n-3); 20:5(n-3); 20:4(n-6); Dalsgaard et al. 2003), sulfate-reducer biomarkers (16:1(n-5); Elvert et al. 2003), and aerobic-methanotrophic biomarkers (16:1(n-8); 16:1(n-6); Bowman et al. 2001) were found (Table 3.4; 3.5). In this case the most stringent similarity cut off that resulted in significantly different groupings was 59% similarity. The main difference between Group C and the remaining groups were the abundant FAs indicative of phytoplanktonic consumption (Table 3.4). Group C also was the most distinct in the 2-D representation of the variables (Figure 3.4), although this was a poor representation of the groupings, as indicated by a stress value of 0.21. Stress values <0.2 are considered to be good representations of the multidimensional data in two dimensions (Clark 1993). Groups A and D were separated by FAs that are not indicative of specific nutritional sources, although 16:1(n-7) and 18:1(n-7) helped identify and differentiate both of these groups. These biomarkers are abundant in sulfide-oxidizing bacteria (McCaffrey et al. 1989), but can also be synthesized by most fauna. The biomarker that contributed to the greatest dissimilarity between Group B and Groups A and D was the aerobic methanotrophic biomarker 16:1(n-8). A combination of site and site-specific isotopic composition of the species correlated with the distribution of these FA samples (BVSTEP/ BIOENV ρ= 0.246, p=0.01), whereas depth was not as important. Further these FA-distinct groupings had carbon isotopic signatures that were significantly different from each other (ANOVA $F_{3,65}$=9.86; p<0.01). Group B was lighter than the remaining three groups and Group D was lighter than Group C, although Group A and Group B and Group A and Group C were not different from each other. Together these lines of evidence indicated

that the FA composition differentiated groups that were mostly fueled by photosynthetic production from the remaining samples (Group C was different from all samples but Group A) and that within the seep, aerobic methanotrophic biomarkers differentiated the grouping, separating those that had the lightest $\delta^{13}C$. The aerobic biomarkers were present in 38 of the FA samples analyzed, which supports the prevalence of aerobic methanotrophy throughout these sampling sites. Notably, even the Group C samples, which were collected from Stations 43 and 84, had fauna with a diet of mainly phytoplanktonic origin, but also with small amounts of aerobic methanotroph biomarkera present within their tissues. These samples were collected from near-seep locations by a 'blind' multicore and could still be under the influence of methane emission.

Species-specific methane-derived carbon estimates identified the importance and magnitude of microbial methanotrophy. Ampharetid-bed macrofaunal biomass was 201 g m^{-2} (Station 261) and 273 g m^{-2} (Station 196). Species-specific isotopic data were available for species representing 88% of the biomass at station 261 and 98% of the biomass from station 196. This allowed species-specific, methane-derived biomass to be calculated using the two-source mixing model of Thurber et al. (2010). Estimates for infaunal biomass derived from methane within the ampharetid beds were 82 - 160 g m^{-2} and 139 - 255 g m^{-2} methane-derived carbon at stations 261 and 196, respectively. We used the respiration rate of the ampharetids (0.29 mmol O_2 g^{-1} min^{-1}, mass in wet weight from Sommer et al. 2010) to estimate the amount of methanotrophic biomass that this community consumes daily. We assumed a 1:1 carbon to oxygen ratio and a 100% assimilation efficiency, to come up with a highly conservative estimate of the amount of methane- derived carbon that this community uses. Although the assumption of 100% assimilation efficiency is not a valid assumption, we chose to err on the side of underestimating methane-derived carbon. Based on these two samples the community

was estimated to consume from 34 to 106 mmol C m^{-2} d^{-1} from methanotrophic bacteria or archaea.

Discussion

A novel seep community

The variety of habitats induced by geochemical heterogeneity at methane seeps act to increase the overall biodiversity on continental margins (Cordes et al. 2010). As such identifying novel seep assemblages is key, not only for characterizing diversity, but providing insight into the underlying mechanisms that drive it. The New Zealand ampharetid beds formed a unique community on the New Zealand margin and had the highest heterotrophic-metazoan density and biomass currently known from methane seeps, adding to its intrigue. Independent of site or location, those samples that contained abundant ampharetid polychaetes had an overall different community composition (Figure 3.2). The species that caused that difference were the ampharetids themselves and dorvilleid polychaetes (Table 3.2), two taxa that typify seep assemblages, and especially microbial mat settings (Sahling et al. 2002; Levin et al. 2003; 2010). This pattern is not unique to New Zealand; ampharetids also drive the differences among seep assemblages in other locations (Menot et al. 2010) and are commonly the most abundant infauna at seeps (Sahling et al. 2002; Levin et al. 2010; Menot et al. 2010; Ritt et al. 2010; Bernadino and Smith 2010). Yet in comparison to these other locations the density of fauna within the New Zealand ampharetid beds is far greater (Figure 3.5). In addition, although only the extreme cases of biomass were measured, these habitats had far greater biomass than any heterotrophic community from soft-sediment seeps currently known (Figure 3.6). Although canyons on the New Zealand margin can exhibit incredibly high benthic biomass (De Leo et al. 2010), the isotopic (Thurber et al. 2010) and FA composition (this study) from within the ampharetid beds demonstrate that neither surface or terrestrial

productivity of this region drive the high seep infaunal abundance. Instead methanotroph-microbial production is fueling this incredibly high-biomass and dense community.

We hypothesize that the abundant oxygen in the water column combined with the engineering role of the ampharetids and ample methane, leads to these remarkable densities. In contrast to areas such as Hydrate Ridge, OR and Eel River, CA which occur either within or below oxygen minimum zones (Levin et al. 2010), having oxygen levels of 0.40-0.47 ml l^{-1} (Sahling et al. 2002) and 0.24-0.48 ml l^{-1} (Levin et al. 2003) respectively, New Zealand's margin is bathed in water with oxygen concentrations of 4.5 ml l^{-1} (Sommer et al. 2010) and does not have a strong oxygen minimum due to the relatively recent ventilation of its water mass. Pointing to the role of oxygen in structuring the benthic fauna of New Zealand ampharetid beds is the abundance of crustaceans, including gammarid amphipods that are uncommon in areas that are oxygen stressed (Levin 2003) yet reached maximum densities of 25,000 ind. m^{-2} in New Zealand (Table 3.3). Ampeliscid amphipods, which were part of this ampharetid-bed community, are sometimes abundant at the lower limit of oxygen minimum zones (Levin 2003), yet they were only a fraction of the amphipod diversity present in the New Zealand ampharetid beds. This greater oxygen allows greater total respiration within the benthic boundary layer leading to the observed high infaunal abundance.

Bioirrigation by ampharetids likely increases the availability of oxygen within the sediment, favoring a deeper distribution of fauna. Microbial mats at Eel River, CA seeps have 91% of their fauna within the top 2 cm likely due to the high levels of sulfide caused by intense AOM deeper within the sediment fueled by high methane flux (Levin et al. 2003). This sulfide also favored low diversity and a fauna that could handle high sulfide concentrations, notably the dorvilleids (Levin et al. 2003). In the ampharetid beds, which were areas of the highest methane flux in New Zealand (Sommer et al. 2010), 92% of the community was relegated to the top 5cm, extending 3 cm deeper into the sediment than the Eel River microbial

mat. The distribution of the ampharetid bed community was more similar to clam beds; clam beds have 29% of their macrofaunal community below 2cm (Levin et al. 2003) and ampharetid beds have 26% of their community below 2cm. This deeper distribution of clam bed fauna is likely due to the bioirrigation of the sediment by the clams. We suggest that the ampharetid beds provide the same ecosystem engineering role that the seep clams provide. Through bioirrigating the sediment, the ampharetids facilitate a deeper distribution of both themselves as well as a spionid and dorvilleid polychaetes, leading to greater access of chemosynthetic nutrition and higher densities for the entire community.

Aerobic Methanotrophy

Further supporting the importance of aerobic processes was the imbalance between carbon demand (macrofaunal methane-derived carbon) and the C production by anaerobic methane oxidizing archaea. A species-specific mixing model, which used wide ranging endpoints to encompass all likely scenarios of isotopic mixing, projected minimum daily methanotroph biomass consumed by these infaunal communities to be 34 or 56 mmol C m^{-2} d^{-1}. These values likely underestimate the actual methane-fueled microbial biomass used by the macrofaunal communities yet were within the measured sediment community total oxygen utilization rate, which reached a maximum of 117 mmol m^{-2} d^{-1} (Figure 3.7; Sommer et al. 2010). By scaling up respiration based on density rather than biomass, Sommer et al. (2010) estimated that the oxygen requirements of the ampharetid community was 30.8 mmol O_2 m^{-2} d^{-1} which is in approximate agreement with our biomass-based estimate, except that our estimate deals in units of methane-derived carbon rather than oxygen. Independent of which of these numbers is accurate, the rate of anaerobic methane oxidation was insufficient to cover the demand of this community; AOM rates measured within these ampharetid beds were 17 mmol C m^{-2} d^{-1} yet the anaerobic methane oxidizing consortia growth rate was only 0.1 mmol

C m^{-2} d^{-1} (Figure 3.7; Sommer et al. 2010). To support the metazoan community through anaerobic methanotrophy, the entire AOM population would have to double twice a day to fulfill our most conservative estimates that is 340 times greater than the growth rate observed. Although sulfate reducing biomarkers were present, providing indications that part of the AOM consortia might be consumed, anaerobic processes were not sufficient to supply the observed methane-derived carbon requirements of macrofaunal biomass within the ampharetid beds.

Biomarkers provided strong support for aerobic methane oxidation as the main source of nutrition for the ampharetid bed community. The FAs present within this community included both 16:1(n-6) and 16:1(n-8) that are found in Type I aerobic methanotrophs (Bowman et al. 2001). In addition, 16:1(n-8) helped to discriminate among the FA groupings matching the lightest carbon isotopic signature that was found in Group B (Figure 3.4). Groups A and D of the FA analysis had a diversity of biomarkers present indicating that they were fed by a combination of seep bacteria and potentially Archaea including sulfide oxidizers, sulfate reducers, and aerobic methanotrophs. Although the high concentration of aerobic methanotroph biomarkers differentiated Group B from the other three groups, many of the samples had these biomarkers, just not to the high degree that Group B did. The clear reliance on methane-based biomass from the isotopic analysis combined with the abundance of aerobic methanotroph biomarkers suggest that members of this community consume aerobic methanotrophs but the diversity of other biomarkers indicate that this community is not composed of species which are aerobic methanotroph specialists. This microbial metabolism is the dominant nutritional source for the infaunal community.

This aerobic methanotrophic-fueled community co-occurred with the highest measures of methane flux reported to date. The methane flux, which reached a maximum of 264 mmol CH_4 m^{-2} d^{-1}, is more than double any measured methane emission currently known

(Sommer et al. 2010). While this methane provided sufficient methane reactants to support the microbial growth used by the metazoan community (Figure 3.7), this unique confluence of methane emission and aerobic methanotroph-fueled biomass raises the question of whether the consumption of these methanotrophs by ampharetids caused the increased methane release, either through top-down forcing on the aerobic methanotrophs themselves or by ampharetid tubes acting as conduits that, combined with bioirrigation, facilitate methane release from sediments into the water column.

In addition, bioirrigation may alter the microbial processes within the sediment in a form of "bacterial farming". Shallow water infauna use this technique to cultivate bacteria within their burrow walls leading to increased carbon fixation through hypothesized nitrogen based chemoautotrophic production (Reichardt 1988). Although ampharetids form tubes rather than burrows, the role of the increased surface area caused by their tubes may favor aerobic processes, especially in light of the high water column oxygen content. The ampharetids themselves were not the only group that used this aerobic methanotrophic biomass (Table 3.5) and it is possible that they facilitate transfer of this chemosynthetic energy to the rest of the fauna present within the beds. It is unknown whether the underlying geological forcing favors aerobic processes due to high methane flux rates that exceed that capacity of anaerobic processes or whether the bioirrigation of the ampharetids drives the unexpected aerobic-methane oxidation rate.

The importance of aerobic methanotrophs in the methane cycle is not unique to New Zealand ampharetid beds. In a recent study, more than 40% of the microbial community within a hydrocarbon seep microbial mat at Coal Point, CA was composed of aerobic methanotrophs, which had the same (n-6) and (n-8) biomarkers observed here (Ding and Valentine 2008). At Håkon Mosby Mud Volcano, another well oxygenated seep setting, nematodes consumed aerobic methanotrophic production (Van Gaever et al. 2003). In rice

paddies, aerobic methanotrophs are preferentially grazed upon by protists (Murase and Frenzel 2007). Yet it remains unknown how consumption of aerobic methanotrophs impacts the biogechemical cycling and methane emission at each of these locations. The New Zealand ampharetid beds, due to their increased methane emission, present a model system to study whether infauna consume the sediment filter and thus enhance the release of methane into the overlying water column and potentially our atmosphere.

Conclusions

In this study we described a community whose abundance and biomass is among the densest infaunal methane-seep communities known. The ampharetid-dominated community is largely fueled by methane-derived carbon and aerobic methane-oxidizing biomarkers are widespread, both of which highlight the importance of aerobic methanotrophy providing energy to this novel community. As this community co-occurs with the highest rate of methane emission currently known, it provides a model system for future studies on the impact of grazing on methane cycling in sediments. This newly described ampharetid bed habitat is one more example of how methane seeps add to the overall biodiversity present on our continental margins.

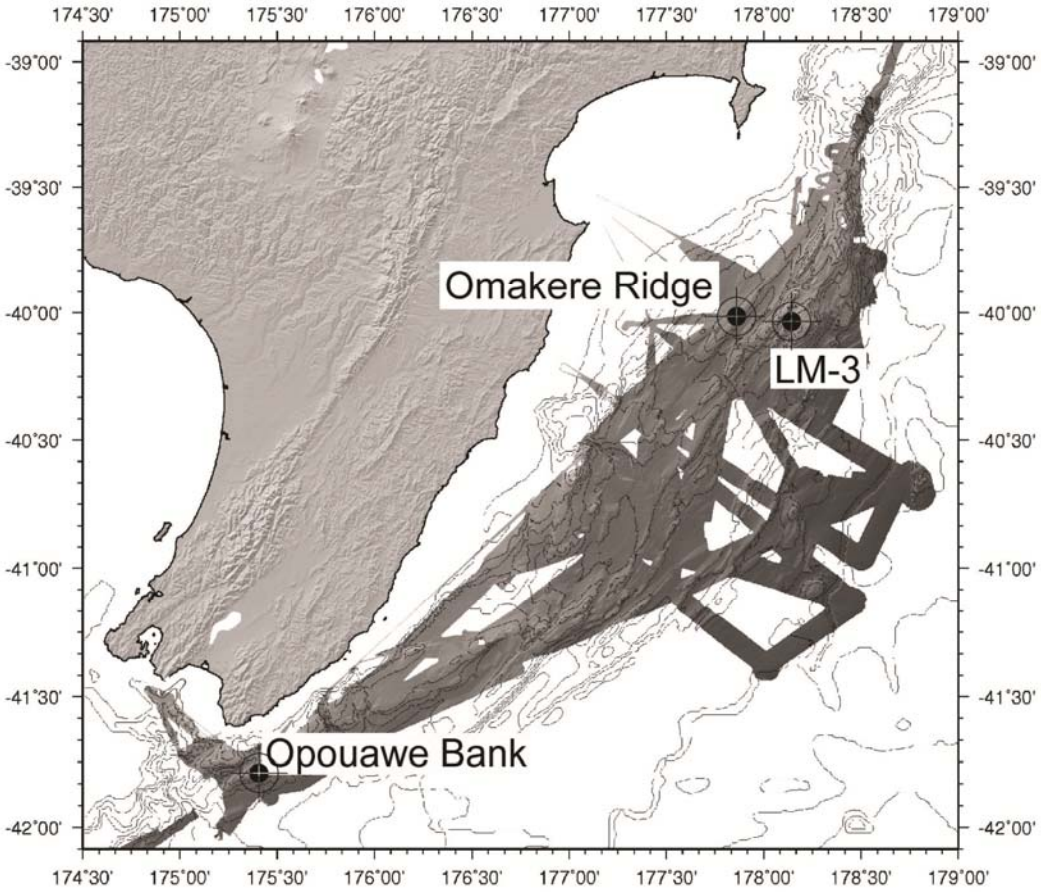

Figure 3.1 Sampling locations of methane seeps off the North Island, New Zealand

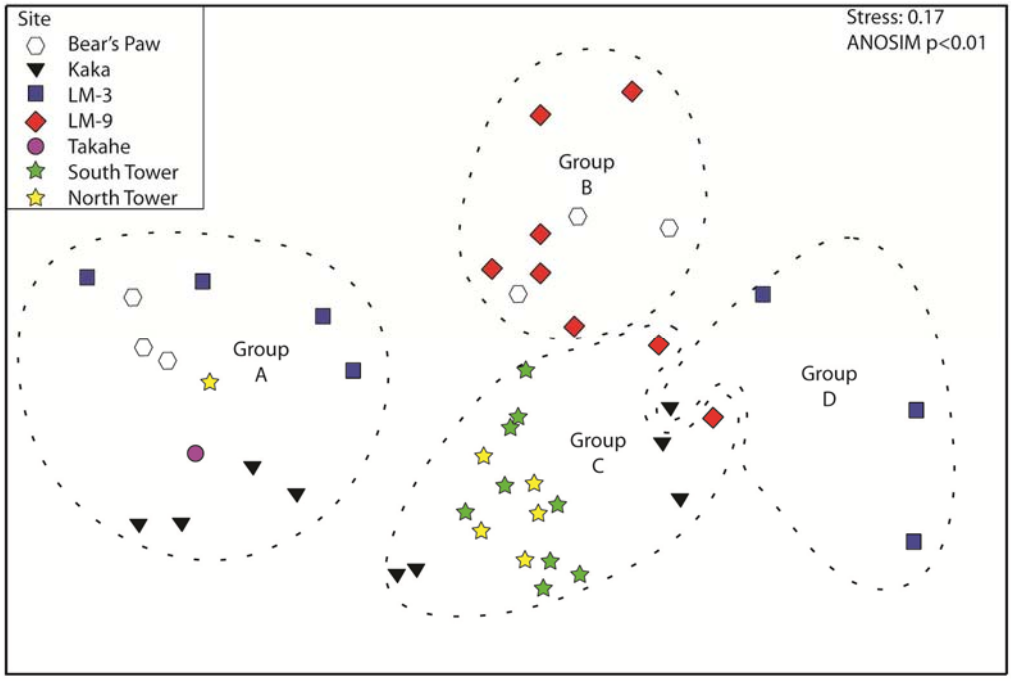

Figure 3.2 A 2D representation of the similarity of New Zealand methane-seep infaunal communities. Significant different groupings as tested by an analysis of similarity (ANOSIM) are indicated by dotted lines.

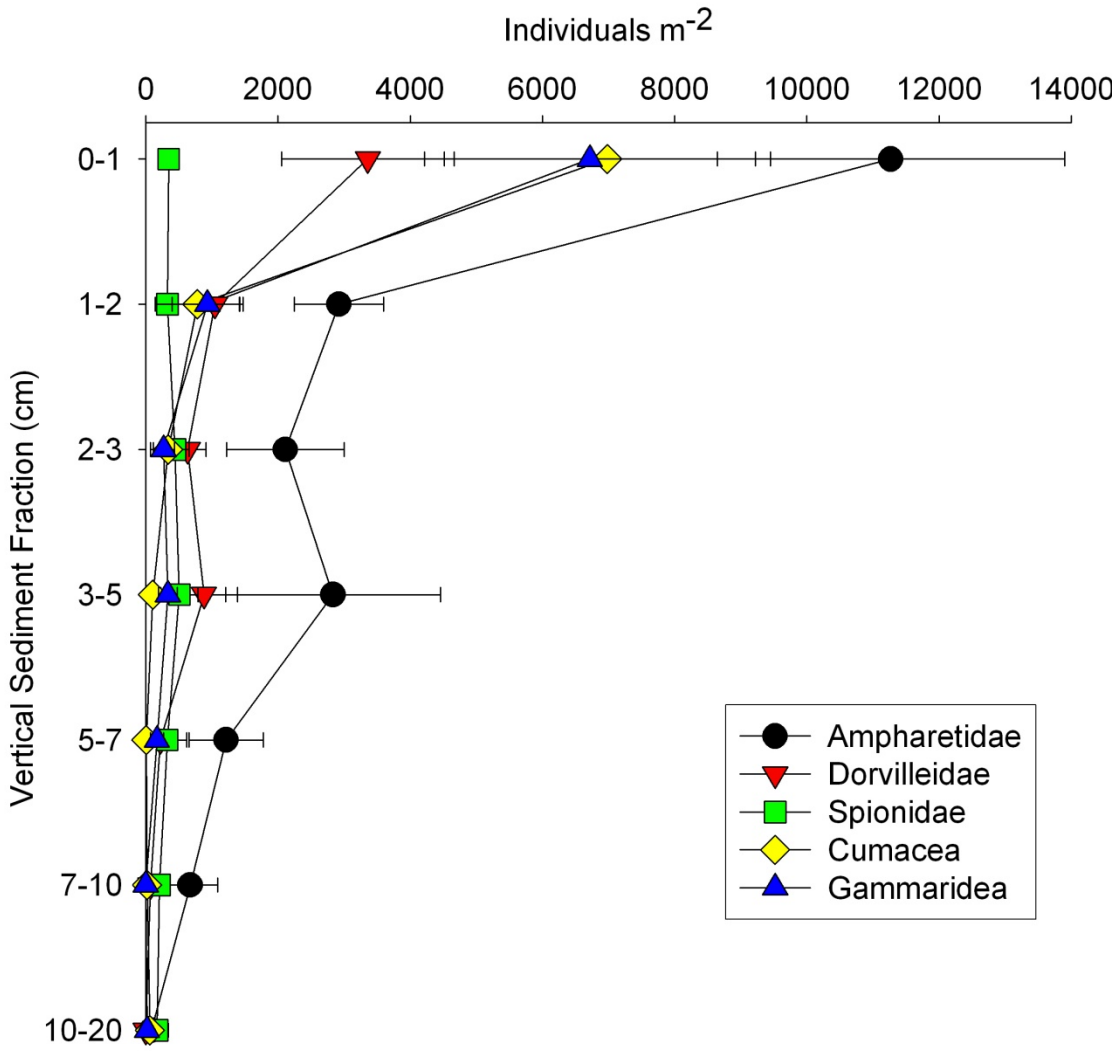

Figure 3.3 Vertical distribution of dominant taxa within ampharetid bed communities.

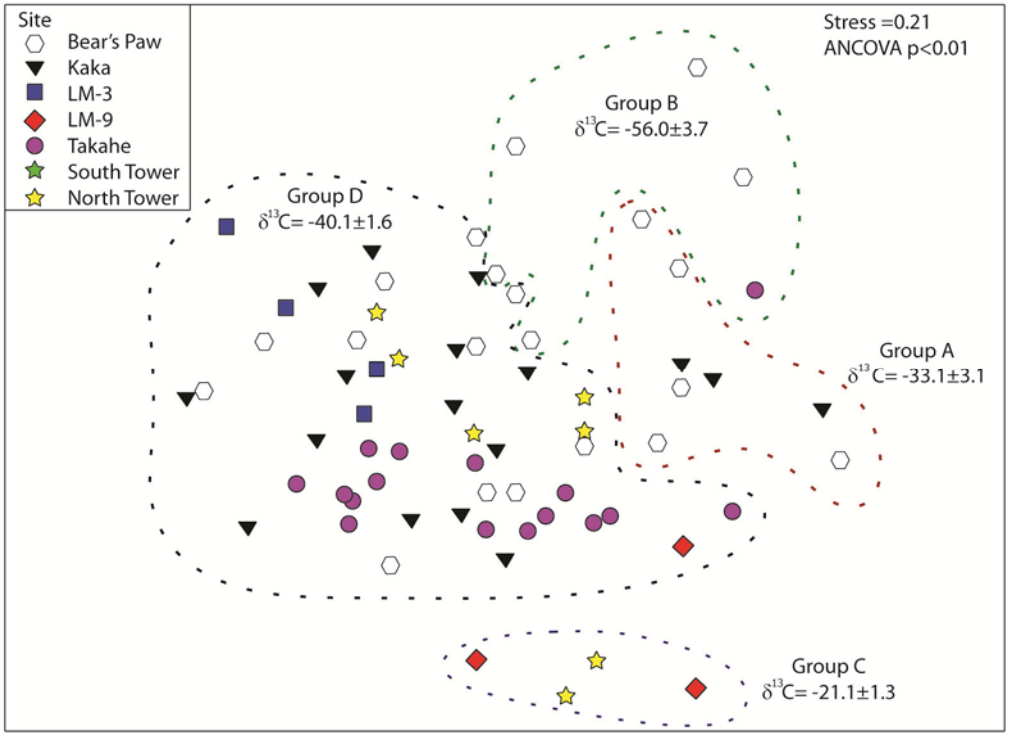

Figure 3.4 A 2D representation of the similarity among fatty acid samples. Significantly different groupings, as tested by an analysis of similarity (ANOSIM), are indicated by dotted lines. Mean isotopic composition for each group are given.

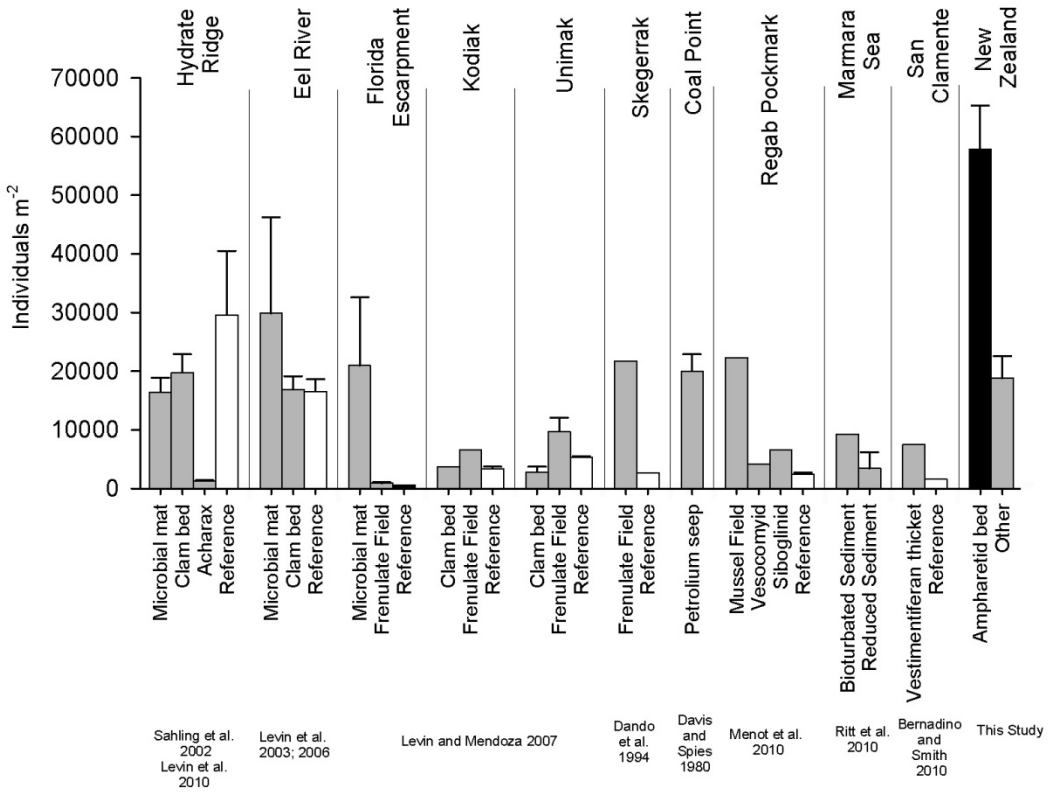

Figure 3.5 Ampharetid bed macrofaunal abundance compared to other methane seep communities. For Hydrate Ridge all abundances are from Levin et al. (2010) except for "Acharax" which is from Sahling et al. (2002) since Levin et al. (2010) used the same size sieve as the present study and is thus more comparable.

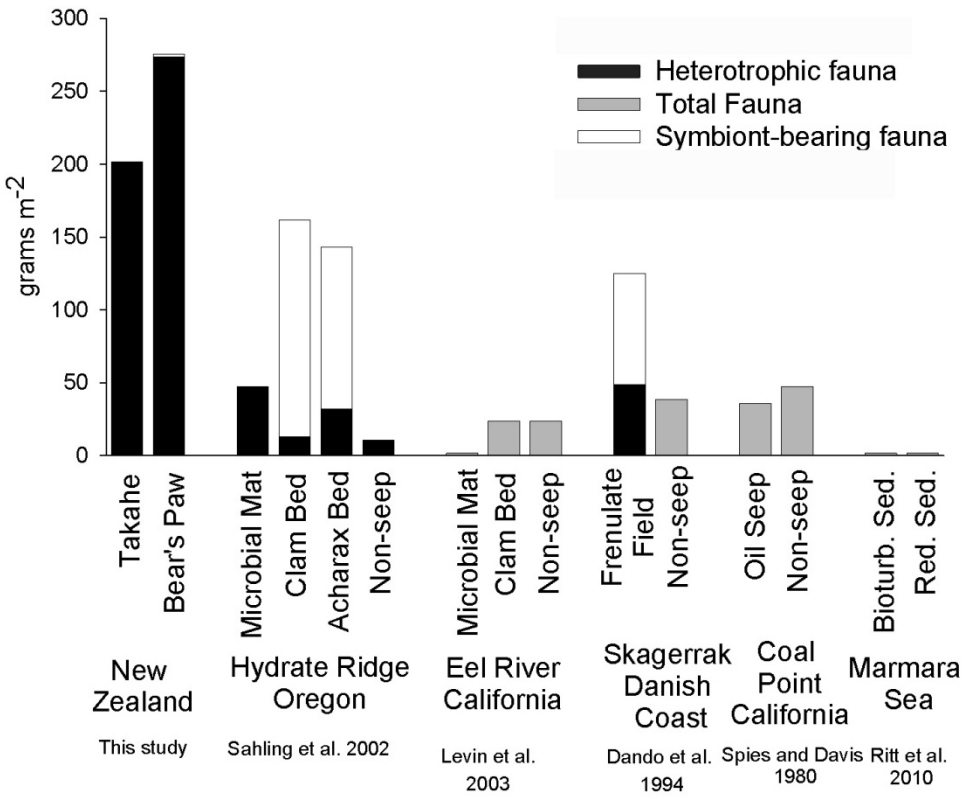

Figure 3.6 Wet-weight biomass of ampharetid bed communities from New Zealand in comparison to other seep infaunal communities. Grey bars indicate a combination of heterotrophic and symbiont bearing (chemosynthetic) fauna. Bioturb. Sed. = Bioturbated Sediment; Red. Sed. = Reduced sediment.

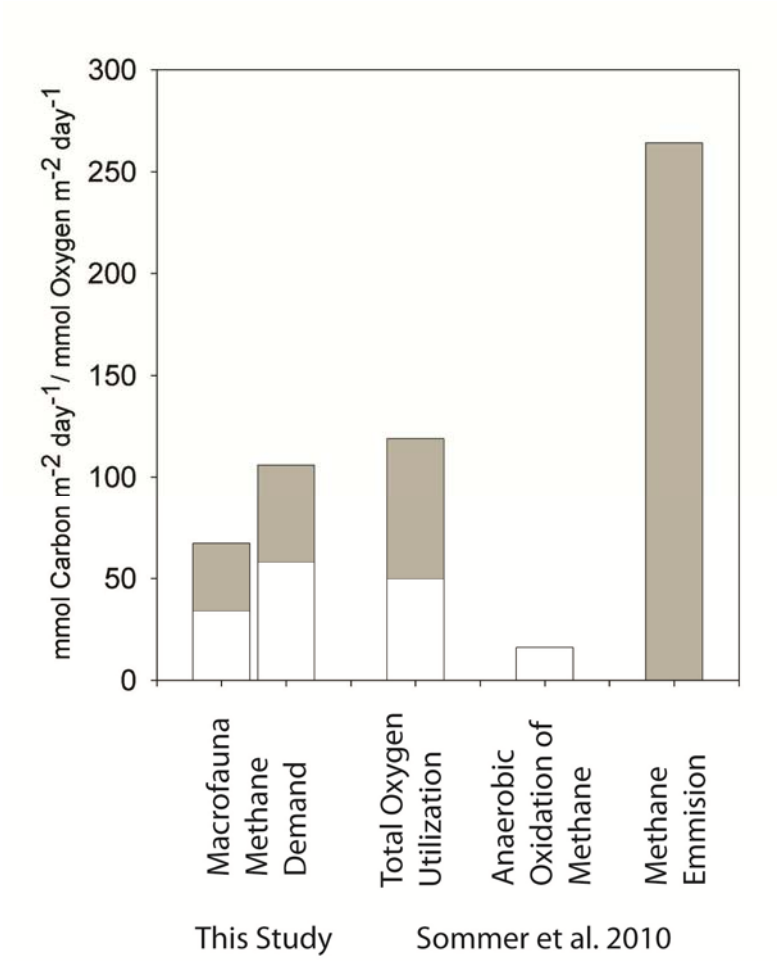

Figure 3.7 Macrofaunal methane demand from two ampharetid beds in comparison to the total oxygen utilization, standing stock of anaerobic oxidation of methane (Note: growth rate of was 0.1 mmol C m-2 day-1) and maximum methane emission from ampharetid bed communities. White bar indicates minimum estimate and grey bar indicates maximum conservative estimate.

Table 3.1 Study locations, sites, macrofaunal density, number of fatty acid (FA) analysis run from each site. Mean carbon stable isotopic signature with standard error and sample size given, and the wet-weight biomass of two samples. Sites in bold are ampharetid bed sites and those in italics had a subset of the samples collected belonging to the "non-seep" habitat.

Location	Site	Station	Density	FA	Stable isotopic signature	Mass
			n m^{-2}	n	$\delta^{13}C$ ± SE (n)	g m^{-2}
Omekere Ridge	LM-9	*46*		3	-25.7 ± 1.2 (12)	
	LM-9	49	6,585		-23.8 ± 1.6 (3)	
	LM-9	54	12,131			
	LM-9	57	7,380		-30.5 ± 2.0 (19)	
	Kaka	**261**	74,527	8	-35.6 ± 1.9 (28)	201
	Kaka	262	9,040			
	Kaka	**242**	40,871	5	-29.5 ± 0.9 (31)	
	Kaka	*232*		5	-33.2 ± 1.7 (15)	
	Bear's paw	186	5,602	2	-37.6 ± 1.8 (13)	
	Bear's paw	195		4	-44.3 ± 3.1 (8)	
	Bear's paw	**196**	58,357	16	-46.4 ± 1.6 (45)	273
LM-3	LM-3	**216**	33,486	4	-52.5 ± 1.7 (21)	
	LM-3	**259**	39,980			
	LM-3	260	5,645			
Opouawe bank	North Tower	84	14,848	2	-19.4 ± 0.6 (9)	
	North Tower	86	34,027		-24.7 ± 1.3 (11)	
	North Tower	112	28,266		-20.6 ± 0.9 (21)	
	North Tower	**290**	49,274	6	-48.7 ± 3.1 (12)	
	North Tower	291	39,725			
	South Tower	116	29,157		-27.2 ± 1.1 (11)	
	Takahe	*309*		17	-37.9 ± 1.0 (64)	
	Takahe	**315**	84,034			

Table 3.2 SIMPER results indicating which macrofaunal taxa differentiated the groupings identified in Figure 2. Polychaete* indicates that the family was not identifiable.

	Group A		Group B		Group C		Group D	
Group A	**Σ Similarity**	**55**	**Σ Dissimilarity**	**73**	**Σ Dissimilarity**	**69**	**Σ Dissimilarity**	**80**
	Ampharetidae	30	Ampharetidae	20	Ampharetidae	15	Ampharetidae	17
	Gammeridae	18	Cumacea	10	Cumacea	8	Cumacea	11
	Cumacea	15	Dorvilleidae	10	Dorvilleidae	7	Dorvilleidae	9
	Dorvilleidae	12	Gammeridae	9	Gammeridae	5	Gammeridae	9
Group B			**Σ Similarity**	**49**	**Σ Dissimilarity**	**61**	**Σ Dissimilarity**	**68**
			Tanaidacea	16	Spionidae	7	Oweniidae	9
			Cumacea	12	Gammeridae	5	Polychaete*	5
			Gammeridae	12	Bivalve	4	Cumacea	4
			Isopoda	11	Paraonidae	4	Hesionidae	4
			Spionidae	10				
Group C					**Σ Similarity**	**51**	**Σ Dissimilarity**	**68**
					Spionidae	13	Spionidae	6
					Tanaidacea	10	Oweniidae	5
					Gammeridae	9	Gammeridae	5
					Isopoda	7	Tanaidacea	4
Group D							**Σ Similarity**	**52**
							Oweniidae	20
							Polychaete*	13
							Paraonidae	8
							Spionidae	8

Table 3.3 Composition of infaunal communities along the New Zealand margin. Group A is the ampharetid bed community. Number of cores are given in parentheses and standard error among cores (not stations) is given.

		Group A (13)	Group B (9)	Group C (20)	Group D (4)
Annelida	Ampharetidae	21,126 ± 3,418	42 ± 45	191 ± 121	127 ± 52
	Amphinomidae	529 ± 255	42 ± 45	777 ± 356	0 ± 0
	Capitellidae	725 ± 353	127 ± 78	280 ± 132	64 ± 37
	Chaetopteridae	0 ± 0	14 ± 21	0 ± 0	0 ± 0
	Cirratulidae	10 ± 10	283 ± 182	293 ± 67	191 ± 82
	Cossuridae	39 ± 22	42 ± 45	414 ± 181	0 ± 0
	Dorvilleidae	7,414 ± 2,101	42 ± 32	108 ± 50	0 ± 0
	Fauvelopsidae	0 ± 0	28 ± 28	45 ± 45	0 ± 0
	Flabelligeridae	0 ± 0	28 ± 28	70 ± 25	64 ± 37
	Glyceridae	108 ± 50	28 ± 28	471 ± 104	64 ± 37
	Hesionidae	0 ± 0	14 ± 21	178 ± 31	382 ± 201
	Hirunidae	0 ± 0	14 ± 21	19 ± 14	0 ± 0
	Lumbrineridae	10 ± 10	71 ± 65	108 ± 27	0 ± 0
	Magelonidae	0 ± 0	0 ± 0	0 ± 0	32 ± 32
	Maldanidae	20 ± 13	113 ± 67	204 ± 47	32 ± 32
	Nephtyidae	0 ± 0	42 ± 32	6 ± 6	0 ± 0
	Nereididae	10 ± 10	28 ± 42	13 ± 13	0 ± 0
	Oligochaeta	0 ± 0	325 ± 276	605 ± 162	0 ± 0
	Onuphidae	0 ± 0	0 ± 0	19 ± 14	64 ± 37
	Opheliidae	10 ± 10	113 ± 50	815 ± 124	0 ± 0
	Orbiniidae	323 ± 126	28 ± 28	204 ± 52	64 ± 64
	Oweniidae	0 ± 0	0 ± 0	45 ± 19	1,401 ± 238
	Paraonidae	617 ± 444	127 ± 71	1,789 ± 784	255 ± 74
	Phyllodocidae	0 ± 0	71 ± 46	19 ± 10	0 ± 0
	Pisionidae	0 ± 0	14 ± 21	0 ± 0	0 ± 0
	Polynoidae	29 ± 15	57 ± 56	153 ± 38	64 ± 37
	Sabellidae	10 ± 10	85 ± 45	38 ± 16	95 ± 95
	scale worm	0 ± 0	14 ± 21	25 ± 20	0 ± 0
	Scalebrigmatid	0 ± 0	0 ± 0	45 ± 17	0 ± 0
	Siboglinidae	372 ± 301	14 ± 21	242 ± 102	0 ± 0
	Sphaerodoridae	0 ± 0	0 ± 0	51 ± 17	0 ± 0
	Spionidae	1,655 ± 595	467 ± 146	4,074 ± 644	350 ± 150
	Sternaspidae	0 ± 0	0 ± 0	6 ± 6	0 ± 0
	Syllidae	78 ± 68	325 ± 153	102 ± 35	95 ± 95
	Terrebellidae	0 ± 0	42 ± 45	64 ± 28	0 ± 0
	Trichobranchidae	0 ± 0	0 ± 0	32 ± 13	0 ± 0
	unknown	49 ± 31	28 ± 28	318 ± 101	573 ± 82
	Polychaete unid.	0 ± 0	0 ± 0	19 ± 10	95 ± 61
	Total Polychaete	**33,134 ± 4,272**	**2,674 ± 695**	**11,841 ± 1,599**	**4,011 ± 483**
Arthropoda	Acari	0 ± 0	14 ± 21	0 ± 0	0 ± 0
	Caprellidea	0 ± 0	0 ± 0	6 ± 6	0 ± 0
	Copepoda	353 ± 155	57 ± 65	306 ± 147	0 ± 0
	Crustacea unid.	0 ± 0	0 ± 0	19 ± 14	32 ± 32
	Cumacea	9,765 ± 2,749	665 ± 293	547 ± 145	95 ± 61
	Decapoda unid.	10 ± 10	0 ± 0	0 ± 0	0 ± 0
	Gammeridea	8,707 ± 1,946	637 ± 242	2,655 ± 528	255 ± 127
	Isopoda	539 ± 166	552 ± 230	1,095 ± 180	191 ± 82
	Ostracoda	69 ± 59	0 ± 0	439 ± 116	95 ± 61
	Pycnogoinida	20 ± 13	0 ± 0	0 ± 0	0 ± 0
	Stomatopoda	10 ± 10	0 ± 0	0 ± 0	0 ± 0
	Tanaidacea	852 ± 432	905 ± 284	2,165 ± 384	191 ± 64
	Total Arthropoda	**20,323 ± 3,565**	**2,829 ± 754**	**7,232 ± 893**	**859 ± 246**

Table 3.3 cont.

		Group A (13)	Group B (9)	Group C (20)	Group D (4)
Echinodemata	Asteroidea	0 ± 0	0 ± 0	6 ± 6	0 ± 0
	Echinoidea	0 ± 0	0 ± 0	19 ± 14	0 ± 0
	Holothuroidea	0 ± 0	99 ± 89	70 ± 42	0 ± 0
	Ophiuroidea	0 ± 0	57 ± 65	83 ± 36	64 ± 37
	Total Echnidermata	**0 ± 0**	**156 ± 94**	**178 ± 49**	**64 ± 37**
Mollusca	Aplacophora	59 ± 49	57 ± 46	95 ± 34	0 ± 0
	Bivalve	206 ± 88	99 ± 126	1,038 ± 159	95 ± 32
	Patellogastropoda	59 ± 27	0 ± 0	0 ± 0	0 ± 0
	Prosobranchia	1,175 ± 742	14 ± 21	51 ± 17	95 ± 32
	Scaphopoda	0 ± 0	14 ± 21	185 ± 64	0 ± 0
	Solemyidae	88 ± 44	0 ± 0	95 ± 58	0 ± 0
	Total Mollusca	**1,587 ± 761**	**184 ± 135**	**1,464 ± 165**	**191 ± 37**
Protista	Foraminifera	20 ± 20	0 ± 0	1,305 ± 512	64 ± 64
	Bathysiphon	0 ± 0	0 ± 0	688 ± 279	0 ± 0
	Gromidae	10 ± 10	28 ± 28	1,210 ± 404	32 ± 32
	Xenophyophora	0 ± 0	0 ± 0	127 ± 69	159 ± 95
	Total Protists	**29 ± 21**	**28 ± 28**	**3,330 ± 789**	**255 ± 156**
Other	Filamentous Bacteria	0 ± 0	0 ± 0	121 ± 96	0 ± 0
	Chaetognatha	0 ± 0	14 ± 21	0 ± 0	0 ± 0
	Cnidaria	0 ± 0	28 ± 42	76 ± 46	32 ± 32
	Hydrozoa	0 ± 0	0 ± 0	57 ± 33	0 ± 0
	Nematoda	206 ± 112	0 ± 0	223 ± 185	0 ± 0
	Nemertea	1,420 ± 401	396 ± 275	579 ± 129	127 ± 74
	Phoronida	0 ± 0	0 ± 0	6 ± 6	255 ± 214
	Platyhelminthes	10 ± 10	0 ± 0	6 ± 6	0 ± 0
	Porifera	0 ± 0	0 ± 0	6 ± 6	414 ± 373
	Priapulid	0 ± 0	0 ± 0	6 ± 6	0 ± 0
	Sipunculid	20 ± 13	28 ± 42	25 ± 15	0 ± 0
	Other	0 ± 0	0 ± 0	115 ± 76	64 ± 37
All Fauna	**SUM**	**56,728 ± 4,784**	**6,338 ± 1,204**	**25,267 ± 2,494**	**6,271 ± 700**

Stations: Group A = 196, 242, 261, 216, 259; Group B = 186, 49, 57; Group C = 262, 54, 84, 86; 112. 116, 291; Group D = 262, 260.

Table 3.4 SIMPER results indicating which fatty acids differentiated the groupings identified in Figure 4.

	Group A		Group B		Group C		Group D	
Group A	**Σ Similarity**	**69**	**Σ Dissimilarity**	**41**	**Σ Dissimilarity**	**46**	**Σ Dissimilarity**	**43**
	16:0	16	16:1(n-8)	6	22:6(n-3)	8	20:1(n-13)	7
	18:1(n-7)	16	20:5(n-3)	5	20:4(n-6)	7	18:0	6
	20:5(n-3)	9	16:2a	5	20:1(n-13)	6	20:5(n-3)	6
	16:1(n-7)	9	16:1	5	18:0	5	22:1(n-9)	5
Group B			**Σ Similarity**	**67**	**Σ Dissimilarity**	**48**	**Σ Dissimilarity**	**43**
			16:0	13	22:6(n-3)	7	16:1(n-8)	6
			16:1(n-7)	13	16:1(n-7)	6	16:1(n-7)	5
			18:1(n-7)	10	20:5(n-3)	6	16:2a	5
			18:0	8	16:1(n-8)	5	16:2b	5
Group C					**Σ Similarity**	**67**	**Σ Dissimilarity**	**43**
					16:0	15	22:6(n-3)	9
					20:5(n-3)	13	20:5(n-3	8
					18:0	12	20:4(n-6)	7
					18:1(n-7)	10	20:1	5
Group D							**Σ Similarity**	**66**
							16:0	21
							18:0	15
							18:1(n-7)	13
							18:1(n-9)	9

Table 3.5 Fatty acid (FA) and stable isotopic composition of each of the different fatty acid clusters. Percent of FA is given for those FAs which made up more than 1% in any sample. grey shading indicates aerobic methanotroph biomarkers, red indicates sulfate reducing bacteria biomarkers, and green indicates phytoplanktonic biomarkers.

	Group A	Group B	Group C	Group D
$\delta^{13}C$	-33.2 ± 3.1	-56.0 ± 3.7	-21.1 ± 1.3	-40.9 ± 1.6
14:0	2.3 ± 0.6	2.0 ± 0.4	1.4 ± 1.0	3.0 ± 0.4
14Ca	0.0 ± 0.0	0.1 ± 0.1	0.5 ± 0.3	0.0 ± 0.0
14Cb	0.0 ± 0.0	0.0 ± 0.0	0.4 ± 0.4	0.0 ± 0.0
*i*15	0.1 ± 0.1	0.0 ± 0.0	0.0 ± 0.0	0.1 ± 0.1
*a*15	0.0 ± 0.0	0.1 ± 0.1	0.0 ± 0.0	0.0 ± 0.0
15:0	0.3 ± 0.2	0.3 ± 0.1	1.1 ± 0.2	0.2 ± 0.1
16:1a	0.5 ± 0.3	3.4 ± 1.2	0.0 ± 0.0	0.1 ± 0.0
16:1(n-8)	0.4 ± 0.3	4.9 ± 1.0	0.4 ± 0.3	0.3 ± 0.1
16:1(n-7)	6.2 ± 1.4	14.3 ± 1.5	1.9 ± 0.6	4.2 ± 0.5
16:1(n-6)	0.6 ± 0.3	0.6 ± 0.6	0.0 ± 0.0	0.1 ± 0.0
16:2a	1.1 ± 0.5	3.6 ± 1.1	0.0 ± 0.0	0.4 ± 0.1
16:1(n-5)	0.8 ± 0.2	2.2 ± 0.3	0.8 ± 0.4	0.5 ± 0.1
16:2b	0.1 ± 0.1	3.1 ± 0.9	0.0 ± 0.0	0.1 ± 0.0
16:0	21.8 ± 2.5	19.5 ± 4.2	17.3 ± 1.7	34.8 ± 1.5
*i*16(n-5)*	0.0 ± 0.0	0.1 ± 0.0	0.0 ± 0.0	0.2 ± 0.1
*i*17:0	0.3 ± 0.1	0.3 ± 0.2	0.1 ± 0.1	0.0 ± 0.0
17:0	0.3 ± 0.1	0.6 ± 0.2	2.2 ± 0.6	0.3 ± 0.1
18:2a	0.1 ± 0.1	0.1 ± 0.1	0.0 ± 0.0	0.1 ± 0.0
18:2b	0.3 ± 0.1	0.1 ± 0.0	0.0 ± 0.0	0.1 ± 0.0
18:2(n-6)	1.9 ± 0.4	1.0 ± 0.2	0.6 ± 0.3	0.9 ± 0.1
18:1(n-9)	5.9 ± 1.3	8.0 ± 3.7	6.3 ± 3.8	5.9 ± 0.8
18:3	0.0 ± 0.0	0.8 ± 0.6	0.0 ± 0.0	0.1 ± 0.1
18:1(n-7)	24.5 ± 4.9	8.5 ± 1.6	7.5 ± 1.9	11.0 ± 0.8
18:2c	4.5 ± 2.0	2.5 ± 0.5	0.5 ± 0.2	1.4 ± 0.3
18:1(n-5)	5.1 ± 2.1	0.9 ± 0.3	1.0 ± 0.5	2.1 ± 0.4
18:2d	0.3 ± 0.1	0.6 ± 0.4	0.0 ± 0.0	0.2 ± 0.1
18:0	3.0 ± 0.7	7.7 ± 2.0	13.6 ± 4.5	12.8 ± 0.6
cycl18w9,10	0.4 ± 0.2	0.4 ± 0.2	1.1 ± 0.7	0.2 ± 0.1
19:0	0.0 ± 0.0	0.0 ± 0.0	0.1 ± 0.1	0.0 ± 0.0
20:4(n-6)	0.0 ± 0.0	0.5 ± 0.4	6.3 ± 2.8	0.6 ± 0.1
20:5(n-3)	8.3 ± 1.6	3.4 ± 1.9	15.6 ± 4.8	3.9 ± 0.6
20:2(n-9)	0.7 ± 0.3	0.2 ± 0.1	0.1 ± 0.1	0.0 ± 0.0
20:3a	0.0 ± 0.0	0.2 ± 0.1	0.2 ± 0.2	0.4 ± 0.1
20:1(n-13)	3.9 ± 0.9	2.1 ± 1.0	0.0 ± 0.0	0.0 ± 0.0
20:1(n-9)	0.0 ± 0.0	0.9 ± 0.4	2.0 ± 1.3	2.0 ± 0.3
20:1a	3.5 ± 0.5	0.6 ± 0.2	4.2 ± 2.4	1.3 ± 0.2
20:2b	0.2 ± 0.2	0.1 ± 0.1	0.0 ± 0.0	0.3 ± 0.1
20:0	0.0 ± 0.0	0.2 ± 0.1	0.0 ± 0.0	0.2 ± 0.0
15i-?	0.0 ± 0.0	0.1 ± 0.1	0.4 ± 0.2	0.1 ± 0.0
Unknown	0.5 ± 0.3	0.2 ± 0.1	0.0 ± 0.0	0.0 ± 0.0
22:6(n-3)	0.3 ± 0.3	0.3 ± 0.3	8.8 ± 3.8	0.5 ± 0.2
20:2c	0.1 ± 0.1	0.5 ± 0.3	0.2 ± 0.1	0.2 ± 0.1
20:2d	0.6 ± 0.2	1.9 ± 0.9	2.6 ± 1.4	3.4 ± 0.8
Unknown	0.3 ± 0.3	0.1 ± 0.1	0.0 ± 0.0	4.5 ± 0.9
22:1(n-9)	0.0 ± 0.0	2.2 ± 1.3	0.5 ± 0.3	2.5 ± 0.3
cyclo22	0.0 ± 0.0	0.0 ± 0.0	0.1 ± 0.1	0.4 ± 0.3
22:1a	0.0 ± 0.0	0.0 ± 0.0	0.5 ± 0.3	0.1 ± 0.0

Group A: Ampharetidae sp. 1; *Ophryotrocha platykephale*(3); Parougia sp. 1(1); Gammarid sp. 1; Gammarid sp. 2; Sheath forming bacteria. **Group B:** Cumacea (2); Gammarid sp. 3; Orbiniid sp.1 (3). **Group C:** Lumbrinerid sp.1; Nemertean; Oligochaeta sp.1; Spionid sp.1. **Group D:** Isopoda sp.1; Ampharetidae sp. 2 (6); Ampharetidae sp. 1 (7); Amphinomidae sp. 1 (2); Aplacophora sp.1; *Capitella* sp.; Cumacea (4); Gammarid sp. 3; Maldanid; Spionidae sp.2; Nemertean; *O. platykephale* (3); Orbiniidae sp.1 (3): *Parougia* sp. 1 (4); *Parougia* sp. 2; Dorvilleid sp. 1 (2); Spionid sp.3; Gammarid sp. 1 (3); Scale worm; Gammarid sp. 2; Spionid sp.4 (3); Gammarid sp. 4 (2).

References

Baco AR, Rowden AA, Levin LA, Smith CR, Bowden DA (2010) Initial characterization of cold seep faunal communities on the New Zealand Hikurangi margin. Mar Geol 272:251-259

Bagarinao R (1992) Sulfide as an environmental factor and toxicant: tolerance and adaptations in aquatic organisms. Aquat Toxicol 24:21-62

Bernadino A, Smith CR (2010) Community structure of infaunal macrobenthos around vestimentiferan thickets at the San Clemente cold seep, NE Pacific. Marine Ecology 31: 608-621.

Boetius A, Suess E (2004) Hydrate Ridge: a natural laboratory for the study of microbial life fueled by methane from near-surface gas hydrates. Chem Geol 205:291-310

Boetius A, Rabenschlag K, Schubert CJ , Richert D, Widdle F, Gieske A, Amann R, Jorgensen BB, Witte U, Pfannkuche O (2000) A marine microbial consortium apparently mediating anaerobic oxidation of methane. Nature 407:623-626

Bowman JP, Skerratt JH, Nichols PD, Sly LI (1991) Phospholipid fatty acid and lipopolysaccharide fatty acid signature lipids in methane-utilizing bacteria. FEMS Microbiol Ecol 85:15– 22

Clark KR (1993) Non-parametric multivariate analyses of changes in community structure. Austral J Ecol 18:117-143

Colaco A, Desbruyeres D, Guezennec J (2007) Polar lipid fatty acids as indicators of trophic associationsin deep-sea vent system community. Mar Ecol 28:15-24

Conway N, Kennicutt II M, Van Dover C (1994) Stable isotopes in the study of marine chemosynthetic based ecosystems. In: Lajtha K, Michener R, editors. Stable isotopes in ecology and environmental sciences. London: Blackwell. pp. 158–186.

Cordes EE, Hourdez S, Predmore BL, Redding ML, Fisher CR (2005) Succession of hydrocarbon seep communities associated with the long-lived foundation species *Lamellibrachia luymesi*. Mar Ecol Prog Ser 305: 17-29.

Cordes EE, Cunha MR, Galéron J, Mora C, Olu-Le Roy K, et al. (2010) The influence of geological, geochemical, and biogenic habitat heterogeneity on seep biodiversity. Mar Ecol 31: 51-65.

Dalsgaard J, St John M, Kattner G, Müller-Navarra D, Hagen W (2003) Fatty acid trophic markers in the pelagic marine environment. Adv Mar Biol 46:225–340

Dattagupta S, Arther MA, Fisher CR (2008) Modification of sediment geochemistry by the hydrocarbon seep tubeworm *Lamellibrachia luymesi:* a combined empirical and modeling approach. Geochim Cosmochim Acta 72:2298-2315

De Leo FC, Smith CR, Rowden AA, Bowden DA, Clark MR (2010) Submarine canyons: hotspots of benthic biodiversity and productivity in the deep sea. Proc R Soc B 277:2783-2792

Deines P, Bodelier PLE, Eller G (2007) Methane-derived carbon flows through methane-oxidizing bacteria to higher trophic levels in aquatic systems. Environ Microbiol 9:1126-1134

Ding H, Valentine DL (2008) Methanotrophic bacteria occupy benthic microbial mats in shallow marine hydrocarbon seeps, Coal Oil Point, California. J Geo Res 113:1-11 doi: 10.1029/2007JG000537

Eller G, Deines P, Grey J, Richnow HH, Kruger M (2005) Methane cycling in lake sediments and its influence on chironomid larval $\delta^{13}C$. FEMS Microbial Ecol 54:339-350

Elvert M, Boetius A, Knittel K, Jorgensen BB (2003) Characterization of specific membrane fatty acids as chemotaxonomic markers for sulfate-reducing bacteria involved in anaerobic oxidation of methane. Geomocrbiol J 20:403-419

Greinert J, Lewis KB, Bialas J, Pecher IA, Rowden A, Bowden DA, De Batist M, Linke P (2010) Methane seepage along the Hikurangi margin, New Zealand: Overview of studies in 2006 and 2007 and new evidence from visual, bathymetric and hydroacoustic investigations. Mar Geol 272:6-25.

Howell KL, Pond DW, Billett DSM, Tyler PA (2003) Feeding ecology of deep-sea seastars (Echinodermata:Asteroidea):a fatty-acid biomarker approach. Mar Ecol Prog Ser 225:193-206

Hudson IR, Pond DW, Billett DSM, Tyler PA, Lampitt RS, Wolff GA (2004) Temporal variations in fatty acid composition of deep-sea holothuruans: evidence of bentho-pelagic coupling. Mar Ecol Prog Ser 281:109-120Kharlamenko et al. 2001

Kharlamenko VI, Kiyashko SI, Imbs AB, Vyshkvartzev DI (2001) Identification of food sources of invertebrates from the seagrass *Zostera marina* community using carbon and sulfer stable isotope ratio and fatty acid analysis. Mar Ecol Prog Ser 220:103-117

Kiyashko SI, Imbs AB, Narita T, Svetashev VI, Wada E (2004) Fatty acid composition of aquatic insect larvae *Stictochironomus pictulus* (Diptera: Chironomidae): evidence of feeding upon methanotrophic bacteria. Comp Biochem Physiol B 139:705-711

Levin LA (2003) Oxygen minimum zone benthos: adaptation and community response to hypoxia. Oceanogr Mar Biol Ann Rev 41:1-45.

Levin LA (2005) Ecology of cold seep sediments: interactions of fauna with flow, chemistry and microbes. Oceanogr Mar Biol Ann Rev 43:1-46

Levin LA, Michener R (2002) Isotopic evidence of chemosynthesis-based nutrition of macrobenthos:the lightness of being at Pacific methane seeps. Limnol Oceanog 47:1336–1345

Levin LA, Ziebis W, Mendoza G, Growney V, Tryon M, Brown K, Mahn C, Gieskes J, Rathburn A (2003) Spatial heterogeneity of macrofauna at northern California

methane seeps: the influence of sulfide concentration and fluid flow. Mar Ecol Prog Ser 265:123–139

Levin LA, Mendoza GF, Gonzalez JP, Thurber AR, Cordes EE (2010) Diversity of bathyal macrofauna on the northeastern Pacific margin: the influence of methane seeps and oxygen minimum zones. Mar Ecol 31:94-110

Lewis T, Nichols PD, McMeekin TA (2000) Evaluation of extraction methods for recovery of fatty acids from lipid-producing microheterotrophs. J Microbiol Methods 43: 107-116

Linke P, Wallmann K, Suess E, Hensen C, Rehder G (2005) In situ benthic fluxes from an intermittently active mud volcano at the Costa Rica convergent margin. Earth Planet Sci Lett 235:79-95

MacAvoy SE, Fisher CR, Carney RS, Macko SA (2005) Nutritional associations among fauna at hydrocarbon seep communities in the Gulf of Mexico. Mar Ecol Prog Ser 292:51-60

MacAvoy SE, Macko SA, Carney RS (2003) Links between chemosynthetic production and mobile predators on the Louisiana continental slope: stable carbon isotopes of specific fatty acids. Chem Geol 201:229-237

McCaffrey MA, Farrington JW, Repeta DJ (1989) Geochemical implications of the lipid composition of *Thioploca spp*. from the Peru upwelling region – 15^{o}S. Org Geochem 14:61–68

Menot L, Galéron J, Olu K, Caprais J-C, Crassous P, Khripounoff A, Sibuet M (2010) Spatial heterogeneity of macrofaunal communities in and near a giant pockmark area in the deep Gulf of Guinea. Mar Ecol 31:78-93

Murase J, Frenzel P (2007) A methane-driven microbial food web in a wetland rice soil. Environ Microbiol 9:3025-3034

Naudits L, Greinert J, Poort J, Belza J, Vangampelaere E, Boone D, Linke P, Henriet J-P, De Batist M (2010) Active venting sites on the gas-hydrate-bearing Hikurangi Margin, off New Zealand: Diffusive- versus bubble-released methane. Mar Geol 272:233-250

Nichols PD, Guckert JB, White DC (1986) Determination of monounsaturated fatty acid double-bond position and geometry for microbial monocultures and complex consortia by capillary GC-MS of their dimethyl disulphide adducts. J Microbiol Meth 5:49–55

Olu-Le Roy K, Caprais, J-C, Fifis A, Fabri M-C, Galéron J, Budzinsky H, Le Ménach K, Khripounoff A, Ondréas H, Sibuet M (2007) Cold-seep assemblages on a giant pockmark off West Africa: spatial patterns and environmental control. Mar Ecol 28:115-130

Orphan VJ, Ussler III W, Naehr TH, House CH, Hinrichs K-U, Paull CK (2004) Geological, geochemical, and mucrobiological heterogeneity of the seafloor around methane vents in the Eel River Basin, offshore California. Chem Geol 205:265-289.

Orphan VJ, House CH, Hinrichs KU, Mckeegan KD, Delong EF (2001) Methane-consuming archaea revealed by directly coupled isotopic and phylogenetic analysis. Science 293:484–487

Orphan VJ, House CH, Hinrichs KU, McKeegan KD, DeLong EF (2002) Multiple archaeal groups mediate methane oxidation in anoxic cold seep sediments. Proc Nat Acad Sci USA 99**:**7663–7668

Pond DW, Dixon DR, Bell MV, Fallick AE, Sargent JR (1997) Occurrence of 16: 2(n-4) and 18: 2(n-4) fatty acids in the lipids of the hydrothermal vent shrimps *Rimicaris exoculata* and *Alvinocaris markensis*: nutritional and trophic implications. Mar Ecol Prog Ser 156, 167-174

Reichardt W (1988) Impact of bioturbation by *Arenicola marina* on microbiological parameters in intertidal sediments. Mar Ecol Prog Ser 44:149-158

Rieley G, Van Dover CL, Hedrick DB, Eglinton G (1999) Trophic ecology of *Rimicaris exoculata*: combined lipid abundance/stable isotope approach. Mar Biol 133:495–499

Ritt B, Sarrazin J, Caprais J-C, Noël P, Gauthier O, Pierre C, Henry P, Desbruyères D (2010) First insights into the structure and environmental setting of cold-seep communities in the Marmara Sea. Deep-Sea Res I 57:1120-1136

Sahling H, Richert D, Lee RW, Linke P, Suess E (2002) Macrofaunal community structure and sulfide flux at gas hydrate deposits from the Cascadia convergent margin, NE Pacific. Mar Ecol Prog Ser. 231:121-138

Sibuet M, Olu K (1998) Biogeography, biodiversity and fluid dependence of deep-sea cold-seep communities at active and passive margins. Deep-Sea Res II 45: 517-567.

Somero GN, Childress JJ, Anderson AE (1989) Transport, metabolism, and detoxification of hydrogen sulfide in animals from sulfide-rich marine environments. Aquatic Sci 1:591-614

Sommer S, Linke P, Pfannkucke O, Schleicher T, Schneider v. Deimling J, Reitz A, Haeckel M, Flogel S, Hensen C (2009) Seabed methane emission and the habitat of frenulate tubeworms on the Captain Arutyunov mud volcano (Gulf of Cadiz). Mar Ecol Prog Ser 382:69-86

Sommer S, Linke P, Pfannkucke O, Neimann H, Truede T (2010) Benthic respiration in a seep habitat dominated by dense beds of ampharetid polychaetes at the Hikurangi Margin (New Zealand). Mar Geol 272: 223-232

Sommer S, Pfannkucke O, Linke P, Luff R, Greinert J, Drews M, Gubsch, Pieper M, Poser M, Viergutz (2006) Efficiency of the benthic filter:Biological control of emission of dissolved methane from sediments containing shallow gas hydrates at Hydrate Ridge. Global Biogeochem Cycles. 20:1-14. doi:10.1029/2004GB002389

Thurber AR (2007) Diets of Antarctic sponges: links between the pelagic microbial loop and benthic metazoan food web. Mar Ecol Prog Ser 351:77-89

Thurber AR (Submitted) Diet-dependant incorporation of biomarkers: Biases associated with food-web studies using stable isotopic and fatty acid analysis. Oecologia.

Thurber AR, Kröger K, Neira C, Wiklund H, Levin LA (2010) Stable isotope signatures and methane use by New Zealand cold seep benthos. Mar Geol 272:260-269

Torres ME, McManus J, Hammond DE, de Angelis MA, Heeschen KU, Colbert SL, Tryon MD, Brown KM, Suess E (2002) Fluid and chemical fluxes in and out of sediments hosting methane hydrate deposits on Hydrate Ridge, OR. Earth Planet Sci Lett 201:525-540

Truede T, Boetius A, Knittel K, Wallmann K, Jørgensen BB (2003) Anaerobic oxidation of methane above gas hydrates at Hydrate Ridge, NE Pacific Ocean. Mar Ecol Prog Ser 264:1-14

Tryon MD, Brown KM (2001) Complex flow patterns through Hydrate Ridge and their impact on seep biota. Geophys Res Lett 28:2863-2866

Van Gaever S, Moodley L, Pasotti F, Houtekamer M, Middelburg JJ, Danovaro R, Vanrousel A (2009) Trophic specialization of metazoan meiofauna at the Håkon Mosby Mud Volcano:fatty acid biomarker isotope evidence. Mar Biol 156:1289-1296

Acknowledgments

We are indebted to (in alphabetical order) Amy Baco, Kerstin Kröger, Peter Linke, Carlos Neira, Olaf Pfannkuche, Craig R. Smith and Stefan Sommer, for making this research possible. We thank Jens Greinert, David Bowden, Angelo Bernardino, Helena Wiklund and the captains, crews, and science parties of RV SONNE-SO191 and RV TANGAROA-TAN0616 for additional assistance at sea. Lipid analysis was made possible due to the kind lending of instrument time by William Gerwick and the support of his lab including Cameron Coates and Jo Nunnery. The map on which Fig. 1 is based was provided courtesy of Jens Greinert. Jennifer Gonzalez assisted tremendously with the sorting of infauna and processing of isotope samples in the laboratory. We thank Bruce Deck (Scripps Institution of Oceanography — SIO) and Ray Lee (Washington State University) for conducting isotopic analyses and the SIO Graduate Office for supplying funding to analyze many of the samples through the SIO analytical facility. Funding was provided by the Sidney E. Frank Foundation,

The Michael M. Mullin Memorial Fellowship and the United States NOAA Office of Exploration Grant Nos.: NA17RJ1231 and NA050AR417076, United States National Science Foundation grant OCE 0425317, OCE-0826254 and OCE-0939557and NIWA Capability Fund project CRFH073 and a University of California Academic Senate to LA Levin and W Gerwick. Chapter 3, in part, is currently being prepared for submission for publication of the material. Thurber, Andrew R.; Levin, Lisa A.; Rowden, Ashley A. The dissertation author was the primary investigator and author of this paper.

CHAPTER 4.

DIET-DEPENDENT INCORPORATION OF BIOMARKERS: IMPLICATIONS FOR FOOD-WEB STUDIES USING STABLE ISOTOPIC AND FATTY ACID ANALYSES

Abstract

Metazoan consumption of Bacteria and Archaea may impact key microbially-mediated processes, yet techniques to quantify these trophic linkages must be evaluated in the laboratory before robust conclusions can be drawn from field observations. In this laboratory-based feeding study, an annelid, *Ophryotrocha labronica*, was raised on eukaryotic, bacterial, or archaeal food sources to test whether current fatty acid and stable isotopic paradigms are appropriate to quantitatively model metazoan consumption of microbial food sources. This annelid's carbon tissue-diet shift, $\Delta^{13}C$ = - 3.6 to +3.6 per mil, was neither zero nor constant, but instead was a function of the $\delta^{13}C$ value and the C:N ratio of the food. Nitrogen isotopic ratio of *O. labronica* was unique for each food source and in all cases was enriched in ^{14}N compared to its food source. $\delta^{15}N$ tissue-diet shifts ranged from -0.8 to -3.0 per mil in contrast to commonly applied values of +2.3 to 3.4 to define a species trophic level. Fatty acid profiles within this species were largely independent of diet. Polyunsaturated fatty acids, commonly used as a metric for phytoplanktonic input and not provided by the food sources, were present in *O. labronica* tissues, potentially indicating the ability of this species to synthesize these fatty acids. Whereas field studies have shown the necessity and utility of these biomarker approaches, tissue-diet shifts based on the literature could erroneously characterize the diet of this species, indicating incorrect carbon source, trophic level, or reliance on certain types of phytoplankton.

Introduction

Understanding energy transfer throughout food webs, from bacteria to top predators, has been an underlying theme of ecology since shortly after the term "food chain" was coined (Elton 1927; Linderman 1942). The discovery that microbial processes, performed by both Archaea and Bacteria provide diverse ecosystem services and facilitate biogeochemical cycling in pelagic (Herndl et al. 2005; Partensky et al. 1999) and benthic realms (Francis et al. 2005; Sommer et al. 2006) has lead to renewed study of top-down forcing on bacterial communities (e.g. Pernthaler 2005; Frias-Lopez et al. 2009). Direct consumption of bacteria has been shown to decrease bacterial productivity (e.g. Lebaron et al. 2001; Spivak et al. 2007), increase bacterial productivity (e.g. Mikola and Setala 1998; Jiang 2007), and shift bacterial community composition (Duffy et al. 2003; Wardle et al. 2004; Spivak et al. 2007). As the role of grazing appears to be system- and species-dependent, quantitative techniques are necessary to allow rapid identification and differentiation of microbial food sources within a larger food web. This will allow recognition of which interactions are critical to ecosystem functioning. Biomarker approaches, including stable isotopic and fatty acid analyses, identify trophic linkages. Yet the laboratory-based experiments do not currently exist that allow accurate interpretation of these analyses when dealing with microbial food sources. In this study we use a species of polychaete belonging to the family Dorvilleidae, which typically inhabits environments rich in Bacteria and Archaea, to test the applicability of biomarker approaches for quantifying bactivory and the consumptions of Archaea within metazoan food webs.

Stable isotopic and fatty acid analysis are two techniques which have the potential to reveal food-web interactions. Animals are thought to preferentially excrete ^{14}N over ^{15}N and respire ^{12}C over ^{13}C leading to a changing isotopic ratio with each successive step within a

food chain (Minagawa and Wada 1974; Peterson and Fry 1987; McCutchan et al. 2003). When these ratios are compared to a standard they are termed $\delta^{15}N$ and $\delta^{13}C$, respectively. In application, the carbon isotopic shift between a species' diet and its tissue, referred to as its tissue-diet shift or $\Delta^{13}C$, is small (between 0 and 1 ‰), making $\delta^{13}C$ indicative of the carbon source at the base of a food web rather than trophic position (DeNeiro and Epstien 1978). $\Delta^{15}N$, the tissue-diet shift for nitrogen, changes with each successive trophic level, providing insight into the food source and trophic level at which a consumer feeds. Since this landmark observation of tissue-diet shifts (Minagawa and Wada 1974; Peterson and Fry 1987), the refinement of $\Delta^{13}C$ and $\Delta^{15}N$ has been the focus of many studies and reviews (e.g. Gannes et al. 1997; Vander Zanden and Rasmussen 2001; Post et al. 2002; McCutchan et al. 2003). Most consider food chains based on photosynthetic primary producers. Accurate measure of $\Delta^{13}C$ and $\Delta^{15}N$ is key to using isotopic data to construct the quantitative models now employed to identify energy flow and trophic linkages (e.g. Phillips and Koch 2002; Schmidt et al. 2007; van Oevelen et al. 2010), but few test the isotope shifts that result from microbial food sources.

Fatty acid analysis is based on the underlying knowledge that many fatty acids (FAs), constituents of lipids including cell membranes that vary by carbon length, double-bond position and branching pattern, are incorporated from food items as it is energetically favorable to *de novo* synthesis. Many food sources have either unique FAs or a unique distribution of FAs which can be traced into a consumer's tissue (Dalsgaard et al. 2003). Although FA analysis has been applied qualitatively to trophic questions (e.g. Pond et al. 1995; Kharlemenko et al. 2001; Iverson et al. 2001; Thurber 2007; Jeffries et al. 2009), only a small number of studies have measured the tissue-diet shift, ΔFA, necessary to gain quantitative information about a consumer's food source (Iverson et al. 2004; 2007; Wang et

al. 2010). These few studies have all been performed on birds and mammals. The success of the these biomarker techniques directly rely on the accurate characterization of $\Delta^{13}C$, $\Delta^{15}N$, and ΔFA, without which quantitative models are not possible.

A key group that has received little attention in tissue-diet shift laboratory studies is the ubiquitous Annelida. This phylum is a dominant component of marine sediment fauna throughout the world, occupying many trophic roles from grazers and deposit feeders to predators (Fauchald and Jumars 1979). The potential for trophic interaction between the worms and the abundant microbes in the sediment make this group a likely consumer of Bacteria and Archaea. One family of Annelida, the Dorvilleidae, are well adapted to habitats with high microbial biomass. Their known ability to feed on sulfide-oxidizing bacteria and potentially methane-oxidizing Archaea (Levin and Michener 2002; Levin and Mendoza 2007), make members of this family a model system to test measures of $\Delta^{13}C$, $\Delta^{15}N$, and ΔFA. In this study, we use a laboratory-based approach to measure tissue-diet shifts between *Ophryotrocha labronica* and food sources from each of the domains of life. We test the hypothesis that when a species is fed Bacteria and Archaea its $\delta^{13}C$ and lipid content reflects that of its diet and it has a uniform increase in $\delta^{15}N$ from its food source, as expected from paradigms constructed from our knowledge of species fed eukaryotic diets.

Materials and Methods

This study uses a shallow-water species of dorvilleid polychaete, *O. labronica,* as a model to identify how biomarkers are reflected in the tissues of an annelid. This species was collected from an Italian harbor and had been in culture in the laboratory at Scripps Institution of Oceanography since early 2006. Adult stocks were raised on *Spinacia oleracea* until they deposited a brood which was transferred to fresh seawater without food; from this point on all

seawater used was 0.2 μm filtered and contained two broad-spectrum antibiotics, 50μM kanamycin monosulfate and 50μM streptomycin sulfate, to eliminate or minimize microbial growth and minimize processing of the food sources provided. *Ophryotrocha labronica* deposits broods of ca. 30 to 100 offspring which hatch as individuals 0.2 mm in length (pers. obs.). Upon hatching, single clutches were split among separate petri dishes and fed one of the following freeze-dried foods: eukaryotic sources 1) *S. oleracea* (spinach), 2) *Oryza sp.* (rice); bacterial food sources 3) *Photobacterium profundum* 3TCK *(*a gram-negative γ-proteobacterium) 4) *Bacillus subtilis* (a gram-positive firmicute); or archaeal food sources 4) *Halobacterium salinarium* 5) *Haloferax volcanii* (both halophilic Euryarchaea). All bacterial and archaeal food sources were provided by E. Eloe, Scripps Institution of Oceanography from laboratory cultures. *Spinacia oleracea* and *Oryza* sp. were purchased locally. The same cultures and food stocks were used throughout the experiment, except for *H. volcanii* for which two cultures were grown from the same parent stock. Because no isotopic difference was observed between the separate cultures they are treated as one from this point forward. Food sources were provided in unlimited supply; approximately 1.6 mg of food was sufficient for up to 7 individuals to grow to > 10 setigers in a 22^{o}C incubator. Individuals were harvested when they reached approximate adult size (10-14 setigerous segments) for both isotopic and FA analysis. Prior to being frozen at -80 ^{o}C for analysis, individuals were placed in filtered seawater overnight without food to allow gut evacuation and then rinsed in Milli-Q water. Gut evacuation was confirmed by inspection of the gut through their transparent body wall.

Fatty acid and isotopic analysis was performed using methods and instruments tuned for minimal biomass on both *O. labronica* and its food sources. Isotopic analysis was performed on 2-4 individuals per sample and a similar weight of each food (0.25±0.02 mg) . These samples were dried at 60 ^{o}C and acidified with either $PtCl_2$ or H_2PO_4 (there was no

significant impact of acid type on isotope signatures; Paired-T test $p>0.05$ for both C and N). Samples were analyzed on either a Eurovector elemental analyzer interfaced with a continuous flow Micromass Isoprime isotope ratio mass spectrometer at Washington State University or a Thermo Finnigan Delta Xp Plus with a Costech 4010 Elemental Analyzer at the Scripps Institution of Oceanography analytical facility. Comparable samples were run at both facilities with no discrepancy among the instruments. Isotopic ratios are expressed as $\delta^{13}C$ or $\delta^{15}N$ in units of per mil (‰). Standards were Pee Dee Belemnite for $\delta^{13}C$ and atmospheric nitrogen gas for $\delta^{15}N$.

Lipids were extracted using the method of Lewis et al. (2000) in a one step extraction-transesterification reaction on freeze dried material. This technique is especially effective for small-biomass samples. All glassware used in the extractions was sonicated for 15 min with four washes (1x soap, 2x water, 1x DI water) and heated in a muffle furnace for four hours at 500 ^{o}C. Contaminants were extracted from the glassware by solvents following the same extraction protocol which the samples would undergo to remove any remaining lipids within the vials and blanks were run concurrently with all sample sets. Worms or food sources were placed in these pre-extracted 12ml screw-top glass vials with PTFE lined lids at which point they were freeze dried. The extraction solvent, 3ml of 10:1:1 methanol: chloroform: hydrochloric acid (v:v:v), was added and the samples were ground with a glass rod in the extraction solvent and sonicated for 10-15 minutes. After heating to 90 degrees C for 1 hour, samples were allowed to cool, and one ml of Milli-Q water was added. The newly formed fatty acid methyl esters were extracted in 3 aliquots of 2ml 4:1 chloroform: hexanes (v:v). Samples were blown to dryness in N_2, weighed, and brought up in an appropriate amount of the chloroform: hexanes solution for injection and analysis by GC- MS on a Thermo Finnigan Trace GC/MS with a TR-5MS 60m x 0.32μm i.d. column in positive ion mode. Sample oven

conditions were an initial hold at 60 ^{o}C for 1 minute, heating from 60^{o}C to 180^{o}C at 12 ^{o}C per minute, then an increase to 250 ^{o}C at 2.5 ^{o}C per minute where samples were held for 30 minutes. Blanks were run with all batches and all solvents were ACS grade or better. All sample chromatograms were corrected for any peaks eluting in the blank. Due to the small sample sizes, GC-MS analysis, was chosen over GC-FID to increase detection sensitivity. Thus whereas internal comparisons within this study are valid, absolute concentrations are not quantitatively comparable with other studies. Peak integration and identification were performed based on the mass spectra using Xcaliber © software (Thermo Scientific) on full mass spectra and comparison to known standards (Supelco 37 Component FAME mix and Supelco Bacterial Acid Methyl Ester mix, Sigma-Aldrich), and dimethyl disulfide derivatization (following Nichols et al. 1986) for identification of mono-unsaturated bond location.

Samples were statistically treated to determine: (1) if there were differences among the δ^{13}C and δ^{15}N of food sources (one-way Analysis of Variance – ANOVA); (2) if there were differences among isotope signatures of species fed those food sources (also with a one-way ANOVA), and (3) if the differences between food source and consumer tissues represented a significant Δ^{13}C or Δ^{15}N - T-test. Regression analyses were performed between tissue and mean-diet isotopic composition to identify if there was a linear trend between these values, as would be expected from a uniform tissue-diet shift. Univariate statistical analysis was performed with Systat ver. 10 and no transformations were necessary to fulfill the underlying assumptions of the tests. Homogeneity of variance was evaluated graphically and normality was tested using the non-parametric Kolmogorov–Smirnov test. For ANOVA analyses, a Tukey post-hoc test was used to identify significant treatments in the event of a significant factor. For the fatty acid profiles, multidimensional scaling (MDS) was used to plot

differences in the overall lipid profiles within the tissue of *O. labronica* fed each of the food sources. A pair-wise analysis of similarity (ANOSIM) tested whether food source was a determining factor in the lipid profile of *O. labronica.* Both MDS and ANOSIM were performed using log(x+1) transformed data based on Bray-Curtis similarity in Primer (ver. 6). In all instances, we used a significance level of 0.05. Univariate statistical analysis was not performed on FA data due to abundant zeros which made assumptions of homogeneity of variance invalid.

Results

Diet Influence on Carbon and Nitrogen Isotopic Signatures

Ophryotrocha labronica diet influences its isotopic composition but $\Delta^{13}C$ was not uniform among food sources (Figure 4.1). Food sources had distinct $\delta^{13}C$ signatures from each other ($F_{5,26}$=47.8; $p<0.001$) with *P. profundum* being different from all other food sources and the remaining food sources each different from four of the other five (Figure 4.1). Yet *O. labronica* fed these diets did not retain a significantly-different isotopic signature ($F_{5,19}$=2.338; p=0.08) as would be expected if there was a consistent tissue-diet shift. $\Delta^{13}C$ for all of diets ranged from -3.6 to 3.6 ‰ but only the worms fed *P. profundum* and *Oryza sp.,* exhibited significant isotopic differences between food source and tissue (Table 4.1). Those that did have a significant difference from their diets, and hence a significant tissue-diet shift, did not shift in the same direction; *Oryza* sp. caused an increase in consumer $\delta^{13}C$ and *P. profundum* caused a decrease. The range of $\delta^{13}C$ for *O. labronica* fed *P. profundum* was very large, ranging from -23 to -18 ‰, yet the consumer tissue's $\delta^{13}C$ was consistently lighter than its food source of *P. profundum*. When looking across all treatments, there was a linear decrease in $\Delta^{13}C$ as a function of $\delta^{13}C$ of the diet as indicated by slope not equal to 1 in the regression

analyses where $\delta^{13}C_{tissue}$=-16.25 + 0.294 x $\delta^{13}C_{diet}$ (R^2=0.20, $F_{1,23}$=5.87, p=0.02). The fit of this line was improved when food source C:N ratio, a measure of food quality, was included as an independent variable resulting in $\delta^{13}C_{tissue}$=-13.59 + 0.44 x $\delta^{13}C_{diet}$ + 0.06 x C:N (R_{adj}^2=0.28, $F_{2,22}$=5.58, p=0.01). *Oryza* sp. had a high C:N ratio which greatly influenced the fit of the line. This can be clearly seen when a regression is fit both with and without *Oryza* sp. By removing *Oryza* sp. from this regression analysis the R^2 value is increased from 0.20 to 0.34 (Figure 4.2). Whereas these regressions do not explain much of the inherent variance of $\delta^{13}C_{tissue}$, indicated by the low R^2 values) they do explain the mean values, suggesting that mean $\delta^{13}C_{tissue}$ can be largely explained by mean $\delta^{13}C_{diet}$ when sample sizes are increased. When only means are considered across all treatments, 84% of the variance was explained by a regression, $\delta^{13}C_{tissue}$=-13.30 + 0.45x$\delta^{13}C_{diet}$ + 0.07 x C:N (R_{adj}^2=0.84, $F_{2,3}$=13.72, p=0.03). This highlights the fact that isotopic measures of a species based on one or two individuals is unlikely to accurately characterize the $\delta^{13}C$ of the food source even when corrected for $\Delta^{13}C$.

There was no clear pattern among food domains with the eukaryotes and the bacteria having the largest $\Delta^{13}C$ (Table 4.1). Both archaeal food source treatments yielded the smallest values of $\Delta^{13}C$ yet there was no significant difference among the $\Delta^{13}C$ for bacteria and archaeal treatments. Therefore these differences are less than the inherent variance in $\Delta^{13}C$ among food sources, independent of domain (bacteria, archaea, eukaryotes).

There was no consistent $\Delta^{15}N$ for *O. labronica*, yet all food sources resulted in a decrease in $\delta^{15}N$ (Figure 4.1). Nitrogen isotopic values were not uniform among food sources or *O. labronica* fed those food sources. *Halobacterium salinarium* and *S. oleracea* were less depleted in ^{15}N than *Oryza sp.* and *H. volcanii* ($F_{5,19}$=3.6; p=0.02 –significance indicated on Figure 4.1) and this resulted in a difference in *O. labronica*'s $\delta^{15}N$ for those individuals fed *H.*

volcanii and *S. oleracea* ($F_{5,26}$=7.52; p<0.001). In all instances the tissue-diet shift resulted in a decrease of $\delta^{15}N$ from its diet, favoring incorporation of the lighter isotope, although only *O. labronica* fed either *H. salinarium* and *S. oleracea* were significantly different in $\delta^{15}N$ from their food source with $\Delta^{15}N$ values of -2.8 and -3.0, respectively. C:N ratio of the food sources did not impact these results as the two significant tissue-diet shifts came from food sources which had similar C:N ratios to those food sources which did not cause a shift. O*ryza* sp., the food which had the most distinct C:N ratio, had a $\Delta^{15}N$ shift in its consumer's tissue similar to *O. labronica* fed a diet with a comparatively small C:N ratio. As with Carbon there was not a slope of 1 between $\delta^{15}N_{tissue}$ and $\delta^{15}N_{diet}$ indicating that $\Delta^{15}N$ varied with $\delta^{15}N_{diet}$ ($\delta^{15}N_{tissue}$ = 0.23 x $\delta^{15}N_{diet}$ + 0.61; R^2=0.29, $F_{1,23}$=9.4, p<0.01). This relationship was not improved by including C:N ratio.

Diet Influence on Fatty Acid Signatures

Fatty acids in the food sources were not uniformly incorporated into the tissues of *O. labronica*. Food sources had FAs which differed in their chain length and branching patterns (Table 4.2). The most distinct food sources were the two archaeal species, which contained no FAs and *B. subtilis* whose FA distribution was largely composed of branched FAs and the saturated 15 carbon FA (15:0; Table 4.2). Lipid extraction of both archaeal species were attempted using the same protocol and had results equivalent to concurrently run blanks. The *Oryza sp.* profile had an abundance of an 18:2 FA whose retention time matched that of the (n-6) FA standard. Whereas *S. oleracea* also contained this unsaturated18 carbon FA, it was unique in having 62% of its fatty acid composition composed of a 18 carbon FA with three double bonds. *Photobacterium profundum* contained the "classic" bacterial profile, dominated by (n-7) monounsaturated FAs. All eukaryotic and bacterial food sources contained the saturated 16:0 FA. FAs less than 14 carbon lengths are not included in this analysis nor are

peaks which were not FAs based on mass spectra. We used a 0.5% cut off for inclusion in the analysis, eliminating FAs which were not greater than this value in any sample.

Ophryotrocha labronica had a diverse distribution of FAs which were largely independent of those available from their food (Table 4.2). Individuals fed *H. volcanii* had the least diversity, containing only 14 FAs, whereas the remaining food sources yielded 20 FA's in *O. labronica* tissues. The FAs which were present in *O. labronica*'s tissues included essential FAs, 20:4(n-6) and 20:5(n-3), branched and one cyclic FA independent of food source (Table 4.2). Each food source did not result in a distinct overall FA pattern in the *O. labronica* fed those food sources. There were significant differences between *Oryza sp.* and *S. oleracea* (R=0.36, p=0.038), and between *B. subtilis* and both *Oryza* sp. (R=0.45, p=0.012) and *S. oleracea* (R=0.48, p=0.029) based on the ANOSIM pair-wise analysis, but there were no other significant pair-wise comparisons. This was apparent visually as indicated by the absence of groupings defined by food source in an MDS plot whose 2-dimensional stress indicated it sufficiently displayed these multidimensional data (Figure 4.3). No food source, regardless of how unique its FA composition, resulted in a predictable fatty acid profile in *O. labronica*.

Divergence from the mean FA distribution of *O. labronica* reveals differences among the food sources (Figure 4.4; Table 4.2). Within the individuals fed *B. subtilis* there was a consistent enrichment of both a14:0, i15:0 and 15:0 between diet and tissues. In contrast, individuals fed *H. volcanii* synthesized a greater proportion of 18:0 than the mean distribution in addition to 16:0. There appeared to be an increase of all three constituents of *P. profundum* in its consumer compared to the mean distribution of FA within *O. labronica,* yet *P. profundum*'s FAs were 39% 16:0 and this high amount of FA input resulted in minimal increase in 16:0 in *P. profundum's* consumer compared to the mean. In addition, *P. profundum*

had 47% of its FAs made up of 16:1(n-7) and this FA was <3% divergent among *O. labronica* fed any food source, even though *P. profundum* was the only species to provide this FA. *Oryza sp.* consumers had mild increases in four of the FAs provided by *Oryza* sp. but there was no resultant increase in 14:0. Individuals fed *S. oleracea* only appeared to incorporate 16:0 from its diet and had no enrichment of the 16:1(n-3)*, 16:2, or 18:3 FA which were either unique as in the first two cases, or completely dominant in the case of 18:3, constituting 62% of the *S. oleracea*'s FA profile. What is potentially most striking is that whereas both *P. profundum* and *Oryza* sp. provided a food source which was made up of approximately 38% 16:0, the worms fed these diets differed by 2.4 fold in their concentration of this FA. There was less incorporation in the *P. profundum*-fed individuals. Although there was large variance among replicates of *O. labronica* fed each food source, when this variance was removed, (i.e. mean FA distribution in *O. labronica* as a function of food source was used) the signature of a given food source began to become apparent, but the pattern of FA uptake among food sources was not uniform.

Overall this species has a distinct fatty acid signature that is largely independent of its diet although it appears to uptake certain components from its diet. FA uptake was not uniform among food sources. By knowing the distribution of FAs within the food sources we were able to find similarities, but without this *a priori* knowledge of the food sources we would not be able discriminate any clear pattern (Figure 4.3). Furthermore those food sources which provided unique FAs which would have been useful biomarkers to identify consumers fed that diet were not represented in the worm tissues. This was highlighted by a lack of 18:3 in *O. labronica* fed *S. oleracea*.

A diversity of FAs were synthesized or transformed by *O. labronica*. The only FA that was provided by all the bacterial and eukaryotic food sources was 16:0, yet *O. labronica*

fed these diverse food sources had the same 20 FAs. These included the polyunsaturated fatty acids 20:4(n-6) and 20:5(n-3) that were not present in any of their food sources and the unsaturated 18:2 FA that was only present in the two eukaryotic food sources. This overall fatty acid profile was also present in the tissue of *O. labronica* fed *H. salinarium* despite the fact that this species of Archaea contains no FA. Only *H. volcanii*-fed *O. labronica* had a reduced diversity of FAs, yet they still contained 20:4(n-6) and 20:5(n-3). *O. labronica* appears to be able to synthesize every FA that we found in this annelid.

Discussion

Isotopic Implications

The observed isotopic tissue-diet shifts were both large in comparison those previously found (McCutchan et al. 2003) and surprisingly these tissue-diet shifts varied with the food source consumed. In this study, one annelid species fed all the domains of life had a $\Delta^{13}C$ range of -3.6 to +3.6. This range is larger than the -2.7 to +3.4 ‰ found in a recent review (McClutchan et al. 2003) covering many animal phyla. Previous investigators have found large ranges of $\Delta^{13}C$ for polychaetes: -0.2 to 2.1 for *Capitella capitata* [sic] (Haines and Montegue 1979); +1.3 to +2.1 for *Pseudopolydora kempi japonica* (Hentchell 1998); and -2.2 to +3.9 for *Nereis diversicolor* (Jackson and Harkness 1987). Both *C. capitata* [sic] and *N. diversicolor* also had distinct shifts depending on the food source. Yet these studies either lacked replication (Haines and Montegue 1979) or started with adults and relied upon tissue turnover during a four-month period to evaluate $\Delta^{13}C$ (Jackson and Harkness 1987). Data from the present study, which raised the model species from birth and took advantage of the increased throughput and decreased cost of isotopic analysis since 1979, support many of their findings. This phenomenon is not limited to annelids. Two recent studies found $\Delta^{13}C$ values

with a larger range than observed in *O. labronica*, including a mammal whose $\Delta^{13}C$ ranged from -8.8 to 0.6 (Caut et al. 2008) and an amphipod whose $\Delta^{13}C$ ranged from -10 to -2 (Crawley et al. 2007), both of which were a function of the food source fed. By analyzing whole organisms and not extracting lipids from these samples, the $\Delta^{13}C$ measured within this study should have been more negative $\Delta^{13}C$ than many studies (McCutchan et al. 2003). Yet, these methodological considerations do not explain the food- dependent $\Delta^{13}C$ or the large shifts I observed.

Whereas a universal tissue-diet shift has been commonly applied to food web studies, food quality and food amount in relation to metabolic needs impact the magnitude of $\Delta^{13}C$ and $\Delta^{15}N$. Consumed food can be directly incorporated into a consumer's tissue or catabolized and respired/excreted or resynthesized prior to incorporation into its tissues (Auerswald et al. 2010). Within a food source, molecules are not homogeneous in their isotopic composition (DeNeiro and Epstien 1977). This means that a consumer's tissue reflects the sum of many different tissue-diet shifts whose values are a function differential incorporation and starting isotopic composition. Differential incorporation of food source molecules are manifested with proteins being largely directly incorporated into a consumer's tissue whereas carbohydrates and many lipids are catabolized before being rebuilt from components – as such the proteins would have very low $\Delta^{13}C$ and carbohydrates and lipids would have a larger $\Delta^{13}C$ (Ambrose and Norr 1993; Fantle et al. 1999). This non-uniform reprocessing of compounds is called isotopic routing (Schwarcz 1991). In mixed diets where one, sometimes minor, food source is high in protein, the isotopic content of the consumer tissue preferentially reflects the isotopic composition of the food source with the high protein content. Food sources with divergent C:N ratios also cause greater tissue-diet shifts. A larger C:N ratio causes a greater $\Delta^{13}C$ due to increased respiration and lower $\Delta^{15}N$ due to nitrogen limitation (Webb et al. 1998; Adams and

Sterner 2000; Phillips and Koch 2002). Greater amounts of food also allow rapid deposition of body mass and consumer tissues will take less time to reflect the isotopic signature of the food source (Carelton and Martinez del Rio 2010). In times of famine, $\Delta^{15}N$ is extremely high since the consumer's tissues are degraded during starvation and so ^{14}N is excreted creating an essential infinitely large tissue-diet shift (Hobson et al. 1993). All of these factors work together to create the $\Delta^{13}C$ and $\Delta^{15}N$ for the bulk tissue within a consumer.

In this study we tried to minimize many of the aforementioned artifacts associated with tissue-diet fractionation and still observed a food-source dependent tissue-diet shift. By raising *O. labronica* from hatching on the prescribed diet we avoided problems with incomplete isotopic turnover from previous food sources. $\Delta^{15}N$ values, always <0, were not indicative of starvation. Isotopic routing impacts on these estimates were minimized since all food sources were fed in monoculture and the whole organism was sampled, eliminating divergent incorporation among tissue types. However, food sources did have different biochemical compositions (i.e. lipids available to be incorporated and C:N ratio). The C:N ratio did impact $\Delta^{13}C$ but to a lesser extent than the starting food source $\delta^{13}C$; this ratio had no impact on $\Delta^{15}N$.

Tissue-diet shifts as a function of food source $\delta^{13}C$ have been emphasized in four studies to date (Hilderbrand et al. 1996; Felicciti et al. 2003; McCutchen et al. 2003; Caut et al. 2008). The effect of tissue-diet shifts as a function of food source isotopic composition may be very pronounced when food source endpoints are far from each other, such as those studies using tracers (i.e. Blair et al. 1996; Aberle and Witte 2003) or methane-derived food sources (i.e. Levin and Michener 2002; Thurber et al. 2010). If I apply the regression equation relating $\delta^{13}C_{tissue}$ to $\delta^{13}C_{diet}$ measured within this study to estimate the value of $\Delta^{13}C$ of infauna fed a methane-based diet (using the $\delta^{13}C$ of -62 observed in Thurber et al. (2010) and resulting in a

estimated $\delta^{13}C_{tissue}$ of -32 ‰) we would have a $\Delta^{13}C$ of 27 ‰. This extrapolation is only suggestive without directed further study, yet the magnitude is great enough to warrant this research. Aueswald et al. (2010) calls into question the relationship of $\Delta^{13}C$ to $\delta^{13}C_{diet}$ as observed by Caut et al. (2009) stating that it is a statistical artifact. As shown here by using the direct relationship between $\delta^{13}C_{diet}$ to $\delta^{13}C_{tissue}$ we have avoided this artifact and still see a non-uniform incorporation. Not incorporating this diet-specific shift into mixing models will cause an inaccurate estimation of carbon source which will be magnified with each trophic step.

Essential Fatty Acids in Annelids.

The fatty acid composition of a species has broad implications for its survivorship and reproductive success (Berge and Barnathan 2005). Increasing length and unsaturation state (i.e. number of double bonds) increases the fluidity of cellular membranes. This results in a FA profile that changes in proportion to ambient temperature (Taghon 1988; Chu and Graeves 1991) and pressure (Allen et al. 1999). Especially key are certain types of FAs, referred to as the "essential fatty acids", which are necessary for growth and reproduction (Stanley-Samuelson 1994). Most taxa cannot synthesize them *de novo* and instead must get them from their diet (Iverson 2009).

A specific suite of enzymes allows lipid synthesis and the addition of double bonds and elongation of both synthesized and diet-derived FAs. Desaturases add a double bond at a specific position along the carbon back bone of a fatty acid. The naming scheme numerically identifies at which carbon from the carboxyl end this double bond is placed, i.e. a Δ^9 desaturase converts 16:0 to 16:1(n-7) or 18:0 to 18:1(n-9). The type of desaturases which a species possesses limits which FAs it can create from a food source; the essential fatty acids are those which cannot be synthesized without specific precursors. These precursors in

terrestrial habitats are 18:3(n-3) and 18:2(n-6), FAs which are transformed by Δ^9 and Δ^5 desaturases into those which are commonly available in the marine environment 20:5(n-3) and 22:6(n-3). Although the desaturase diversity has been studied in many animals, the desaturases present within annelids remains largely unknown, although unique desaturases are known from other marine invertebrate phyla (Berge and Barnathan 2005; Gostinčar et al. 2010).

A surprise from this laboratory study was the ubiquity of the essential FAs in individuals that were fed diets which did not contain essential FAs, suggesting the presence of desaturases not known to occur within most animal phyla. *Ophryotrocha labronica* appears to be able to synthesize both 20:4(n-6) and 20:5(n-3) from diets that specifically do not include any FAs, i.e. the two archaeal food sources, and diets that do not provide the precursors for their synthesis, the two bacterial food sources. Although *S. oleracea* provided both 18:3 and 18:2 FAs, the precursors that are used in terrestrial systems, *O. labronica* fed *S. oleracea* had lower PUFAs than those fed other diets. There is some debate as to whether or not these starting points are functional for marine systems and thus may not act as precursors for this species (Pond et al. 2002). Without showing the specific enzymatic pathway or the presence of those necessary desaturases, this study can only suggest that *O. labronica* is able to synthesize essential fatty acids. In addition to this study, the most compelling evidence that supports the ability of Polychaeta to synthesize PUFAs is the presence of 20:5(n-3) and 20:4(n-6) in the symbiont-bearing, mouthless and gutless hydrothermal vent worm, *Ridgea piscesae* (Pond et al. 2002). Although the source of these PUFAs remain unknown, and could derive from their symbionts, it is the best example of an annelid which likely derives its PUFAs from bacterial origin or synthesizes them within the deep-sea (Pond et al. 2002). Both nematodes (Spychalla et al. 1997) and heterotrophic ciliates and flagellates (Zhukova and Kharlamenko 1999) are

also now known to be able to synthesize these FAs and further research is warranted to determine if annelids may as well.

The ability to synthesize essential FAs and not be dependent on one's food source for them may be a key advantage for the success of polychaetes. Polychaetes are abundant in many habitats where PUFAs are not abundant including both hydrothermal vents and methane seeps where microbial production largely fuels metazoan fauna (Fisher 1990; Levin 2005; Thurber et al. 2007). Many, but not all bacteria (Nichols 2003) do not form essential FAs and so those deep-sea animals which normally subsist by consuming bacteria would either need to wait for periodic photosynthetic deposition, such as a seasonal phytodetritus pulses (Billett et al. 1983), or synthesize them *de novo*. Deep-sea fauna have limited access to essential FAs which are stripped in the water column from sinking particles (Wakeham et al. 1997) and polychaetes are ubiquitous within these deeper habitats far removed from the sun. The Dorvilleidae, the family of polychaetes to which *O. labronica* belongs, has been present since at least the Mesozoic, if not the Paleozoic era (Courtinat 1998), and the ability to synthesize essential fatty acids may have aided its persistence throughout geological time.

Fatty acid analyses in food webs

While every effort was made to minimize microbial reprocessing of the food sources throughout this experiment, it is unlikely that we were completely successful in eliminating all microbial growth. 15:0, 17:0, and branched FAs were present in *O. labronica* fed all of the food sources. These FAs are thought be derived from microbial biomass. The least affected of all of the food sources was the Archaea, *H. volcanii*, and this food source still resulted in 9.6% of the total FAs within *O. labronica* appearing to be bacterial. Unlike the aforementioned siboglinid polychaete, *R. piscesae,* the dorvilleids are not known to have chemoautotrophic symbionts. Annelids however, are known to have microbial flora to aid in digestion which

could impact biomarker uptake and modification, including essential FA formation (Sampedro et al. 2006). The presence of gut symbionts was not assessed, but as *O. labronica* was able to grow to reproduction on all food sources, in no instance did the antibiotics used eliminate necessary processing of the food sources by potential gut symbionts. On the other hand, increased gut flora processing would have further differentiated the FAs profile of *O. labronica* from that of its food sources. Microbial processing may be an integral part of how a food source is reflected in the tissue of a consumer and an inherent aspect of using biomarkers to identify a species diet.

Fatty acid analysis has been shown to be a powerful tool to identify qualitative food web links and can provide quantitative application in certain systems, yet great care must be used when interpreting field results without careful laboratory study. In a landmark paper, Iverson et al. (2004) was able to use laboratory-based analysis of a marine mammal to come up with a model sufficient to provide reliable tissue-diet shifts for each of the FAs present within the consumer's tissue. They were then able to accurately apply this to the field. Within the Annelida, *Capitella sp.* has been shown to have a FA composition reflecting its diet, yet the diets tested provided 18 different FAs in contrast to our study in which each of our food sources provided between zero and seven FAs. This resulted in *O.labronica* having to synthesize most of its FAs and likely led to FA profiles distinct from those of the species' diet (Figure 4.3). In a study similar to this one, ciliates and flagellates were fed food sources which lack FA diversity and this resulted in a similar impressive diversity of FAs in these consumers' tissues (Zhukova and Kharlamenko 1999). This finding suggests that when a food source is limited in its diversity of FAs, the FA signature of the consumer reflects its diet less. In addition, many short chain (i.e. 16:0 and shorter) FAs are catabolized rather than incorporated, contributing to why *O. labronica* does not reflect its diet – 16:0 was the dominant FA of three of the food sources present with other short chain FAs being present

along with them. As bacteria commonly have a profile dominated by short chain FAs, it is likely that bacterial FAs are routinely underrepresented in bactivorous fauna. As no unique archaeal biomarkers were found within the FAs of the consumer, Archaea are not resolvable within a FA-derived food web.

For complex invertebrate food webs, FA analysis has been applied to successfully to tease apart divergent food sources and so is a valid approach for identifying interactions (e.g. Colaco et al. 2007; Kharlamenko et al. 2001). Yet as we've shown here, not all biomarkers are reflected in a species' diet. When temperature, metabolism, and species were held constant, only *B. subtilis* resulted in *O. labronica* tissues enrichment in diet-provided FAs, and even then *O. labronica*'s lipid pattern was discernable from only two of the other food sources. The absence of unique dietary FAs in the tissue of a consumer does not mean that it is not consuming a particular food source. These results show that cellular machinery can be more important than diet in the FA profile of certain invertebrates. We hypothesize that this is simply because, unlike "higher" organisms, annelids are adapted to FA-poor diets and thus have a greater abundance of desaturases, or gut symbionts, than is currently recognized. This suggests that we are a long way from being able to apply quantitative metrics to the incorporation of FAs by this abundant and diverse group of invertebrates.

Conclusion

In this paper we have demonstrated that, as Gannes et al. (1997) pointed out, further laboratory studies are still critical in our evaluation of the quantitative nature of food web biomarkers. We have shown that:

1) Archaeal consumption results in a FA profile indistinct from other food sources.

2) Unique FA biomarkers from a food source are not necessarily incorporated into consumer tissues and so a lack of biomarker does not indicate a lack of consumption.

3) Carbon tissue-diet shifts vary and can be both a function of food source $\delta^{13}C$ and C:N ratio.

4) $\Delta^{15}N$ values were negative for *O. labronica*, making estimation of the trophic level of *O. labronica* and potentially many annelids difficult.

While this study presents the challenges which face coupling microbial processes with metazoans diets, it highlights how Bacteria and Archaea are viable but not quantitatively tractable food source for at least one species of polychaete. In addition we show how essential fatty acids are available to this species even when not provided by their food source. Further studies are needed to identify whether the patterns we observed for two types of biomarkers are common among other annelid and invertebrate taxa.

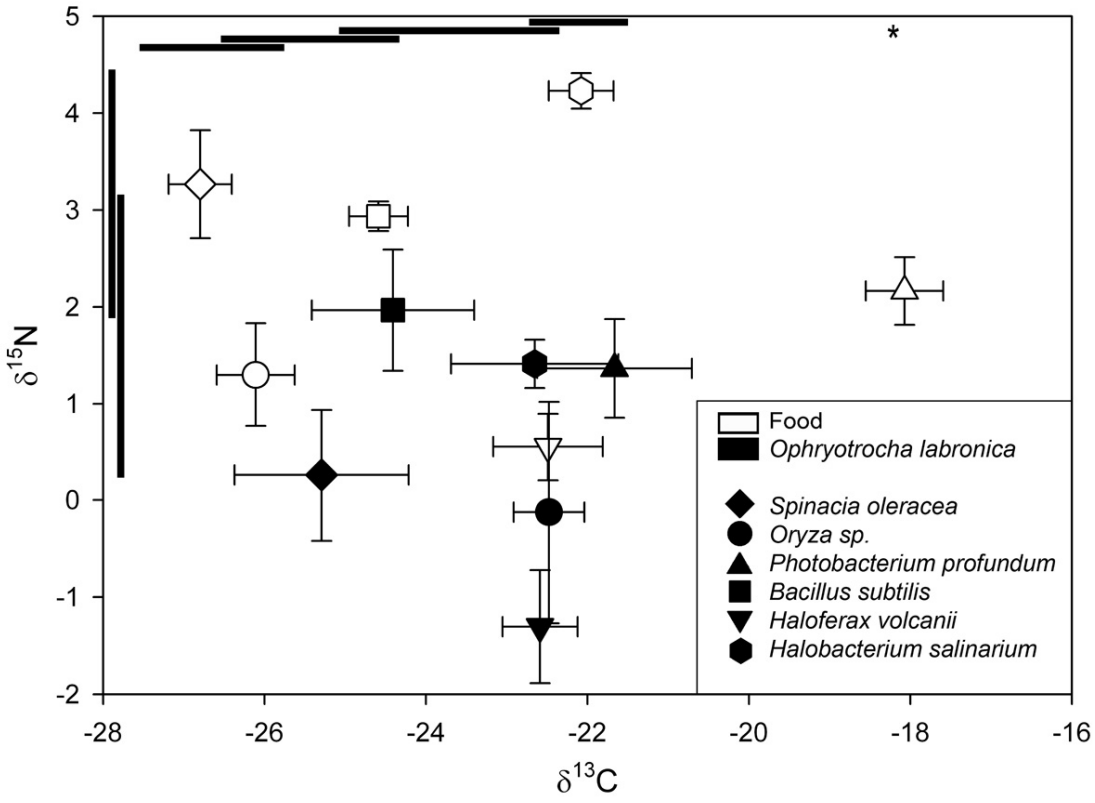

Figure 4.1 Carbon and nitrogen stable isotopic composition of six food sources and *Ophryotrocha labronica* fed those food sources. Significant differences in food sources are indicated by bars with horizontal bars showing significant differences in carbon and vertical differences in nitrogen. Points which fall under the same bar are not significantly different from each other. An asterisk indicates the isotopic composition of that food source is significantly different from all other food sources. See text for statistical treatment. Error bars are standard error.

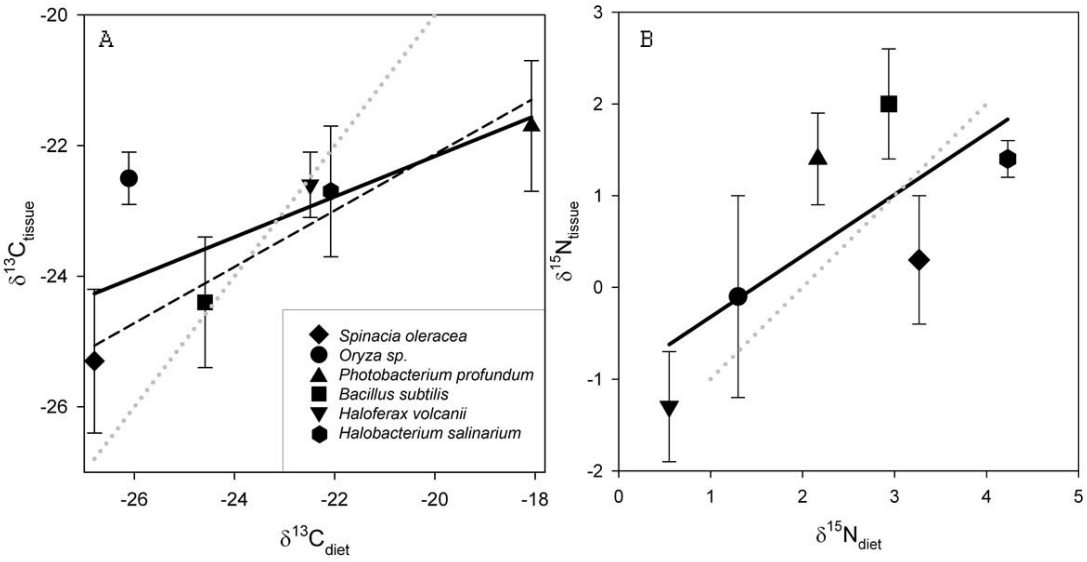

Figure 4.2 Relationship between A) $\delta^{13}C_{diet}$ and $\delta^{13}C_{tissue}$ and B) $\delta^{15}N_{diet}$ and $\delta^{15}N_{tissue}$ for *Ophryotrocha labronica* fed the indicated diets. Solid lines are linear regressions based on all data. Dotted grey lines indicate a slope of one or the slope of the line predicted by a constant tissue-diet shift independent of food source. Dashed black line in A) indicates the regression fit when *Oryza* sp. is not included in the analysis. See text for regression equations and fit. Error bars are standard error.

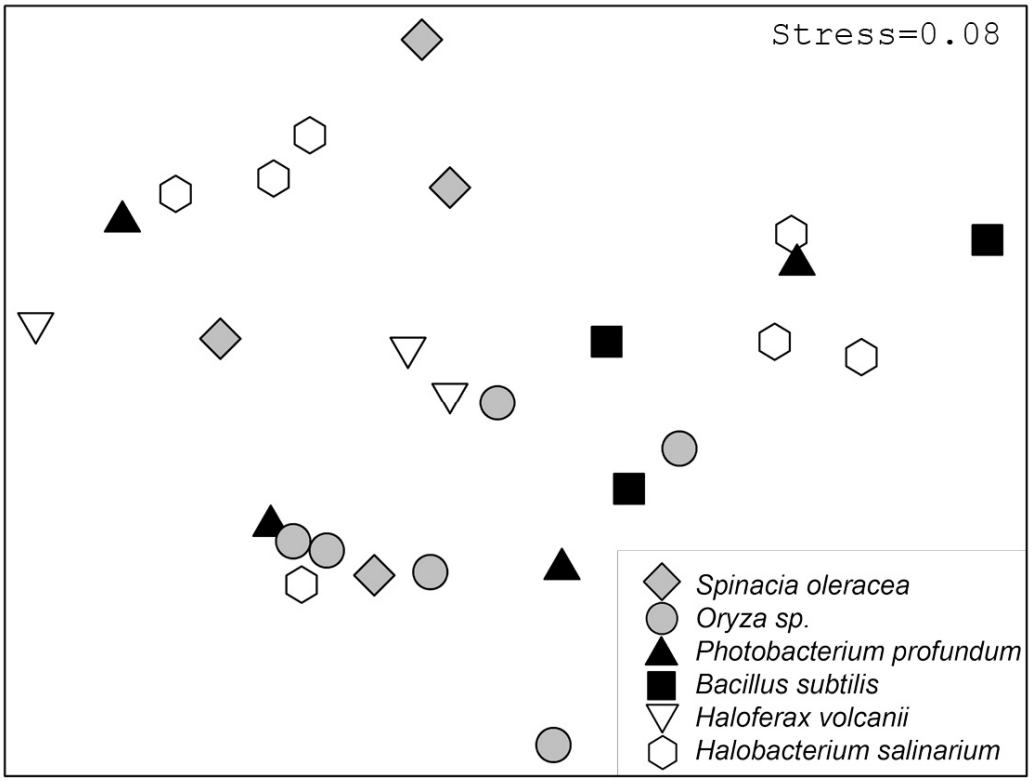

Figure 4.3 Multidimensional Scaling of log(x+1) fatty acid profiles of *Ophryotrocha labronica* fed six food sources. Worms fed eukaryotic food sources are in grey, bacterial in black, and archaeal in white.

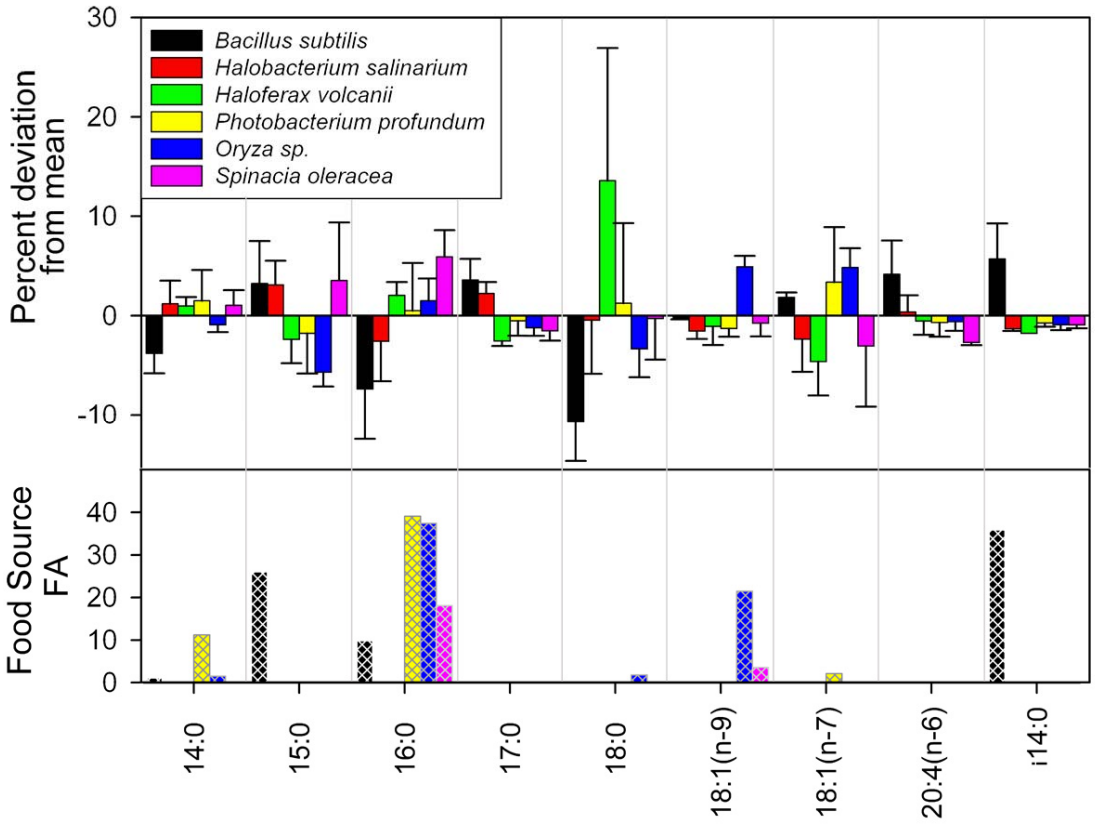

Figure 4.4 Deviation from the mean fatty acid profile for *Ophryotrocha labronica* fed six different diets. Food-source fatty acid distribution is presented in the lower panel in hashed bars.

Table 4.1 Mean tissue-diet shift for carbon, $\Delta^{13}C$, and nitrogen, $\Delta^{15}N$, stable isotopic composition between *Ophryotrocha labronica* and six different diets. Statistical results indicate differences between the diet and tissue with a significant value indicating that they were different, df= degrees freedom and significant p-values are in bold. C:N ratio is given of each food source. SE = standard error.

	Domain	**Tissue-Diet Shift**		**T-test Between Diet and *O. labronica***		**C:N ratio**
Diet		**$\Delta^{13}C$**	**$\Delta^{15}N$**	**$\delta^{13}C$**	**$\delta^{15}N$**	**± SE**
Bacillus subtilis	Bacteria	0.2	-1.0	$T_{df=7}$=-0.19; p=0.86	$T_{df=7}$=1.7; p=0.14	4.1 ± 0.02
Halobacterium salinarium	Archaea	-0.6	-2.8	$T_{df=7}$= 0.57; p=0.59	$T_{df=7}$=9.4; **p<0.01**	3.6 ± 0.04
Haloferax volcanii	Archaea	-0.1	-1.9	$T_{df=6}$= 0.13; p=0.91	$T_{df=6}$=2.3; p=0.06	4.2 ± 0.23
Photobacterium profundum	Bacteria	-3.6	-0.8	$T_{df=8}$= 3.4; **p=0.01**	$T_{df=8}$=1.3; p=0.24	3.8 ± 0.07
Oryza sp.	Eukaryote	3.6	-1.4	$T_{df=10}$= -4.8**; p<0.01**	$T_{df=10}$=1.3; p=0.22	40.1 ± 2.86
Spinacia oleracea	Eukaryote	1.5	-3.0	$T_{df=7}$= -1.7; p=0.14	$T_{df=7}$=3.2; **p=0.01**	7.7 ± 0.96

Table 4.2 Fatty acid (FA) composition of *Ophryotrocha labronica* reared on six food sources and the fatty acid composition of those food sources. Archaeal food sources had no FAs present. Bold numbers indicate percent of the total FA within the species (± Standard Error). FAs are named after the number of carbons in their carbon back bone followed by the number of double bonds present. The (n-x) notation indicates the position of the first double bond (x) relative to the terminal end of the FA and those preceded by an i or a are branched. Number of replicates is given in parentheses after the food source.

	Ophryotrocha labronica															**Source**			
Fatty Acid	*Bacillus subtilis (3)*			*Photobacterium profundum (4)*			*Oryza sp. (6)*			*Spinacia oleracea (4)*			*Halobacterium salinarium (7)*			*Haloferax volcanii (3)*			*Bacillus subtilis*	*Photobacterium profundum*	*Oryza sp.*	*Spinacia oleracea*
14:0	**3.2**	±	2.0	**8.5**	±	3.1	**6.1**	±	0.7	**8.0**	±	1.5	**8.2**	±	2.3	**8.0**	±	0.9	**1.0**	**11.2**	**1.5**	0.0
15:0	**11.7**	±	4.3	**6.7**	±	4.0	**2.8**	±	1.4	**12.0**	±	5.8	**11.6**	±	2.4	**6.1**	±	2.4	**26.0**	0.0	0.0	0.0
16:0	**18.4**	±	5.1	**26.3**	±	4.8	**27.3**	±	2.2	**31.7**	±	2.7	**23.2**	±	4.0	**27.8**	±	1.4	**9.8**	**39.1**	**37.4**	**18.0**
16:1 (n-9)	**0.3**	±	0.3	**0.1**	±	0.1	0.0	±	0.0	**1.7**	±	0.8	**0.6**	±	0.3	**1.4**	±	0.7	0.0	0.0	0.0	0.0
16:1 (n-7)	**0.3**	±	0.3	**2.7**	±	1.6	**1.6**	±	0.9	**0.9**	±	0.6	**0.4**	±	0.2	0.0	±	0.0	0.0	**47.7**	0.0	0.0
16:1 (n-3)*	0.0			0.0			0.0			0.0			0.0			0.0			0.0	0.0	0.0	**1.8**
16:2	0.0			0.0			0.0			0.0			0.0			0.0			0.0	0.0	0.0	**5.6**
17:0	**6.6**	±	2.1	**2.5**	±	1.5	**1.8**	±	0.8	**1.5**	±	1.0	**5.3**	±	1.2	**0.5**	±	0.5	0.0	0.0	0.0	0.0
18:0	**11.0**	±	4.0	**23.0**	±	8.1	**18.4**	±	2.8	**21.5**	±	4.1	**21.3**	±	5.4	**35.3**	±	13.3	0.0	0.0	**1.8**	**tr**
18:1 (n-9)	**3.5**	±	0.1	**2.4**	±	0.8	**8.6**	±	1.1	**3.0**	±	1.3	**2.2**	±	0.8	**2.6**	±	1.9	0.0	0.0	**21.5**	**3.5**
18:1 (n-7)	**12.7**	±	0.5	**14.2**	±	5.5	**15.7**	±	1.9	**7.8**	±	6.1	**8.5**	±	3.3	**6.2**	±	3.4	0.0	**2.0**	0.0	0.0
18:2 (n-6)	**2.0**	±	0.4	**1.2**	±	0.5	**3.7**	±	0.6	**0.5**	±	0.3	**1.0**	±	0.4	**1.3**	±	0.7	0.0	0.0	**38.0**	**9.1**
18:3	0.0			0.0			0.0			0.0			0.0			0.0			0.0	0.0	0.0	**62.0**
20:1 (n-13)	**5.3**	±	0.7	**1.0**	±	1.0	**2.5**	±	1.4	**1.8**	±	0.9	**2.7**	±	1.3	**3.1**	±	1.3	0.0	0.0	0.0	0.0
20:2	0.0	±	0.0	0.0	±	0.0	**1.4**	±	1.0	0.0	±	0.0	0.0	±	0.0	0.0	±	0.0	0.0	0.0	0.0	0.0
20:4 (n-6)	**7.3**	±	3.4	**2.5**	±	1.4	**2.6**	±	0.9	**0.5**	±	0.3	**3.5**	±	1.7	**2.6**	±	1.4	0.0	0.0	0.0	0.0
20:5 (n-3)	**2.0**	±	0.9	**1.1**	±	0.7	**0.9**	±	0.5	**1.1**	±	0.7	**1.2**	±	0.6	**2.3**	±	1.4	0.0	0.0	0.0	0.0
i15:0	**7.5**	±	3.6	**1.0**	±	0.4	**0.9**	±	0.5	**0.9**	±	0.3	**0.5**	±	0.2	0.0	±	0.0	**35.8**	0.0	0.0	0.0
a15:0	**1.2**	±	0.3	**1.9**	±	0.9	**0.5**	±	0.3	**1.5**	±	0.9	**1.3**	±	0.5	**0.3**	±	0.3	0.0	0.0	0.0	0.0
i16:0	**2.1**	±	1.2	**2.9**	±	1.9	**0.4**	±	0.3	**1.5**	±	1.5	**3.6**	±	1.1	0.0	±	0.0	**3.7**	0.0	0.0	0.0
i17:0	**3.0**	±	1.6	**0.1**	±	0.1	**0.5**	±	0.4	**0.1**	±	0.1	**0.2**	±	0.1	0.0	±	0.0	**14.2**	0.0	0.0	0.0
a17:0	**0.6**	±	0.4	**0.5**	±	0.3	**2.4**	±	1.8	**2.4**	±	1.1	**1.5**	±	0.4	**2.4**	±	0.8	**9.5**	0.0	0.0	0.0
i18:0	**0.1**	±	0.1	**0.0**	±	0.0	**0.2**	±	0.2	**0.1**	±	0.1	**1.3**	±	1.1	0.0	±	0.0	0.0	0.0	0.0	0.0
cyclo18	**0.8**	±	0.8	**0.8**	±	0.5	**0.3**	±	0.3	**1.1**	±	1.1	**0.4**	±	0.3	0.0	±	0.0	0.0	0.0	0.0	0.0

* double bond position is not confirmed

References

Aberle N, Witte U (2003) Deep-sea macrofauna exposed to a simulated sedimentation event in the abyssal NE Atlantic: in situ pulse-chase experiments using ^{13}C-labelled phytodetritus. Mar Ecol Prog Ser 251:37-47

Adams TS, Sterner RW (2000) The effects of dietary nitrogen on trophic level ^{15}N enrichment. Limnol Oceangr 45:601-607

Allen EE, Facciotti D, Bartlett DH (1999) Monounsaturated but not polyunsaturated fatty acids are required for growth of the deep-sea bacterium *Photobacterium profundum* SSP at High Pressure and low Temperature. Enriron Microbiol 65:1710-1720

Ambrose SH, Norr L (1993) Carbon isotopic evidence for routing of dietary protein to bone collagen, and whole diet to bone apatite carbonate: Purified diet growth experiments. In: Lambert J, Grupe G (eds) Molecular archaeology of prehistoric human bone. Springer, New York, pp 1-37

Auerswald K, Wittmer MHOM, Zazzo A, Shäufele R, Schnyder H (2010) Biases in the analysis of stable isotope discrimination in food webs. J Appl Ecol 47:936-941. doi: 10.111/j.1365-2664.2009.01764.x

Berge J-P, Barnathan G (2005) Fatty acids from lipids of marine organisms: molecular biodiversity, roles as biomarkers, biologically active compounds, and economical aspects. Adv Biochem Engin Biotechnol 96:49-125

Billett DSM, Lampitt RS, Rice AL, Mantoura RFC (1983) Seasonal sedimentation of phytoplankton to the deep-sea benthos. Nature 302: 52-522

Blair NE, Levin LA, DeMaster DJ, Plaia G.(1996) The short-term fate of fresh algal carbon in continental slope sediments. Limnol Oceanogr 41:1208-1219

Carleton SA, Martinez del Rio C (2010) Growth and catabolism in isotopic incorporation: a new formulation and experimental data. Funct Ecol 24:805-812. doi: 10.1111/j.1365-2435.2010.01700.x

Caut S, Angulo E, Courchamp F (2008) Discrimination factors (Δ^{15}N and Δ^{13}C) in an omnivorous consumer: effect of diet isotopic ratio. Funct Ecol 22:255-263. doi: 10.1111/j.1365-2435.2007.01360.x

Caut S, Angulo E, Courchamp F (2009) Variation in discrimination factors (Δ^{15}N and Δ^{13}C): the effect of diet isotopic values and applications for diet reconstruction. J App Ecol 46:443–453

Caut S, Angulo E, Courchamp F (2008) Discrimination factors (Δ^{15}N and Δ^{13}C) in an omnivorous consumer: effect of diet isotopic ratio. Funct Ecol 22:255-263. doi: 10.1111/j.1365-2435.2007.01360.x

Chu FLE, Graeves J (1991) Metabolism of palmitic, linoleic, and linolenic acids in adult oysters, *Crossostrea virginica.* Mar Biol 110:229-236

Colaco A, Desbruyeres D, Guezennec J (2007) Polar lipid fatty acids as indicators of trophic associationsin deep-sea vent system community. Mar Ecol 28:15-24

Courtinat B (1998) New general and new species of scolecodonts (fossil annelids) with paleoenvironmental and evolutionary considerations. Micropaleontol 44:435-440

Crawley KR, Hyndes GA, Vanderlkift MA (2007) Variation among diets in discrimination of d13C and D15N in the amphipod *Allorchestes compressa*. J Exp Mar Biol Ecol 249:370-377.

Dalsgaard J, St John M, Kattner G, Müller-Navarra D, Hagen W (2003) Fatty acid trophic markers in the pelagic marine environment. Adv Mar Biol 46:225–340

DeNeiro MJ, Epstien S (1977) Mechanism of carbon isotope fractionation associated with lipid synthesis. Science 197:261-263

DeNeiro MJ, Epstien S (1978) Influence of diet on the distribution of carbon isotopes in animals. Geochim Cosmochim Acta 42:495-506

Duffy JE, Richardson JP, Canuel EA (2003) Grazer diversity effects on ecosystem functioning in seagrass beds. Ecol Lett 6:637-645

Elton C (1927) Animal ecology. Sidgwick and Jackson, Ltd. London

Fantle MS, Dittel AI, Schwalm SM, Epifanio CE, Fogel ML (1999) A food web analysis of a juvenile blue crab, *Callinectes sapidus*, using stable isotopes in whole animals and individual amino acids. Oecologia 120:416-426

Fauchald K, Jumars PA (1979) The diet of worms: a study of polychaete feeding guilds. Oceangr Mar Biol Ann Rev 17:193-284

Felicciti LA, Schartz CC, Rye RO, Haroldson MA, Gunther KA, Phillips DL, Robbins CT (2003) Use of sulfer and nitrogen stable isotopes to determine the importance of whitebark pine nuts to Yellowstone grizzly bears. Can J Zool 81:763-770

Fisher CR (1990) Chemoautotrophic and methanotrophic symbioses in marine invertebrates. Rev Aquat Sci 2:399–436

Francis CA, Roverts KJ, Beman JM, Eantoro AE, Oakley BB (2005) Ubiquity and diversity of ammonia-oxidizing archaea in water columns and sediments of the ocean. Proc Nat Acad Sci 102:14683-14688

Frias-Lopez J, Thompson A, Waldbauer J, Chisholm SW (2009) User of stable isotope-labeled cells to identify active grazers of picocyanobacteria in ocean surface waters. Environ Microbiol 11:512-525. doi:10.1111/j.1462-2920.2008.01793.x

Gannes LZ, O'Brien DM, Marínez del Rio C (1997) Stable isotopes in animal ecology: assumptions, caveats, and a call for more laboratory experiments. Ecology 78:1271-1276

Gostinčar C, Turk M, Gunde-Cimerman N (2010) The evolution of fatty acid desaturases and Cytochrome *b*5 in eukaryotes. J Membrane Biol 233:63-72

Haines EB, Montegue CL (1979) Food source of estuarine invertebrates analyzed using $^{13}C/^{12}C$ ratios. Ecology 60:48-56

Hentchell BT (1998) Intraspecific variations in $\delta^{13}C$ indicate ontogenetic diet changes in deposit-feeding polychaetes. Ecology 79: 1357-1370

Herndl GJ, Reinthaler T, Tiera E, van Aken H, Veth C, Pernthaler A, Pernthaler J (2005) Contribution of Archaea to total prokaryotic production in the deep Atlantic Ocean. App Environ Microbiol 71: 2303-2309

Hilderbrand GV, Farley SD, Robbins CT, Hanley TA, Titus K, Servheen C (1996) Use of stable isotopes to determine diets of living and extinct bears. Can J Zool 74:2080-2088

Hobson KA, Alusauskas RT, Clark RG (1993) Stable-Nitrogen isotope enrichment in avian tissues due to fasting and nutritional stress: implications for isotopic analyses of diet. Condor 95:388-394

Iverson SJ (2009) Tracing aquatic food webs using fatty acids: from qualitative indicators to quantitative determination. IN: Arts M, Brett M, Kainz M (eds) Lipids in aquatic ecosystems. Springer, New York. pp 281- 307

Iverson SJ, MacDonald J, Smith LK (2001) Changes in diet of free-ranging black bears in years of contrasting food availability revealed through milk fatty acids. Can J Zool 79:2268–2279

Iverson SJ, Field C, Don Bowen W, Blanchard W (2004) Quantitative fatty acid signature analysis: a new method for estimating predator diets. Ecol Monogr 74: 211-235

Iverson SJ, Springer AM, Kitaysky AS (2007) Seabirds as indicators of food web structure and ecosystem variability: qualitative and quantitative diet analyses using fatty acids. Mar Ecol Prog Ser 352:235-244. doi:10.3354/meps07073

Jackson D, Harkness DD (1987) The use and interpretation of d13C values as a means of establishing dietary composition. OIKOS 48: 258-264

Jeffreys RM, Wolff GA, Murty SJ (2009) The trophic ecology of key megafaunal species at the Pakistan Margin: Evidence from stable isotopes and lipid biomarkers. Deep-Sea Res I 56:1816-1833

Jiang L (2007) Negative selection effects suppress relationships between bacterial diversity and ecosystem functioning. Ecology 88:1075-1085

Kharlamenko VI, Kiyashko SI, Imbs AB, Vyshkvartzev DI (2001) Identification of food sources of invertebrates from the seagrass *Zostera marina* community using carbon and sulfer stable isotope ratio and fatty acid analysis. Mar Ecol Prog Ser 220:103-117

Lebaron P, Servais P, Troussellier M, Courties C, Muyzer G, Bernard L, Schäfer H, Pukell R, Stackerbrandt R, Guindulain T, Vives-Rego J (2001) Microbial community dynamics in Mediterranean nutrient-enriched seawater mesocosms: changes in abundance, activity and composition. FEMS Microbial Ecol 34:255-266

Levin LA (2005) Ecology of cold seep sediments: interactions of fauna with flow, chemistry and microbes. Oceanogr Mar Biol Ann Rev 43:1-46

Levin LA, Mendoza GF (2007) Community structure and nutrition of deep methane-seep macrobenthos from the North Pacific (Aleutian) Margin and the Gulf of Mexico (Florida Escarpment). Mar Ecol 28:131-151

Levin LA, Michener RH (2002) Isotopic evidence for chemosynthesis based nutrition of macrobenthos: the lightness of being at Pacific methane seeps. Limnol Oceangr 47:1336-1345

Lewis T, Nichols PD, McMeekin TA (2000) Evaluation of extraction methods for recovery of fatty acids from lipid-producing microheterotrophs. J Microbiol Meth 43:107-116

Linderman RL (1942) The trophic-dynamic aspect of ecology. Ecology 23:339-417

McCutchan Jr. JH, Lewis WM, Kendall C, McGrath C (2003) Variation in trophic shift for stable isotope ratios of carbon, nitrogen, and sulfer. OIKOS 102:378-390

Mikola J, Setala H (1998) Evidence of trophic cascades in an experimental microbial- based soil food web. Ecology 79:153-164

Minagawa M, Wada W (1974) Stepwise enrichment of ^{15}N along food chains: Future evidence and the relation between $\delta^{15}N$ and animal age. Geochim Cosmochim Acta 48:1135-1140

Nichols DS (2003) Prokaryotes and the input of polyunsaturated fatty acids to the marine food web. FEMS Microbiol Let 210: 1-7

Nichols PD, Guckert JB, White DC (1986) Determination of monounsaturated fatty acid double-bond position and geometry for microbial monocultures and complex consortia by capillary GC-MS of their dimethyl disulphide adducts. J Microbiol Met 5:49-55

Partensky F, Hess WR, Vaulot D (1999) *Prochlorococcus*, a marine photosynthetic prokaryote of global significance. Microbiol Mol Biol Rev 63:106-127

Pernthaler J (2005) Predation on prokaryotes in the water column and its ecological implications. Nat Rev 3:537-546

Peterson BJ, Fry B (1987) Stable isotopes in ecosystem studies. Ann Rev Ecol Syst 18:293-320

Phillips DL, Koch PK (2002) Incorporating concentration dependence in stable isotope mixing models. Oecologia 130:114-235

Pond DW, Allen CE, Bell MC, Van Dover CL, Fallick AE, Dixon DR, Sargent JR (2002) Origins of long-chain polyunsaturated fatty acids in the hydrothermal vent worms *Ridgea piscesae* and *Protis hydrothermica*. Mar Ecol Prog Ser 225:210-226

Post DM (2002) Using stable isotopes to estimate trophic position: models, methods, and assumptions. Ecology 83:703-718

Sampedro L , Jeannotte R, Whalen JK (2006) Trophic transfer of fatty acids from gut microbiota to the earthworm *Lubricus terrestris* L. Soil Biol Biochem 38:2188-2198

Schmidt SN, Olden JD, Solomon CT, Vander Zanden MJ (2007) Quantitative approaches to the analysis of stable isotope food web data. Ecology 88:2793-2802

Schwarcz HP (1991) Some theoretical aspects of isotope paleodiet studies. J Archaeol Sci 18:261-275

Sommer S, Pfannkucke O, Linke P, Luff R, Greinert J, Drews M, Gubsch, Pieper M, Poser M, Viergutz (2006) Efficiency of the benthic filter: Biological control of emission of dissolved methane from sediments containing shallow gas hydrates at Hydrate Ridge. Global Biogeochem Cycles. 20:1-14. doi:10.1029/2004GB002389

Spivak AC, Canuel EA, Duffy E, Richards JP (2007) Top-down and bottom-up controls on sediment organic matter composition in an experimental seagrass ecosystem. Limnol Oceanogr 52:2595-2607

Spychalla JP, Kinney AJ, Brose J (1997) Identification of an animal w-3 fatty acid desaturase by heterologous expression in *Arabidopsis*. Proc Natl Acad Sci 94:1142-1147

Stanley-Samuelson DW (1994) The biological significance of prostaglandins and related eicosanoids in invertebrates. Amer Zool 34:589-598

Taghon GL (1988) Phospholipid fatty acid composition of the deep-sea hydrothermal vent polychaete *Paralvinella palmiformis* (Polychaeta- Ampharetidae): effects of thermal regime and comparison with two shallow-water confamilial species. Comp Biochem Physiol B 91:593-596

Thurber AR (2007) Diets of Antarctic sponges: links between the pelagic microbial loop and the benthic metazoan food web. Mar Ecol Prog Ser 351:77-89

Thurber AR, Kröger K, Neira C, Wiklund H, Levin LA (2010) Stable isotope signatures and methane use by New Zealand cold seep benthos. Mar Geol 272:260-269

van Oevelen D, Van den Meersche K, Meysman FLR, Soetaert K, Middelburg JJ, Vézina AF (2010) Quantifying food web flows using linear inverse models. Ecosystems 13:32-45. doi: 10.1007/s10021-009-9297-6

Vander Zanden MJ, Rasmussen JB (2001) Variations in $\delta^{15}N$ and $\delta^{13}C$ trophic fractionation: implications for aquatic food web studies. Limnol Oceanogr 46:2061-2066

Wakeham SG, Hedges JI, Lee C, Peterson ML, Hernes PJ (1997) Composition and transport of lipid biomarkers through the water column and surficial sediments of the equatorial Pacific Ocean. Deep-Sea Res II 44:2131-2162

Wang SW, Hollmén TE, Iverson SJ (2010) Validating quantitative fatty acid signature analysis to estimate diets of spectacled and steller's eiders (*Somateria fishcheri* and *Polysticta stelleri*). J Comp Physiol B 180:125-139. doi 10.1007/s00360-009-0393-x

Wardle DA, Yeates GW, Williamson M, Bonner KI, Barker GM (2004) Linking aboveground and belowground communities: the indirect influence of aphid species identity and diversity on three trophic level soil food web. OIKOS 107:283-294

Webb SC, Hedges REM, Simpson SJ (1998) Diet quality influences the $\delta^{13}C$ and $\delta^{15}N$ of locusts and their biochemical components. J Exp Biol 201:2903-2911

Zhukova NV, Kharlamenko VI (1999) Sources of essential fatty acids in the marine microbial loop. Aquatic Microbiol Ecol 17:153-157

Acknowledgements.

I would like to thank Dr. Lisa A. Levin for conceptual input. Dr. William Gerwick, Cameron Coates, Jo Nunnery, and Dr. Tak Suyama provided access to the GC-MS which was crucial for this study. Emiley Eloe and Dr. Douglas Bartlett supplied the cultures of archaeal and bacterial food sources used, without which this study would not have been possible. Geoff Cook, Jen Gonzalez, and Christina Smith helped with the lab work. *Ophryotrocha labronica* were kindly provided by Dr. Daniella Prevedelli. Support was provided by NSF Grant OCE 0425317 and OCE 0826254, the University of California Academic Senate, Michael M. Mullin Memorial Fellowship, University of California Marine Council Coastal Environmental Quality Initiative, and Sidney E. Frank foundation. This chapter, in part, is a submitted for publication in Oecologia. The dissertation author was the primary investigator and author of this paper.

CHAPTER 5.

ARCHAEA IN METAZOAN DIETS

Abstract

Archaea are among the most abundant life forms on the planet but their role as a food source for metazoans has yet to be explored. In this study we test whether: (1) Archaea provide a food source sufficient to allow metazoan fauna to complete their life cycle; (2) neutral lipids provide a biomarker that can be used to identify archaeal consumers; and (3) archaea are consumed by metazoans that live at deep-sea methane seeps. In the laboratory, we demonstrated that a dorvilleid polychaete species, *Ophryotrocha labronica*, can complete its life cycle on monocultures of two different strains of Euryarchaea. This identified archaea as a nutritious and digestible food source sufficient to sustain metazoan populations. Although both Euryarchaea strains had unique archaeal lipids, none of these were incorporated into the *O. labronica* fed these food sources. Thus we were unable to identify an archaeal lipid within metazoans tissue that could serve as a biomarker. At methane seeps, sulfate-reducing bacteria form aggregations with anaerobic-methane oxidizing archaea (ANMEs). The sulfate-reducing bacteria contain isotopically- and structurally-unique fatty acids that were incorporated into tissues of an endolithofaunal species of dorvilleid polychaete from the Costa Rica margin, documenting consumption of archaeal-bacterial aggregates. Fatty acid composition of several dorvilleid species from soft-sediment methane seep habitats on the California and Oregon margins provides further evidence that consumption of archaeal-bacterial aggregates is a widespread methane-seep phenomenon. The confirmed consumption of archaea by metazoans, a trophic process we here call archivory, suggests that the biogeochemical reactions mediated by archaea could be impacted by metazoan grazing.

Introduction

Trophic interactions represent the most important class of feedback phenomena on our planet (Worm and Duffy 2005), but we have yet to integrate one of the most abundant forms of life in the oceans, Archaea (Lipp et al. 2008), into our understanding of these trophic relationships. In addition to their ubiquity (Karner et al. 2001; Francis et al. 2005; Pearson et al. 2008), Archaea perform key ecosystem services, including nitrification (Beman and Francis 2006), methane oxidation (Truede et al. 2003), and chemosynthetic production (Boetius and Suess 2004; Herndl et al. 2005; Wuchter et al. 2003). These services are likely impacted by grazing pressure, a "top-down" force that can cause drastic changes in productivity and nutrient cycling (Belovsky and Slade 2000; McNaughton 1995). Integrating archaea into our understanding of marine-trophic relationships may provide fundamental information about mechanisms that control archaeal-driven biogeochemical cycling. Providing the first conclusive evidence of a trophic linkage between Archaea and Metazoa, this study demonstrates that Archaea offer all of the necessary nutrients to at least one group of animal and identifies archaeal-bacterial aggregates as a primary food source for methane-seep fauna.

Methane-seep habitats provide an ecosystem with abundant, isotopically-distinct archaea which mitigate the release of the green-house gas methane. As methane is released from vast sub-seafloor reservoirs, whose volume is estimated to be 5 to 25 x 10^{17} grams C globally (Milkov 2004), it is initially oxidized by aggregates of bacteria and archaea (ANMEs) using sulfate as an electron acceptor (Boetius et al. 2000; Orphan et al. 2001; 2002). This chemoautotrophic process, the anaerobic oxidation of methane (AOM), is thought to be one of the main methane sinks on the planet (Valentine et al. 2001; Truede et al. 2003) and keeps marine methane out of the atmosphere. In addition to this ecosystem service of methane mitigation, ANMEs also act as deep-sea engineers by creating hard substrate in the form of authigenic carbonates, as a byproduct of AOM (Greinert et al. 2001; Luff et al. 2004). Within

the ANME aggregates, AOM is compartmentalized with archaea oxidizing methane (methanotrophy) and bacteria performing the sulfate reduction (although other electron acceptors can be used; Beal 2009). As methane in many cases has a distinct ^{13}C to ^{12}C ratio (Whiticar 1998- $\delta^{13}C$ notation is explained within) these aggregates possess a distinct, isotopically light carbon isotopic composition; Methanotrophic archaeal bulk $\delta^{13}C$ ranges between -30 and -100‰ and ANME associated sulfate-reducing bacteria $\delta^{13}C$ values range from -15 to -70 ‰ (Orphan et al. 2002). In most cases these values are far removed from those of photosynthetic production, which normally has a $\delta^{13}C$ value of -15 to -25 ‰ (Fry and Sherr 1994). In addition to their unique carbon-isotopic composition, both methanotrophic archaea and sulfate-reducing bacteria within these habitats have unique membrane lipids which also exhibit a highly negative (or "light") carbon-isotopic composition. Archaeal lipids from ANME consortia are composed of repeating isoprene units and have $\delta^{13}C$ values that range between -128 to -76 ‰ (Elvert and Suess 1999; Boetius et al. 2000; Hinrichs et al. 2000). Sulfate-reducing bacteria within these same consortia are largely composed of 16:1(n-5), cyc17, and/or *a*15:0 and 18:1(n-7) fatty acids (FAs), with $\delta^{13}C$ values between -112 ‰ and approximately -65 ‰ (Blumenberg et al. 2004; Elvert et al. 2003; Neimann and Elvert 2008). The FAs are named using the scheme (carbon chain length):(number of double bonds) and the location of the first double bond from the terminal methyl end given as X in the (n-X) notation. Cyc17 indicates a ring structure and a and i prefixes indicate a branch in the anteiso or iso position, respectively. These ANME aggregates, which perform a key ecosystem service and have both biomass and lipids with unique carbon-isotopic composition, routinely occur in the top four centimeters of sediment at methane seeps (Elvert et al. 2003; Knittel et al. 2003). This shallow sediment depth places them in contact with metazoan grazers that mostly belong to the polychaete family Dorvilleidae.

The isotopically-labeled archaea at methane seeps provide a model system to explore archivory, a term we coin to mean the consumption of archaea. For heterotrophs, their carbon-isotopic signature is derived from the isotopic signature of the primary producer that they or their prey feed upon (DeNeiro and Epstein 1978). Within methane seeps, members of the aforementioned Dorvilleidae, have been found with isotopically light $\delta^{13}C$ values potentially reflecting consumption of ANME aggregates (Levin and Michener 2002; Levin and Mendoza 2007; Thurber et al. 2010). This has suggested the existence of archivory, yet aerobic methanotrophs, including α-, δ-, and γ- proteobacteria but not archaea (Murase and Frenzel 2007; Ding and Valentine 2008) also have a light, methane-derived isotopic composition (Elvert et al. 2000; Werne et al. 2002). In addition, all chemoautotrophic producers, including abundant sulfide-oxidizing bacteria, can incorporate a ^{13}C-depleted isotopic signature from a ^{13}C-depleted DIC pool (Fisher 1990). Both of these mechanisms can provide a light isotopic signature to a consumer that has not consumed archaea. Thus, other biomarker approaches must be taken to identify archivory.

Grazer lipids are partially derived from their diet, providing a powerful tool for tracking microbial consumption (Dalsgaard et al. 2003). This phenomenon is best known for FAs, a component of both Eukaryotic and Bacterial cell membranes, which can provide a quantitative measure of food web linkages (Iverson 2009). In seep settings, key FA biomarkers include 16:1(n-7) and 18:1(n-7) that are abundant in sulfide-oxidizing bacteria (McCaffrey et al. 1989), the aforementioned 16:1(n-5) and cyc17 that are abundant in sulfate-reducing bacteria (Elvert et al. 2003; Blumberg et al. 2004), and 16:1(n-6) and 16:1(n-8) that are indicative of aerobic methanotrophs (Bowman et al. 1991). Composition of photosynthetic production can be identified by Polyunsaturated Fatty Acids (PUFAs) including 22:6(n-3) and 20:5(n-3) (reviewed in Dalsgaard et al. 2003). Archaeal lipids potentially provide a unique biomarker for tracking consumption of Archaea. Although these

archaeal biomarkers are very diagnostic, their incorporation into metazoan tissues has yet to be documented, limiting their utility in food-web studies.

Due to the ubiquity of dorvilleids in archaea-fueled methane seep sediments (Levin and Michener 2002; Levin et al. 2003; Levin 2005; Levin and Mendoza 2007; Menot et al. 2010; Ritt et al. 2010), we chose to use this polychaete family to study archivory. Dorvilleids are tolerant to sulfide stress allowing them to numerically dominant in microbial-mat covered sediments at seeps (Levin et al. 2003; Levin 2005), a habitat that has high ANME abundance (Boetius and Suess 2004). Archaea are known to prevail in low-energy systems and to grow slowly (Valentine 2007), thus it is unclear if archaea are a food source that is nutritious enough to support persistent metazoan populations. Some bacteria can pass through deposit-feeder guts undamaged (Lopez and Levinton 1987) and the unique, highly stable cell membranes of archaea (van de Vossenberg et al. 1998) may provide protection from digestion. We have chosen to study a taxon whose range overlaps with archaea, with the hypothesis that they are adapted to feeding upon this Domain. As a first step towards identifying if archaea are a viable and utilized food source, we combined laboratory-based feeding assays with trophic studies in soft-sediment and authigenic-carbonate seep habitats to answer the questions:

(1) Can metazoans survive and reproduce on a diet exclusively of archaea?

(2) Is there evidence for archaeal consumption by metazoans in natural populations?

(3) Does an archaeal diet manifest itself in consumer lipid signatures?

(4) Is there a trophic interaction between grazers and ANME aggregates?

Materials and Methods

Sample collection and preparation

To test if archaeal biomass provides sufficient nutrition for sustaining metazoan populations and to identify archivory biomarkers in biomass completely derived from an

archaeal diet, we raised a species of dorvilleid polychaete on archaea within the laboratory. The shallow water dorvilleid, *Ophryotrocha labronica,* was raised on monocultures of two types of halophilic Euryarchaea, *Halobacterium salinarium* and *Haloferax volcanii*. For a control, *O. labronica* was raised on a bacterium *Bacillus subtilis*, to provide a non-archaeal food-source for lipid comparison. *Ophryotrocha labronica* was also raised for 44-48 days on a diet of the aforementioned archaeal food sources or *Oryza* sp., *B. subtilis*, *Photobacterium profundum,* or *Spinacia oleracea* (four food sources representing Eukarya and Bacteria) to determine whether growth rates differ between individuals fed archaea and individuals fed the other domains of life. These prokaryotic food sources were freeze dried and fed to freshly hatched *O. labronica* at 22^{o}C in 0.2 μm filtered seawater (FSW) containing two bacterial-protein-synthesis inhibiting antibiotics, 50μM kanamycin monosulfate and 50μM streptomycin sulfate. This antibiotic treatment was used to minimize bacterial processing of the archaeal food before it was consumed by *O. labronica*. Archaeal food sources were provided by E. Eloe, Scripps Institution of Oceanography (SIO) from laboratory cultures and *O. labronica* was collected from an Italian harbor and has been in culture at SIO since 2006. Upon reaching near adult size, approximately 1.4 mm, *O. labronica* was allowed to evacuate its gut overnight in FSW (gut evacuation was obvious through the usually transparent body wall), frozen at -80^{o}C and then freeze dried for later lipid analysis.

We then sought out metazoans that live in habitats with plentiful archaea. Two deep-sea, methane-rich habitats were chosen due to their likely or known high abundance of Archaea; Authigenic carbonates precipitated on Mound 12 off Costa Rica (8^{o} 55.8'N 84^{o}18.8'W) and soft-sediment seep habitats at Eel River off northern California (40^{o}47.1'N 124^{o} 35.68'W) and at Hydrate Ridge off Oregon (44^{o}40.1'N 125^{o} 05.8'W). Authigenic carbonate rocks collected from Costa Rica during RV *Atlantis* cruise 15-44 (Rock L2; 21 February- 8 March, 2009) and 15-59 (Rock E3; January 6-12, 2010). The rocks were

recovered by the submersible DSRV *Alvin* from 1000m in insulated boxes. Carbonates were broken open with a chisel and endolithofauna removed. For the metazoans, we focused on a single undescribed dorvilleid polychaete species within the genus *Dorvillea* which was found living within the rock itself. In addition a portion of rock E3 was analyzed for its microbial community; archaeal community structure was measured by creating and sequencing a 16S rRNA gene library and fatty acids were extracted to identify the bacterial community present. Archaeal aggregates were imaged using DAPI staining and epiflourescent microscopy.

Soft-sediment seep habitats off CA and OR with high abundance of Archaea (Orphan et al. 2001; Elvert et al. 2003; Knittel et al. 2003; Boetius and Suess 2004), were sampled during RV *Atlantis* cruises 15-7 (July 13-27, 2006) and 15-11 (September 26-October10, 2006) using the DSRV *Alvin.* Sediment was collected using 6.3cm diameter push cores or "scoops" from clam beds and microbial mats at depths of 500-880 m. These sediment samples were sieved on a 300-μm sieve and sorted live yielding five species of dorvilleid polychaetes for analysis. Animals were identified to putative species and placed in 25 μm-filtered, cold seawater overnight to allow gut evacuation. All field collected samples were frozen at -80^{o}C for lipid analysis or prepared for isotopic analysis.

Lipid analyses

Neutral lipid and fatty acid analyses were performed to characterize food sources and diets of laboratory-reared and field-collected animals. Neutral lipids were measured from both laboratory food sources as well as all dorvilleids. Key archaeal lipids, including hydroxyarchaeol, archaeol, crocetane, and PMI are present in the neutral lipid fraction (Obe et al. 2006) and provided possible archivory biomarkers. Neutral lipids were repeatedly extracted ultrasonically in methanol/chloroform/10% trichloroacetic acid (TCA) (2:1:0.8 v/v/v) (modified from Obe et al. 2006). After 30 minutes sonication, samples were spun down,

supernatant removed and fresh extraction solvent added, this was repeated four times and the supernatants collected in a fresh vial. Milli-Q water and methanol were then added to create a final ratio of 1:1:0.9 (methanol/chloroform/10% TCA) at which point the TCA was removed by repeated washing with 5:4 methanol: H_2O. The sample was dried under N_2 gas and saponified in 6% potassium hydroxide (KOH) in methanol for 3 hrs at 80^{o}C. After being allowed to cool the neutral lipids were extracted 4 times in hexane. The remaining KOH:methanol was acidified to a pH of 1 and re-extracted with hexane. This hexane contains the "polar" fraction (FAs) and is not discussed further except for one instance where the $\delta^{13}C$ values of neutral and polar lipids were analyzed in *Dorvillea* sp. from authigenic-carbonate. Neutral lipids were blown down to dryness in conical vials, and transferred to lined injection vials. 10µl of pyridine and 10µl of BSTFA +1%TMCS (N,O-bis(trimethylsilyl)triflouroacetamide) were added (Fisher scientific) and the vials were heated to 70^{o}C for 60 min in nitrogen flushed vials to derivatize carboxylic acid with a trimethylsilyl group. All syringes that were used with the BSTFA and samples for this stage were flushed with N_2. After cooling the samples were blown to dryness and brought back into hexane before injection on a GC-MS. All glassware used in the extractions (both this and those described below) was sonicated for 15 min with four washes (1x soap, 2x water, 1x DI water) and heated in a muffle furnace for four hours at 500 ^{o}C. Contaminants were extracted from the glassware by solvents following the same extraction protocol that the samples would undergo to remove any remaining lipids within the vials. Blanks were run concurrently with all sample sets. Samples were extracted in 12ml screw-top glass vials with PTFE lined lids.

Fatty acids of field-collected individuals and rock E3 were extracted using a one-step extraction-transesterification reaction to identify the food sources consumed by these species. This technique was chosen due to its effectiveness at extracting very small (<0.2 mg) biomass samples. This reaction used an extraction solvent of 3ml of 10:1:1 methanol: chloroform:

hydrochloric acid (v:v:v; Lewis et al. 2000), which was added to the previously freeze-dried samples. Samples were ground within this solvent using a glass rod prior to being sonicated for 10-15 minutes. After heating to 90^{O}C for 1 hour in a dry block, samples were allowed to cool, and one ml of Milli-Q water was added. The newly formed fatty acid methyl esters were extracted in 3 aliquots of 2ml 4:1 chloroform: hexanes (v:v). Samples were blown to dryness in N_2, weighed, and brought up in an appropriate amount of the chloroform: hexanes mixture for injection and analysis by GC- MS. The extraction-transesterification method was modified to extract the E3 carbonate. 1.3g of rock was pulverized in a methanol cleaned, dry-ice chilled mortar and pestle and then added to a vial with methanol: chloroform: hydrochloric acid (HCl) extraction solvent. 12N HCl was added until degassing stopped (from the carbonates reaction with the extraction solvent) until a final pH of 1.5 was achieved (the starting pH of the solvent). From that point forward the rock was extracted as above.

Due to the small biomass of most dorvilleids, GC-MS analysis, being highly sensitive but less quantitative than GC-FID, was employed. Thus whereas internal comparisons within this study are valid, absolute concentrations are not quantitatively comparable with values generated by other instruments. All samples were analyzed on a Thermo Finnigan Trace GC/MS with a TR-5MS 60m x 0.32μm i.d. column in positive ion mode. Sample oven conditions for fatty acid analysis were an initial hold at 60 ^{o}C for 1 minute, heating from 60^{o}C to 180^{o}C at 12^{o}C per minute, then an increase to 250 ^{o}C at 2.5 ^{o}C per minute where samples were held for 30 minutes. Neutral lipids were injected at 70 ^{o}C and raised to 160 ^{o}C at 20 ^{o}C per minute and then at 4 ^{o}C per minute to 310 ^{o}C. Blanks were run with all batches and all solvents were ACS grade or better. In the instance where blanks did indicate peaks, these were subtracted from co-extracted and analyzed samples. Peak integration and identification were performed based on the full mass spectra using Xcaliber © software (Thermo Scientific), comparison to known standards (Supelco 37 Component FAME mix and Supelco Bacterial

Acid Methyl Ester mix, Sigma-Aldrich), and dimethyl-disulfide derivatization (following Nichols et al. 1986) for identification of mono-unsaturated bond location. Identification of neutral lipids was based on comparison to published mass spectra.

Carbon isotopic analyses

Three types of isotopic analysis were performed on field-collected samples to track methane-derived carbon, potentially indicative of archivory: "Bulk $\delta^{13}C$", "Bulk-Lipid $\delta^{13}C$", and "Compound-Specific $\delta^{13}C$". "Bulk $\delta^{13}C$" is the carbon isotopic composition of the non-lipid extracted dorvilleid biomass. For this analysis, individuals, or fractions thereof, were placed in tin-boats at sea, dried at 60^{o}C overnight, and acidified with 1% $PtCl_2$ to remove any inorganic carbon. "Bulk-Lipid $\delta^{13}C$" was the separate analysis of polar and neutral lipids within *Dorvillea* sp. Lipids, and thus biomarkers, which are directly incorporated from methanotrophic archaea should have a light carbon isotopic signature. By separately measuring the $\delta^{13}C$ of each of these lipid fractions we can identify which of them might contain an archaeal biomarker. To do this we used the neutral lipid extraction technique but evaporated both polar and neutral fractions into doubled tin boats. A concurrent solvent and extraction blank was run and the samples were corrected for this. These "Bulk $\delta^{13}C$" and "Bulk-Lipid $\delta^{13}C$" samples were analyzed on a Eurovector elemental analyzer interfaced with a continuous flow Micromass Isoprime isotope ratio mass spectrometer at Washington State University, a Finnigan Conflow 2 continuous flow system and a Fisons NA 1500 elemental analyzer coupled to a Finnegan Delta S isotope ratio mass spectrometer at Boston University, or a continuous flow PDZ Europa 20/20 isotope ratio mass spectrometer at UC Davis.

"Compound-specific $\delta^{13}C$" was used to identify the isotopic composition of each of the FAs present within both rock E3 and the *Dorvillea* sp. which inhabited it. This allows fine-

scale identification of which FAs are both present within the food source (the rock) and are incorporated into *Dorvillea* tissues. FAs were extracted using the one-step extraction-transesterification, the FA composition identified and percent FA calculated, then analyzed at the University of Davis Stable Isotope Facility on a Thermo GC/C-IRMS system composed of a Trace GC Ultra gas chromatograph (Thermo Electron Corp., Milan, Italy) coupled to a Delta V Advantage isotope ratio mass spectrometer. Each FA isotopic composition was corrected for the C added by methylation from the methanol used and a blank was run concurrently to determine whether any of the FAs were likely a mixture of contaminants.

Results

Ophrotrocha labronica grew and reproduced on archaeal food sources yet did not incorporate an archaeal lipid signature. *O. labronica* grew from 0.2 mm (post hatching) to approximately 1.3mm (adult size) on monospecific diets of both *H. salinarium* (n=13 separate cohorts) and *H. volcanii (n=12* separate cohorts). *Ophryotrocha labronica* fed *H. volcanii* (n=1; 4 young hatched) and of *H. salinarium* (n=3; 1 brood = 33 eggs; 5-12 young hatched from other 2 replicates) produced broods in 45-48 days; the same amount of time it took *O. labronica* fed *B. subtilis* (n=3; 9, 13, and 36 young hatched), *P. profundum* (n=1; 5 young hatched),*Oryza sp.* (n=1; brood = 21 eggs) and *S. oleracea* (n=1; 6 young hatched) to produce broods and offspring. Mean growth rate of *O. labronica* over a 44-47 day period did not vary as a function of food source (Figure 5.1; $F_{5,29}$=1.36, p=0.27). Archaeal food sources were sufficient to allow *O. labronica* to close its life cycle and did not negatively affect this species' mean growth rate. Both strains of Euryarchaea had a neutral lipid composition which included repeating isoprene units, including squalene and similar molecules (Table 5.1). The worms fed these two archaeal species did not incorporate these molecules and instead had a neutral lipid profile consisting largely of cholesterol and other common sterols. With the exception of β-

sitosterol, these same compounds were found in an individual fed the bacterium *B. subtilis* (Table 5.1). None of the neutral lipids in archaea-fed *O. labronica* tissues were archaeal specific, despite the fact that this species could grow to reproduction on an Archaeal monoculture.

Although archivory biomarkers were not detected, sulfate-reducing bacterial biomarkers allowed us to identify ANME aggregates as the main food source for the *Dorvillea* sp. inhabiting authigenic-carbonate. Within rock E3, we found microbial aggregates (Figure 5.2) and a microbial community dominated by ANME type-II aggregates; type-I aggregates were also present. 16S rRNA gene analysis identified 68% percent of archaeal diversity as belonging to the ANME type-II, whereas 10% belonged to ANME type-I. The fatty acid composition of rock E3 was largely composed of ^{13}C-depleted FAs indicative of ANME-associated, sulfate-reducing bacteria, as well. The two most abundant FAs, cyc17:0 and 16:1(n-5), each comprised more than 20% percent of the total FA composition of the rock (Figure 5.3) and are common in sulfate-reducing bacteria associated with ANME type-II aggregates (Elvert et al. 2003; Blumenburg et al 2004). The isotopic signatures of these two FAs, with δ^{13}C values of -115 ‰ and -110 ‰ respectively, provided further evidence that they are derived from sulfate-reducing bacteria coupled to anaerobic-methane oxidation. The FA which had the lightest isotopic signature was a15:0, with a δ^{13}C value of -127‰. This FA made up 11% of the FA composition of those bacteria present within the carbonate and is a biomarker found in sulfate-reducing bacteria associated with ANME Type-1 aggregates. These FA profiles mirror the 16S gene data indicating that the majority of the microbial community within the rock was ANME type-II aggregates with a smaller subset belonging to the type-I. Both 16:0 and 18:0 were much heavier than the other FAs present, and although these data were corrected for concurrently run blanks, they also exhibited trace contaminants from the sample processing and thus their isotopic values are unlikely to represent the isotopic

composition of those FAs from the sample. 16:1(n-6) and 16:1(n-8) FAs were not present; these would have indicated bacterial aerobic methanotrophs within the carbonate habitat.

The *Dorvillea* sp. inhabiting these carbonates consumed ANME aggregates as their main food source. Among the isotopically lightest metazoans on record, the bulk carbon isotopic signatures of *Dorvillea* sp. were as low as -101 ‰ (rock L2) and within rock E3 this species had a mean $\delta^{13}C$ of -91.7 ± 3.5 (SE) ‰ (n= 10). The individual with a bulk $\delta^{13}C$ of -101 ‰, had polar-lipid $\delta^{13}C$ = -116 ‰ and neutral lipid $\delta^{13}C$ relatively heavy at -68 ‰. This indicated that the lightest carbon, and thus biomarkers from methanotroph biomass, are incorporated into the polar-lipid fraction rather than the neutral lipids. Although the neutral-lipid fraction also showed clear incorporation of methane-derived carbon (-68 ‰ is still very light), this isotopic composition is far removed from the sulfate-reducing lipid isotopic composition (here -110 ‰ at the heaviest; Figure 5.3). As sulfate-reducing biomarkers are always isotopically heavier than archaeal lipid biomarkers (Blumenberg et al. 2004; Niemann and Elvert 2008), it is unlikely that the archaeal lipids formed the building blocks of the neutral lipids within *Dorvillea* sp. In addition the neutral-lipid composition of this species was similar to that of *O. labronica* raised in the laboratory on *B. subtilis* or the Euryarchaea, indicating that the dorvilleid neutral lipid signature is not diet specific (Table 5.1).

The *Dorvillea* sp. lipid profile included FAs derived from ANME-associated, sulfate-reducing bacteria (Figure 5.3). These FAs included 16:1(n-5), which composed 1.4-1.8 % of the total fatty acids present within *Dorvillea* sp. from rocks E3 and L2. The FA 18:1(n-5), which can be synthesized by eukaryotes if they are provided with 16:1(n-5), also formed between 3.3 and 5.3 percent of the *Dorvillea*'s FA profile. Both of these (n-5) FAs had isotopic signatures within 3‰ of the sulfate-reducing bacteria (n-5) FA. This indicates that these FAs were derived from the carbonate AOM consortia. The remaining FAs present within this species had isotopic signatures that were < -100 ‰ (except for a 20:0 FA that was -95 ‰)

also clearly revealing incorporation of methane-derived carbon. Even two polyunsaturated fatty acids, 20:5(n-3) and 20:4(n-6), which are commonly used as indicators of phytoplanktonic production, had $\delta^{13}C$ values between -103‰ and -109‰, indicating they were formed *in situ* by either consumed bacteria or the dorvilleids. Together, these lines of evidence suggest that *Dorvillea* sp. incorporates markers from sulfate-reducing bacteria but its fatty acid signature and therefore its diet is entirely composed of methane-derived carbon originating with AOM.

We can ask whether consuming the AOM consortia is an evolutionary oddity limited to carbonate habitats or a common occurrence. We examined 5 species of dorvilleids from NE Pacific seeps that co-occurred with AOM consortia. The $\delta^{13}C$ composition of these species varied between -19.5 and -57.9 ‰ indicating use of a diversity of food sources, including potentially photosynthetic and AOM-derived organic matter. As with the carbonate endolithofauna, a subset of these dorvilleids possessed (n-5) fatty acids (Table 5.2). The distribution of these FAs was not uniform among the species; instead the greater the composition of (n-5) FAs the lighter the $\delta^{13}C$ (Figure 5.4). This simple relationship between percent (n-5) and $\delta^{13}C$ explained 50% of the variance observed in the carbon isotopic composition of these species ($F_{1,20}$=20.4, $p<0.01$; R^2=50.5):

$$\delta^{13}C = -3.5 \times \sum [16:1(n-5) + 18:1(n-5)] + -28.2 \qquad (1)$$

Although one individual appeared to have a large impact on this regression, as it's FA composition was 10.1% (n-5) FAs, removing this individual increased the negative slope of the regression to -5.6 and but had little effect on the variance explained ($F_{1,19}$=17.1, $p<0.01$; R^2=47.4). Thus, we have chosen to retain all data. Inclusion of the (n-7) FAs, common in

sulfide-oxidizing bacteria (McCaffrey et al. 1989), only improved the fit of the model by 1.5%. A regression of isotope signature against percent (n-7) FAs, explained 20% of the variance ($F_{1,20}$=5.30, p=0.03; R^2=20.9). There was a small percentage of 16:1(n-6) FA present in three of the dorvilleid species, which are FAs indicative of aerobic methanotrophy, yet these were a minor component of the lipid profile (Table 5.2). The neutral lipids within the seep-sediment dorvilleid species had a sterol composition similar to that of the carbonate endolithofauna and those of the *O. labronica* reared in the laboratory on archaeal and bacterial diets (Table 5.1). Together these observations support the hypothesis that the Eel River and Hydrate Ridge dorvilleids consume AOM aggregates. Furthermore, as both the laboratory and field study found, unique neutral lipids were not found in species for which all other evidence suggested archaeal consumption.

Discussion

Archaeal biomarkers

Archaea are a ubiquitous domain of life, and in addition to their previously recognized importance, are now known to be capable of supporting growth and reproduction of heterotrophic metazoans. Archaea are abundant throughout the water column below 1000 m (Karner et al. 2001**,** Herndl et al. 2005, Francis et al. 2005), in the southern ocean (Church et al. 2003), oxygen minimum zones (Francis et al. 2005), sediments greater than 1m below the seafloor (Biddle et al. 2006)**,** and in reducing ecosystems such as methane seeps (Boetius and Suess 2004). Within the meso- and bathy-pelagic depths, archaea fix carbon chemosynthetically (Wutchter et al. 2003; Herndl et al. 2005; Ingalls et al. 2006) which support bacterial and archaeal populations (Hansman et al. 2009). Symbiotic relationships are known between archaea and ciliates (van Hoek et al. 2000), sponges (Preston et al. 1996), and even terrestrial ruminants (Joblin 2005), defining a key role for archaea in supporting

eukaryotes. In each of these systems and symbioses, archaea are abundant and likely biogeochemically and ecologically important. Attempts to amplify archaeal 16S rRNA from *Dorvillea* sp. from E3 (S. Goffredi pers. com.) confirmed that dorvilleids do not have archaeal symbionts. Thus, this family of polychaete provides the first evidence for the ecological role of archaea as a food source for heterotrophic metazoans. Notably, the ability to identify the trophic role of archaea will be hindered without archivory biomarkers.

Although the archaea used as food sources in this study provided diagnostic neutral-lipid biomarkers, those species that consumed archaea did not incorporate these lipids, nor did they appear to derive their neutral lipids from them. Archaeal biomarkers were not found in species fed a monoculture of archaea or those that clearly consumed archaeal aggregates. The neutral lipids present within the Euryarchaea fed to *O. labronica* contained compounds similar in structure to crocetene and PMI, two characteristic lipids found in anaerobic-methane oxidizing archaea at seeps (Figure 5.5; Sprott et al. 1990; Hinrichs et al. 2000; Werne et al. 2002; Pancoast et al. 2000). Neither lab-reared nor field-collected dorvilleids had any of these compounds present (Table 5.1).

If archaeal lipids form the building blocks for eukaryotic sterol synthesis, compound specific analysis of these sterols may be an alternative approach to identifying archivory. Both crocetane and PMI are some of the most ^{13}C depleted lipids within methanotrophic Archaea. In a broad review of these two lipids from seep habitats, neither was found to have a $\delta^{13}C$ value heavier than -83 ‰ (Niemann and Elvert 2008). In addition, crocetane and PMI have a structure similar to squalene, a lipid provided by both archaeal food sources in the laboratory, which is a precursor of cholesterol during sterol biosynthesis (Kanazawa 2001). Yet, the neutral lipids within the carbonate-dwelling *Dorvillea* sp. had a ^{13}C-enriched $\delta^{13}C$ signature (-68 ‰) despite a bulk biomass $\delta^{13}C$ of -101‰. This neutral fraction was mostly composed of

cholesterol and so it is unlikely formed through incorporation of archaeal lipids; it was far too heavy. The ability to synthesize many sterols has been observed in the polychaete *Capitella* sp. I to augment those provided by its diet (Marsh et al. 1990). The isotopic composition of the neutral lipid fraction of *Dorvillea* sp. and the uniform distribution of sterols within all dorvilleids studied suggests they too synthesize most of their sterols and do not incorporate archaeal lipids as sterol building blocks.

The source of building blocks for the dorvilleid sterols remains a mystery. Acetate is commonly incorporated into sterols in many phyla (Kanazawa et al. 2001) and acetate is used to elongate FAs. *Dorvillea* sp. forms 18:1(n-5) by the addition of acetate to 16:1(n-5) therefore we can use a carbon mass-balance approach to calculate the $\delta^{13}C$ of acetate used by *Dorvillea* sp. This results in an acetate $\delta^{13}C$ estimate of -109 ‰ and -128 ‰ used by *Dorvillea* sp. from rocks L2 and E3, respectively. This does assume that there is no fractionation among which 16:1(n-5) FAs get converted into 18:1(n-5). The same individual which used a $\delta^{13}C$=-109 ‰ acetate had a neutral lipid signature of -68 ‰, thus the incorporation of acetate into the *Dorvillea* sp. neutral-lipid biosynthetic pathway is unlikely. This is only suggestive evidence of the isotopic composition of sterol building blocks. The sterol synthesis pathway may not use the same precursors as FA synthesis and instead could incorporate acetate that has a different isotopic signature than we estimate here.

Bactivory tracing Archivory

By tracking FAs that are present in the sulfate-reducing bacterial component of AOM aggregates, we indirectly identified consumption of Archaea by metazoans. Within the authigenic carbonate habitat we found a microbial community that was dominated by ANME aggregates; 54% of the FAs within the rocks belonged to components of AOM-associated sulfate-reducing bacteria. 43 % of these were FAs most dominant in Type-II ANME

aggregates and 68% of the archaea in the rock belonged to Type-II ANMEs, based on 16S rRNA analysis gene sequence. The remaining 11% of sulfate-reducing biomarkers and 10% of the archaeal diversity belonged to Type-I ANMEs. 18:1(n-7) is also abundant in Type-I ANME aggregates (Elvert et al. 2003; Blumenberg et al. 2004) and comprised 9.4% of the FA within rock E3. This FA is also found within sulfide-oxidizing bacteria (McCaffery et al. 1989) and can be synthesized by eukaryotes (Berge and Barnathan 2005). As such, this FA is not diagnostic for sulfate-reducing bacteria but it likely belongs to Type-I ANMEs aggregates in this particular case. Together these combined FA and 16S rRNA gene sequence results indicate that the dominant available food sources within the rock were ANME aggregates.

Eukaryotes have a suite of enzymes that allow them to form or modify dietary-derived FAs to form their lipid profiles. In addition to being able to elongate FAs by the addition of acetate, eukaryotes can also synthesize a diversity of unsaturated (n-7) and (n-9) FAs and a variety of 20:1 FAs (Kattner and Hagen 1995). Knowledge to date suggests that (n-5) fatty acids are not synthesized by eukaryotes (MacAvoy et al. 2003). This was also one of the few FAs present within *Dorvillea* sp. that this group cannot synthesize (Chapter 4). This means that the rest of its FA profile could be generated by any food source, including archaea. The cyc17 that was abundant within the rocks was not present within the dorvilleid tissues. However a species has the ability to either digest or incorporate a FA and certain FAs are not incorporated even if they are present in a species diet (Chapter 4). As such the abundance of (n-5) fatty acids, isotopically similar to the sulfate-reducing bacteria, indicates that AOM aggregates are the primary food source for the carbonate-dwelling dorvilleids.

This consumption of ANME by dorvilleids occurs at other seep locations, as was previously hypothesized based on isotopic evidence (Levin and Michener 2002). It is likely that dorvilleids are able to harvest these aggregates due to their chitonized jaws that provide a mechanism to scrape the microbial aggregates off of rocks. The mechanism might be

analogous to use of the gastropod radula in harvesting epilithic algae, and make dorvilleids pre-adapted to consume seep aggregates.

Two potential hypotheses may explain the interaction between dorvilleids and the aggregates: (1) dorvilleids consumed the aggregates but only digested the sulfate-reducing bacteria or (2) dorvilleids digested the aggregates en masse and thus their diet is composed of both archaea and sulfate-reducing bacteria. If the latter is true, all compounds within the consumed Archaea would be re-synthesized providing an across- the-board light isotopic signature in both their tissue and lipids. Such signatures were observed in all analyses except for the neutral lipid fraction. Our estimate of a -128 ‰ isotopic signature for acetate indicates that a portion of the *Dorvillea* sp. food source has an isotopic signature that is only found in nature in archaeal lipids. This finding adds further credence to the idea that archaea are consumed, ingested and, and digested during aggregate consumption. The isotopic signature of -127 ‰ for *a*15:0 collected from the rock is potentially the lightest FA known and was (marginally) heavier than the -128 ‰ estimated for acetate. Yet independent of whether dorvilleids were digesting the archaea, they were clearly impacting the aggregates by either digesting just the sulfate-reducing bacteria or the ANME aggregate in its entirety.

Archaea in food webs

Discovery of the importance of the microbial loop in pelagic food webs represents a major revolution in oceanography (Barber and Hilting 2000). But far less is known about microbial roles in benthic food webs and marine sediments, where microbe and species interactions are hard to study. The discovery of the existence and ubiquity of Archaea represents another major discovery, with the potential to transform our understanding of microbial roles in the ocean. But presently both benthic and pelagic food webs at best include

a ‘box’ for bacteria (e.g. Oevelen et al. 2006; Soetart & Oevelen 2009) and never mention Archaea. This is because there is virtually no information about archaeal roles in food webs. In many of the environments where archaea occur in great numbers, they have a carbon-isotopic composition that is indistinct from planktonic production (Hoefs et al. 1997) and no symbionts that can be followed as a biomarker proxy. Yet, as we demonstrate here, Archaea are food sources that can support metazoan growth and are ingested even if they are not digested by infauna. As we have been unsuccessful in identifying a biomarker for archivory, we must instead turn to other techniques, potentially including pulse-chase manipulative approaches (Blair et al. 1997; Aberle and Witte 2003; Witte et al. 2003; Wuchter et al. 2003) or tracing ^{14}C dead radiocarbon into cells, a powerful approach when identifying both archaeal activity in deep-pelagic realms (Ingalls et al. 2006) and their importance for microbes (Hansman et al. 2009).

ANME are thought to be the terminal sink of methane throughout the globe yet the impact of metazoan grazing on ANMEs is unknown. The majority of methane emitted at seeps is consumed within the sediment before it is released into the water column. Aerobic bacteria and ANME’s form a “sediment filter” keeping this green house gas out of the atmosphere (Sommer et al. 2006). For the first time we have shown that the anaerobic part of this sediment filter is consumed by metazoans, with unknown ramifications for the biogeochemical cycling of methane within these seeps. Observation of this phenomenon within authigenic carbonates, habitats that are widespread on margins, opens a new avenue of C cycling investigation. To date carbonates have not been appreciated as a filter for escaping methane. Archaea, even at methane seeps (Orphan et al. 2004), exist without sulfate-reducing symbionts. We still have no techniques to resolve if and how their populations are impacted by grazing. By showing that ANME consumption can be identified from the incorporation of AOM-associated, sulfate-reducing bacteria FAs, we have taken a first step towards identifying the impact of microbial-

metazoan interactions on methane cycling. This domain of life may interact with metazoans in many yet-to be discovered ways.

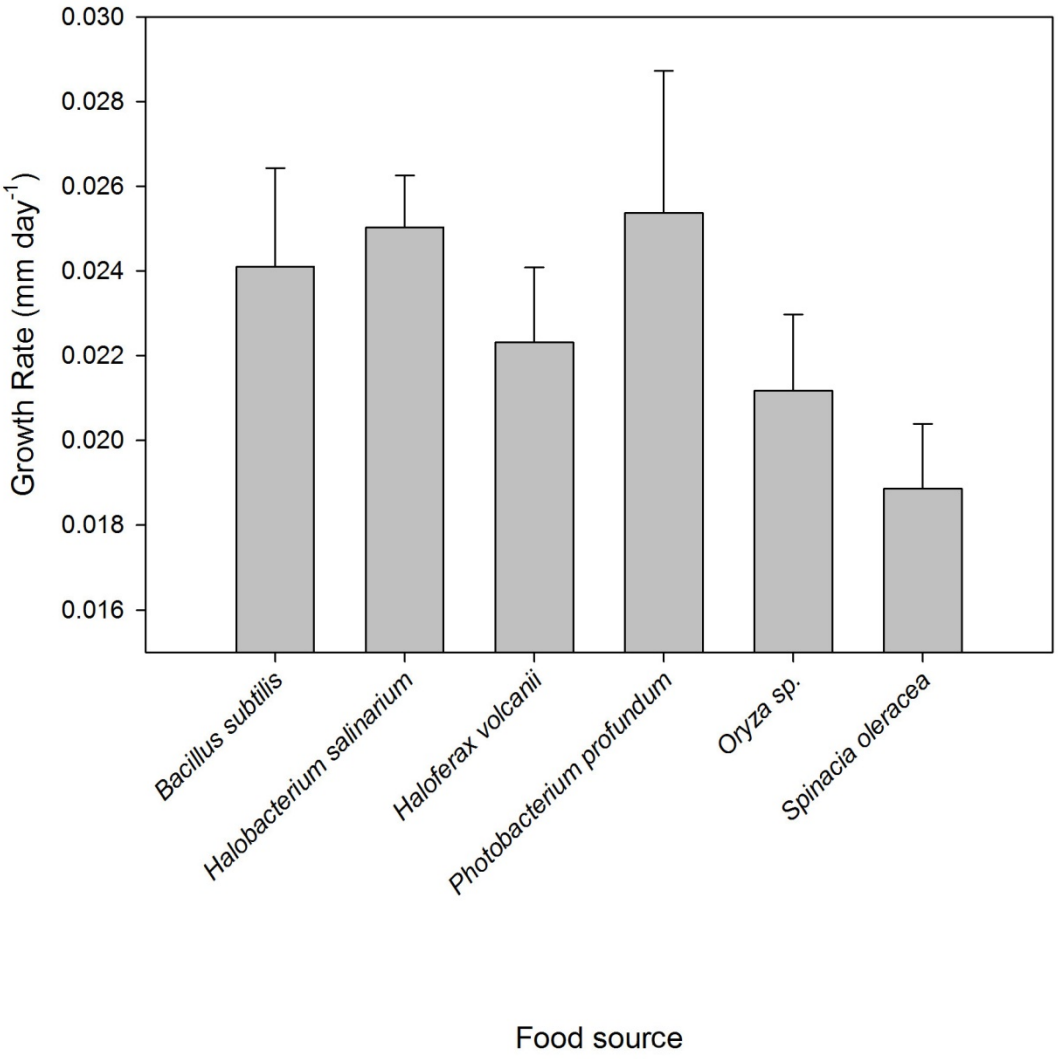

Figure 5.1 Mean daily growth rate of *Ophryotrocha lobronica* over a 44 to 47 day period as a function of food source. Error bars = 1 SE.

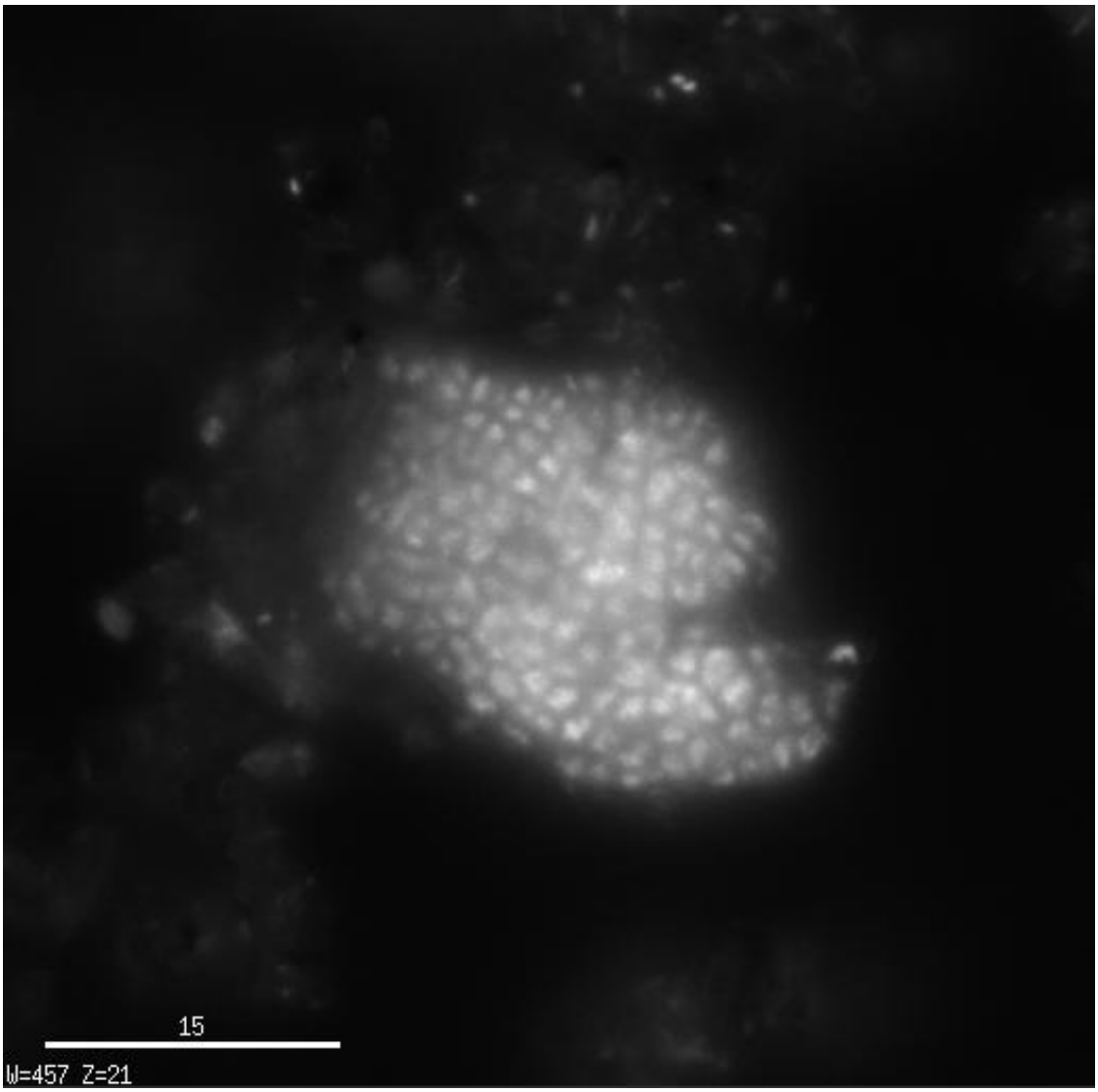

Figure 5.2 Micrograph of ANME aggregate from inside rock "E3" stained with DAPI. Scale bar = 15μm (Credit: Jeffrey Marlow)

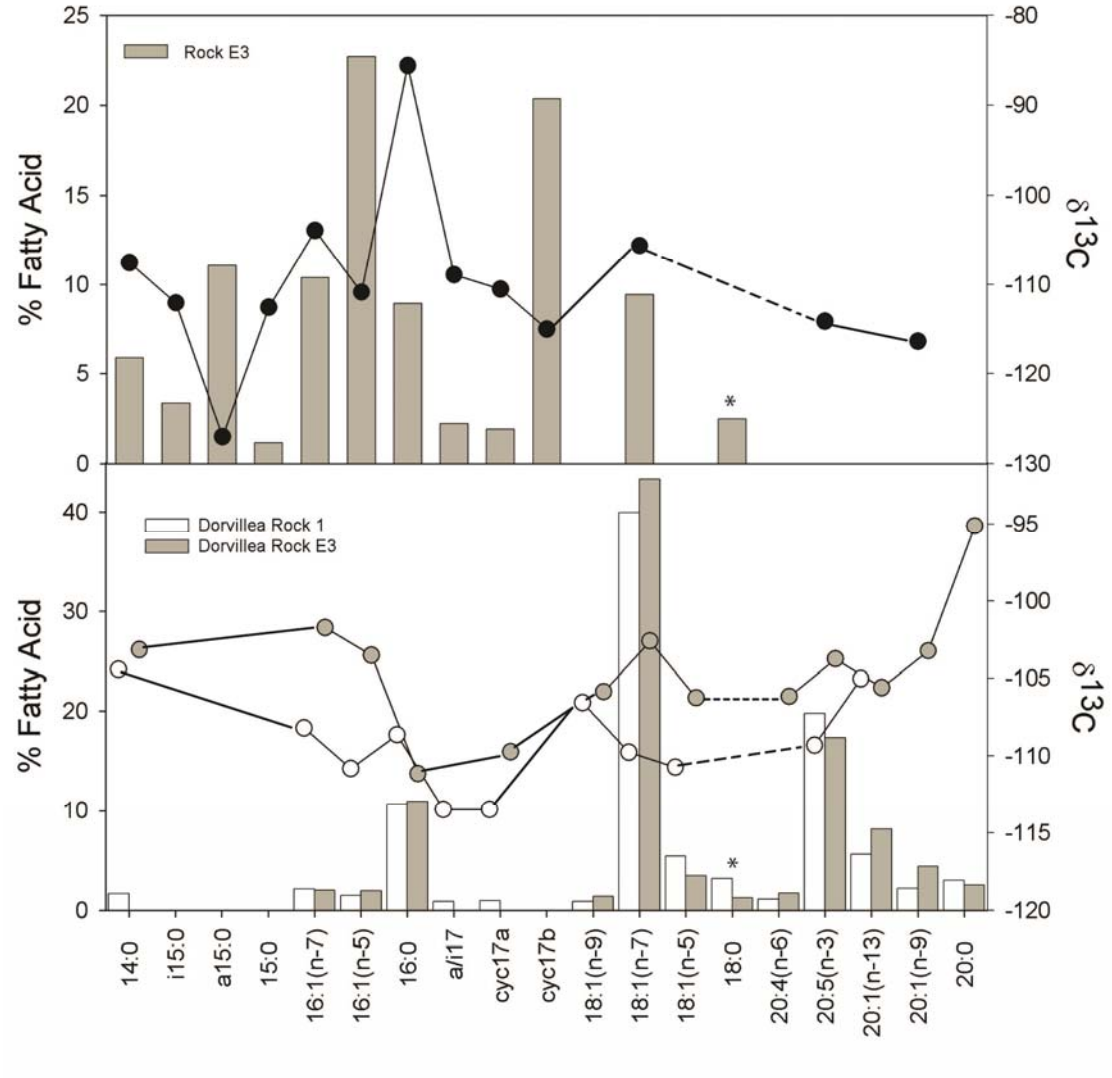

Figure 5.3 Carbon isotopic composition of fatty acids and fatty acid distribution within (upper panel) carbonate rocks and (lower panel) *Dorvillea* sp. Left y-axis and bars are percent fatty acid and right y-axis and points are isotopic composition. Asterisks indicate that isotopic composition was potentially largely impacted by contaminants (see text for more details). Value estimates for this omitted FA ranged between -143 to -45 ‰. 18:2 and 20:1(n-11) were left off this figure as they were <2% in only one individual of *Dorvillea* sp.

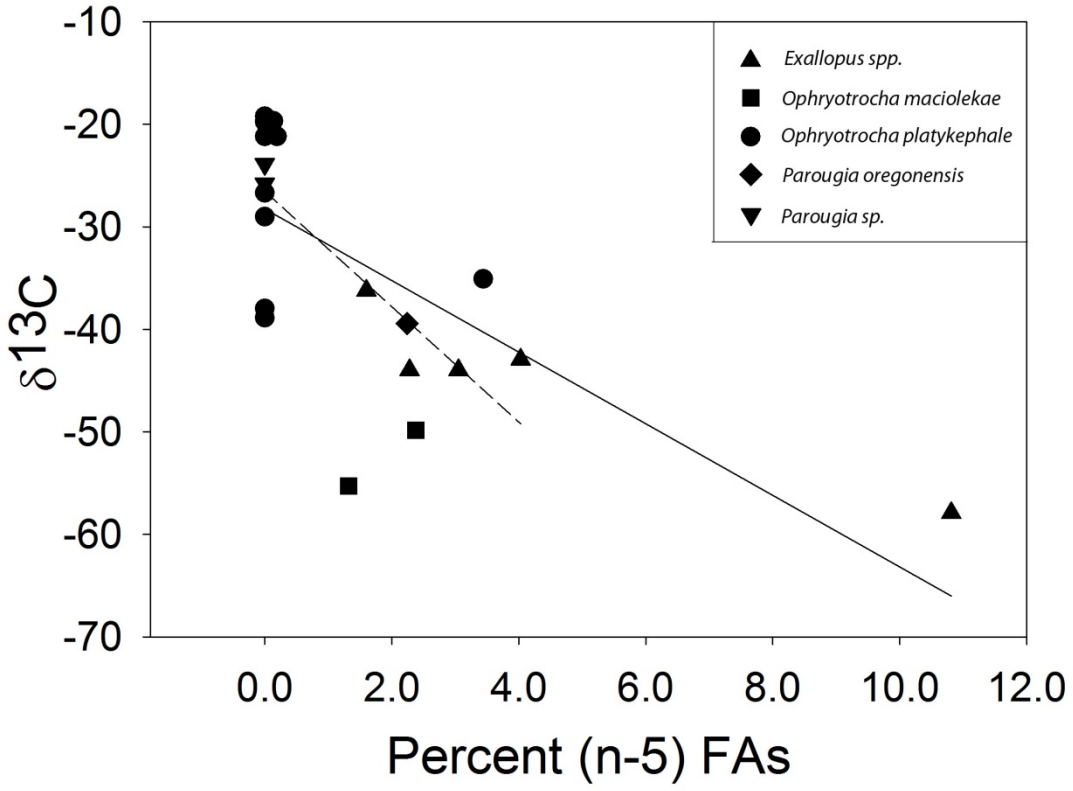

Figure 5.4 Relationship between carbon isotopic composition and sum of 16:1(n-5) and 18:1(n-5) FAs present within 5 species of polychaete from Eel River and Hydrate Ridge. Solid line is a regression including all dorvilleid polychaetes in which both isotopic and FA data are available within a single sample. Dotted line indicates regression if point to the far right is removed. Symbols indicate species.

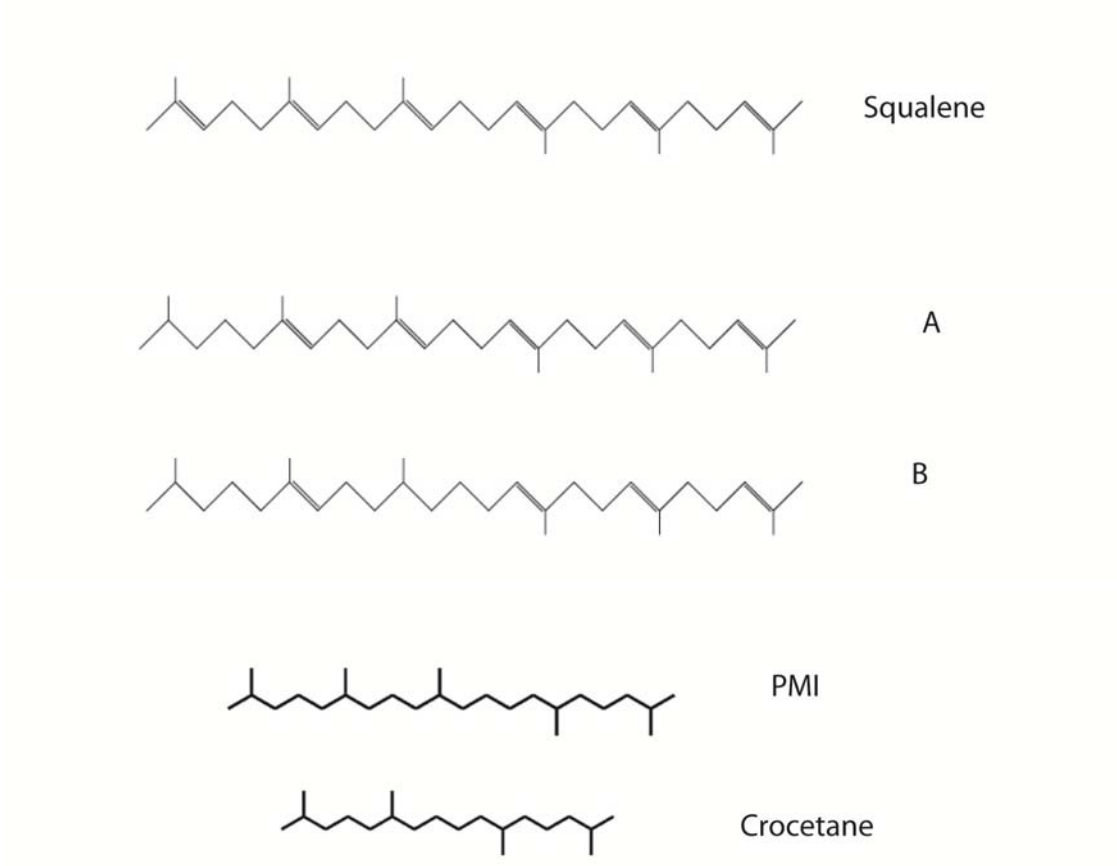

Figure 5.5 Most abundant neutral lipids present within the two species of Euryarchaea used in the laboratory feeding study (squalene, A, and B) and those present within methane seep Euryarchaea (PMI, crocetane from Blumenberg et al. 2004). Location of double bonds for A and B are approximate and in Table 5.1 A and B include all isomers of these molecules.

Table 5.1 Percent neutral lipid composition of dorvilleid polychaetes and *Ophryotrocha labronica* fed Euryarchaea in the laboratory. Dorvilleids include those collected from cold-seep habitats. Archaea are identified in bold. Tr = trace; nd = not detected potentially due to methodology or concentration analyzed. M.W. = Molecular weight of TMS derivative. Other indicates that its mass spectra was not able to be conclusively identified. Asterisks indicates probable identity. A and B are more saturated molecules of squalene (and shown in Figure 5.5).

Chemical name	Formula	M.W.	*Dorvillea sp.*	*O. labronica* fed *H. volcanii*	*O. labronica* fed *H. salinarium*	*O. labronica* fed *B. subtilis*	*Parougia oregonensis*	*Exallopus spp.*	*Ophryotrocha maciolekae*	*Ophryotrocha platykephale*	***H. volcanii***	***H. salinarium***
Cholesterol	$C_{27}H_{46}O$	458	41.5	69.1	77.2	81.6	71.6	87.2	82.8	81.5		
Desmosterol	$C_{27}H_{44}O$	456	27.1	9.6	12.5	tr		3.5	7.8	13.7		
Brassicasterol	$C_{28}H_{46}O$	470	25.3	8.6	tr	nd	12.8		4.3	4.7		
Cholestanol	$C_{29}H_{52}O$	488						1.9				
Other							6.3	4.6				
β- sitosterol	$C_{29}H_{50}O$	486	6.1*	12.7	nd	tr	9.2	2.9	nd			
Squalene	410										60.3	3.1
A	412										30.7	4.3
B	414										7.4	81.2
Phytol		nd	nd	nd	nd	nd	nd	nd	nd	nd	0.7	11.3
C20 Isoprene	370	nd	nd	nd	nd	nd	nd	nd	nd	nd	1.1	
C15 Isoprene	294	nd	nd	nd	nd	nd	nd	nd	nd	nd	2.5	

Table 5.2 Fatty acid (FA) fraction of total FA profile of each species included in analysis. Isotopic data are provided for either a fraction of the individual extracted for lipids or from individuals within the same core or scoop sample. Standard error is given. Only data are presented with samples that corresponded to an isotopic measure and only FAs are presented that made up at least 1% of any one sample. * means that double-bond position was estimated from retention time rather than DMDS adduct formation.

	Exallopus spp.	*Ophryotrocha maciolekae*	*Ophryotrocha platykephale*	*Parougia oregonensis*	*Parougia sp.*	*Dorvillea sp.*
n	5	3	11	2	1	2
$\delta^{13}C$	-45.0 ± 3.5	-24.5 ± 0.6	-26.2 ± 2.4	-52.6	-39.4	-91.5
14:0	0.023 ± 0.004	0.035 ± 0.009	0.015 ± 0.004	0.024	0.000	0.009
16:1(n-7)	0.117 ± 0.013	0.045 ± 0.019	0.056 ± 0.011	0.024	0.033	0.019
16:1(n-6)	0.006 ± 0.002	0.000 ± 0.000	0.001 ± 0.001	0.001	0.000	0.000
16:1(n-5)	0.031 ± 0.013	0.000 ± 0.000	0.002 ± 0.001	0.006	0.008	0.016
16:0	0.160 ± 0.018	0.256 ± 0.052	0.202 ± 0.034	0.117	0.115	0.110
18:2(n-6)c	0.016 ± 0.003	0.004 ± 0.004	0.016 ± 0.004	0.003	0.000	0.005
18:1(n-9)t	0.004 ± 0.004	0.012 ± 0.012	0.003 ± 0.003	0.000	0.000	0.000
18:1(n-9)c	0.070 ± 0.058	0.082 ± 0.069	0.025 ± 0.004	0.010	0.008	0.014
18:2(n-6)t	0.016 ± 0.016	0.014 ± 0.007	0.004 ± 0.004	0.000	0.000	0.000
18:1(n-7)	0.278 ± 0.067	0.074 ± 0.037	0.220 ± 0.036	0.485	0.483	0.399
18:2b	0.069 ± 0.020	0.003 ± 0.003	0.064 ± 0.012	0.033	0.000	0.000
18:1(n-5)	0.013 ± 0.005	0.000 ± 0.000	0.002 ± 0.002	0.013	0.014	0.044
18:0	0.039 ± 0.019	0.203 ± 0.093	0.094 ± 0.024	0.027	0.025	0.032
cyc19	0.000 ± 0.000	0.000 ± 0.000	0.009 ± 0.003	0.000	0.007	0.000
20:4(n-6)	0.006 ± 0.002	0.025 ± 0.014	0.010 ± 0.003	0.006	0.023	0.014
20:5(n-3)	0.076 ± 0.018	0.138 ± 0.054	0.094 ± 0.017	0.078	0.216	0.188
20:2	0.009 ± 0.009	0.030 ± 0.015	0.030 ± 0.009	0.008	0.000	0.000
20:1(n-13)	0.029 ± 0.008	0.022 ± 0.022	0.011 ± 0.008	0.038	0.056	0.069
20:1(n-9)*	0.000 ± 0.000	0.009 ± 0.009	0.000 ± 0.000	0.000	0.000	0.000
20:1(n-7)	0.013 ± 0.006	0.000 ± 0.000	0.009 ± 0.005	0.006	0.011	0.007
20:1a	0.004 ± 0.004	0.007 ± 0.007	0.008 ± 0.006	0.000	0.000	0.032
20:3n3or6	0.004 ± 0.004	0.000 ± 0.000	0.017 ± 0.006	0.000	0.000	0.000
20:0	0.005 ± 0.005	0.019 ± 0.009	0.005 ± 0.003	0.000	0.000	0.030
21:0	0.000 ± 0.000	0.000 ± 0.000	0.001 ± 0.000	0.000	0.000	0.000
22:0	0.000 ± 0.000	0.000 ± 0.000	0.005 ± 0.003	0.033	0.000	0.000
23:0	0.000 ± 0.000	0.004 ± 0.004	0.032 ± 0.025	0.039	0.000	0.000
24:1	0.000 ± 0.000	0.000 ± 0.000	0.003 ± 0.003	0.000	0.000	0.000
24:0	0.000 ± 0.000	0.000 ± 0.000	0.003 ± 0.003	0.000	0.000	0.000

References

Aberle N, Witte U (2003) Deep-sea macrofauna exposed to a simulated sedimentation event in the abyssal NE Atlantic: in situ pulse-chase experiments using ^{13}C-labelled phytodetritus. Mar Ecol Prog Ser 251:37-47

Barber RT, Hilting AK (2000) Achievements in biological oceanography. In: 50 Years of Ocean Discovery. Ocean Studies Board. Washington DC, National Academy Press. pp11–21

Beal EJ, House CH, Orphan VJ (2009) Manganese- and Iron- Dependent marine methane oxidation. Science 325:184-187

Belovsky GE, Slade JB (2000) Insect herbivory accelerates nutrient cycling and increases plant production. Proc Natl Acad Sci USA 97:14412-14417

Beman JM, Francis CA (2006) Diversity of ammonia-oxidizing archaea and bacteria in the sediments of a hypernutrified subtropical estuary: Bahia del Tobari, Mexico. Appl Environ Microbiol 72:7767-7777

Berge J-P, Barnathan G (2005) Fatty acids from lipids of marine organisms:molecular biodiversity, roles as biomarkers, biologically active compounds, and economical aspects. Adv Biochem Engin Biotechnol 96:49-125

Biddle JF, Lipp JS, Lever MA, Lloyd KG, Sørensen KB, Anderson R, Fredricks HF, Elvert M, Kelly TJ, Schrag DP, Sogin ML, Brenchley JE, Teske A, House CH, Hinrichs K-U (2006) Heterotrophic Archaea dominate sedimentary subsurface ecosystems off Peru. Proc Nat Acad Sci 103:3846-3851

Billett DSM, Lampitt RS, Rice AL, Mantoura RFC (1983) Seasonal sedimentation of phytoplankton to the deep-sea benthos. Nature 302: 52-522

Blumenberg M, Kruger M, Nauhaus K, Talbot HM, Oppermann BI, Seifert R, Pape T, Michaelis W (2006) Biosynthesis of hopanoids by sulfate-reducing bacteria (genus *Desulfiovibrio*) Environ Microbiol doi:10.1111/j.1462-2920.2006.01014.x

Blumenberg M, Seifert R, Reitner J, Pape T, Michaelis W (2004) Membrane lipid patterns typify distinct anaerobic methanotrophic consortia. Proc Nat Acad Sci 30:11111-11116

Boetius A, Rabenschlag K, Schubert CJ, Richert D, Widdle F, Gieske A, Amann R, Jorgensen BB, Witte U, Pfannkuche O (2000) A marine microbial consortium apparently mediating anaerobic oxidation of methane. Nature 407:623-626

Boetius A, Suess E (2004) Hydrate Ridge: a natural laboratory for the study of microbial life fueled by methane from near-surface gas hydrates. Chem Geol 205:291-310

Bowman JP, Skerratt JH, Nichols PD, Sly LI (1991) Phospholipid fatty acid and lipopolysaccharide fatty acid signature lipids in methane-utilizing bacteria. FEMS Microbiol Ecol 85:15– 22

Church MJ, DeLong EF, Ducklow HW, Karner MB, Preston CM, Karl DM (2003) Abundance and distribution of planktonic *Archaea* and *Bacteria* in the waters west of the Antarctic Peninsula. Limnol Oceangr 48:1893-1902

Conway NM, Kennnicult II MC, Van Dover CL (1994) Stable isotopes in the study of marine chemosynthetic-based ecosystems. In: Lajtha K, Michener HR (eds) Stable Isotopes in Ecology and Environmental Science, Blackwell, Oxford, pp. 158–186

Dalsgaard J, St John M, Kattner G, Müller-Navarra D, Hagen W (2003) Fatty acid trophic markers in the pelagic marine environment. Adv Mar Biol 46:225–340

DeNeiro MJ, Epstien S (1978) Influence of diet on the distribution of carbon isotopes in animals. Geochim Cosmochim Acta 42:495-506

Ding H, Valentine DL (2008) Methanotrophic bacteria occupy benthic microbial mats in shallow marine hydrocarbon seeps, Coal Oil Point, California. J Geo Res 113:1-11 doi: 10.1029/2007JG000537

Elvert M, Greinert J, Suess E, Whiticar MJ (2000) Archaea mediating anaerobic methane oxidation in deep-sea sediments at cold seeps of the eastern aleutian subduction zone. Organic Geochem 31:1175-1187

Elvert M, Boetius A, Knittel K, Jorgensen BB (2003) Characterization of specific membrane fatty acids as chemotaxonomic markers for sulfate-reducing bacteria involved in anaerobic oxidation of methane. Geomocrbiol J 20:403-419

Elvert M, Suess E (1999) Anaerobic methane oxidation associated with marine gas hydrates: superlight c-isotopes from saturated and unsaturated C20 and C25 irregular isoprenoids. Naturwissenchaften 86:295-300

Fisher CR (1990) Chemoautotrophic and methanotrophic symbioses in marine invertebrates. Rev Aquat Sci 2:399–436

Francis CA, Roberts KJ, Beman JM, Santoro AE, Oakley BB (2005) Ubiquity and diversity of ammonia-oxidizing archaea in water columns and sediments of the oceans. Proc Nat Acad Sci 102:14683-14688

Fry B, Sherr EB (1994) $\delta^{13}C$ measurements as indicators of carbon flow in marine and freshwater systems. Contrib Mar Sci 27:13-46

Greinert J, Bohrmann G, Suess E (2001) Gas hydrate-associated carbonates and methane-venting at Hydrate Ridge classification, distribution, and origin of authigenic lithologies, Geophys Monogr 124:99-113

Hansman RL, Griffin S, Watson JT, Druffel ERM, Ingalls AE, Pearson A, Aluwihare LI (2009) The radiocarbon signature of microorganisms in the mesopelagic ocean. Proc Nat Acad Sci 106:6513-6518

Herndl GJ, Reinthaler T, Tiera E, van Aken H, Veth C, Pernthaler A, Pernthaler J (2005) Contribution of Archaea to total prokaryotic production in the deep Atlantic Ocean. App Environ Microbiol 71: 2303-2309

Hinrichs KU, Summons RE, Orphan V, Sylva SP, Hayes JM (2000) Molecular and isotopic analysis of anaerobic methane-oxidizing communities in marine sediments. Org Geochem 31:1685–1701

Hoefs MJL, Schouten S, de Leeuw JW, King LL, Wakeham SG, Sinninghe Damsté HS (1997) Ether lipids of planktonic Archaea in the marine water column. Appl Environ Microbiol 63:3090-3095

Ingalls AE, Shah SR, Hansman RL, Aluwihare LI, Santos GM, Druffel ERM, Pearson A (2006) Quantifying archaeal community autotrophy in the mesopelagic ocean using natural radiocarbon. Proc Nat Acad Sci 103:6442-6447

Iverson SJ (2009) Tracing aquatic food webs using fatty acids: from qualitative indicators to quantitative determination. IN: Arts M, Brett M, Kainz M (eds) Lipids in aquatic ecosystems. Springer, New York. pp 281- 307

Joblin K (2005) Methanogenic archaea. IN: Makkear HPS, McSweeny CS (eds) Methods in gut microbial ecology for ruminants. Springer, New York, pp 47-53

Kanazawa A (2001) Sterols in marine invertebrates. Fisheries Sci 67:997-1007.

Karner MB, EF Delong, Karl DM (2001) Archaeal dominance in the mesopelagic zone of the Pacific Ocean. Nature 409:507-510

Kattner G, Hagen W (1995) Lipid metabolism of the Antarctic euphausiid *Euphausia crystallorophias* and its ecological implications. Mar Ecol Prog Ser 170:203-213

Knittel K, Boetius A, Lemke A, Eilers H, Lochte K, Pfannkucke O, Linke P (2003) Activity, distribution, and diversity of sulfate reducers and other bacteria in sediments above gas hydrate (Cascadia Margin, Oregon). Geomicrobiol J 20:269-294

Levin LA (2005) Ecology of cold seep sediments: interactions of fauna with flow, chemistry and microbes. Oceanogr Mar Biol Ann Rev 43:1-46

Levin LA, Mendoza GF (2007) Community structure and nutrition of deep methane-seep macrobenthos from the North Pacific (Aleutian) Margin and the Gulf of Mexico (Florida Escarpment). Mar Ecol 28:131-151

Levin LA, Michener R (2002) Isotopic evidence of chemosynthesis-based nutrition of macrobenthos:the lightness of being at Pacific methane seeps. Limnol Oceanog 47:1336–1345

Levin LA, Ziebis W, Mendoza G, Growney V, Tryon M, Brown K, Mahn C, Gieskes J, Rathburn A (2003) Spatial heterogeneity of macrofauna at northern California methane seeps:the influence of sulfide concentration and fluid flow. Mar Ecol Prog Ser 265:123–139

Lewis T, Nichols PD, McMeekin TA (2000) Evaluation of extraction methods for recovery of fatty acids from lipid-producing microheterotrophs. J Microbiol Methods 43: 107-116.

Lipp JS, Morono Y, Inagaki F, Hinrichs K-U (2008) Significant contribution of archaea to extant biomass in marine subsurface sediments. Nature 424:991-994

Lopez GR, Levinton JS (1987) Ecology of deposit-feeding animals in marine sediments. Quarterly Review of Biology 62: 235-260

Luff R, Wallmann K, Aloisi G (2004) Numerical modeling of carbonate crust formation at cold vent sites: significance for fluid and methane budgets and chemosynthetic biological communities. Eart Planet Sci Lett 22:337-353

MacAvoy SE, Macko SA, Carney RS (2003) Links between chemosynthetic production and mobile predators on the Louisiana continental slope: stable carbon isotopes of specific fatty acids. Chem Geol 201:229-237

Marsh AG, Harvey HR, Gremaré A, Tenore KR (1990) Dietary effects on oocyte yolk-composition in *Capitella* sp. I (Annelida: Polychaeta): fatty acids and sterols. Mar Biol 106:369-374

McCaffrey MA, Farrington JW, Repeta DJ (1989) Geochemical implications of the lipid composition of *Thioploca spp*. from the Peru upwelling region – 15°S. Org Geochem 14:61–68

McCutchan Jr. JH, Lewis WM, Kendall C, McGrath CC (2003) Variation in trophic shift for stable isotope ratios of carbon, nitrogen, and sulfur. Oikos 102: 378-390.

McNaughton SJ (1985) Ecology of a grazing ecosystem: the Serengeti. Ecol Monogr 55:259-294.

Menot L, Galéron J, Olu K, Caprais J-C, Crassous P, Khripounoff A, Sibuet M (2010) Spatial heterogeneity of macrofaunal communities in and near a giant pockmark area in the deep Gulf of Guinea. Mar Ecol 31:78-93

Milkov AV (2004) Molecular and stable isotope compositions of natural gas hydrates:A revised global dataset and basic interpretations in the context of geological settings. Org Geochem 36:681-702

Murase J, Frenzel P (2007) A methane-driven microbial food web in a wetland rice soil. Environ Microbiol 9:3025-3034

Neimann H, Elvert M (2008) Diagnostic lipid biomarker and stable carbon isotope signatures of microbial communities mediating the anaerobic oxidation of methane with sulphate. Org Geochem 39:1669-1677.

Nichols PD, Guckert JB, White DC (1986) Determination of monounsaturated fatty acid double-bond position and geometry for microbial monocultures and complex consortia by capillary GC-MS of their dimethyl disulphide adducts. J Microbiol Meth 5:49–55

Niemann H, Elvert M (2008) Diagnostic lipid biomarker and stable carbon isotope signatures of microbial communities mediating the anaerobic oxidation of methane with sulphate. Org Geochem 39:1668-1677

Obe M, Sakata S, Tsunogai U (2006) Polar and neutral isopranyl glycerol ether lipids as biomarkers of archaea in near-surface sediments from the Nankai trough. Org Geochem 37:1643-1654

van Oevelen D, Moodley L, Soetaert K, Middelburg JJ (2006) The trophic significance of bacterial carbon in marine intertidal sediment: results of an in situ stable isotope labeling study. Limnol Oceanogr 51:2349-2359

Orphan VJ, House CH, Hinrichs KU, Mckeegan KD, Delong EF (2001) Methane-consuming archaea revealed by directly coupled isotopic and phylogenetic analysis. Science 293:484–487

Orphan VJ, House CH, Hinrichs KU, McKeegan KD, DeLong EF (2002) Multiple archaeal groups mediate methane oxidation in anoxic cold seep sediments. Proc Nat Acad Sci USA 99**:**7663–7668

Orphan VJ, Ussler III W, Naehr TH, House CH, Hinrichs K-U, Paull CK (2004) Geological, geochemical, and microbiological heterogeneity of the seafloor around methane vents in the Eel River Basin, offshore California. Chem Geol 205:265-289.

Pancost, RD, Sinninghe Damste JS, De Lint S, Van Der Maarel MJEC, Gottschal JC, Medinaut Shipboard Scientific Party (2000) Biomarker evidence for widespread anaerobic methane oxidation in Mediterranean sediments by a consortium of methanogenic archaea and bacteria. Appl Environ Microbiol 66:1126–1132

Preston CM, Ying Wu K, Molinski TF, DeLong EF (1996) A psychrophilic crenarchaeon inhabits a marine sponge: Cenarchaeum symbiosum gen. nov., sp. nov. Proc Nat Acad Sci 93:6241-6246.

Ritt B, Sarrazin J, Caprais J-C, Noël P, Gauthier O, Pierre C, Henry P, Desbruyères D (2010) First insights into the structure and environmental setting of cold-seep communities in the Marmara Sea. Deep-Sea Res I 57:1120-1136Sampedro L , Jeannotte R, Whalen JK (2006) Trophic transfer of fatty acids from gut microbiota to the earthworm *Lubricus terrestris* L. Soil Biol Biochem 38:2188-2198

Soetart K, van Oevelen D (2009) Modeling food web interactions in benthic deep-sea ecosystems: a practical guide. Oceanogr 22:128-143

Sommer S, Pfannkucke O, Linke P, Luff R, Greinert J, Drews M, Gubsch, Pieper M, Poser M, Viergutz (2006) Efficiency of the benthic filter: Biological control of emission of dissolved methane from sediments containing shallow gas hydrates at Hydrate Ridge. Global Biogeochem Cycles. 20:1-14. doi:10.1029/2004GB002389

Sprott GD, Ekiel I, Dicaire C (1990) Novel, Acid-labile, Hydroydiether lipid cores in methanogenic bacteria. J Biological Chem 23:13735-13740

Spychalla JP, Kinney AJ, Brose J (1997) Identification of an animal w-3 fatty acid desaturase by heterologous expression in *Arabidopsis*. Proc Natl Acad Sci 94:1142-1147

Stadnitskaia A, Bouloubassi I, Elvert M, Hinrichs K-U, Sinninghe Damsté JS (2008) Extended hydroxyarchaeol, a novel lipid biomarker for anaerobic methanotrophy in cold seep habitats. Org Geochem 30:1007-1014

Thurber AR (submitted) Diet-dependant incorporation of biomarkers: Biases associated with food-web studies using stable isotopic and fatty acid analysis. Oecologia.

Thurber AR, Kröger K, Neira C, Wiklund H, Levin LA (2010) Stable isotope signatures and methane use by New Zealand cold seep benthos. Mar Geol 272:260-269

Truede T, Boetius A, Knittel K, Wallmann K, Jørgensen BB (2003) Anaerobic oxidation of methane above gas hydrates at Hydrate Ridge, NE Pacific Ocean. Mar Ecol Prog Ser 264:1-14

Valentine DL (2007) Adaptations to energy stress dictate the ecology and evolution of the Archaea. Nat Rev Microbiol 5:316-323

Valentine DL, Blanton DC, Reeburgh WS, kastner M (2001) Water column methane oxidation adjacent to an area of active hydrate dissociation, Eel River Basin. Geochim Cosmochim Acta 65:2633-2640

Van de Vossenberg JLCM, Driessen AJM, Konings WN (1998) The essence of being extremophilic: the role of the unique archaeal membrane lipids. Extremophiles 2:163-170.

van Hoek AHAM, van Alen TA, Sprakel VSI, Leunissen JAM, Brigge T, Bogels GD, Hackstein JHP (2000) Multiple acquisition of methanogenic archaeal symbionts by anaerobic ciliates. Mol Biol Evol 17: 251-258

Werne JP, Baas M, Sinninghe Damste JS (2002) Molecular isotopic tracing of carbon flow and trophic relationships in a methane-supported benthic microbial community. Limnol Oceanogr 47:1694-1701

Whiticar MJ (1998) Carbon and hydrogen isotope systematic of bacterial formation and oxidation of methane. Chem Geol 161:291-314

Witte U, Aberle N, Sand M, Wenshöfer F (2003) Rapid response of a deep-sea benthic community to POM enrichment: an in situ experimental study. Mar Ecol Prog Ser 251:27-36

Worm B, Duffy JE (2003) Biodiversity, productivity, and stability in real food webs. Trends Ecol Evo 18:628-632.

Wuchter C, Schouten S, Boshker HTS, Sinninghe Damste JS (2003) Bicarbonate uptake by marine Crenarchaeota. FEMS Microbiol Lett 219:203-20

Acknowledgments

We are indebted to the Captains, Crew, Alvin group and Science parties from AT 15-9; 15-11; 15-44; 15-59. Guillermo Mendoza, Jennifer Gonzalez, Brigitte Ebbe, Ken Halanych, Ray Lee and Greg Rouse all helped tremendously at sea with sorting and identification of the dorvilleid species. Dr. William Gerwick provided access to the analytical instrumentation necessary to carry out this research and Cameron Coates, Jo Nunnery and Tak Suyama were always present to help trouble shoot analytical problems. This research was supported by four NSF Grants OCE 0425317, OCE 0826254, NSF OCE-0242034, and OCE-0939557 grants to LA Levin, in addition to the Michael M Mullin Memorial fellowship, Sidney E Frank foundation Fellowship, and the graduate office of Scripps Institution of Oceanography. Chapter 5, in part, is currently being prepared for submission for publication of the material. Thurber, Andrew R.; Levin, Lisa A.; Orphan, Victoria J. The dissertation author was the primary investigator and author of this paper.

CHAPTER 6.

DANCING FOR FOOD IN THE DEEP SEA:

BACTERIAL FARMING BY A NEW SPECIES OF YETI CRAB

Abstract

Vent and seep animals harness chemosynthetic energy to thrive far from the sun's energy. While symbiont-derived energy fuels many taxa, vent crustaceans have remained an enigma; these shrimps, crabs, and barnacles, possess a phylogenetically distinct group of chemosynthetic bacterial epibionts, yet the role of these symbionts has remained unclear. We test whether a new species of Yeti crab, which we describe as *Kiwa puravida* n. sp., farms the epibiotic bacteria that it grows on its chelipeds (claws); chelipeds that the crab waves in fluid escaping from a deep-sea methane seep. Lipid and isotope analyses identify epibiotic bacteria as the crab's main food source and *K. puravida* n. sp. has highly-modified setae (hairs) on its 3rd maxilliped (a mouth appendage) which it uses to harvest these bacteria. The ε- and γ-proteobacteria that this methane-seep species feeds upon are related to hydrothermal-vent decapod epibionts, yet the two species of Yeti crabs' bacterial symbionts are more closely related to symbionts from more geographically and phylogenetically separated hosts than to each other. Although it remains unknown whether evolutionary history or environmental similarities explain the divergent host-symbiont phylogenies we observed, *K. puravida* n. sp. highlights the connection among cold-seep and hydrothermal-vent fauna. The discovery of this new species, only the second within a family described in 2005, stresses how much remains undiscovered on our continental margins.

Introduction

From ants that use symbiotic bacteria to protect the fungi that they farm (Currie et al. 2001) to polychaetes that "garden" bacteria (Grossman and Reichart 1991), animals have developed a diversity of mechanisms to increase their symbionts' productivity and health. Few places provide as many examples of these symbioses as reducing systems, including hydrothermal vents and cold seeps, where shrimp, mussels, clams, and mouthless tubeworms are fueled by their chemoautotrophic bacterial symbionts (Felbeck 1981; Cavanaugh et al. 1981; Childress et al. 1986; Schmaljohann et al. 1990; Dupperon et al. 2005; Peterson et al. 2009). As we try to understand how these systems function, novel species are constantly revealed. In 2005 a new family of crab was discovered at a hydrothermal vent with chelipeds (claws) covered in dense setae and epibiotic bacteria, an appearance that lead to this species, *Kiwa hirsuta*, to be called the "Yeti crab" (Macpherson et al. 2005). Only a single individual of *K. hirsuta* was collected leaving the ecology and role of its bacterial epibionts largely unknown (Macpherson et al. 2005; Goffredi et al. 2008). During June 2006, we discovered a second species of Yeti crab, which we formally describe here at *Kiwa puravida* n. sp., swinging its bacteria-laden chelipeds rhythmically at a Costa Rican methane seep (Figures 6.1A-C and 1F). In this study, we describe how this new species farms its epibiotic bacteria in a unique form of symbiosis.

The symbiont- host interactions of epibiont bearing hydrothermal vent crustaceans have remained perplexing; these shrimp, barnacles, and crabs, share a distinct phylogeny of chemosynthetic epibionts (Goffredi 2010) but if and how they harvest their symbionts has remained elusive (summarized in Peterson et al. 2009). The best studied of this group is the vent shrimp *Rimicaris exoculata* that gains a large proportion of its energy from the ε- and γ-proteobacteria symbionts that grow inside its carapace and on its enlarged mouthparts

(Segonzac et al. 1993; Gebruk et al. 1993; 2000; Polz et al. 1998; Peterson et al. 2009). What remains unknown is how *R. exoculata* harvests its bacteria. Competing hypotheses suggest that *R. exoculata* either uses its chelipeds to transfer its epibiotic bacteria to its mouth (Gebruk et al 1993) or consumes its discarded bacterial-rich exoskeleton after molting (Gebruk et al 1993). This has led some to question the nutritional role of these symbionts (Peterson et al. 2009). Vent barnacles also appear to have morphological adaptation to harvest their symbionts (Southward and Newman 1998), but no observations support this hypothesis. Only the vent crab *Shinkaia crosnieri,* has been observed to scrape off its epibiotic bacteria and transfer them to its mouth, providing a clear mechanism for symbiont harvesting (Miyake et al. 2007). Yet the importance of *S. crosnieri*'s symbionts to its overall nutrition remains unknown. Although symbiont affinities and the presence of enzymes necessary for carbon fixation indicate that *K. hirsuta* may rely on its chemosynthetic symbionts for a food source, it has not been observed to consume them (Goffredi et al. 2008; Peterson et al. 2009; Goffredi 2010).

A key aspect of farming, a form of mutualistic symbiosis, is the direct trophic transfer of energy from a symbiont to its host, a phenomenon that can be clearly shown through biomarker analysis. Biomarkers, specifically carbon isotopic and fatty acid (FA) analyses, track a signature from an individual's diet into its tissues providing a time integrated view of what that species eats (Dalsgaard et al. 2003; McCutchan et al. 2003). Chemosynthetic and photosynthetic derived biomass commonly differ in the ratio of carbon-13 to carbon-12 and the length, bonding and branching patterns of certain FAs in their lipid membranes (Conway et al. 1994; MacAvoy et al. 2002; Colaco et al. 2007). Consumers derive their isotopic and FA composition from their diet (DeNiero and Epstien 1978; Dalsgaard et al. 2003). Through analysis of an individual tissue their main food sources can be identified. In certain cases, rare or unique FAs can be traced from a symbiont into their host, and provides a robust measure of

direct consumption. An example of this is *R. exoculata*, as its bacteria have relatively unique 16:2(n-4) and 18:2 (n-4) FAs that can be traced into its biomass (Pond et al. 1997). Isotopic and FA analyses of *K. puravida* n. sp. may provide insight about its consumption of chemoautotrophic production and identify whether it is gaining energy from its symbionts or not.

Vents and seeps are both fueled by similar chemical reactions which has lead to cross ecosystem comparisons since the first seep community was discovered (Paul et al. 1984; DiMeo et al. 2000; Wolff 2005; Vrijenhoek et al. 2007). Symbionts have been especially enlightening in demonstrating the similarity among these habitats (Di Meo et al. 2000; Cavanaugh et al. 2006; Vrihenhoek et al. 2007). An initial description of the epibionts found on the Costa Rican *Kiwa* species found provocative cross-ecosystem similarities among vent and seep crustacean epibionts (Goffredi et al. 2008). Here we build upon that research through description of the host's phylogeny, and adding additional epibiont analysis. Our comparison of host and symbiont evolutionary histories now provides better understanding of the biogeography of these disparate "islands" of chemoautotrophy in the deep-sea, and tests the hypothesis that *K. puravida* n. sp. farms its epibiotic bacteria.

Materials and Methods

Specimens were collected with DSRV Alvin on RV Atlantis Cruises AT 15-5 and AT 15-44 during June 16, 2006 and February 22– March 23, 2009, respectively, at Mound 12 off Costa Rica (8^{o} 55.8'N 84^{o}18.8'W) at depths of 1000– 1040 m. One specimen was collected at Mound 11, although few individuals were observed there. Specimens were preserved in 8% buffered formalin or 95% Ethanol. In certain instances a pereopod was removed for isotopic,

genetic, epibiont, and fatty acid analysis and frozen at -80^{o}C. Video footage was collected during both cruises as well as AT 15-59 from the same site in January 2010.

Measurements of specimens are given in millimeters (mm) and indicate the postorbital carapace length unless otherwise indicated. Specimens are deposited at the Smithsonian (Holotype and Paratype 1); University of Costa Rica (Paratype 2). Additional specimens are being deposited at NIWA Invertebrate Collection, Wellington, New Zealand, and the Scripps Institution of Oceanography Benthic Invertebrate Collection. Descriptions were prepared using DELTA (DEscriptive Language for Taxonomy; Dallwitz et al. 1997). Drawings were made using a WACOM Intuous3 Graphics Tablet and Adobe Illustrator CS2-CS4.

Stable isotopic and fatty acid (FA) analyses were performed on those specimens that underwent molecular analysis (shown in Figure 6.3). Stable isotopic analysis was performed on muscle tissue of additional specimens, collected during cruises 15-44 and 15-59 at which time particulate organic carbon (POC) isotopic measurements were also made. POC isotopic analysis was performed on surface and water at the depth of the seep location to get a maximal estimate of potential planktonic isotopic signature for this region. 0.2 mg of tissue, bulk plankton, or scraping of the GF/Fs were placed in tin boats, dried at 60^{o}C overnight, acidified with 1% $PtCl_2$ and analyzed on a Eurovector elemental analyzer interfaced with a continuous flow Micromass Isoprime isotope ratio mass spectrometer at Washington State University in the lab of Dr. Raymond Lee. Isotope ratios are expressed as $\delta^{13}C$ or $\delta^{15}N$ in units of per mil (‰). Standards were Pee Dee Belemnite for $\delta^{13}C$ and nitrogen gas for $\delta^{15}N$ (atmospheric) using the standard notation (Conway et al. 1994). Fatty acids were extracted in a one step extraction-transesterification method (Lewis et al. 2000) from bacteria-laden setae tips, muscle tissue and from plankton collected via CTD and filtered on a 64μm sieve. This plankton sample was collected directly over Mound 12 within 12 hours of collection of those *K.*

puravida n. sp. specimens that underwent FA analysis. Freeze-dried tissue was placed in 3ml MeOH:HCl: $CHCl_3$ (10:1:1 v/v/v) at 60^{o}C for 60 min, cooled and 1 ml Milli-Q H_2O added prior to extraction in hexane:chloroform, (4:1 v/v), and dried over sodium sulfate. FAs were analyzed on a Thermo Finnegan Trace GC/MS and peak integration was performed using Xcaliber software. Percentage of total FAs are given for abundant FAs defined as those which composed more than 1.0% from any of the samples. As peak area measurements from mass spectra are not a function of concentration alone (detector response varies with FA analyzed), these FA data are comparable within this study only.

Molecular analyses were performed on specimens collected during 2006. Genomic DNA was isolated from ethanol-preserved muscle (50 mg) and treated with the QiagenDNeasy isolation kit, according to manufacturer's instructions (Qiagen Inc., Valencia, CA). Polymerase chain reaction (PCR) conditions for amplification of the gene regions were as follows: 100 ng of template DNA, 5 µl 10X buffer (supplied by manufacturer), 5 µl $MgCl_2$ (2.5 µM), 2 µl of each primer (10 µM final conc.), 2.5 units of Taq polymerase (Promega Inc., WI), 5 µl of a 2mM stock solution of dNTPs, and sterile water to a final-volume of 25 µl. A ≈2000 bp fragment of the 18S rRNA gene was amplified with universal 18S rDNA primers, 18e (5'-CTGGTTGATCCTGCCAGT-3') and 18P (5'-TAATGATCCTTCCGCAGGTTCACCT-3') (Halanych et al. 1998). PCR products were sequenced bidirectionally with an ABI 3100 DNA sequencer (Applied Biosystems Inc., Foster City, CA). GenBank 18S rRNA sequences (Anomura: AF439381-AF439391, Z14062; *Upogebia affinis*: AF439392) were aligned with the yeti crab 18S rRNA (DQ219316) using ClustalX^2 followed by manual checking. Secondary structure of rRNA (i.e. stems and loops) was inferred using the program GeneBee (Brodsky et al. 1995). Bayesian inference of phylogeny was performed using MrBayes v3.0B4 (Huelsenbeck and Ronquist 2001) with data partitions using RNA secondary structure. Six chains were run simultaneously for 1,100,000

generations and trees sampled every 1000 generations. The first 1000 trees were discarded as "burn in" and Bayesian posterior probabilities were estimated on the 95% majority rule consensus. The portion of the mitochondrial genome including Cytochrome Oxidase I (COI) and the intervening region to Cytochrome Oxidase II (COII) was amplified using previously published primers and conditions (Macpherson et al. 2005) to determine tRNA composition and order. 16S rRNA genes from bacterial genomic DNA isolated from hairs on pereopods were amplified using 27F and 1492 primers. 16S rRNA gene PCR products were cloned and sequenced using published protocols (Goffredi et al. 2008). A phylogenetic tree for the ε-proteobacteria was constructed using MUSCLE (Edgar 2004) including all ε-proteobacteria from *K. hirsute* and those from *S. crosnieri* and *Rimicaris* spp. found to be most closely related to the ribotypes of *K. puravida*. The phylogenetic tree was constructed from the second iteration using the nearest neighbor algorithm.

Results and Discussion

Nutrition and Farming

During submersible dives with the DSRV Alvin off of Costa Rica, *K. puravida* n. sp. were observed to have a patchy distribution on the tops and within crevices of carbonate outcroppings, on *Lamellibrachia* cf. *barhami* colonies, amongst bathymodiolin mussels, and in pits within carbonate rocks with alvinocarid shrimp (Figure 6.1C and 6.1F). The presence of these other symbiont-bearing species indicates that these areas have active methane-seep fluid release. This new *Kiwa* species was not observed scavenging food, a strategy previously suggested for its congener, *K. hirsuta* (Macpherson et al. 2005). In addition, *K. puravida* n. sp. were often seen using their chelipeds to force shrimp away which got close to them; the crab made no obvious attempt to capture these shrimp. However, individuals were commonly

observed slowly waving their chelipeds (pereopod 1) back and forth in these areas of active seepage.

Both isotopic and FA biomarker approaches identified that *K. puravida* n. sp. used its epibiotic bacteria as its main food source. The carbon isotopic composition of this species ($\delta^{13}C_{muscle}$ = -20.1 to -44.2 ‰, n= 30) was significantly lighter than phytoplanktonic production in this community ($\delta^{13}C_{plankton}$ =-16 to -21 ‰, n =18: T-test t=-8.9, df=42.8, $p<0.001$), clearly indicating a chemoautotrophic food source for *K. puravida* n. sp. The light and wide ranging isotopic values of this species indicate that sulfide- and potentially methane-oxidation fuel this chemoautotrophic symbiosis (Conway et al. 1994). *Kiwa puravida* n. sp.'s muscle fatty acid profile was also divergent from the planktonic FA composition and mirrored that of its bacteria-laden setae (Table 6.1; Figure 6.2). The $FA_{plankton}$ composition included an abundance of polyunsaturated fatty acids (PUFAs) with 18% of the FA composition made up by 22:6(n-3) and 7 % from 20:5(n-3); both diagnostic for photosynthetic production (Dalsgaard et al. 2003 but see Nichols 2003). In contrast, 20:5(n-3) was not common in the *K. puravida* n. sp. tissue composing only 3 and 5 % of the FAs measured and was never observed in either of the specimens' setae sampled. 22:6(n-3) was present between 4 and 1% in the tissue but was present in one of the specimens' setae sampled, comprising 6% of the total FAs. 16:2 and 18:2 FAs, which are abundant in *R. exoculata* symbionts (Pond et al. 1997), were present on *K. puravida* n. sp.'s bacteria-setae and tissue sample with the majority being within the tissues; the sum of the two diene FAs comprised 33 % of both specimens' tissue samples. 16:2 biomarkers have also been found in limited abundance in mussel tissues (Volkan et al. 1989) and diatoms (Volkman et al. 1989) yet were not found in a species of Bathymodiolin mussel from Costa Rica (Thurber, Pers. Obs.) or the phytoplankton sample collected. Whereas the isotopic composition of this species does not eliminate the possibility that *K. puravida* n.

sp. may be a scavenger or consume symbionts-bearing fauna, we did not observe them grazing upon other fauna and the unique 16:2 FA within their tissues further makes this lifestyle less probable. The monounsaturated fatty acid, 16:1(n-7), a common constituent of sulfide-oxidizing bacteria (McCaffrey et al. 1989), was always more than four times as abundant in tissue and spines of *K. puravida* n. sp. compared to the plankton sample. The presence of 16:2 FA, an abundance of 16:1(n-7), the similarity of bacteria-laden setae with muscle tissue, and the isotopic composition indicative of chemosynthetic nutrition, strongly support the hypothesis that *K. puravida* n. sp.'s main food source is the epibiotic bacteria growing on its setae.

In addition to this biomarker evidence, *K. puravida* n. sp. possessed both morphological and behavioral adaptations to harvest its symbionts. *Kiwa puravida* n. sp. had specialized comb-shaped setae on its 3rd maxilliped (a mouth appendage; Figure 6.1D) that it uses to scrape bacteria off of its whip-like barbed setae (WBSs, see description below for further detail) which adorn its chelipeds, sternum, and pereopods before transferring the harvested bacteria into its mouth (Figure 6.1G). Dissection of an individual revealed that the bacterial filaments were commonly stuck within these comb-row setae, indicating that the crabs were effective at removing the filaments from their setae (Figure 6.1H). Bacterial filaments were found in *K. puravida* n. sp.'s cardiac stomach demonstrating that they are transferred into its mouth, an observation similar to what has been recorded in *R. exoculata* (Zbinden and Cambon-Bonavita 2003).

In addition to gaining energy from its epibionts, for a species to farm bacteria it must also facilitate the growth of its symbionts. In a minimalist sense, *K. puravida* n. sp. does this by providing an attachment substrate for its bacteria, yet through its continual cheliped movement, *K. puravida* n. sp. likely facilitates increased symbiont productivity as well.

Chemoautotrophic symbionts require access to oxygen from the water column and reduced compounds, i.e. sulfide or methane, from the seep. During periods of carbon fixation, a boundary layer depleted in one or more of these solutes likely develops which then limits symbiont productivity. This is analogous to reef-building corals whose photosynthetic symbionts become carbon limited during periods of high productivity (Lesser et al. 1994). In coral symbioses, carbon limitation becomes ameliorated at increased current speeds or mixing of the water column which replenishes these boundary layers (Jokiel et al 1978; Dennison and Barnes 1988). We hypothesize that *K. puravida* n. sp. waves its chelipeds to shear off boundary layers formed by their epibionts productivity, increasing both their symbionts and, in turn, their own access to food. As in corals, boundary layers are greatest in areas of reduced flow, such as pits and depressions (Petterson et al. 1991), which is a habitat where *K. puravida* n. sp. commonly occurs, making this behavior even more adaptive. In other words, the cheliped waving motion may be similar to a farmer fertilizing his crops to increase productivity and yield.

In addition to bacteria, detritus was observed both attached to the bacteria-laden setae and was present within the *Kiwa* mouth. As potential photosynthetic fatty acid biomarkers were observed, albeit minimally, both within the tissue and the setae, it seems likely that this species may periodically augment its diet through sweeping up detritus, the source of this photosynthetically-derived particulate organic matter. Yet this did not appear to be the main food source for *K. puravida* n. sp..

Ecology and Behavior

In addition to its bacteria harvesting, this species demonstrated intriguing intra-species interactions. An individual that appeared to have recently molted due to its minimal bacterial covering, began grappling with a larger specimen that it approached. This ended in a

dominance display where the challenged individual forced the challenging individual off the carbonate outcropping while both individuals had their chelipeds spread apart. As decapods commonly reproduce after molting, as has also been observed in the hydrothermal vent *S. crosnieri* (Miyake et al. 2007), the individual that was forced off may have been inseminated during this display or this may have been a behavior demonstrating how this species competes for space in areas of active seepage.

Phylogenetic affinities and biogeography

Both morphology and molecular data support *K. puravida* n. sp. as a new species of Kiwaidae. The type species of the Kiwaidae, *K. hirsuta* that was collected from 2228 m at a hydrothermal vent, is closely related to but genetically distinct from the methane-seep species described here, having a COI nucleotide similarity of 86% and a 2% divergence in their 18S rRNA sequence (Figure 6.3). Furthermore, both *Kiwa* species have four tRNAs between COI and COII in the mitochondrial genome (Leu(CUN), Leu(UUR), Ala, Gly); this appears to be a unique feature to Kiwaidae (see Hickerson and Cunningham 2000; Morrison et al. 2002; Yang and Yang 2008). Of significant note, *S. crosnieri* and *K. puravida* n. sp. are distinct both morphologically and genetically, having a 77% COI nucleotide similarity, which conforms with the family-level differences between these two taxa (Costa et al. 2007).

A total of 33 bacterial sequences were collected from a single individual of *K. puravida* n. sp. that included 18 ε-proteobacteria, five δ-proteobacteria, two γ-proteobacteria, and four bacteroidetes taxa (Table 6.2). The γ-proteobacteria recovered were highly similar to the other epibionts collected from reducing-habitat decapods, including the *S. crosnieri* and *R. exoculata*, being 97% and 98% similar among the four taxa (Table 6.2; Figure 6.4). Within the ε-proteobacteria, 17 fell within the Marine Group 1, Thiovulgaceae, and all of the ε-proteobacteria were between 95– 98% similar to epibionts of *K. hirsuta* and *S. crosnieri* and

94 – 98 % similar to epibionts similar to *R. exoculata* epibionts. The remaining ribotypes were most similar to environmental samples collected from cold seep, hydrothermal vent, and cave systems with complex sulfur cycling.

Although ε-proteobacteria ribotypes were diverse on *K. puravida* n. sp., the isotopic composition of this host was more indicative of a γ-proteobacterial diet. Epsilon proteobacteria use the reductive tricarboxylic acid (rTCA) cycle to fix carbon that leads to a heavy isotopic signature of both microbial biomass and consumers thereof (Sirevag 1974; Quadant et al. 1977; Suzuki et al. 2006). In contrast γ-proteobacteria mostly use the reductive pentose phosphate cycle, better known as the Calvin Benson Bessham cycle (Hugler and Sievert, in press), and can be either sulfide oxidizers or methanotrophic (Childress et al. 1986). Although *R. exoculata* has both ε- and γ-proteobacteria (Peterson et al. 2009), its isotopic signature is indicative of symbionts that use the rTCA cycle, e.g. $\delta^{13}C$ =-9.4 to -12.3 ‰ (Polz et al. 1998), suggesting that this species mostly consumes its ε- proteobacterial symbionts. In contrast, *K. puravida* n. sp.'s $\delta^{13}C$ < -20 ‰ is more indicative of a food source mainly composed of their γ-proteobacterial epibionts. The mostly negative isotopic values also suggest that this species may be consuming methanotrophic symbionts, yet negative isotopic composition can simply result from fixing carbon that was previously impacted by methane cycling (Fisher 1990). As fixation pathway is not the only factor that influences symbiont isotopic value, we cannot conclusively dismiss the nutritional role of ε-proteobacteria for *K. puravida* n. sp.. Furthermore the ε-proteobacteria may also be vestigial symbionts retained from ancestral hydrothermal affinities of the *Kiwa* genus.

While the similarity among the epibionts and hosts further supports a close evolutionary relationship between methane seep and hydrothermal vent fauna, it suggests the

trajectory of epibiont colonization is likely independent of host radiation across the oceans and potentially dependent on the local environment. Fifteen of *K. puravida* n. sp.'s eighteen ε-proteobacterial symbionts were more similar to symbionts on *S. crosnieri,* a crab that occurs >13,000 km away from *K. puravida* n. sp.*'s* known range, rather than *K. hirsuta, K. puravida* n. sp.'s congener, which occurs 6,500 km away (Table 6.2; Figure 6.4). Host species identity is not always a determining factor in symbiont identity (Vrijenhoek et al. 2007), but both evolutionary and environmental factors appear to impact microbial biogeography (Hughes et al. 2006). The dissimilarity of host and symbiont phylogeny may be the result of independent symbiont colonization events of the two species of *Kiwa* during their evolutionary history, with a potential symbiont source from across the Pacific Ocean from *S. crosnieri*. Conversely, environmental factors at vents and seeps, such as methane and sulfide concentration, may be more important than temperature and thus the symbionts identities indicate a habitat similarity between *S. crosnieri* and *K. puravida* n. sp.. In any case, the bacteria symbionts of reducing-habitat decapods are recruiting from vast distances across the ocean or a series of as-of-yet unknown stepping stones.

Broader implications

This new species is only the second within a family discovered in 2005, yet this species and discoveries like it are in jeopardy due to the expanding exploitation of continental margins habitats. Fishers are harvesting deeper stocks and mineral and methane mining is either proposed or planned in the near future (Glover and Smith 2003). Methane seeps provide heterogeneous habitats (Cordes et al. 2010) and long-lived foundational species (e.g. *Lamellibrachia* spp. (Cordes et al. 2005), making them areas of increased biodiversity (Sibuet and Olu 1998) and vulnerability to exploitation. *Kiwa puravida* n. sp. is currently found at

only two locations that together cover less than 1km^2 of the seafloor, suggesting extreme vulnerability to human exploitation.

Species Description

Family KIWAIDAE Macpherson, Jones & Segonzac, 2005

Kiwaidae Macpherson, Jones and Segonzac, 2005: 712

Diagnosis.

Body depressed, symmetrical. Carapace calcified, slightly convex, smooth. Rostrum well developed, triangular. Cervical grooves clearly distinct between gastric and anterior branchial regions and between anterior and posterior branchial regions; either side of mesogastric region with small sharply defined pit. Cardiac region small and depressed and separated from branchial regions by shallow grooves. Anterior branchial regions well delimited and separated by short median longitudinal groove; small W-shaped groove over this groove. Posterior branchial regions separated by median longitudinal groove. Intestinal region well circumscribed and separated from branchial regions by distinct grooves. Posterior half of pterygostomian flap with two longitudinal and subparallel carina. Abdominal segments smooth, not folded against thorax; telson folded beneath preceding abdominal somite, with a median transverse suture and a longitudinal suture in the posterior half of telson; uropods spatulate. Epistome unarmed. Mandibular cutting edge with chitinous teeth along incisor process. Sternal plate between third maxillipeds (sternite 3) well developed, strongly produced anteriorly; sternal plate between fifth pereopods (sternite 8) absent. Eyes strongly reduced to small soft tissue, not calcified, movable, without pigment, inserted near antennulae. Antennal peduncle 5-segmented, without antennal scale; flagellum of moderate length. Third maxillipeds with crista dentata in proximal half to third of ischium; epipods absent. Chelipeds

(pereopod 1) strong, subequal, and greatly elongate; dense corneous spinules along distal portion of occlusal margin. Walking legs (pereopods 2–4) stout, with claw-like dactyli bearing dense corneous spinules along flexor margin. Fifth pereopod chelated, inserted below sternite 7, insertion not visible ventrally. Male first pleopod absent, pleopods 2–5 reduced, uniramous. Gills with four pairs of arthrobranchs (a pair each on P1–P4), 2 vestigial arthrobranchs on third maxilliped; pleurobranchs absent.

Genus *Kiwa* Macpherson, Jones & Segonzac, 2005

Kiwa Macpherson, Jones and Segonzac, 2005: 712

Diagnosis. — as for family

Kiwa puravida n. sp.

Figures 6.1A and 6.1B; Figures 6.4–6.6.

Material examined.

Type specimens***:*** HOLOTYPE: ♂ (30 mm), Costa Rica, 8° 55.8'N 84°18.8'W, 1007 m, 15 May 2006, RV *Atlantis* and DSRV *Alvin*, Alvin Dive (AD) 4200, Scoop net (Accession number – added after acceptance). PARATYPE: ♂ (24.1 mm), same as holotype (Accession number– added after acceptance). PARATYPE: ♀ (21.5 mm), 997 m, 22 February 2009, RV *Atlantis* and DSRV *Alvin*, Biobox (MZUCR-2673-01).

Other material examined: Juvenile (2.5 mm), 997 m, 22 February 2009, RV *Atlantis* and DSRV *Alvin* . ♂ (6.2 mm); ♂ (9.5 mm); ♀ (11.9 mm); ♂ (14.1 mm); ♂ (17.9 mm) ; ♂ (30.2 mm); ♀ (17.2 mm); ♀ (4.7 mm), AD4511, March 5, 2009: ♂ (11.2 mm); ♀ (24.5 mm); ♀ (19.7 mm); ♂ (20.9 mm); ♀ (11.6 mm); Juvenile (3.9 mm). AD 4502, Feb. 23, 2009: ♂ (4.2 mm) (Accession Numbers– added after acceptance).

Etymology - puravida, is a conjunction of the Spanish words “pura” and “vida” meaning pure life and is a common saying within Costa Rica, in whose waters these specimens were collected in. The genus is feminine as is the species name.

Description

Carapace:

1.3 times as long as broad (including rostrum) (1.5 times without rostrum). Dorsal surface unarmed and sparsely setose with stiff, barbed setae (SBS, Supplemental 3g, right image). Hepatic and epigastric regions depressed; distinct pit on either side in posterior gastric region. Region between the anterior and posterior portion of the cervical groove with distinct ∞-shaped groove. Frontal margin oblique, relatively straight, with large tooth near rostrum. Anterolateral margin rounded, lateral margin slightly divergent posteriorly (widest at distal quarter); slightly irregular with small granule at anterior margin of posterior branchial region, immediately posterior to deep groove. Posterior margin unarmed. Rostrum broadly triangular, horizontal, 0.2 times the length of remaining carapace; dorsal surface dorsally convex on either side of median ridge, smooth and sparsely furnished with SBS (dense cluster at apex); lateral margins slightly convex, irregular with granules but straight. Pterygostomian flap

lateral surface granulate, with additional short striae in median portion and with two separate longitudinal carinae under posterior branchial region; anterior margin produced into a spine.

Sternum

Sternal plastron 1.6 times as wide as long (at mid-length), convex lateral margins; surface smooth, sparsely furnished with fine whip-like barbed setae (WBS, Figure 6.7E left), lateral margins serrated. Sternite 3, with strong spine at lateral midlength, anterior portion forming a roughly equilateral triangle, with large granules along lateral margins. Sternite 4 2.3 times as wide as sternite 3, anterior margin shallowly concave, anterior midline grooved. Anterolateral margin produced to tooth not overreaching sternite 3 and with large granules laterally. Sternite 6 widest. Posterior margin of sternite 7 deeply concave and deep median emargination.

Abdomen

Tergites sparsely setose with SBS. Pleura each with anterior transverse carina and medially depressed; pleural margins of segments 2–6 strongly tapering and with concave anterior margins. Telson 1.1 times as broad as long; distal portions 2.6 times length of proximal portion, distally distinctly bi-lobed with median notch (0.4 times the length of distal portion).

Antennal peduncle

Article 1 distomesial margin unarmed, distolateral margin produced to 3 small distal spines; article 2 with strong lateral projection reaching end of article 4, strongly toothed and with additional prominent ventral spine; article 3 laterally and distally toothed, nearly reaches

distal end of segment 4. Penultimate article with 3 distal spines (2 mesial and 1 lateral); ultimate article armed with 1 dorsal and 1 ventral spine. Sparsely furnished with thick SBS.

Maxilliped 3

Surface smooth and unarmed except for small granules at bases of plumose setae; coxa with fine serration along distal border, fully calcified (not corneous); ischium with 20 teeth on proximal third of mesial ridge. Two types of setae present including CRS (Figure 6.1D and 6.1H; Figure 6.7E) on ventral and distal carpus, propodus and dactylus and WBS on dorsal portion of all segments.

Pereopod 1 (cheliped)

Strongly spinose, 2.6 times as long as carapace (excluding rostrum) (2.1 times including rostrum). Ischium with 2 dorsal distal spines, serrated along mesial margin. Merus with scattered strong spines, most prominent along mesial margin, with 6 distal spines. Carpus with multiple longitudinal rows of spines, with 6 distal spines, length of carpus slightly longer than palm. Propodus with palm 1.8 times as long as high, with distinct rows of spines. Length of dactylus 0.7 times as long as propodus, proximal tooth on lateral margin; occlusal margin distally hollowed, opposable margins strongly gaping proximally with prominent median tooth; fingers each distally with strong triangular corneous tooth. Ventral portion of ischium and merus densely furnished with WBS setae, remaining surfaces uniformly covered with SBS.

Pereopods 2–4

Ambulatory legs similar. Surface covered with tubercular processes on meri, carpi and propodi. Merus dorsal margin with spines and large granules; with 8 spines on dorsal crest on

P2 (including distal spine), ventral margin with row of tubercular processes, 1.4–1.0 times as long as propodus (for P2 and P4, respectively). Carpus, dorsal margin serrated with spines and tubercular processes. Propodus 2.1–1.9 times as long as dactylus (from P2–P4), extensor margin spinose, flexor margin with 6–7 corneous spines along distal third of margin, distal-most paired. Dactylus straight; flexor margin with 13, 12–15 inclined and slender corneous spines along entire length (P2, P3–P4, excluding distal spine). Dense fields of plumose WBS distributed along ventral portions of ishia and meri.

Gill structure

Phyllobranchiate gills; 2 arthrobranchs each on the cheliped and the walking legs (P2-P4); pair of vestigial, lamellar gills on third maxilliped, none on P5; pleurobranchs are absent.

Remarks

Neither of the original two specimens were complete, the male holotype specimen is lacking the posterior left two walking legs (P3 and P4), the male paratype specimen is lacking the right cheliped and the two posterior right walking legs. Sixteen additional specimens were collected during 2009 which included 7 females between carapace length (including rostrum) 4.9 and 24.5 mm and 7 male specimens between 7.4 and 38.6 mm. A single specimen, 4.6 mm, had potentially developing gonopores, indicating that it was female and this specimen and those smaller were classified as juveniles. Female gonopores were clearly visible making identification of sex possible (Figure 6.7F).

The overall morphology and morphometrics of the paratypes and other specimens examined agree with the holotype, except for a variance in the shape of the rostrum: the rostrum of one of the paratypes is not evenly triangular but more leaf-shaped along the left margin.

Kiwa puravida n. sp. is similar to *K. hirsuta* (Macpherson et al. 2006) but can be clearly distinguished by the following characters:

- frontal margin with prominent tooth at base of rostrum in *K. puravida* n. sp. (*K. hirsuta* only has a small tooth; Figure 6.5E and 6.6A).
- pteryogostomian flap covered with large granules and short striae in addition to longitudinal carinae, anteriorly produced to spine and with short, scattered setae (*K. hirsuta* only has a few scattered granules in the anterior portion, anteriorly rounded and without setae; Figure 6.6A and 6.6B).
- the proportions of the anterior and posterior portions of the telson differ with *K. puravida* n. sp. having a distinctly larger posterior portion (1.6 to 2.4 times a long as anterior portion) compared to *K. hirsuta* (0.8). Additionally, the distal cleft of the telson is distinctly deeper in the new species with the distal portion of the telson in *K. hirsuta* being only shallowly emarginated (Figure 6.6F and 6.6C). The extent of the cleft was reduced in a specimen whose carapace was 4.7 mm and should not be used as a distinguishing feature in small specimens.
- anterior portion of sternite 3 in the shape of a wider triangle with length-to-width ratio 0.7 (*K. hirsuta* sternite 3 anterior portion is acute with approximate length-to-width ratio of 1.4; Figure 6.6F and 6.6C).
- anterior portion of sternite 4 is shallowly concave (*K. hirsuta* anterior margin of sternite 4 is deeply concave; Figure 6.6F and 6.6C).
- lateral margins of sternal plastron are distinctly serrated (smooth in *K. hirsuta*; Figure 6.6F and 6.6C).
- all articles of the antennal peduncle are distinctly more spiny and with the prominent lateral process on article 2, reaching the distal margin of article 4 (instead of only reaching to midlength in *K. hirsuta*; Figure 6.6C).

- the coxa of the third maxilliped is distally not strongly produced, only slightly serrate and without corneous spines (distal border strongly produced and denticulate with each tooth with corneous margin in *K. hirsuta;* Figure 6.6D).
- each tip of the cheliped fingers bear a single corneous spine only (Figure 6.7D) while in *Kiwa hirsuta* bears two corneous tips on the fixed finger.
- propodi of walking legs with 4–8 movable corneous spines along distal half portion of flexor margin (*K. hirsuta* has 11–16 spines along nearly the entire margin Figure 6.5B–6.4D).

The various types of setae that cover the surfaces of the body and appendages in both species remain intriguing. Macpherson et al. (2006) describe the setation as dense long plumose setae (similar to WBS) mainly on sternum and ventral surface of pereopods and rigid chitinous seta with barbules (analogous to our SBS) inserted in pairs mainly on the merus of the cheliped. Unlike the rigid chitinous setae of *K. hirsuta*, the SBS of *K. puravida* n. sp. were covered with bacteria, even though the density of bacteria was much reduced compared to the WBS. The barbules on WBS were not easily visible except under 200x power magnification. The comb-row setae, which were not reported on *K. hirsuta,* were limited to the carpus, propodus and dactylus of the third maxilliped (Figure 6.1D and 6.6E). The second maxilliped of *K. puravida* n. sp. had comb-row setae present but with much reduced combs.

The diagnosis of the family Kiwaidae and genus *Kiwa* is adjusted; the presence of the row of corneous spines on the coxa of the third maxilliped is excluded as this character varies between the two species now known in genus *Kiwa.* However, the presence of a dense row of corneous spinules along distal margins of the cheliped fingers is added. Furthermore, the gill structure appears to be unique in this family compared to other anomurans, specifically

involving the presence of only four pairs of arthrobranchs with gills absent from the third maxilliped. The closely related Chirostylidae have an additional pair of arthrobranchs on the third maxilliped. Albuneids, hippids and aeglids are comparably more similar in having a pair of arthrobranchs on P1– P4 and a single arthrobranch on the maxilliped (McLaughlin et al. 2007).

Additionally, the two *Kiwa* species differ in their habitat. The new species was collected from a methane seep at 1000-m depth while *K. hirsuta* was observed and collected at greater depth (exceeding 2200m) at a hydrothermal vent. The collection locations of *K. hirsuta* and *K. puravida* n. sp. are 6,500 km apart.

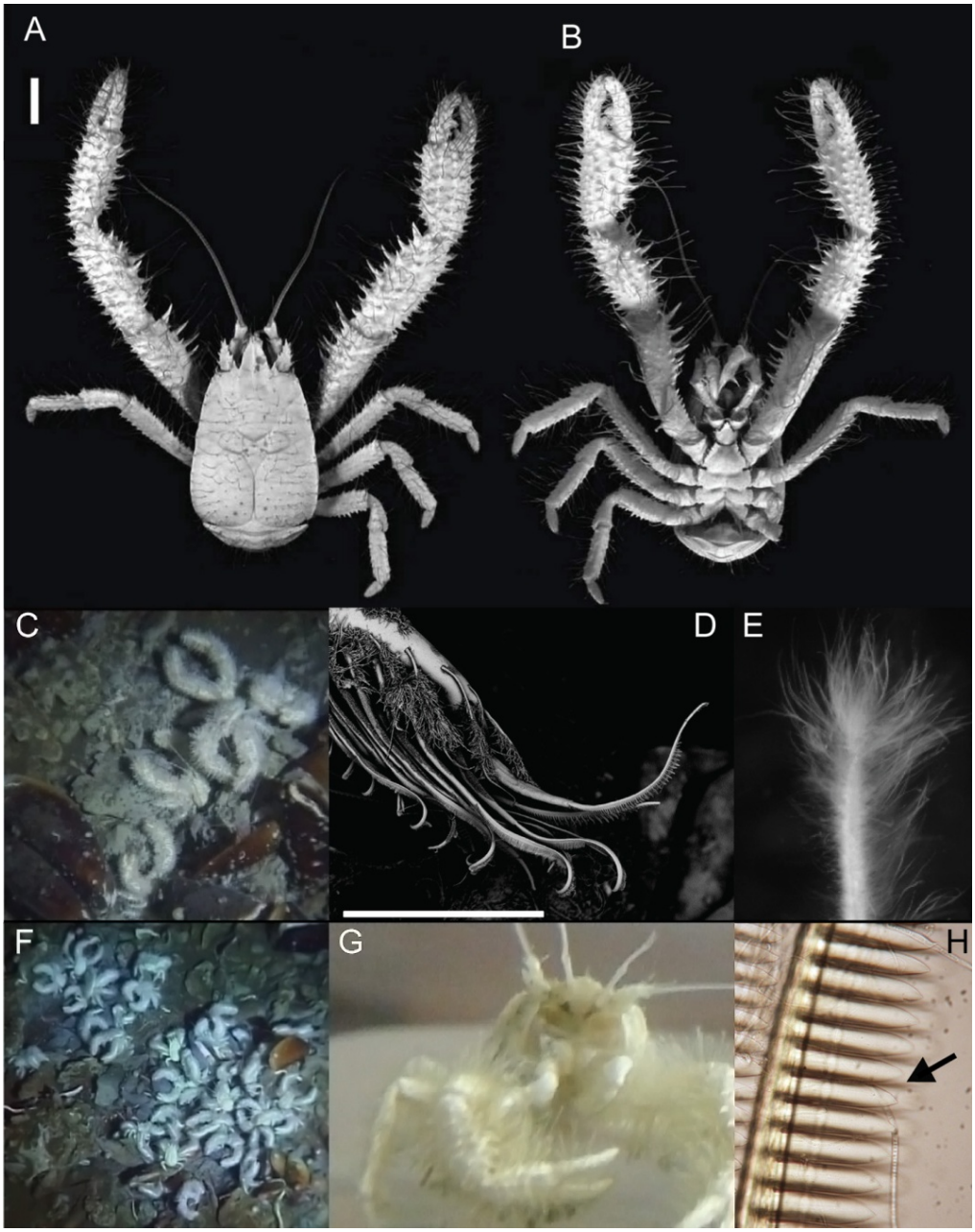

Figure 6.1 *Kiwa puravida* n. sp. holotype, *in situ* images, and morphologic and behavioral adaptations to harvest its bacteria. *Kiwa puravida* n. sp. male holotype: (A) Dorsal view. (B) Ventral view (A and B scale bar = 10mm; credit: Shane Ahyong, NIWA Wellington). (C) *in situ* next to bathymodiolin mussels (D) scanning electron micrograph of *K. puravida* n. sp.'s 3rd maxilliped and the comb-row setae that it uses to harvest its bacteria (scale bar = 150µm credit; Shana Goffredi, Occidental College]. (E) Setae covered by bacteria from 3rd pereopod (see Figure 6.7E for scale). (F) Dense aggregation *in situ*. (G) Shipboard photo of *K. puravida* n. sp. using its 3rd maxilliped to harvest its epibiotic bacteria. (H) Comb-row setae with bacteria filaments stuck among combs (indicated by arrow).

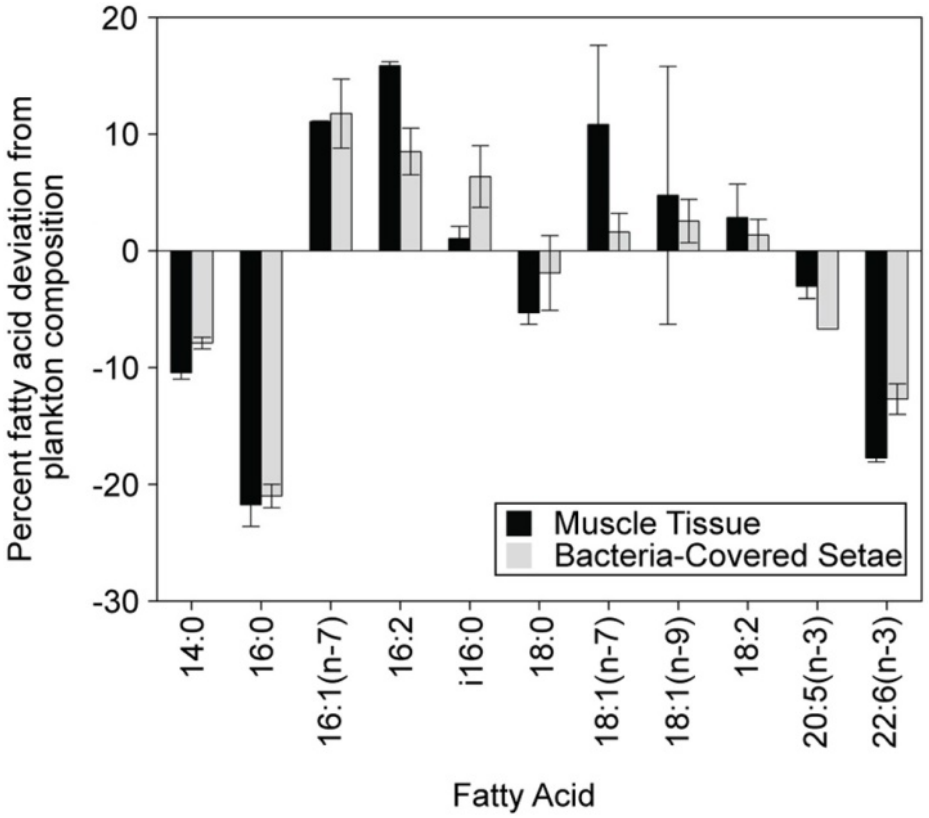

Figure 6.2 Fatty acid composition of muscle tissue and bacteria-laden setae in relation to plankton. Mean fatty acid composition of abundant (>1‰ of the total fatty acids present in any of the samples) fatty acids of muscle and bacteria-laden setae from 3rd or 4th pereopod of *Kiwa puravida* n. sp. subtracted from the fatty acid composition of plankton collected from the overlying water column. Error bars = range. N=2.

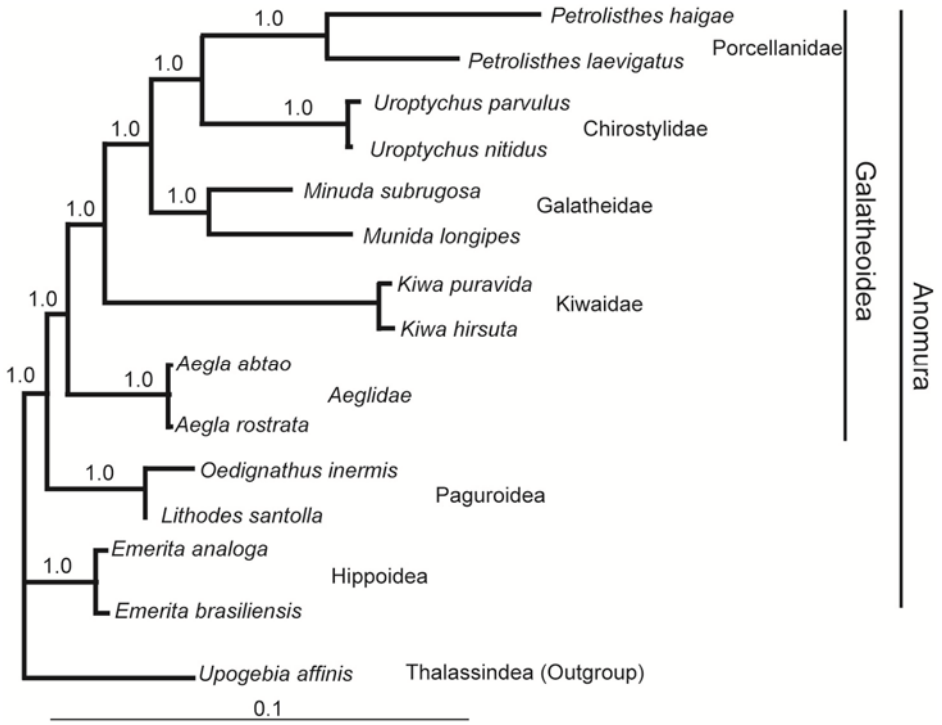

Figure 6.3 Bayesian phylogenetic tree based of 18S rRNA gene sequence, rooted using *Upogebia affinis*.

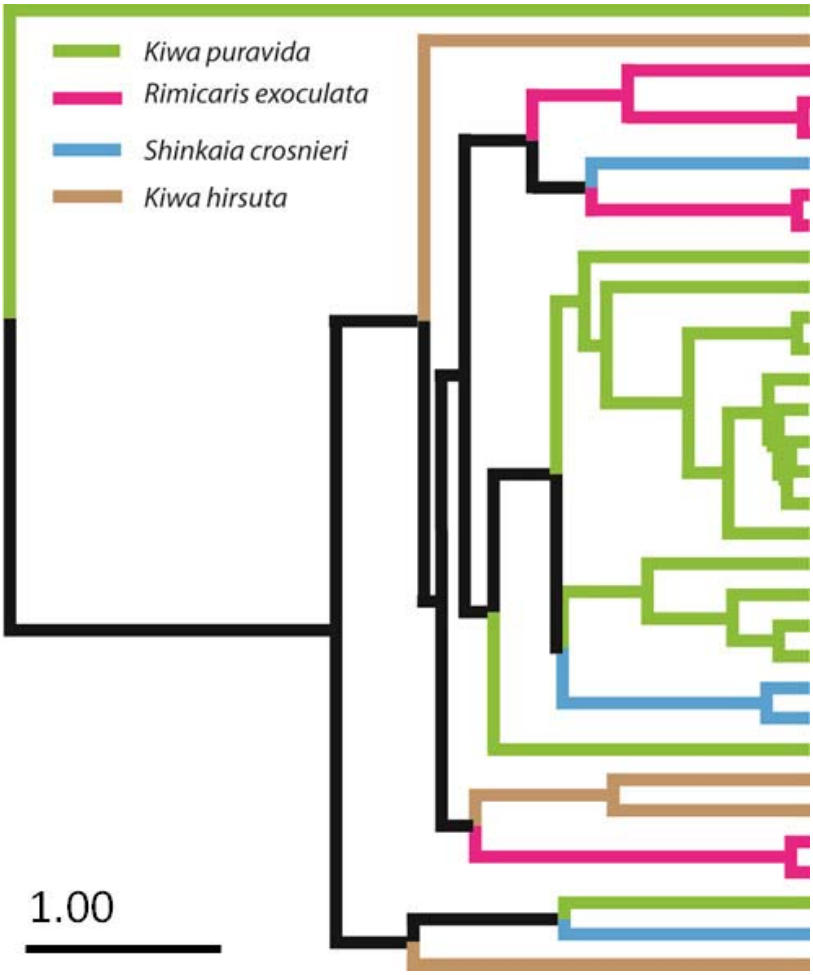

Figure 6.4 16S rRNA gene phylogeny of ε-proteobacteria decapod symbionts created using the MUSCLE algorithm (Edgar 2004).

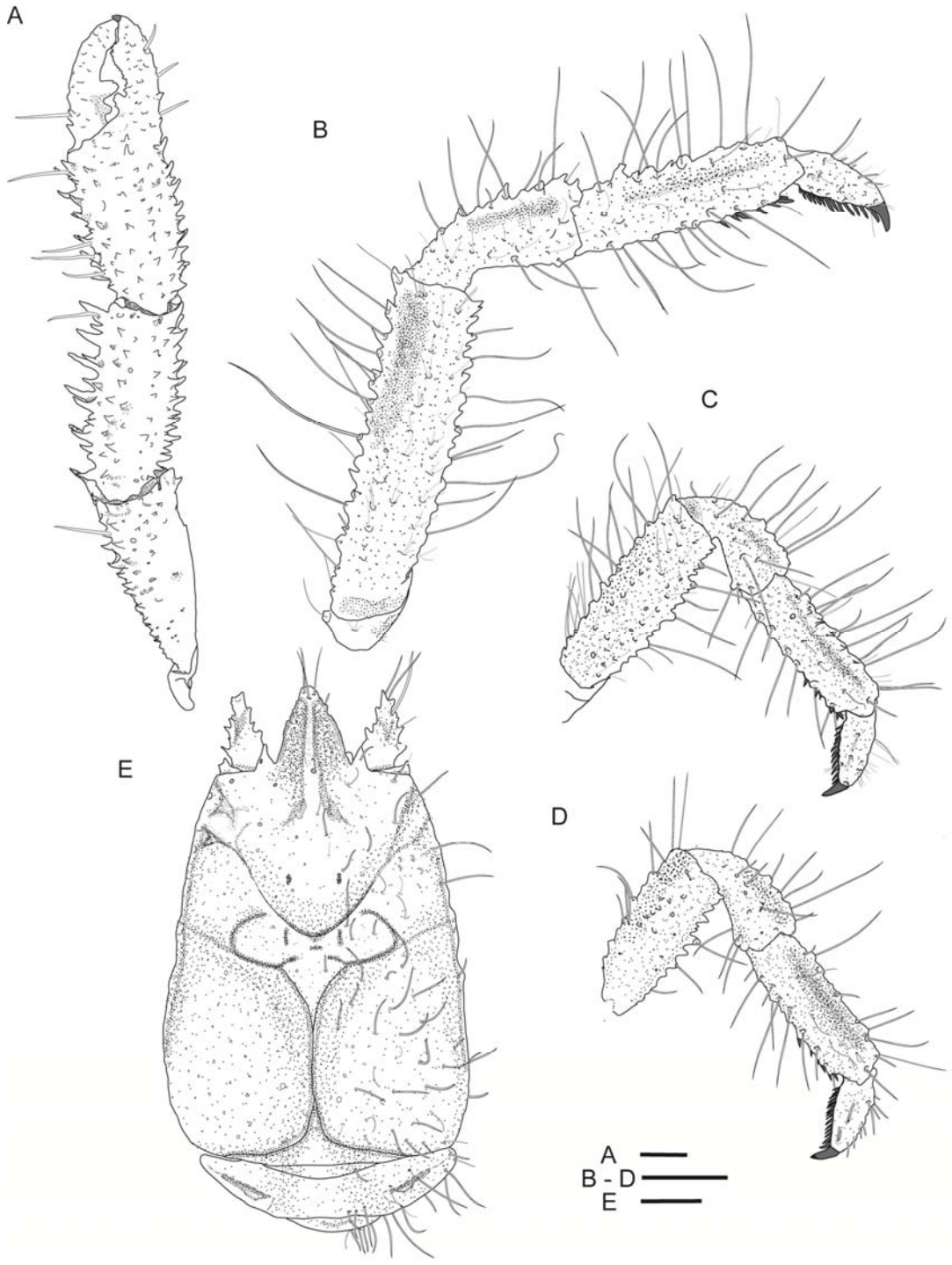

Figure 6.5 *Kiwa puravida* n. sp. male holotype. (A) Pereopod 1 (cheliped). (B) Pereopod 2 (1st walking leg). (C) Pereopod 3. (D) Pereopod 4. (E) Carapace. Scale bars = 5mm.

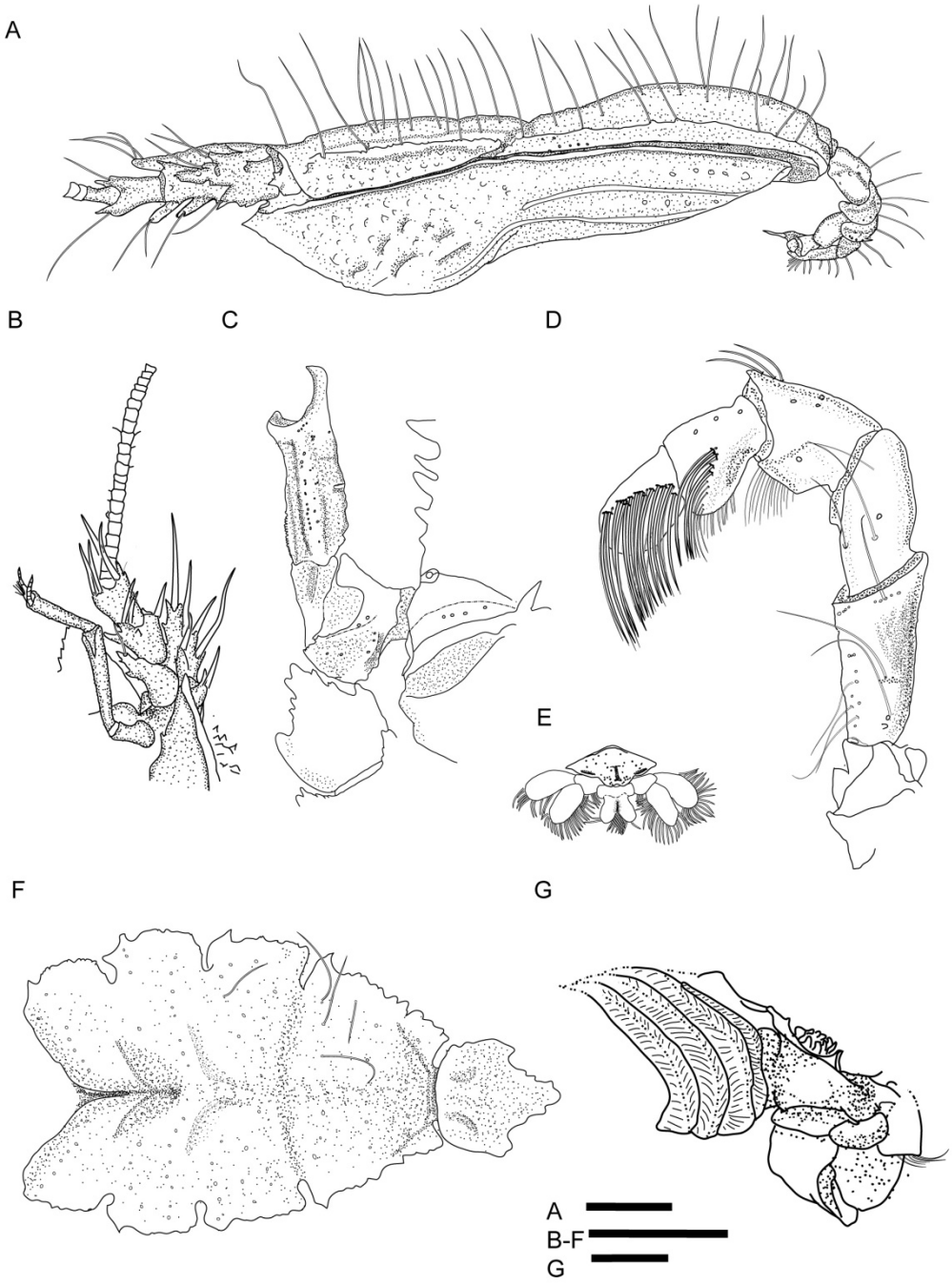

Figure 6.6 *Kiwa puravida* n. sp. male holotype. (A) Lateral view carapace and abdomen. (B) Antennule and antenna left and anterior part of ptergostomial flap. (C) Basis-ischium of third maxilliped, mesial view. (D) Third maxilliped. (E) Sixth segment of abdomen. (F) Sternal plastron. (G) Male paratype gill arrangement. Scale bars = 5mm.

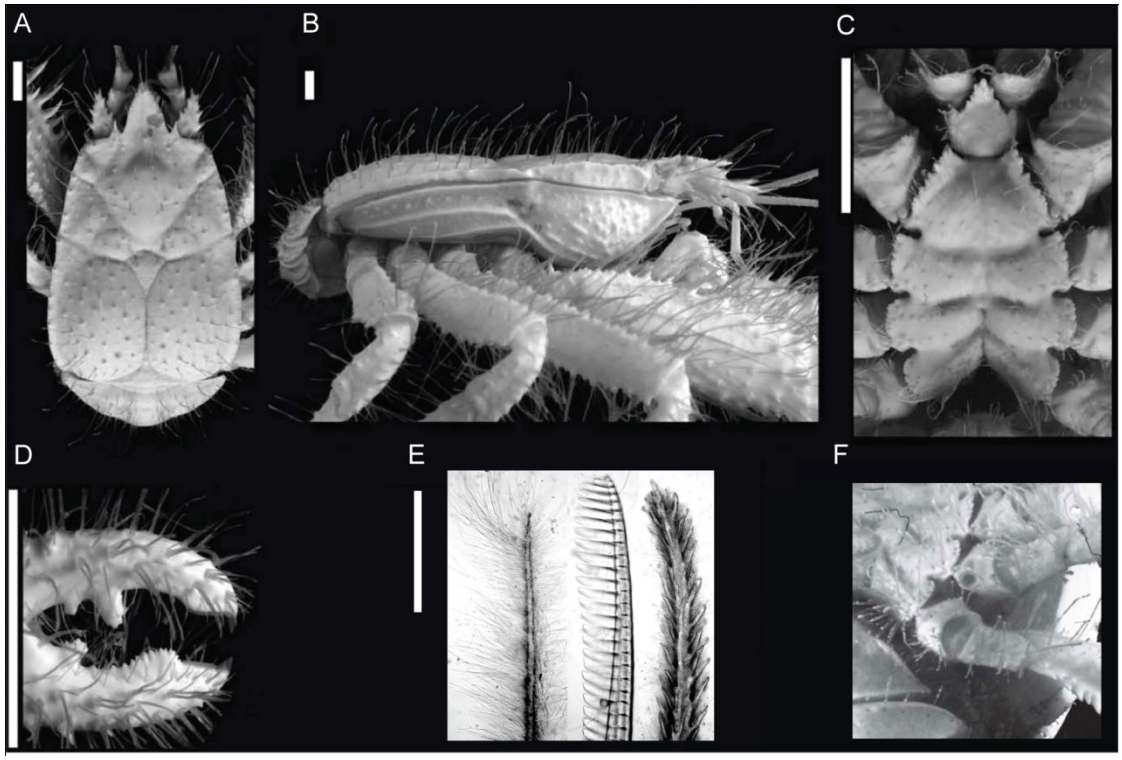

Figure 6.7 *Kiwa puravida* n. sp. male holotype. (A) Dorsal carapace. (B) Lateral view. (C) Sternal plastron. (D) Finger and thumb on cheliped (E) Whip-like barbed setae (left), comb-row setae (middle), and stout barbed setae (right). (G) *K. puravida* n. sp. female gonopore on third pereopod. Scale bars: A-D = 10mm; E =500µm. (A-D credit: Shane Ahyong, NIWA Wellington)

Table 6.1 $\delta^{13}C$ and $\delta^{15}N$ and fatty acid composition of abundant (>1‰ in any sample) fatty acids within the 3rd or 4th pereopod from *Kiwa puravida* n. sp. or plankton from the overlying water column. nd – not detected.

	K. puravida		*K. puravida*		Plankton
	Tissue	**Spine**	**Tissue**	**Spine**	
$\delta^{13}C$	-20.1	-19.5	-21.5	-23.8	-16.8
$\delta^{15}N$	8.5	5.66	6.5	5.66	10.6
FA					
14:0	1.5	3.0	0.4	4.0	11.4
16:0	12.4	10.3	8.7	12.3	32.3
16:1(n-7)	13.6	17.3	13.7	11.4	2.6
16:2	16.2	10.5	15.5	6.5	nd
iso-16:0	2.1	3.7	nd	9.0	nd
18:0	6.5	5.7	4.5	12.1	10.8
18:1 (n-7)	17.6	3.2	4	nd	nd
18:1 (n-9)	nd	10.7	22.1	7	6.3
18:2	5.7	2.7	nd	nd	nd
20:5(n-3)	2.6	nd	4.7	nd	6.7
22:6(n-3)	0	4.1	0.7	6.7	18.1

Table 6.2 Relationship between *Kiwa puravida* epibiont fauna and sequence available in GenBank as of 9/15/2009 using 16S rRNA gene sequence data

		Most similar sequence			*Kiwa hirsuta*		*Shinkaia crosnieri*		*Rimicarus exoculata*	
Group ID	**Ascension #**	**Source**	**% Sim.**	**Ascension #**	**% Sim.**	**Ascension #**	**% Sim.**	**Ascension #**	**% Sim.**	**Ascension #**
ε-Proteobacteria	Contig_0373	*S. crosnieri* Epibiont	96%	EU107475.1	96%	EU265786.1	96%	EU107475.1	96%	FM203406.1
	Contig_354	Hydrothermal Sediment	97%	FJ535278.1	97%	EU265787.1	97%	AB476173.1	97%	FN393026.1
	Contig_0357	*S. crosnieri* Epibiont	97%	AB440170.1	96%	EU265787.1	97%	AB440170.1	96%	FM203395.1
	Contig_0358	*S. crosnieri* Epibiont	97%	EU107475.1	96%	EU265786.1	97%	EU107475.1	96%	FM203406.1
	Contig_0361	*S. crosnieri* Epibiont	97%	EU107475.1	96%	EU265787.1	97%	EU107475.1	96%	FM203396.1
	Contig_0362	*S. crosnieri* Epibiont	96%	EU107475.1	95%	EU265786.1	96%	EU107475.1	96%	FM203406.1
	Contig_0363	Peltospiridae Epibiont	96%	AY531601.1	95%	EU265793.1	96%	AB476188.1	94%	FM203398.1
	Contig_0364	*S. crosnieri* Epibiont	96%	EU107475.1	96%	EU265785.1	96%	EU107475.1	96%	FM203396.1
	Contig_0365	*S. crosnieri* Epibiont	97%	EU107475.1	96%	EU265787.1	97%	EU107475.1	96%	FM203395.1
	Contig_0369	*S. crosnieri* Epibiont	96%	EU107475.1	96%	EU265786.1	96%	EU107475.1	96%	FM203406.1
	Contig_0370	*S. crosnieri* Epibiont	96%	EU107475.1	95%	EU265785.1	96%	EU107475.1	95%	FM203395.1
	Contig_0376	*S. crosnieri* Epibiont	96%	EU107475.1	95%	EU265786.1	96%	EU107475.1	96%	FM203406.1
	Contig_0380	*S. crosnieri* Epibiont	97%	EU107475.1	96%	EU265786.1	97%	EU107475.1	95%	FM203395.1
	Contig_0382	*S. crosnieri* Epibiont	97%	AB440170.1	95%	EU265787.1	97%	AB440170.1	96%	FM203406.1
	Contig_0383	*K. hirsuta* Epibiont	96%	EU265787.1	96%	EU265787.1	97%	AB440170.1	95%	FM203395.1
	Contig_0378	*S. crosnieri* Epibiont	97%	EU107475.1	96%	EU265787.1	97%	EU107475.1	96%	FM203395.1
	Contig_0359	9N Hydrothermal Bacterial Mat	96%	AY075127.1	95%	EU265787.1	96%	AB440170.1	95%	FM203377.1
	Contig_0355	*K. hirsuta* Epibiont	98%	EU265786.1	98%	EU265786.1	98%	EU107475.1	96%	FN393028.1
δ-Proteobacteria	Contig_0374	HR Methane Seep Sediment	98%	AJ535238.1	95%	EU265788.1	< 92%		< 92%	
	Contig_0377	HR Methane Seep Sediment	99%	AJ535238.1	95%	EU265788.1	< 92%		< 92%	
	Contig_0379	Peltospiridae Epibiont	94%	AY531586.1	<89%		< 89%		< 89%	
	Contig_0360	Peltospiridae Epibiont	93%	AY355303.2	<91%		< 91%		< 91%	
	Contig_0372	HR Methane Seep Sediment	89%	AJ535236.1	< 87%		< 87%		< 87%	
Bacteriodetes	Contig_0367	Methane Seep Sediment	97%	AM745131.1	<90%		< 90%		< 90%	
	Contig_0368	Haakon Mosby Sediment	98%	AJ704707.1	92%	EU265797.1	< 87%	AB476194.1	< 84%	
	Contig_0385	Peltospiridae Epibiont	97%	AY531558.1	< 87%		< 87%		< 87%	
	Contig_0375	Peltospiridae Epibiont	97%	AY531558.1	< 87%		< 87%		< 87%	
γ - Proteobacteria	Contig_0352	*K. hirsuta* Epibiont	98%	EU265784.1	98%	EU265784.1	98%	AB476177.1	98%	FM203402.1
	Contig_0353	*K. hirsuta* Epibiont	97%	EU265791.1	97%	EU265791.1	97%	AB476177.1	97%	FM203375.1
Unresolved	Contig_0371	Hydrothermal Sulfide Structure	97%	AB293157.1	< 72%		< 72%		< 72%	
	Contig_0381	*Lamellibrachia* Tube	90%	FM212619.1	< 78%		< 78%		< 78%	
	Contig_0384	Sulfate-Reducing Cave	89%	FJ716411.1	< 82%		< 82%		< 82%	

References

Brodsky LI, Ivanov VV, Kalaidzidis YAL, Leontovitch AM, Nikolaev VK, et al. (1995) Genebee-Net – internet-based server for analyzing biopolymers structure. Biochemistry-Moscow 60: 923-928.

Cavanaugh CM, Gardiner SL, Jones ML, Jannasch HW, Waterbury JB (1981) Prokaryotic cells in the hydrothermal vent tube worm *Riftia pachyptila*: Possible chemoautotrophic symbionts. Science 213: 340-342.

Cavanaugh CM, McKiness ZP, Newton ILG, Stewart FJ (2006) Marine Chemosynthetic symbioses. Prokaryotes 1: 475-507.

Childress JJ, Fisher CR, Brooks JM, Kennicutt MC, Bidigare R, Anderson AE (1986) A methanotrophic marine molluscan (Bivalvia, Mytilidae) symbiosis: mussels fueled by gas. Science 233: 1306–1308.

Colaco A, Desbruyeres D, Guezennec J (2007) Polar lipid fatty acids as indicators of trophic associations in a deep-sea vent system community. Mar Ecol 28: 15-24.

Conway N, Kennicutt II M, Van Dover C (1994) Stable isotopes in the study of marine chemosynthetic based ecosystems. In: Lajtha K, Michener R, editors. Stable isotopes in ecology and environmental sciences. London: Blackwell. pp. 158–186.

Cordes EE, Cunha MR, Galéron J, Mora C, Olu-Le Roy K, et al. (2010) The influence of geological, geochemical, and biogenic habitat heterogeneity on seep biodiversity. Mar Ecol 31: 51-65.

Cordes EE, Hourdez S, Predmore BL, Redding ML, Fisher CR (2005) Succession of hydrocarbon seep communities associated with the long-lived foundation species *Lamellibrachia luymesi*. Mar Ecol Prog Ser 305: 17-29.

Costa FO, deWaard JR, Boutillier J, Ratnasingham S, Dooh R, et al. (2007) Biological identification through DNA barcodes: the case of the Crustacea. Can. J. Fish. Aquat. Sci. 64: 272-295.

Currie CR, Scott JA, Summerbell RC, Malloch D (2001) Fungus-growing ants use antibiotic-production bacteria to control garden parasites. Nature 398: 701-704.

Dallwitz MJ, Paine TA, Zurcher EJ (1997) User's guide to the DELTA system. A general system for processing taxonomic descriptions. 4.08. CSIRO Division of Entomology, Canberra.

Dalsgaard J, St. John M, Kattner G, Müller-Navarra D (2003) Fatty acid trophic markers in the pelagic marine environment. Adv Mar Biol 46: 225-340.

DeNiero MJ, Epstien S (1978) Influence of diet on the distribution of carbon isotopes in animals. Geochim Cosmochim Acta 42: 495-506.

Dennison WC, Barnes DJ (1988) Effect of water motion on coral photosynthesis and calcification. J Exp Mar Biol Ecol 115: 67-77.

Di Meo CA, Wilbur AE, Holben WE, Feldman RA, Vrijenhoek RC, et al. (2000) Genetic variation among endosymbionts of widely distributed vestimentiferan tubeworms. Appl Environ Microbiol 66: 651-658.

Dupperon S, Nadalig T, Caprais J-C, Sibuet M, Fiala-Médioni, A, et al. (2005) Duel symbiosis in a *Bathymodiolus* sp. mussel from a methane seep on the Gabon Continental Margin (Southeast Atlantic): 16S rRNA phylogeny and distribution of the symbionts in gills. Appl Environ Microbiol 71: 1694-1700.

Edgar RC (2004) MUSCLE: a multiple sequence alignment method with reduced time and space complexity. BMC Bioinformatics 5:113

Felbeck H (1981) Chemoautotrophic potential of the hydrothermal vent tube worm, Riftia pachyptila Jones (Vestimentifera). Science 213: 336-338.

Fisher CR (1990) Chemoautotrophic and methanotrophic symbioses in marine invertebrates. Rev Aquat Sci 2: 399-436.

Gebruk AV, Pimenov NV, Savvichev AS (1993) Feeding specialization of bresiliid shrimps in the TAG site hydrothermal community. Mar Ecol Prog Ser 98: 247-253.

Gebruk AV, Southward EC, Kennedy H, Southward AJ (2000) Food sources, behavior, and distribution of hydrothermal vent shrimps at the Mid-Atlantic Ridge. J Mar Biol Ass U K 80: 485-499.

Glover AG, Smith CR (2003) The deep-sea floor ecosystem: current status and prospects of anthropogenic change by the year 2025. Environ Conserv 30: 219-241.

Goffredi SK (2010) Indigenous ectosymbiotic bacteria associated with diverse hydrothermal vent invertebrates. Environ Microbiol Rep 2: 479-488.

Goffredi SK, Jones WJ, Erhlich H, Springer A, Vrijenhoek RC (2008) Epibiotic bacteria associated with the recently discovered Yeti crab, *Kiwa hirsuta.* Environ Microbiol 10: 2623-2635.

Grossman S, Reichart W (1991) Impact of *Arenicola marina* on bacteria in intertidal sediments. Mar Ecol Prog Ser 77: 85-93.

Halanych KM, Lutz RA, Vrijenhoek RC (1998) Evolutionary origins and age of vestimentiferan tubeworms. Cah Biol Mar 39: 355-358.

Hickerson MJ, Cunningham CW (2000) Dramatic mitochondrial gene rearrangements in the hermit crab Pagurus longicarpus (Crustacea, Anomura). Mol Biol Evol 17: 639.

Huelsenbeck JP, Ronquist F (2001) MRBAYES: Bayesian inference of phylogenetic trees. Bioinformatics 17: 745-746.

Hughes Martiny JB, Bohannan BJM, Brown JH, Colwell RK, Fuhrman JA, et al. (2006) Microbial biogeography: putting microorganisms on the map. Nat Rev Microbiol 4: 102-112.

Hugler M, Sievert SM (in press) Beyond the Calvin Cycle: autotrophic carbon fixation in the ocean. Annu Rev Mar Sci.

Jokiel PL (1978) Effects of water motion on reef corals. J Exp Mar Biol Ecol 35: 87-97.

Lesser MP, Weis VM, Patterson MR, Jokiel PL (1994) Effects of morphology and water motion on carbon delivery and productivity in the reef coral, *Pocillopora damicornis* (Linnaeus): Diffusion barriers, inorganic carbon limitation, and biochemical plasticity. J Exp Mar Biol Ecol 178: 153-179.

Lewis T, Nichols PD, McMeekin TA (2000) Evaluation of extraction methods for recovery of fatty acids from lipid-producing microheterotrophs. J Microbiol Methods 43: 107-116.

MacAvoy SE, Macko SA, Joye SB (2002) Fatty acid carbon isotope signatures in chemosynthetic mussels and tube worms from Gulf of Mexico hydrocarbon seep communities. 185: 1-8.

MacPherson E, Jones W, Segonzac M (2005) A new squat lobster family of Galatheoidea (Crustacea, Decapoda, Anomura) from the hydrothermal vents of the Pacific- Antarctic Ridge. Zoosystema 27: 709-723

McCaffrey MA, Farrington JW, Repeta DJ (1989) Geochemical implications of the lipid composition of *Thioploca spp*. from the Peru upwelling region – 15^{o}S. Org Geochem 14: 61–68.

McCutchan Jr. JH, Lewis WM, Kendall C, McGrath CC (2003) Variation in trophic shift for stable isotope ratios of carbon, nitrogen, and sulfur. Oikos 102: 378-390.

McLaughlin PA, Lemaitre R, Sorhannus U (2007) Hermit crab phylogeny: A reappraisal and its "fall-out." J Crust Biol 27: 97-105.

Miyake H, Kitada M, Tsuchida S, Okuyama Y, Nakamura K (2007) Ecological aspects of hydrothermal vent animals in captivity at atmospheric pressure. Mar Ecol 28: 86-92.

Morrison CL, Harvey AW, Lavery S, Tieu K, Huang Y, Cunningham CW (2002) Mitochondrial gene rearrangements confirm the parallel evolution of the crab-like form. Proc R Soc London Ser B 269: 345-350.

Nichols DS (2003) Prokaryotes and the input of polyunsaturated fatty acids to the marine food web. FEMS Microbiol Lett 219: 1-7.

Patterson MR, Sebens KP, Olson RR (1991) In situ measurements of flow effects on primary production and dark respiration in reef corals. Limnol Oceanogr 36: 936-948.

Paul CK, Hecker B, Comeau R, Freeman-Lynde RP, Neumann C, et al. (1984) Biological communities at the Florida Escarpment resemble hydrothermal vent taxa. Science 226: 965-967.

Petersen JM, Ramette A, Lott C, Cambon-Bonavita M-A, Zbinden M, Dubilier N (2009) Dual symbiosis of the vent shrimp *Rimicaris* exoculata with filamentous gamma- and epsilonproteobacteria at four Mid-Atlantic Ridge hydrothermal vent fields. Environ Microbiol 12: 2204-2218.

Polz MF, Robinson JJ, Cavanaugh CM, van Dover CL (1998) Trophic ecology of massive shrimp aggregations at a Mid-Atlantic Ridge hydrothermal vent site. Limnol Oceanogr 43: 1631-1638.

Pond DW, Dixon DR, Bell MV, Fallick AE, Sargent JR (1997) Occurrence of 16: 2(n-4) and 18: 2(n-4) fatty acids in the lipids of the hydrothermal vent shrimps *Rimicaris exoculata* and *Alvinocaris markensis*: nutritional and trophic implications. Mar Ecol Prog Ser 156, 167-174.

Quadant L, Gottschalk G, Ziegler H, Stichler W (1977) Isotope discrimination by photosynthetic bacteria. FEMS Microbiol Lett 1: 125-128.

Saito H (2008) Unusual novel n-4 polyunsaturated fatty acids in cold-seep mussels (*Bathymodiolus japonicus* and *Bathymodiolus platifrons*), origination from symbiontic methanotrophic bacteria. J Chromatrogr A 1200: 242-254.

Schmaljohann R, Faber E, Whiticar MJ, Dando PR (1990) Co-existence of methane- and sulpher-based endosymbioses between bacteria and invertebrates at a site in the Skegerrak. Mar Ecol Prog Ser 61: 119-124.

Segonzac M, Desaintlaurent M, Casanova B (1993) Enigma of trophic adaptation of the shrimp Alvinocarididae in hydrothermal areas along the Mid-Atlantic Ridge. Cah Biol Mar 34: 535-571.

Sibuet M, Olu K (1998) Biogeography, biodiversity and fluid dependence of deep-sea cold-seep communities at active and passive margins. Deep-Sea Res II 45: 517-567.

Sirevag R (1974) Further studies on carbon dioxide fixation in *Chlorobium*. Arch Microbiol 98: 3-18.

Southward AJ, Newman WA (1998) Ectosymbiosis between filamentous sulphur bacteria and stalked barnacle (Scalpellomorpha, Neolepadinae) from the Lau Back Arc Basin, Tonga. Cah Biol Mar 39: 259-262.

Suzuki Y, Kojima S, Sasaki T, Suzuki M, Utsumi T, et al. (2006) Host-symbiont relationships in hydrothermal vent gastropods of the genus *Alvinoconcha* from the Southwest Pacfic. Appl Environ Microbiol 72: 1388-1393.

Volkman JK, Barrett SM, Blackburn SI, Mansour MP, Sikes EL, Gelin F (1989) Microalgal biomarkers: a review of recent research development. Org Geochem 29: 1163-1179.

Vrijenhoek RC, Duhaime M, Jones WJ (2007) Subtype variation among bacterial endosymbionts of tubeworms (Annelida: Siboglinidae) from the Gulf of California. Biol Bull 212: 180-184.

Wolff R (2005) Composition and endemism of the deep-sea hydrothermal vent fauna. Cah Biol Mar 46: 97-104

Yang JS, Yang WJ (2008) The complete mitochondrial genome sequence of the hydrothermal vent galatheid crab *Shinkaia crosnieri* (Crustacea : Decapoda : Anomura): A novel arrangement and incomplete tRNA suite. BMC Genomics 9: 257-270.

Zbinden M, Cambon-Bonavita MA (2003) Occurrence of *Deferribacterales* and *Entomoplasmatales* in the deep-sea alvinocarid shrimp *Rimicaris exoculata* gut. FEMS Microbiol Ecol 46: 23-30.

Acknowledgements

We would like to thank Lisa A. Levin and Shana Goffredi for comments, Shane Ahyong for photographs and advice and Ashley A. Rowden, Mike Tryon, and Captains, Crew, Science Parties, and the Alvin Group of AT 15-5, 15-44, 15-59 for making this research possible. The species was discovered thanks to the insight of Alvin pilot Gavin Eppard who immediately recognized its novelty. This research was supported by NSF OCE-0242034, OCE-0826254 and OCE-0939557, New Zealand Foundation for Research, Science and Technology (project C01X0502), the David & Lucile Packard Foundation, Monterey Bay Aquarium Research Institute, Michael M. Mullin Memorial Fellowship, Sydney E. Frank Foundation, and Census of Marine Life-Training AWard for New Investigators (TAWNI). The funders had no role in study design, data collection and analysis, decision to publish, or preparation of the manuscript. This chapter, in part, is a submitted for publication in a 2010 issue of PLoS ONE (Thurber AR, Jones WJ, Schnabel, K). The dissertation author was the primary investigator and author of this paper.

CHAPTER 7.

DISCUSSION

Biomarker techniques, including fatty acid (FA) and stable isotopic analysis, provide a time-integrating measure of trophic linkages. These techniques have become powerful and often-applied tools in marine and terrestrial systems (e.g. Stapp et al. 1999; Felicitti et al. 2003; Iverson et al. 2004). In deep-sea systems, the large challenges associated with manipulative experiments and long-term observation, has led to widespread application of both of these tools to megafauna (e.g. Howell et al. 2003; MacAvoy et al. 2003; 2005), macrofauna (e.g. Van Dover et al. 2002; Levin and Michener 2002; Levin et al. 2003), meiofauna (Van Graever 2009; Ingals et al. 2010), bacteria and Archaea (Hinrichs et al. 2000; Orphan et al. 2001; Elvert et al. 2003), providing novel insights into ecosystem functioning. Yet, the underlying assumptions and widespread application of both of these approaches are commonly based on analyses of large data sets (Daslgaard et al. 2003; McClutchen et al. 2003), which provide trends but ignore species-specific variation. The ramifications of not having species-specific incorporation estimates were clear throughout this dissertation. By using a laboratory-based study to test the underlying assumptions of lipid and isotopic analysis for a polychaete species (**Chapter 4),** I found that neither the isotopic enrichment nor fatty acid profile was tractable in a consumer without *a priori* knowledge of the food source. While this added credence to a highly-conservative mixing models used to estimate methane-derived carbon at New Zealand methane seeps (**Chapter 2),** it also helped explain many of the patterns that I observed in the remaining Chapters, including the high abundance of polyunsaturated FAs (PUFAs) in species that did not consume phytoplankton (**Chapters 3** and **5**), and that certain FA and archaeal lipids were not incorporated into grazer tissue, independent of the amount provided by their food source.

Within metazoan fauna, the importance of PUFAs has lead to these FAs and their precursors to be called the “essential fatty acids.” Even the lay public choses breakfast cereal due to the concentration of PUFAs within different brands, and traditional wisdom suggests that these are entirely derived from primary producers, such as plants or phytoplankton (Berge and Barnathan 2005). In the past two decades we have learned that bacteria and heterotrophic protists also synthesize PUFAs, potentially forming a key source of essential fatty acids to other fauna (Allen et al. 1990; Zhukova and Kharlamenko 1999; Nichols 2003; Sampedro et al. 2006). Thus, I was surprised to find out that PUFAs were prevalent within the tissue of *Ophryotrocha labronica* when raised on a monoculture of food sources that did not contain PUFAs (**Chapter 4**). In addition they were common throughout the ampharetid bed community (**Chapter 3)** and, most shockingly, within a species that had a $\delta^{13}C$ value of -101 ‰ **(Chapter 5)!** Whereas this could have been attributed to these bactivorous, and likely archivorous (Archaea consuming), species augmenting their diet with phytoplankton, $\delta^{13}C$ values of PUFAs within this “-101” species were <-100 ‰, meaning that it must be formed *in situ* by either the worm (as **Chapter 4** would suggest) or by bacteria within the rock or the worm’s gut. Thus, the presence of PUFAs are not, by themselves, conclusive evidence of phytoplankton consumption. It has been suggested that protists are a source of PUFAs to food webs (Zhukova and Kharlamenko 1999), and this study suggests that polychaetes, and potentially many other invertebrate phyla, may also provide PUFAs to the diversity of fauna that consume them.

Another key finding of this dissertation is that an absence of a lipid is not proof that a food source is not consumed (**Chapters 4** and **5)**. In archaeal, eukaryotic, and bacterial food sources, certain lipids, including all of the archaeal lipids analyzed, provided unique signatures that were not incorporated into annelids that consumed them. This finding was key for

interpreting the diet of a species that lived within authigenic carbonate rocks (**Chapter 5).** Although compound-specific FA data indicated that this novel species of *Dorvillea* sp. clearly incorporated most of the FAs available within the carbonate rock, identifying AOM consortia as its main food source, the lack of cyclo17, diagnostic for sulfate-reducing bacteria, was perplexing. Just like the (n-3) FA that was present within *Oryza* (**Chapter 4**), the sulfate reducing biomarker was not incorporated. Although in the past, a lack of archaeal FAs has been used as an indicator that there was unlikely archivory within a species (Phleger et al. 2005), I learned that lipid measures are not appropriate to identify or eliminate archaea as a consumed food source (**Chapter 5**).

Although both isotopic and FA analysis have limitations, they also provide insight into the functioning of methane seeps. Isotopic analysis identified methane-based biomass as an important food source for both infaunal ampharetid beds and a sponge community (**Chapter 2** and **3**). FA analysis combined with other lines of evidence, identified the source of energy for invertebrates within ampharetid beds as aerobic methanotrophs (**Chapter 3**). Furthermore, although PUFA presence does not unequivocally identify consumption of phytoplankton, a high abundance of PUFAs within certain species, when compared to seep fauna and coupled to isotopic measures, identified that certain individuals consume more photosynthetic production even when collected within seep habitats (**Chapter 3**). Using FA, isotopic, and a combination of the two techniques, sulfate-reducing bacteria from archaeal-bacterial aggregates were found to be consumed by metazoans (**Chapter 5)**. And finally, isotopic analysis identified chemosynthetic energy as the main food source for a new species of Yeti Crab, and FA analysis identified this food sources as its epibiotic symbionts (**Chapter 6**). In each of these cases, multidisciplinary approaches allowed me to discover a variety of novel trophic relationships within methane seeps.

What biomarkers can tell us about biogeochemical cycling.

Biomarkers of metazoans provide insight into the dominant biogeochemical cycling that occurs in sediments. Methane flux out of seep sediments is highly episodic and varies on small spatial scales (Tryon and Brown 2001; Levin et al. 2003; Ziebis and Haese 2005; Linke et al. 2010; Naudits et al. 2010). Short term observation may or may not represent the "normal" chemical environment within seeps. In addition, soft-sediment habitats have received the most attention when measuring methane flux as technology currently exists to measure the magnitude of methane release out of these habitats (Tryon et al. 1999; Sommer et al. 2006). Carbonate habitats, precipitated by AOM, have unique methanotrophic Archaea within them (Stadnitskaia et al. 2008) yet do not lend themselves to methane flux measurements. Yet two carbonate habitats were fueled almost entirely by methane (**Chapter 2** and **5**). A sponge community exists off of NZ that subsists off of methane-derived carbon (**Chapter 2**) and a species of dorvilleid lives inside the rocks and consumes ANME aggregates (**Chapter 5**). To have this occur, they must be receiving a constant flux of methane. This highlights how methane released from authigenic carbonates may be an underappreciated source of methane into the water column, and potentially our atmosphere, yet some of this release is mitigated by metazoan methane sinks, including the aforementioned sponge community.

Top down forcing on Methane Emission?

The world's continental margins contain between 5 and 25 x 10^{17} grams C of methane, a green house gas that is 23 times more potent than CO_2 (Milkov 2004). At times throughout earth's history these methane reservoirs have been released into the atmosphere,

causing massive extinction events (Kemp et al. 2005), including losses of 33-55% of species globally (Sepkoski 1996). The majority of methane currently released from these reservoirs is consumed by methanotrophic archaea and sulfate-reducing bacteria through the anaerobic oxidation of methane (Valentine et al. 2001, Truede et al. 2003), attenuating its threat to the global environment. I found that this syntrophic partnership is grazed upon by dorvilleid polychaetes at a variety of seeps (**Chapter 5**). What role might this grazing have on our global carbon cycle? Is the sediment filter, which normally consumes this methane (Sommer et al. 2006), being consumed?

Top-down forcing, including both predation and grazing, can have direct implications for productivity within a food web (Carpenter et al. 1985). Grazing on methanotrophs can impact the rate of methane emission, potentially stimulating methanotroph productivity (lessening methane emission). In New Zealand, I found a habitat with the greatest methane flux and the greatest methanotrophic biomass consumed by metazoan fauna (**Chapter 3**). This could be caused by the ampharetid polychaetes consuming aerobic methanotrophs at a rate that limited the methanotroph productivity and led to methane release. Essentially, the ampharetids may provide a top-down forcing on the microbial community sufficient to cause increased emission of a greenhouse gas. Yet at the same time, through tube formation, they could also increase the oxygenated surface area, promoting aerobic processes and aerobic methane oxidation. This would instead limit the methane release by increasing the surface area for aerobic methanotrophs to live, while grazing them at what fishery scientists would call “maximum sustainable yield”, further decreasing methane flux. Although each of scenarios has a divergent ramification for the role of trophic linkages between infauna and microbial processes, this aerobic, methane-fueled habitat clearly shows that there is potential for strong interplay between metazoans and the biogeochemical cycling in methane seep sediments.

Summary

Throughout this dissertation, I have identified the importance and diversity of microbial production in the diets of metazoans from the scale of the community (**Chapter 2** and **3**) down to the species (**Chapter 5** and **6**). I found that the underlying chemical reactions of this production varied by location and identified the limitations of both fatty acid and stable isotopic techniques for seep food-web studies (**Chapter 4** and **5**). While doing this, I found that polychaetes can grow on Archaea, a domain of life that is currently left out of classical food webs, and identified how archaeal-bacterial aggregates are consumed by infauna (**Chapter 4** and **5**). Finally, I found a habitat where aerobic methane oxidation fuels a high biomass, deep-sea community (**Chapter 3**). This dissertation furthers our knowledge of microbial-metazoan interactions at methane seeps, while providing the necessary underlying evidence that microbially-mediated biogeochemical cycling is connected to the metazoan food web. The impact of grazing pressure on global-methane cycles and microbial processes is a clear next step for deep-sea seep research.

References

Allen EE, Facciotti D, Bartlett DH (1999) Monounsaturated but not polyunsaturated fatty acids are required for growth of the deep-sea bacterium *Photobacterium profundum* SSP at High Pressure and low Temperature. Enriron Microbiol 65:1710-1720

Berge J-P, Barnathan G (2005) Fatty acids from lipids of marine organisms:molecular biodiversity, roles as biomarkers, biologically active compounds, and economical aspects. Adv Biochem Engin Biotechnol 96:49-125

Carpenter SR, Kitchell JF, Hodgson JR (1985) Coscading trophic interactions and lake productivity. Bioscience 35:634-639

Dalsgaard J, St John M, Kattner G, Müller-Navarra D, Hagen W (2003) Fatty acid trophic markers in the pelagic marine environment. Adv Mar Biol 46:225–340

Elvert M, Boetius A, Knittel K, Jorgensen BB (2003) Characterization of specific membrane fatty acids as chemotaxonomic markers for sulfate-reducing bacteria involved in anaerobic oxidation of methane. Geomocrbiol J 20:403-419

Felicciti LA, Schartz CC, Rye RO, Haroldson MA, Gunther KA, Phillips DL, Robbins CT (2003) Use of sulfer and nitrogen stable isotopes to determine the importance of whitebark pine nuts to Yellowstone grizzly bears. Can J Zool 81:763-770

Hinrichs KU, Summons RE, Orphan V, Sylva SP, Hayes JM (2000) Molecular and isotopic analysis of anaerobic methane-oxidizing communities in marine sediments. Org Geochem 31:1685–1701

Howell KL, Pond DW, Billett DSM, Tyler PA (2003) Feeding ecology of deep-sea seastars (Echinodermata:Asteroidea):a fatty-acid biomarker approach. Mar Ecol Prog Ser 225:193-206

Ingels J, Van den Driessche P, De Mesel I, Vanhove S, Moens T, Vanreusel A (2010) Preferred use of bacteria over phytoplankton by deep-sea nematodes in polar regions. Mar Ecol Prog Ser 406:121-133

Iverson SJ, Field C, Don Bowen W, Blanchard W (2004) Quantitative fatty acid signature analysis:a new method for estimating predator diets. Ecol Monogr 74:211-235

Kemp DB, Coe AL, Cohen AS, Schwark L (2005) Astronomical pacing of methane release in the early Jurassic period. Nature 437:396-399

Levin LA, Michener R (2002) Isotopic evidence of chemosynthesis-based nutrition of macrobenthos:the lightness of being at Pacific methane seeps. Limnol Oceanog 47:1336–1345

Levin LA, Ziebis W, Mendoza G, Growney V, Tryon M, Brown K, Mahn C, Gieskes J, Rathburn A (2003) Spatial heterogeneity of macrofauna at northern California methane seeps:the influence of sulfide concentration and fluid flow. Mar Ecol Prog Ser 265:123–139

Linke P, Sommer S, Rovelli L, McGinnis DF (2010) Physical limitation so of dissolved methane fluxes:the role of bottom-boundary layer processes. Mar Geol. 272:209-222

MacAvoy SE, Macko SA, Carney RS (2003) Links between chemosynthetic production and mobile predators on the Louisiana continental slope:stable carbon isotopes of specific fatty acids. Chem Geol 201:229-237

MacAvoy SE, Fisher CR, Carney RS, Macko SA (2005) Nutritional associations among fauna at hydrocarbon seep communities in the Gulf of Mexico. Mar Ecol Prog Ser 292:51-60

McCutchan Jr. JH, Lewis WM, Kendall C, McGrath C (2003) Variation in trophic shift for stable isotope ratios of carbon, nitrogen, and sulfer. OIKOS 102:378-390

Milkov AV (2004) Molecular and stable isotope compositions of natural gas hydrates:A revised global dataset and basic interpretations in the context of geological settings. Org Geochem 36:681-702

Naudits L, Greinert J, Poort J, Belza J, Vangampelaere E, Boone D, Linke P, Henriet J-P, De Batist M (2010) Active venting sites on the gas-hydrate-bearing Hikurangi Margin, off New Zealand:Diffusive- versus bubble-released methane. Mar Geol 272:233-250

Nichols DS (2003) Prokaryotes and the input of polyunsaturated fatty acids to the marine food web. FEMS Microbiol Lett 219:1-7

Orphan VJ, House CH, Hinrichs KU, Mckeegan KD, Delong EF (2001) Methane-consuming archaea revealed by directly coupled isotopic and phylogenetic analysis. Science 293:484–487

Phleger CF, Nelson MM, Groce AK, Cary SC, Coyne K, Gibson JAE, Nichols PD (2005) Lipid biomarkers of deep-sea hydrothermal vent polychaetes – *Alvinella pompejana, A. caudate, Paralvinella grasslei* and *Hesiolyra bergii*. Deep-Sea Res I 52:2333-2352

Sampedro L , Jeannotte R, Whalen JK (2006) Trophic transfer of fatty acids from gut microbiota to the earthworm *Lubricus terrestris* L. Soil Biol Biochem 38:2188-2198

Sepkoski JJ (1996) Patterns of Phanerozoic extinction:A perspective from global data bases. In:Walliser OH (Ed) Global Events and Event Stratigraphy in the Phanerozoic. Springer, Berlin, pp35–51

Sommer S, Pfannkucke O, Linke P, Luff R, Greinert J, Drews M, Gubsch, Pieper M, Poser M, Viergutz (2006) Efficiency of the benthic filter: Biological control of emission of dissolved methane from sediments containing shallow gas hydrates at Hydrate Ridge. Global Biogeochem Cycles. 20:1-14. doi:10.1029/2004GB002389

Stadnitskaia A, Bouloubassi I, Elvert M, Hinrichs K-U, Sinninghe Damsté JS (2008) Extended hydroxyarchaeol, a novel lipid biomarker for anaerobic methanotrophy in cold seep habitats. Org Geochem 30:1007-1014

Stapp P, Polis GA, Piñero FS (1999) Stable isotope reveal strong marine and El Nino effects on island food webs. Nature 401:467-469

Truede T, Boetius A, Knittel K, Wallmann K, Jørgensen BB (2003) Anaerobic oxidation of methane above gas hydrates at Hydrate Ridge, NE Pacific Ocean. Mar Ecol Prog Ser 264:1-14

Tryon MD, Brown KM, Torres ME, Tréhu AM, McManus J, Collier RW (1999) Measurements of transience and downward fluid flow near episodic methane gas vents, Hydrate Ridge, Cascadia. Geology 27:1075-1075

Tryon MD, Brown KM (2001) Complex flow patterns through Hydrate Ridge and their impact on seep biota. Geophys Res Lett 28:2863-2866

Valentine DL, Blanton DC, Reeburgh WS, kastner M (2001) Water column methane oxidation adjacent to an area of active hydrate dissociation, Eel River Basin. Geochim Cosmochim Acta 65:2633-2640

Van Dover CL (2002) Trophic relationships among invertebrates of the Kairei hydrothermal vent field (Central Indian Ridge). Mar Biol 141:761-772

Van Gaever S, Moodley L, Pasotti F, Houtekamer M, Middelburg JJ, Danovaro R, Vanrousel A (2009) Trophic specialization of metazoan meiofauna at the Håkon Mosby Mud Volcano:fatty acid biomarker isotope evidence. Mar Biol 156:1289-1296

Zhukova NV, Kharlamenko VI (1999) Sources of essential fatty acids in the marine microbial loop. Aquatic Microbiol Ecol 17:153-157

Ziebis W, Haese RR (2005) Interactions between fluid flow, geochemistry, and biogeochemical processes at methane seeps. In: Kristensen E, Haese RR, Jostka JE (eds) Interactions between macro- and microorganisms in marine sediments. Coastal and Estuarine studies 60. American Geophysical Union, Washington. p267-298